

Université du Québec
Institut national de la recherche scientifique
Centre Eau Terre Environnement

**ESTIMATION DE LA RECHARGE À PARTIR DE SÉRIES TEMPORELLES
DE LA TEMPÉRATURE DU SOL, DES NIVEAUX D'EAU DANS LES
PUITS ET DE DONNÉES MÉTÉOROLOGIQUES: DÉVELOPPEMENT
MÉTHODOLOGIQUE ET ÉVALUATION DE L'INCERTITUDE**

Par

Jean-Sébastien Gosselin

Thèse présentée pour l'obtention du grade de
Philosophiae Doctor, Ph.D.
en sciences de la Terre

Jury d'évaluation

Examinateur externe	Gerald Flerchinger Ph.D. USDA
Examinateur externe	Asim Biswas Ph.D. Université McGill
Examinateur interne	René Therrien Ph.D. Université Laval
Directeur de recherche	Richard Martel Ph.D. INRS-ETE
Codirecteur de recherche	Christine Rivard Ph.D. CGC
Codirecteur de recherche	René Lefebvre Ph.D. INRS-ETE

Highly organized research is guaranteed to produce nothing new.

- FRANK HERBERT, DUNE

Remerciements

Je tiens d'abord à remercier les membres du jury d'évaluation pour avoir pris le temps de lire ma thèse et pour leurs judicieux commentaires qui ont permis d'améliorer ce travail.

Je remercie ensuite mon directeur, Richard Martel, de même que mes codirecteurs de recherche, Christine Rivard et René Lefebvre, pour leur soutien tout au long de ma thèse. J'ai beaucoup appris de chacun de vous trois et j'en suis très reconnaissant. Merci, Richard, pour ta confiance, ton pragmatisme et pour les qualités humaines et professionnelles dont tu fais preuve dans la gestion et la motivation de ton équipe. Merci, Christine, pour ta grande disponibilité, ton soutien dans les moments stressants et pour la rigueur et précision de tes révisions. Merci, René, pour ta passion contagieuse de l'hydrogéologie, pour tes qualités de communicateur, tes idées innovatrices et ta grande vision et rigueur scientifique.

Je souhaite de plus remercier mes collègues étudiants avec qui j'ai partagé le quotidien pendant ces quelques années à l'INRS. C'est en bonne partie grâce à vous si ces années à l'INRS sont passées si vite et ont été si agréables. Marc, Pierre, Martin, Lorenzo, Patrick, Gabriel, Simon, Guillaume, Emmanuelle, Olivier ainsi qu'à tous ceux que j'oublie, merci. Je remercie également le professeur Erwan Gloaguen sans qui la vie à l'INRS ne serait pas la même. Merci de contribuer, par tes nombreuses initiatives, à rendre l'INRS un lieu agréable à travailler et où il est possible pour nous tous d'échanger, tant du point de vue professionnel que personnel. C'est très inspirant et motivant.

Je remercie également mes parents qui m'ont toujours supporté et encouragé à aller de l'avant dans mes études, même si parfois j'avais de gros doutes. Ça valait vraiment le coup maintenant que c'est fait! Aller à l'université et poursuivre à la maîtrise et au doctorat ont été de très bonnes décisions de vie et je ne voudrais pas refaire les choses autrement.

Enfin, je remercie ma conjointe Marie-Claude et ma fille Léane qui ont su me supporter tout au long de cette aventure et particulièrement à travers la rédaction et la préparation des présentations orales qui me stressent toujours autant. Marie-Claude, tu as été et es toujours une source d'inspiration pour moi. J'admire ta discipline, ta rigueur, de même que ton sens des responsabilités et de l'organisation. Je ne le dirai jamais assez, une chance qu'on t'a. Léane, merci pour ta bonne humeur, ta belle personnalité et ton humour. Je n'aurais pas pu rêver avoir une meilleure fille que toi. Merci d'apporter autant de bonheur et de rires dans ma vie.

Avant-Propos

Cette thèse est composée de deux parties distinctes. La [partie I](#) comprend une synthèse de la démarche et des résultats pour l'ensemble des travaux effectués lors du doctorat. La [partie II](#) est constituée de quatre articles qui ont été écrits au cours du doctorat. Les quatre articles présentés dans la [partie II](#) sont, dans l'ordre:

- [Article 1](#) (compte-rendu de conférence):

Gosselin JS, Rivard C, Paniconi C & Martel R (2011). Applicability of temperature profile techniques for estimating recharge fluxes through the vadose zone. *GeoHydro2011, Joint IAHCNC, CANQUA and AHQ conference proceedings*, pages 1–7, Quebec City, Quebec, Canada. [DOI: 10.13140/RG.2.1.4018.2165](https://doi.org/10.13140/RG.2.1.4018.2165)

- [Article 2](#) (article publié):

Gosselin JS, Rivard C, Martel R & Lefebvre R (2016). Application limits of the interpretation of near-surface temperature time series to assess groundwater recharge. *Journal of Hydrology*, 538:96–108. [DOI: 10.1016/j.jhydrol.2016.03.055](https://doi.org/10.1016/j.jhydrol.2016.03.055).

- [Article 3](#) (à soumettre):

Gosselin JS, Lefebvre R, Martel C & Rivard C (à soumettre). Combined surface and aquifer water budgets to estimate groundwater recharge from daily weather data and well hydrographs.

- [Article 4](#) (à soumettre):

Gosselin JS, Martel C & Rivard C (à soumettre). An algorithm to automate the filling of gaps in daily weather records.

Un guide d'utilisateur du logiciel WHAT, développé dans le cadre du doctorat, est également présenté à l'[annexe A](#). Le logiciel est disponible gratuitement sur la plateforme web GitHub à l'adresse suivante: <https://github.com/jnsebgosselin/WHAT>.

Résumé

De nombreuses méthodes existent pour estimer la recharge, basées sur une grande variété de mesures, mais aucune n'est universelle, chacune ayant ses avantages et ses inconvénients. La recharge varie dans le temps et l'espace sur plusieurs ordres de grandeur. De plus, elle est généralement déduite de mesures indirectes avec des modèles qui reposent sur un ensemble d'hypothèses simplificatrices. Pour ces raisons, une grande incertitude peut être associée à toute estimation de la recharge. C'est pourquoi il est recommandé d'utiliser plusieurs méthodes afin d'accroître le niveau de confiance des valeurs estimées. Ceci ne permet toutefois pas de réduire ni de quantifier l'incertitude sur la recharge. De plus, cette solution n'est pas toujours possible, en raison par exemple de contraintes financières ou des échéanciers des projets. Il y a donc un intérêt pratique et scientifique à améliorer les méthodes d'estimation de la recharge qui sont simples d'application et basées sur des données facilement disponibles. Dans cette optique, cette thèse de doctorat traite de deux de ces méthodes en deux volets distincts.

Le premier volet présente une méthode d'estimation de la recharge utilisant des mesures de températures du sol et basée sur l'inversion d'un modèle numérique du transport advectif et conductif de la chaleur. Pour évaluer ses limites d'applicabilité, la méthode a été testée avec plusieurs séries temporelles synthétiques de températures produites avec le simulateur SHAW (Simultaneous Heat and Water model). Les résultats ont démontré qu'il est possible d'estimer la recharge avec une incertitude de moins de 20 % lorsque les taux annuels sont supérieurs à 200 mm/a. Toutefois, des analyses de sensibilité ont montré qu'une erreur considérable pouvait être associée aux valeurs estimées lorsque l'incertitude sur les paramètres du modèle inverse et sur les mesures de températures était prise en compte. Ces travaux présentent les difficultés associées à l'estimation précise des taux de recharge diffuse par traçage thermique et dressent un portrait des limites d'application et des sources d'erreurs qui peuvent avoir un impact significatif sur la précision de la méthode. Ils suggèrent que cette méthode n'est pas applicable dans la grande majorité des cas pour évaluer des taux de recharge diffuse.

Le second volet de la thèse propose plusieurs développements méthodologiques et informatiques pour l'application d'une méthode d'estimation de la recharge basée sur le calage d'un bilan hydrologique de surface couplé à un bilan en eau d'un aquifère libre à des mesures de niveaux d'eau dans un puits. Un logiciel a été développé pour l'application de la méthode, incluant un algorithme permettant d'estimer et de combler automatiquement les valeurs manquantes dans les séries de données météorologiques quotidiennes qui sont requises par la méthode. Afin d'améliorer la méthode et évaluer l'incertitude, une méthode d'optimisation a été incluse dans le logiciel. Les résultats obtenus suite à l'application de la méthode couplée à un site d'étude confirment qu'elle permet de réduire l'incertitude sur les valeurs de recharge estimées par rapport à l'utilisation des deux méthodes de bilan individuellement en contraignant les valeurs des paramètres hydrologiques.

Abstract

Numerous methods exist to estimate recharge, based on a wide variety of measurements, but none is universal, each having advantages and drawbacks. Recharge can vary in time and space over several orders of magnitude and is generally inferred from indirect measurements with models based on a set of simplifying assumptions. For these reasons, a large uncertainty may be associated with any recharge estimate. Therefore, it is recommended to use multiple methods to increase the confidence level of the estimates. This, however, does not allow the reduction or the quantification of the uncertainty. Moreover, this solution is not always possible due to financial constraints, project deadlines, and data availability. There is thus a practical and scientific interest in improving recharge assessment methods that are simple to apply and based on readily available data. In this context, this thesis tackles two of these methods in two distinct parts.

The first part presents a method based on the inversion of a numerical model of advective and conductive heat transport to infer recharge from soil temperature measurements. To assess its application limits, the method was tested with several synthetic time series of soil temperatures that were produced with the simulator SHAW (Simultaneous Heat and Water model). Results show that this method can assess recharge with an uncertainty lower than 20 % when annual recharge rates are over 200 mm/y. However, sensitivity analyses show that the inaccuracy can become very important when the uncertainty of the inverse model parameters and temperature measurements are taken into account. This work highlights the difficulties associated with the accurate assessment of diffuse recharge rates from temperature measurements and better defines the application limits and various sources of errors of the approach. The results suggest that this method is not applicable in most cases to evaluate diffuse recharge rates under real field conditions.

The second part offers several methodological and software developments for the application of a recharge assessment technique based on the calibration of a soil moisture balance coupled with an unconfined aquifer water budget to an observed well hydrograph. A computer software was developed for the application of the method, which includes an algorithm for estimating and automatically filling the gaps in daily weather datasets that are required by the method. In order to improve the method and evaluate the uncertainty, a global optimization method was included in the software. Application of this coupled method to a study area confirms that it reduces the uncertainty of recharge estimates compared to the use of both methods taken individually by better constraining the range of plausible values of the hydrological parameters.

Table des matières

Dédicace	iii
Remerciements	v
Avant-Propos	vii
Résumé	ix
Abstract	xi
Table des matières	xiii
Liste des figures	xvii
Liste des tableaux	xxiii
Partie I Synthèse	1
Chapitre 1 Introduction	3
1.1 L'eau souterraine	3
1.2 La recharge des eaux souterraines	4
1.3 Méthodes d'estimation de la recharge	6
1.4 Défis liés à l'estimation de la recharge	8
1.5 Traçage thermique	11
1.6 Bilans hydrologiques combinés	13
1.7 Objectifs du doctorat	16
1.7.1 Sous objectifs du volet sur le traçage thermique	16
1.7.2 Sous objectifs du volet sur les bilans hydrologiques combinés	17
Chapitre 2 Traçage thermique	19
2.1 Travaux préliminaires	19
2.1.1 Méthodologie	20
2.1.2 Discussion des résultats	21
2.2 Développement méthodologique et analyse d'incertitude	24
2.2.1 Méthodologie	25
2.2.2 Discussion des résultats	26
Chapitre 3 Bilans hydrologiques combinés	33

3.1	Estimation de la recharge	35
3.1.1	Méthodologie	38
3.1.2	Discussion des résultats	40
3.2	Comblement des données météorologiques journalières manquantes	43
3.2.1	Méthodologie	44
3.2.2	Discussion des résultats	45
Chapitre 4 Conclusion		51
4.1	Traçage thermique	51
4.2	Bilans hydrologiques combinés	53
4.2.1	Estimation de la recharge	53
4.2.2	Comblement des données météorologiques journalières manquantes	55
4.2.3	Logiciel WHAT	56
Partie II Articles		57
Article 1	Applicability of temperature profile techniques for estimating recharge fluxes through the vadose zone	59
Résumé		60
Abstract		60
1	Introduction	60
2	Theoretical basis and literature review	63
3	Methodology	66
3.1	Description of the numerical model	66
3.2	Description of the simulations	68
4	Results and Discussion	69
4.1	Case #1: constant recharge	69
4.2	Case #2 and #3: variable monthly recharge	71
5	Conclusion	73
6	Acknowledgments	74
Article 2	Application limits of the interpretation of near-surface temperature time series to assess groundwater recharge	75
Résumé		76
Abstract		77
1	Introduction	78
1.1	Background	78
1.2	Rationale and Objectives	79
2	Materials and Methods	80
2.1	Overview of the Methodology	80
2.2	Generation of the Synthetic Datasets	82
2.3	Inverse Numerical Model of Heat Transport	88
3	Results	92
3.1	Validation of the HeatFlow1Dz Simulator	92
3.2	Impact of Modeling Errors	94
3.3	Impact of Input Parameter Uncertainty	97
3.4	Impact of Measurement Errors	100

4	Discussion	101
5	Conclusion	103
6	Acknowledgments	105
7	Soil Hydraulic and Thermal Properties	106
Article 3	Combined soil moisture balance and unconfined aquifer water budget to assess recharge from daily weather data and well hydrographs	107
Résumé		108
Abstract		108
1	Introduction	109
2	Method	113
2.1	Surface Water Budget	114
2.2	Aquifer Water Budget	120
2.3	Model Calibration	122
3	Case Study	124
3.1	Material and Method	124
3.2	Results	131
3.3	Discussion	131
4	Conclusion	134
5	Acknowledgments	135
Article 4	An Algorithm to Automate the Filling of Gaps in Daily Weather Records	137
Résumé		138
Abstract		138
1	Introduction	139
2	Description of the Algorithm	140
2.1	Correlation Coefficients Calculations	140
2.2	Selection of the Neighboring Stations	142
2.3	Generation of the Multiple Linear Regression Model	142
2.4	Estimating Missing Daily Values	143
2.5	Uncertainty Assessment of the Estimated Values	144
3	Technical Information on the Use of PyGWD	144
3.1	Input Data	145
3.2	Parameters	145
3.3	Outputs	146
4	Application: The Montérégie Est Case Study	146
4.1	Materials and Method	146
4.2	Results and Discussion	151
4.3	Future Perspectives	156
5	Conclusion	157
6	Acknowledgments	158
7	Appendix	159
7.1	Minimal Working Example of the Gapfilling Algorithm	159
7.2	Example of a weather data input file	161
7.3	Inputs and Functions	162
Références		165

Annexe A	User Manual for WHAT	175
1	Introduction	175
1.1	What is WHAT	175
1.2	Features	175
1.3	Installation and Update	177
1.4	Overview of the Graphical User Interface	178
2	Data Management by Projects	179
2.1	Introduction	179
2.2	Create a New Project	180
2.3	Open a Project	181
2.4	Project Folder Structure Overview	182
3	Creating Gapless Daily Weather Datasets	183
3.1	Downloading and formatting data from the CDCD	183
3.2	Filling the gaps in daily weather records	186

Liste des figures

Partie I Synthèse

1.1	Distribution mondiale de l'eau.	4
1.2	Coupe verticale montrant différentes composantes du cycle de l'eau.	5
1.3	Plages de taux de recharge, échelles spatiales et échelles temporelles pour lesquelles les estimations de recharge sont valides pour diverses techniques d'estimation.	7
1.4	Profils hypothétiques verticaux des températures minimales et maximales dans le sol.	12
1.5	Variation hypothétique du niveau d'eau dans un puits d'observation en réponse aux précipitations.	14
2.1	Répartitions mensuelles de la recharge imposées pour les scénarios #1 à #3.	21
2.2	Résultats pour le scénario #1: recharge constante dans le temps.	22
2.3	Résultats pour le scénario #2: recharge nulle durant l'été.	23
2.4	Résultats pour le scénario #3: recharge importante au printemps et à l'automne.	23
2.5	Erreurs moyennes (ME) et erreurs quadratiques moyennes (RMSE) calculées entre les estimations annuelles de recharge (compilé à partir des flux d'eau résolus sur une base annuelle, semi-annuelle, mensuelle et hebdomadaire) et les valeurs simulées avec SHAW pour chacun des 12 contextes étudiés.	27
2.6	Erreur quadratique moyenne (exprimée en % de la recharge annuelle moyenne) pour les valeurs estimées de recharge obtenues par inversion sur une base hebdomadaire par rapport à la recharge annuelle moyenne simulée pour chaque contexte avec SHAW.	28
2.7	Boîtes à moustaches de Tukey des erreurs calculées sur les taux annuels de recharge estimés sur une période de 20 ans pour les 12 contextes étudiés lorsqu'une incertitude est considérée (a) sur la conductivité thermique du sable, k_{sand} , (b) sur la porosité totale du sol, n , et (c) sur la teneur volumétrique en eau, θ_w , lorsque (d) des erreurs aléatoires sont introduites dans les séries de températures à 1, 3 et 5 m de profondeur (σ_{obs} est la déviation standard des erreurs) et lorsque (e) un biais constant, $bias_{obs}$, est introduit dans la série de températures à 3 m. ÉI correspond à l'écart interquartile et VA aux valeurs aberrantes.	30
3.1	Exemple d'un hydrogramme de puits produit avec le logiciel WHAT.	34
3.2	Simulations équiprobables des niveaux d'eau mesurés dans un puits d'observation en Montérégie Est, Québec avec la méthode présentée par Lefebvre <i>et al.</i> (2011).	37
3.3	Capture d'écran du logiciel WHAT montrant l'interface qui a été développée pour l'estimation de la courbe maîtresse de récession (MRC).	39
3.4	Valeurs modales de recharge annuelle estimées avec la méthode GLUE.	41

3.5	Enveloppe des niveaux d'eau estimés avec la méthode pour l'intervalle de confiance de GLUE de 5 à 95 %	42
3.6	Nuages de points comparant les valeurs estimées et mesurées des températures de l'air (a) minimales, (b) moyennes, (c) maximales et des (d) précipitations journalières à la station <i>Granby</i> située au centre de la région d'étude.	47
3.7	Fonctions de densité de probabilité (FDP) gamma obtenues à partir des précipitations journalières estimées et mesurées à la station météorologique <i>Granby</i>	48

Partie II Articles

Article 1

1	Monthly distribution of groundwater recharge that were used as input to run forward simulations of advective-conductive heat transport with the model developed in section 3.1 . The monthly distribution for each of the three cases is equivalent to an annual groundwater recharge 400 mm/y	68
2	Results for Case #1: constant recharge case.	70
3	Results for Case #2: zero recharge during summer.	72
4	Results for Case #3: uneven spring and fall recharge distribution.	72

Article 2

1	Diagram showing the methodology followed for assessing the estimation error of annual groundwater recharge rates.	81
2	Location of the two weather stations used for this study.	86
3	Yearly and monthly averages for total precipitation and mean air temperature calculated at the Quebec (a) and Toronto (b) airport weather stations for the 1985-2005 period.	87
4	Hourly simulation results for Context #1 (Quebec weather station, sand, bare soil) for the years 1999 to 2001. <i>TOP</i> – Vertical hourly water fluxes calculated with SHAW at depths of 1 and 5 m below the ground surface. <i>MIDDLE</i> – Temperature time series produced with SHAW (solid blue lines) at depths of 1, 3 and 5 m, as well as with the heat transport model at a depth of 3 m after the calibration (dotted black line) and for the no-water flux scenario (dash-dot red line). <i>BOTTOM</i> – Temperature differences calculated between the time series simulated with SHAW and with the heat transport model for the no-water flux scenario at a depth of 3 m.	93
5	Mean Errors (ME) and Root Mean Square Errors (RMSE) calculated between the annual recharge estimates (compiled from water fluxes solved on an annual, semiannual, monthly, and weekly basis) and those produced with SHAW for each of the 12 contexts studied. The mean value (Re) of the actual annual recharge produced with SHAW is also provided.	95
6	Monthly averages of precipitation and recharge simulated with SHAW for the hydrogeological Contexts #1 and #2 to illustrate the impact of the vegetation cover on the time distribution of recharge over the year.	96
7	Root Mean Square Error (RMSE), calculated between the annual groundwater recharge rates estimated with the inverse heat transport model (compiled from water fluxes solved on a weekly basis) and those produced with the SHAW model, expressed in % of the mean annual recharge obtained with SHAW for each hydrogeological context.	96

8	Tukey box plots of the estimation error of the annual groundwater recharge (all contexts pooled together) obtained from the sensitivity analyses for (a) the thermal conductivity of the sand fraction, k_{sand} , (b) the soil total porosity, n , and (c) the soil volumetric water content, θ_w . IQR = Interquartile range.	98
9	Soil thermal diffusivity as a function of (a) the soil total porosity, (b) the sand fraction thermal conductivity, and (c) the soil moisture saturation. The soil thermal diffusivity takes into account the transfer of latent heat of vaporization and was computed from the calibrated model described in section 2.3.1 at a constant temperature of 8 °C (mean value at 3 m). For (a) and (b), the curves were produced for a fixed value of θ_w that corresponds to the average value of θ_w simulated for each soil type at the depth of 1 m with SHAW (see table 2). The dots in (a) and (b) correspond to the soil thermal diffusivity at the actual value of n and k_{sand} used in SHAW in the simulations. In (c), the solid and dotted lines show, respectively, the value of the soil thermal diffusivity within and outside the range of S_w simulated with SHAW (see table 2).	99
10	Tukey box plots of the estimation error of the annual groundwater recharge (all contexts pooled together) obtained after the introduction of (a) random errors in the synthetic temperature time series at 1, 3 and 5 m and (b) a constant bias to the synthetic temperature time series at the depth of 3 m.	100
11	Soil hydraulic characteristic curves for (a) the water retention and (b) the unsaturated hydraulic conductivity computed using the model of Brooks & Corey (1966) and the parameter values presented in table 1.	106
12	Soil thermal characteristic curves for (a) the thermal conductivity of the soil computed with the model of de Vries (1966) compensated for the transport of the latent heat of vaporization with the model of Campbell (1974) and (b) the heat capacity of the soil computed with a standard additive mixing law.	106

Article 3

1	Diagram showing relations between components of the soil moisture balance and aquifer water budget.	114
2	Flowchart showing the functional relationships used to compute daily accumulated P_{acc} and available (P_{avail}) precipitation from mean air temperature (T_{air}) and total precipitation (P_{tot}).	115
3	Diagram showing two soil moisture profiles within the unsaturated zone: one before and another after a rain event that was significant enough to produce recharge. The light shaded area corresponds to the Soil Moisture Deficit (SMD), while the dark shaded area corresponds to water in excess of the field capacity (θ_{FC}) of the soil that is assumed to drain below the root zone as potential recharge.	119
4	Location of the Portneuf area in the St. Lawrence Lowlands, Quebec, Canada (modified after Fagnan <i>et al.</i> , 1999). The map shows the observation well (red circle) located in an unconfined deltaic aquifer whose hydrograph is interpreted in this paper.	125
5	Completion of observation well #5080001 of the Quebec monitoring network (Gouvernement du Québec, 2015) located at Pont-Rouge, in the Portneuf area (see map on figure 4).	127
6	Yearly and monthly weather normals, calculated for the years 1960-2015, for the weather stations STE CHRISTINE located 20 km from the observation well at Pont-Rouge.	128

7	Monthly weather data and hydrograph for the years 1996-2014. (Lower Part): Daily water levels in meters below ground surface (mbgs) from the well #5080001 of the Quebec monitoring network (Gouvernement du Québec, 2015) located at Pont-Rouge, in the Portneuf area (figure 4). (Middle part): Monthly cumulative precipitation. (Top part): Average monthly maximum daily air temperatures. Weather data were compiled from daily values from weather station STE CHRISTINE located 20 km from the well (http://climate.weather.gc.ca/)	129
8	GLUE 5/95 uncertainty limits (grey) for predicted water levels and observed hydrograph (solid blue line). Simulated water levels with the calibrated master recession curve are shown with dashed red lines.	132
9	GLUE modal values for predicted annual groundwater recharge (GLUE 50). The whiskers correspond to the GLUE 5/95 uncertainty limits. Values were calculated for hydrological years by summing daily recharge rates from October 1st of one year to September 30th of the next.	132

Article 4

1	Flowchart of the methodology followed in PyGWD to produce serially complete daily weather datasets.	141
2	Location of the Montérégie Est region, Quebec, Eastern Canada.	147
3	Spatial distribution of the weather stations in (19) and around (13) the Montérégie Est area, southern Quebec, Eastern Canada.	149
4	Monthly weather normals for the weather stations with the highest (<i>Sutton</i>) and lowest (<i>Verchere</i>) annual total precipitation and the warmer (<i>Philipsburg</i>) and colder (<i>Bonsecours</i>) air temperature.	150
5	Scatter plots comparing the predicted versus the measured daily values for (a) minimum air temperature, (b) mean air temperature, (c) maximum air temperature, and (c) precipitation for the <i>Granby</i> weather station.	152
6	Gamma probability density functions (PDF) that were estimated from the estimated (dashed red line) and measured (solid blue line) daily precipitation time series for the <i>Granby</i> weather station. The histogram of the distribution of the measured daily precipitation events is also shown in light blue.	154

Annexes

1	Screenshot of WHAT v4.1.7-beta in Ubuntu-Linux 15.04 showing the <i>About</i> tab.	178
2	Screenshots of WHAT v4.1.7-beta captured in Ubuntu Linux 15.04.	180
3	Screenshot of WHAT v4.1.7-beta in Ubuntu-Linux 15.04 showing the <i>New Project</i> dialog window.	181
4	File organization of the project folders.	183
5	Screenshot of WHAT v4.1.7-beta in Ubuntu-Linux 15.04 showing the <i>Download Data</i> tab.	185
6	Screenshot of WHAT v4.1.7-beta in Ubuntu-Linux 15.04 showing the <i>graphical interface</i> to the online CDCD database.	185
7	Screenshot of WHAT v4.1.7-beta in Ubuntu-Linux 15.04 showing the <i>Fill Data</i> tab.	187
8	Screenshot of WHAT v4.1.7-beta in Ubuntu-Linux 15.04 showing the <i>Fill data for station</i> section. For this setup, missing values in the datasets of the selected weather station (MARIEVILLE) would be filled for the 01/01/1980 to 31/12/2015 period.	188

9	Screenshot of WHAT v4.1.7-beta in Ubuntu-Linux 15.04 showing the <i>Advanced Settings</i> menu.	189
10	Screenshot of WHAT v4.1.7-beta in Ubuntu-Linux 15.04 showing the <i>Regression Model</i> menu.	190
11	Screenshot of WHAT v4.1.7-beta in Ubuntu-Linux 15.04 showing the <i>Advanced Settings</i> menu.	190

Liste des tableaux

Partie I Synthèse

3.1	Valeurs des paramètres hydrologiques utilisés pour la simulation des niveaux d'eau présentés dans les graphiques de la figure 3.2.	37
3.2	Plage de valeurs des paramètres hydrologiques utilisées pour l'estimation de la recharge.	40
3.3	Résumé des résultats de la validation croisée pour les 19 stations météorologiques situées en Montérégie Est pour la période 1980-2009.	45

Partie II Articles

Article 1

1	Published values for the properties used for the calculation of C_{soil} and k_{soil} with equations (2) and (3).	67
---	---	----

Article 2

1	Soil mass fraction of grain sizes (sand, silt, and clay) and Brooks-Corey model parameters for the 3 soil texture classes that were defined in SHAW for the production of synthetic temperature datasets.	85
2	Summary of SHAW modeling results for the 12 contexts considered. These contexts comprise two groups with weather conditions of Quebec and Toronto, respectively, each comprising three soil types (sand, loamy sand and sandy loam) and two land covers for each soil type (bare soil and grass). The table shows mean and range of the soil moisture saturation at the depth of 1 m, the maximum soil frost depth during the 20-year simulation, as well as annual groundwater recharge calculated from the hourly water fluxes at the bottom of the soil profile.	87

Article 3

1	List of model hydrological parameters and calibration ranges.	130
---	---	-----

Article 4

1	List of the 19 weather stations located in the study area along with their location coordinates (Lat. and Long.), elevation (Elev.), percentage of days with missing data, yearly averages for the 1980-2009 period, and mean and standard deviation (SD) for daily precipitation intensity. The mean, maximum, and minimum values for each column are also provided at the bottom. The four weather variables are daily minimum, mean, and maximum daily air temperatures (T_{\min} , T_{mean} , T_{\max}) and daily total precipitation (P_{tot}).	148
2	Results of the cross-validation procedure for the 19 weather stations located within the Montérégie Est study area for the 1980-2009 period. The Root-Mean-Square Error (RMSE), the Mean-Absolute Error (MAE), the Mean Error (ME) and the correlation coefficient (r) are given for each weather variable. The measured, predicted, and estimation error on the mean number of wet days per year ($P_{\text{tot}} > 0 \text{ mm/d}$) are also presented at the end. The minimum, mean, and maximum values for each column are provided at the bottom. The four weather variables are daily minimum, mean, and maximum daily air temperatures (T_{\min} , T_{mean} , T_{\max}) and daily total precipitation (P_{tot}).	153
3	The Root-Mean-Square Error (RMSE), Mean-Absolute Error (MAE), and Mean Error (ME) on daily precipitation are presented for limited ranges in increments of 10 mm/day. These values were computed using all the data pooled together from the 19 stations tested. Mean value and number of occurrences for each range is also presented.	155
4	Example of a weather data input file for weather station BONSECOURS located in Quebec, Canada. Missing data are represented by not-a-number (nan) values.	161
5	List of parameters for version 1.0 of PyGWD.	162
6	List of outputs for version 1.0 of PyGWD. The name of the different files are given for the BROME (7020840) weather station.	163

Première partie

Synthèse

Chapitre 1

Introduction

1.1 L'eau souterraine

Environ 71 % de la surface terrestre est recouverte d'eau, ce qui correspond à un volume d'environ 1386 millions de km³ ([Shiklomanov & Rodda, 2003](#)). De ce volume, seulement 2.53 % sont constitués d'eau douce, dont plus de 69 % sont stockés sous forme solide dans les glaciers, les neiges permanentes et le pergélisol. Environ 30 % sont constitués d'eau souterraine. Le reste de l'eau douce (moins de 1 %) est principalement stockée dans les eaux de surface et l'atmosphère (voir la [figure 1.1](#)). Ainsi, presque 99 % de toute l'eau douce disponible sur Terre sous forme liquide est constituée d'eau souterraine.

L'eau souterraine joue un rôle essentiel dans l'approvisionnement en eau des populations. Près de la moitié des besoins en eau potable dans le monde sont comblés par l'eau souterraine ([WWAP, 2015](#)). Au Canada, c'est près de 30 % de la population qui utilise l'eau souterraine pour leurs besoins domestiques ([Environnement et Changement climatique Canada, 2013](#)), alors qu'au Québec, elle sert à alimenter 20 % de la population sur près de 90 % du territoire habité ([Gouvernement du Québec, 2015](#)). L'eau souterraine est d'ailleurs la ressource en eau potable la plus économiquement accessible et la plus sollicitée au Québec, particulièrement en région rurale. En raison de son importance et des besoins croissants de la population en eau potable, une gestion responsable et durable de cette ressource est essentielle pour assurer le bien-être des générations futures.

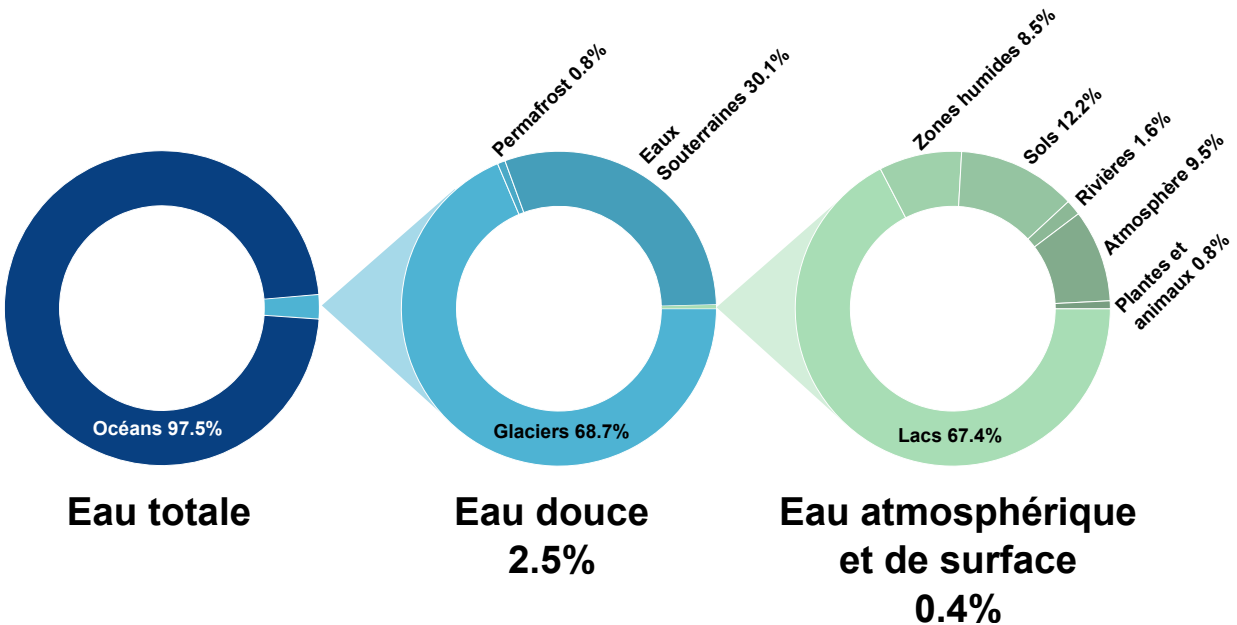


Figure 1.1 – Distribution mondiale de l'eau (adaptée de [UNESCO-WWAP, 2006](#)).

1.2 La recharge des eaux souterraines

La gestion de l'eau souterraine dans une optique de développement durable nécessite la connaissance des taux de recharge puisque celle-ci constitue un élément clé du bilan hydrique qu'il faut connaître pour ne pas surexploriter la ressource. De plus, la recharge joue un rôle important dans le débit des cours d'eau, dans la vulnérabilité des aquifères, dans l'écologie des tourbières (milieux humides) et peut avoir un impact sur certains facteurs socio-économiques ([Alley & Leake, 2004](#); [Sophocleous & Devlin, 2004](#); [Devlin & Sophocleous, 2005](#); [Healy, 2010](#)). La recharge est de plus un intrant important dans de nombreux simulateurs numériques qui sont de plus en plus utilisés pour la caractérisation des aquifères ([Sanford, 2002](#)).

La [figure 1.2](#) schématisse différents processus du cycle de l'eau généralement associés avec la recharge. La *recharge* est communément définie comme l'écoulement de l'eau à travers la zone non saturée et qui atteint la nappe d'eau souterraine ([Freeze & Cherry, 1979](#); [Lerner et al., 1990](#); [Healy, 2010](#)). On qualifie la recharge de “*diffuse*” lorsque cette dernière provient de précipitations qui sont distribuées sur une grande superficie et de “*localisée*” lorsqu'elle provient d'un réservoir d'eau de surface, tels que les rivières et les lacs ([Lerner et al., 1990](#); [Healy, 2010](#)). Cette thèse traite principalement des méthodes pour estimer la recharge diffuse des aquifères.

L'*infiltration* est définie comme le processus par lequel l'eau de surface (provenant des précipitations ou de réservoirs, tel que les rivières et les lacs) pénètre dans le sol. Le *drainage* (souvent considéré comme un terme équivalent à la percolation ou l'infiltration nette) est défini comme le processus par lequel l'eau s'écoule à travers la zone non saturée du sol, vers la nappe (Healy, 2010). Plusieurs méthodes existantes ne fournissent pas une estimation de la recharge proprement dite, mais évaluent plutôt l'infiltration ou encore le drainage. On dit alors que ces méthodes donnent une estimation de la *recharge potentielle*, car il n'est pas certain que toute l'eau infiltrée ou drainée atteigne la nappe. Par exemple, certains bilans hydriques quotidiens et les méthodes lysimétriques permettent généralement d'estimer des taux de recharge potentielle, alors que les méthodes basées sur des mesures de niveaux d'eau dans les puits permettent d'estimer une valeur de la recharge à la nappe.

À noter que la définition de la recharge donnée ci-dessus ne tient pas compte de la recharge des aquifères captifs provenant d'un écoulement d'eau à travers un aquitard. On parlera alors plutôt d'écoulement interaquifère.

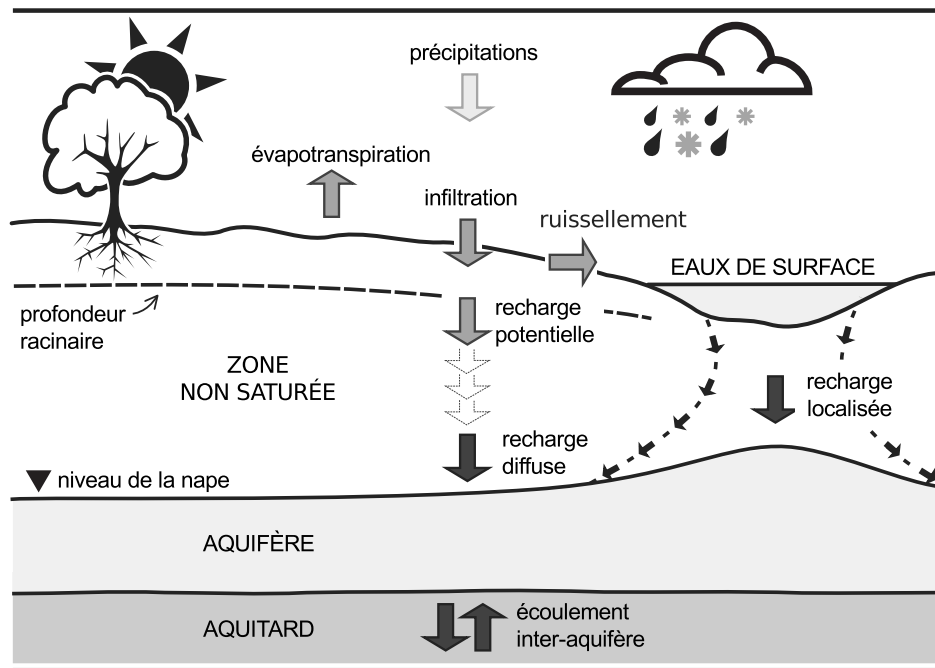


Figure 1.2 – Coupe verticale montrant l'infiltration à la surface du sol, le drainage à travers la zone non saturée (recharge potentielle), la recharge diffuse d'un aquifère à nappe libre provenant des précipitations, la recharge localisée du même aquifère sous un réservoir d'eau de surface et un flux d'eau à travers un aquitard (écoulement interaquifère) entre l'aquifère libre et un aquifère captif (situé sous l'aquitard, non montré sur la figure).

1.3 Méthodes d'estimation de la recharge

De nombreuses méthodes existent pour estimer la recharge, basées sur une grande variété de mesures indirectes, comme les niveaux d'eau dans les puits, les débits de rivières, les traceurs géochimiques et les mesures de températures. Scanlon *et al.* (2002) classent les différentes techniques existantes en trois groupes d'après la zone hydrogéologique où les données utilisées pour estimer la recharge ont été acquises: 1) eaux de surface, 2) zone non saturée et 3) zone saturée. Healy (2010) a adopté une classification similaire où les méthodes y sont regroupées plutôt selon le type de données à partir desquelles la recharge est calculée: 1) données relatives aux eaux de surface, 2) données physiques en zone non saturée et saturée, 3) données géochimiques et 4) données thermiques. Ces approches de classification sont intéressantes, car l'ensemble des méthodes appartenant à un même groupe partagent en général des limites d'application qui sont similaires. Entre autre, les méthodes basées sur des mesures provenant des eaux de surface et de la zone saturée sont plus utilisées dans les régions humides, alors que les techniques basées sur la zone non saturée sont en général mieux adaptées aux régions arides et semi-arides (Scanlon *et al.*, 2002).

Il n'existe toutefois pas de méthode universelle pour estimer la recharge. Les taux de recharge peuvent varier dans le temps et l'espace sur plusieurs ordres de grandeur selon le climat, la géologie, l'hydrologie, la topographie, la couverture végétale et un ensemble de facteurs anthropiques (de Vries & Simmers, 2002; Scanlon *et al.*, 2002; Gee *et al.*, 2009; Healy, 2010). Or, chaque méthode permet d'estimer des taux de recharge à l'intérieur d'une plage de valeurs limitée, avec des échelles d'applications spatiales et temporelles qui varient énormément d'une méthode à l'autre. Ceci est bien illustré sur les graphiques de la figure 1.3, tirés de Scanlon *et al.* (2002), qui présentent des plages plausibles pour les taux de recharge et les échelles d'application spatiales et temporelles de diverses méthodes d'estimation de la recharge.

Il est alors très important que les limites d'application des méthodes sélectionnées pour estimer la recharge permettent de répondre aux objectifs, aux limites financières et à la durée de l'étude. Par exemple, les méthodes basées sur des traceurs géochimiques naturels, tels que le chlore et le carbone, permettent d'obtenir une valeur moyenne de la recharge intégrée sur de longues périodes de temps (figure 1.3b). Ces méthodes ne conviendraient donc pas pour faire un suivi journalier, ou même saisonnier, de la recharge dans un objectif de gestion de la ressource. Toutefois, elles pourraient fournir des informations très utiles pour l'élaboration d'un modèle conceptuel d'écoulement

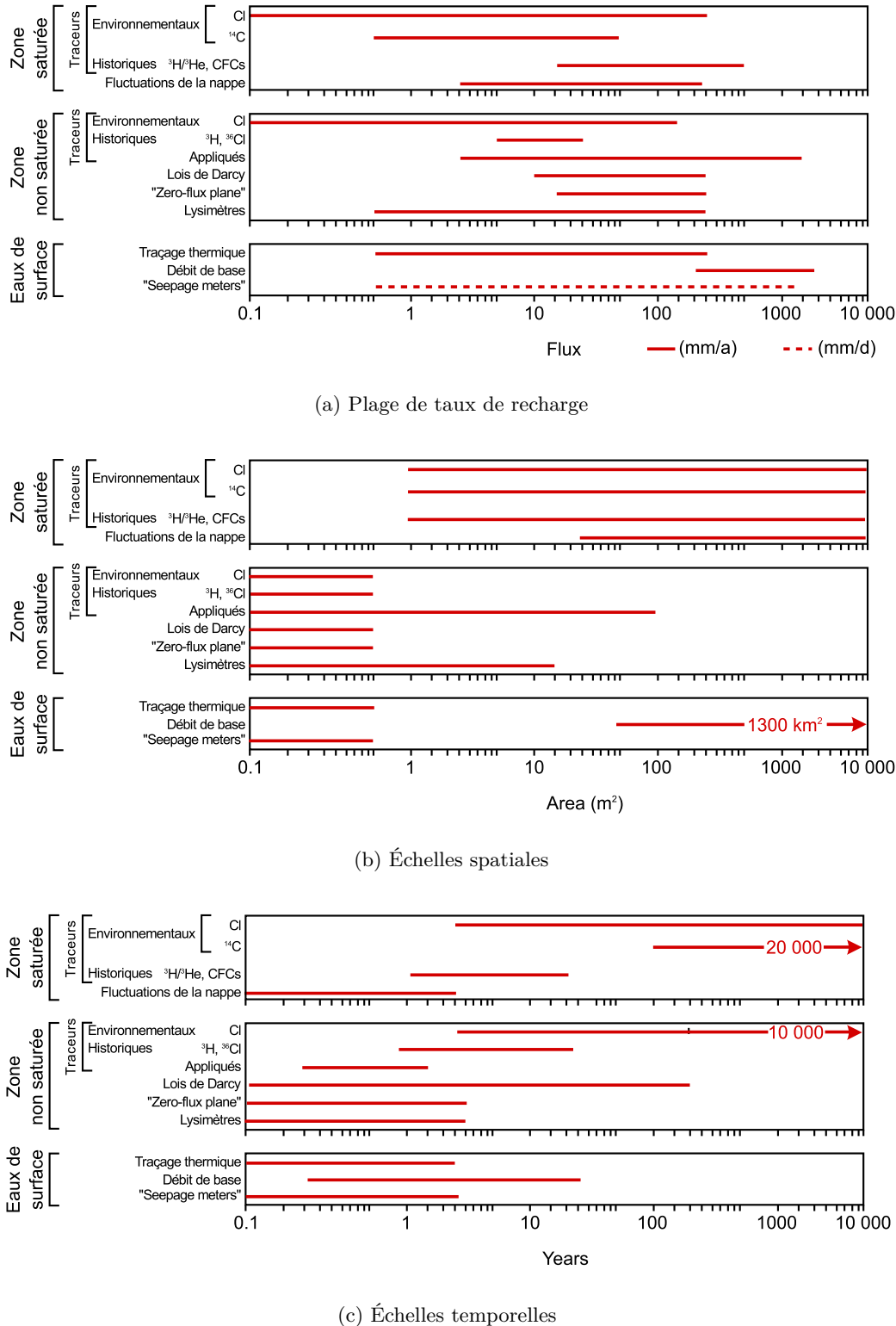


Figure 1.3 – Plages de taux de recharge, échelles spatiales et échelles temporelles pour lesquelles les estimations de recharge sont valides pour diverses techniques d'estimation. Les techniques qui permettent l'estimation de la recharge à l'échelle locale sont représentées par l'intervalle de 0 à 1 m^2 sur la figure 1.3b (adaptée de Healy & Cook, 2002).

à l'échelle régionale (e.g., [Carrier et al., 2013](#)). À l'inverse, les méthodes basées sur l'interprétation des fluctuations des niveaux de la nappe permettent d'estimer la recharge sur une échelle de temps très courte (jours à semaines). Toutefois, la durée sur laquelle les estimations peuvent être calculées est limitée par la quantité de données disponibles et par le fait même, par la durée du projet.

La sélection des méthodes pour estimer la recharge doit également tenir compte du contexte hydrogéologique étudié. Pour la majorité des méthodes existantes, la recharge est déduite de mesures indirectes par le biais de modèles mathématiques. Ces modèles reposent sur un ensemble d'hypothèses simplificatrices qui sont valides pour des conditions hydrogéologiques spécifiques. Par exemple, les méthodes basées sur le traçage thermique sont très utilisées pour caractériser la recharge localisée sous les lacs et les rivières ([Constantz, 2008](#)). Par contre, ces mêmes méthodes ne sont pas nécessairement adaptées pour estimer la recharge diffuse à partir de mesures acquises dans la zone non saturée (voir [chapitre 2](#)). Les hypothèses qui étaient alors valides pour la zone saturée ne le sont pas nécessairement pour la zone non saturée, car les mécanismes de transport de l'eau et de la chaleur ne sont plus les mêmes. Dans un même ordre d'idées, la méthode des fluctuations de la nappe repose sur l'hypothèse que les hausses du niveau de la surface libre de l'aquifère sont le résultat de flux épisodiques de recharge ([Healy & Cook, 2002](#)). Cette méthode n'est donc pas appropriée pour les contextes où les taux de recharge sont faibles et uniformément distribués dans le temps ni pour les contextes où la nappe est captive. L'estimation de la recharge avec des méthodes qui ne sont pas appropriées au contexte hydrogéologique étudié peut mener à des estimations complètement erronées de la recharge. C'est pourquoi une connaissance approfondie des limitations des méthodes utilisées est essentielle en vue de pouvoir caractériser l'incertitude sur l'estimation de la recharge et pouvoir déterminer judicieusement les limites d'application des méthodes pour éviter des erreurs d'estimation importantes.

1.4 Défis liés à l'estimation de la recharge

La recharge est une composante importante à évaluer dans les projets de caractérisation des aquifères, mais celle-ci est difficile à quantifier avec précision. Comme discuté à la section précédente, la recharge est presque toujours déduite de mesures indirectes, à l'aide de méthodes basées sur diverses hypothèses simplificatrices par rapport à la répartition dans le temps et l'espace, de même que sur les processus contrôlant la recharge. Puisque ces hypothèses ne permettent jamais de représenter

parfaitement la réalité, une incertitude importante et difficile à quantifier est généralement associée à toute estimation de la recharge ([Healy, 2010](#)). De plus, étant donné que la recharge ne peut généralement pas être mesurée directement *in situ*, les estimations ne peuvent pas être comparées à des valeurs de référence afin de valider et quantifier l'incertitude des méthodes utilisées.

Puisque la majorité des incertitudes ne peuvent généralement pas être quantifiées, il est recommandé d'utiliser plusieurs méthodes pour évaluer la recharge afin d'accroître le niveau de confiance des estimations obtenues ([de Vries & Simmers, 2002](#); [Scanlon *et al.*, 2002](#); [Healy, 2010](#)). Cette recommandation semble en général avoir été acceptée d'emblée par la communauté scientifique. En effet, le nombre d'études scientifiques réalisées depuis les années 2000 dont l'objectif principal était de comparer les résultats de différentes méthodes existantes pour estimer la recharge est impressionnant (e.g. [Grismer *et al.*, 2000](#); [Arnold *et al.*, 2000](#); [Timlin *et al.*, 2003](#); [Goodrich *et al.*, 2004](#); [Coes *et al.*, 2007](#); [Delin *et al.*, 2007](#); [Heppner *et al.*, 2007](#); [Risser *et al.*, 2009](#); [Sibanda *et al.*, 2009](#); [Obiefuna & Orazulike, 2011](#); [Yin *et al.*, 2011](#); [Aurand & Thamke, 2014](#); [Rivard *et al.*, 2014](#); [Huet *et al.*, 2015](#); [Ringleb *et al.*, 2015](#)).

Cependant, l'application de plusieurs méthodes ne résout pas tous les problèmes relatifs à l'évaluation précise de la recharge des eaux souterraines. Bien que cette approche permette d'augmenter qualitativement le niveau de confiance des estimations obtenues, elle ne permet toutefois pas de réduire ni de quantifier l'incertitude sur la recharge. De plus, l'application de plusieurs méthodes pour estimer la recharge n'est pas toujours possible, en raison par exemple, de contraintes financières ou des échéanciers des projets. Ainsi, l'estimation de la recharge est souvent faite à l'aide de méthodes conventionnelles, telle que la méthode des fluctuations de la nappe basée sur des mesures du niveau des eaux souterraines dans les puits ([Healy & Cook, 2002](#)) ou la méthode des bilans hydrologiques de surface basée sur des données météorologiques facilement disponibles ([Rushton *et al.*, 2006](#)). Même lorsqu'il est possible d'appliquer des méthodes plus complexes (par exemple dans [Croteau *et al.*, 2010](#); [Carrier *et al.*, 2013](#)), la comparaison des résultats avec ceux obtenus à partir d'approches plus simples, dont les limites d'application sont bien connues, est toujours bénéfique et est une pratique qui devrait toujours être encouragée. De plus, la mise à jour sur une base régulière des estimations de la recharge obtenues avec des modèles complexes demande des efforts et des ressources parfois considérables qui ne sont pas toujours possibles. Or, la mise à jour des taux de recharge, qui peuvent être affectés par des changements au niveau du climat ou de l'utilisation du sol par exemple, est un aspect important à considérer dans une optique de gestion durable de la ressource.

Les progrès des dernières décennies en électronique ont mené à la conception de capteurs de données de plus en plus performants et munis d'enregistreurs électroniques autonomes. Cela a permis de faciliter grandement l'acquisition en continu de plusieurs types de mesures pouvant être utilisées pour calculer des taux de recharge. Par exemple, le suivi journalier et même horaire du niveau d'eau dans les puits d'observation peut désormais être fait aisément et de façon abordable grâce à des sondes à pressions autonomes équipées d'un enregistreur de données électronique ([Freeman et al., 2004](#)). De même, de nombreuses sondes thermiques permettent maintenant de mesurer précisément et en quasi-continu des profils verticaux de température dans le sol ou dans des puits d'observation ([Stonestrom & Constantz, 2003](#)). Enfin, des mesures dans le temps de l'humidité du sol dans la zone non saturée, conjointement avec des mesures de température, peuvent maintenant être facilement acquises grâce à des sondes TDR (Time Domain Reflectometry, e.g. [Decagon Devices, 2010](#)). Toutefois, l'interprétation des séries temporelles de données pour estimer des taux de recharge est souvent faite à l'aide de modèles analytiques ou par des approches graphiques dans plusieurs méthodes conventionnelles. Or, ces techniques ne permettent généralement pas d'exploiter pleinement toute l'information contenue dans les données disponibles. Elles sont parfois subjectives, sujettes aux erreurs et laborieuses à utiliser lorsque la quantité de données à analyser est importante.

Il y a donc un intérêt pratique et scientifique à améliorer les méthodes d'estimation de la recharge qui sont simples d'application et basées sur des données facilement disponibles. Entre autres, il est nécessaire d'incorporer des techniques modernes d'assimilation des données et de développer des approches permettant de mieux évaluer l'incertitude de ces méthodes. Dans une optique de gestion durable de la ressource, il est également nécessaire de développer des méthodes qui ne permettent pas uniquement de fournir un portrait statique de la recharge en un temps donné, mais qui permettent de faire un suivi et même de prédire la recharge dans le temps. Cette thèse de doctorat traite de ces aspects pour deux méthodes d'estimation de la recharge. La première méthode est basée sur le traçage thermique dans la zone thermique superficielle du sol (0 à 15 m) et permet d'estimer des taux de recharge potentielle à partir de mesures temporelles de la température du sol. La seconde consiste à combiner la méthode des bilans hydrologiques de surface avec celle des fluctuations de la nappe pour estimer des taux de recharge quotidiens à partir de mesures journalières des précipitations totales, de la température de l'air et du niveau de l'eau souterraine. Le contexte et les avantages et limitations spécifiques à chacune des deux méthodes étudiées sont présentés aux [sections 1.5](#) et [1.6](#).

1.5 Traçage thermique

Le premier volet de cette thèse de doctorat traite de l'estimation de la recharge à partir de séries temporelles de températures mesurées dans la zone thermique superficielle du sol (0 à 15 m), en conditions non saturées, pour un climat froid et humide. Une synthèse des travaux réalisés dans le cadre de ce volet du doctorat est présentée au [chapitre 2](#).

La [figure 1.4](#) montre que le système thermodynamique de sous-surface peut être divisé en une zone superficielle et une zone géothermique ([Parsons, 1970](#)). La zone superficielle est située près de la surface et se caractérise par des variations mesurables de la température du sol en réponse aux cycles journaliers et saisonniers du bilan thermique de surface (variations de la température de l'air, de l'ensoleillement, de la couverture végétale, etc.). L'effet du cycle journalier sur les températures de sous-surface est perceptible jusqu'à 0.1 à 0.3 m de profondeur et jusqu'à 10 à 15 m pour le cycle saisonnier ([Healy, 2010](#)). La zone géothermique est située sous la zone superficielle et est caractérisée par un gradient vertical de température (augmentation d'environ 1 °C par tranche de 20 à 40 m) qui n'est pas influencé de façon significative par les variations annuelles du climat ([Anderson, 2005](#)).

Il est reconnu depuis longtemps dans le domaine de l'hydrogéologie que l'eau circulant dans le sol transporte de la chaleur qui affecte les températures du sol ([Anderson, 2005; Healy, 2010; Rau *et al.*, 2014](#)). La [figure 1.4](#) schématisé l'impact que pourrait produire un écoulement vertical d'eau vers le bas (recharge) ou vers le haut (résurgence) sur les profils verticaux de températures maximales et minimales dans le sol. Les lignes continues et pointillées représentent les profils de température sans et avec un écoulement d'eau respectivement. Par conséquent, les hydrogéologues se sont intéressés depuis les années 1960 à l'utilisation de la chaleur comme traceur naturel pour caractériser qualitativement et quantitativement le mouvement des eaux souterraines (ex.: [Suzuki, 1960; Stallman, 1963, 1965; Bredehoeft & Papadopoulos, 1965](#)). La chaleur est d'ailleurs un traceur naturel qui est bien adapté à l'étude des eaux souterraines pour plusieurs raisons: 1) elle présente un signal dynamique naturel; 2) la théorie du transport couplé de l'eau et de la chaleur est connue depuis longtemps; 3) la température est facilement mesurable à des coûts très abordables et 4) les analyses thermiques peuvent être réalisées avec des outils simples et accessibles ([Anderson, 2005; Healy, 2010](#)).

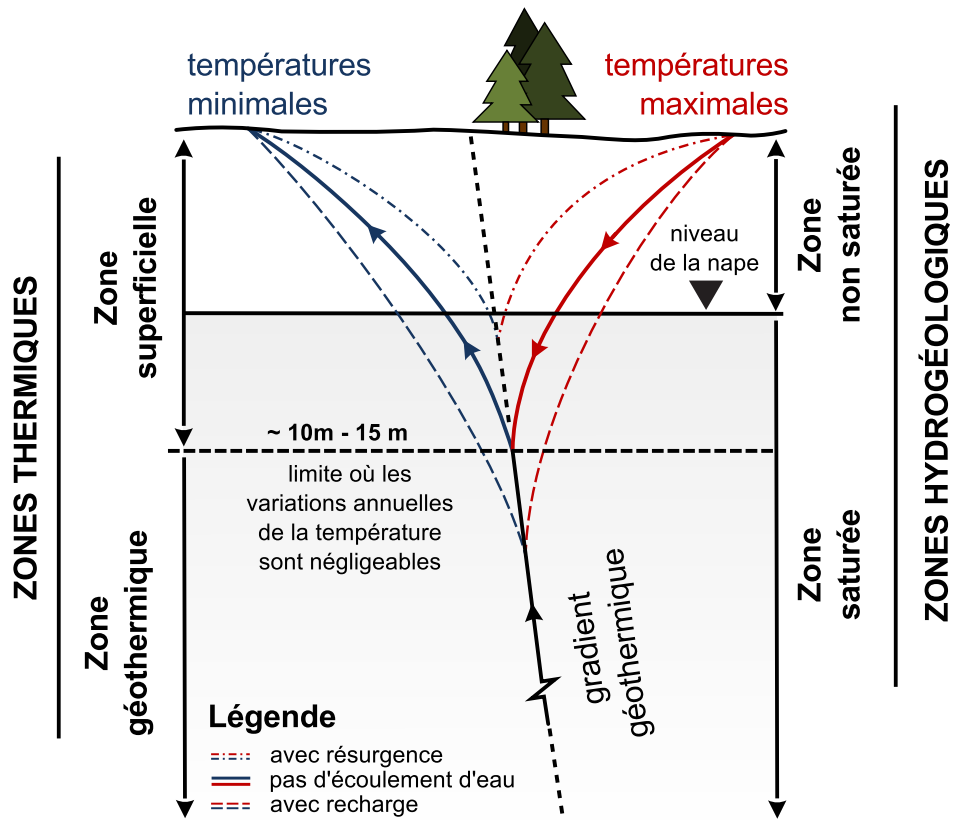


Figure 1.4 – Profils hypothétiques verticaux des températures minimales et maximales dans le sol. L’effet d’un flux de recharge ou de résurgence des eaux souterraines sur les profils de températures est également illustré par des lignes pointillées. Le schéma montre des profondeurs typiques des zones thermiques superficielle et géothermique et des zones hydrogéologiques saturée et non saturée pour un climat humide.

Théoriquement, il est possible de calculer le flux d’écoulement vertical de l’eau à partir de mesures de la température du sol par l’inversion d’un modèle de transport advectif-conductif de la chaleur. À ce titre, Suzuki (1960) et Stallman (1963, 1965) ont été les premiers à utiliser des mesures de températures du sol pour estimer le flux d’écoulement vertical de l’eau souterraine sous des rizières inondées. Leur méthode était basée sur le calage d’une solution analytique de l’équation du transport vertical de la chaleur par advection et conduction à des séries temporelles de températures acquises dans la zone thermique superficielle. Leur solution était valide pour un flux d’écoulement constant à travers un milieu poreux semi-infini et homogène borné en surface par une variation de température sinusoïdale. Parallèlement aux travaux de Suzuki (1960) et Stallman (1963, 1965), Bredehoeft & Papadopoulos (1965) ont présenté une méthode pour estimer le flux d’écoulement vertical de l’eau souterraine dans des couches géologiques semi-confinantes à partir de profils verticaux de températures acquis dans la zone géothermique. Les études mentionnées ci-dessus

ont permis de développer les bases théoriques en hydrogéologie pour l'étude des écoulements de l'eau souterraine à l'aide de mesures de températures de sous-surface.

L'approche présentée par [Stallman \(1965\)](#) a par la suite été largement utilisée pour évaluer l'écoulement des eaux souterraines sous les lacs, les rivières et les zones inondées (ex.: [Lapham, 1989](#); [Taniguchi, 1993](#); [Silliman *et al.*, 1995](#); [Stonestrom & Constantz, 2003](#); [Baskaran *et al.*, 2009](#); [Vandenbohede & Lebbe, 2010a](#)). En revanche, les travaux ayant utilisé les mesures thermiques pour estimer des taux de la recharge naturelle diffuse sont très rares. Les quelques études ayant porté sur ce sujet ont obtenu un succès limité (ex.: [Taniguchi, 1994](#); [Tabbagh *et al.*, 1999](#); [Koo & Kim, 2008](#)). Les résultats de quelques études réalisées dans la zone saturée suggèrent que l'incertitude sur les estimations obtenues avec les techniques basées sur le traçage thermique pourrait être importante (ex.: [Vandenbohede & Lebbe, 2010a,b](#); [Shanafield *et al.*, 2011](#); [Soto-López *et al.*, 2011](#)). Ceci pourrait expliquer les difficultés qui semblent exister quant à l'utilisation de la température pour estimer la recharge naturelle diffuse et comme outil de caractérisation dans les études hydrogéologiques en général ([Anderson, 2005](#); [Healy, 2010](#)).

1.6 Bilans hydrologiques combinés

Le second volet de la thèse porte sur l'estimation de la recharge sur une base quotidienne avec des mesures dans le temps du niveau de l'eau souterraine, de la température de l'air et des précipitations totales. Une synthèse des travaux réalisés dans le cadre de ce volet du doctorat est présentée au [chapitre 3](#).

L'estimation de la recharge par une approche basée sur des mesures de niveaux d'eau dans les puits revêt un intérêt particulier pour les études de caractérisation des aquifères libres pour de multiples raisons: 1) il existe un nombre important de puits d'observation résidentiels, municipaux et gouvernementaux qui peuvent être utilisés pour l'acquisition de ces données; 2) l'apparition durant les années 1990 de technologies (capteurs de pression et enregistreurs de données électroniques) permettant une mesure automatisée des niveaux d'eau dans les puits a rendu ce type de mesures très accessibles ([Freeman *et al.*, 2004](#)); 3) les estimations de la recharge basées sur des niveaux d'eau dans les puits peuvent être représentatives d'une superficie allant de plusieurs mètres à quelques centaines de mètres carrés (voir [figure 1.3b](#)).

Il est possible d'évaluer la recharge à partir de mesures temporelles du niveau de l'eau souterraine avec la méthode des fluctuations de la nappe (WTF: Water Table Fluctuation). Cette technique a été introduite dans les années 1920 et a depuis été largement utilisée dans de nombreuses études (Healy & Cook, 2002). Elle est basée sur la résolution d'un bilan en eau d'un aquifère libre et nécessite une connaissance de la porosité de drainage de l'aquifère. En général, l'application de la méthode consiste à interpréter graphiquement les hausses du niveau d'eau liées aux épisodes de recharge (ex.: Rasmussen & Andreasen, 1959). Plus précisément, la recharge est estimée en multipliant la porosité de drainage de l'aquifère par la différence entre le pic d'une hausse du niveau de l'eau en réponse aux précipitations et le point sur la courbe de récession extrapolée jusqu'au moment du pic (voir figure 1.5). Cette pratique peut toutefois être subjective, prend du temps, et n'est pas adaptée à un grand réseau de puits d'observation où les niveaux des eaux souterraines sont mesurés sur une base quotidienne (ou plus) avec des capteurs de pression automatiques. Pour cette raison, des efforts ont été faits au cours des dernières années pour automatiser cette méthode en utilisant une courbe maîtresse de récession (ex.: Heppner & Nimmo, 2005; Posavec *et al.*, 2006). Une des difficultés majeures dans l'application de la méthode WTF consiste à estimer la valeur de la porosité de drainage de l'aquifère avec précision (Healy & Cook, 2002). Cela est particulièrement vrai pour les milieux fracturés qui sont généralement caractérisés par des porosités de drainage faibles auxquelles sont associées une erreur relative importante.

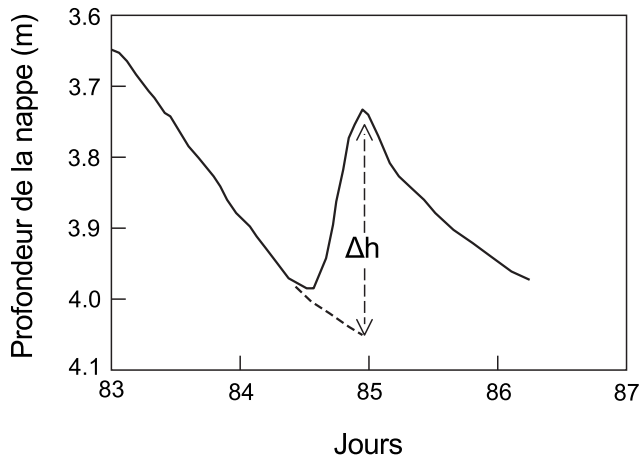


Figure 1.5
Variation hypothétique du niveau d'eau dans un puits d'observation en réponse aux précipitations. La dimension Δh correspond à la différence entre le pic de la remontée du niveau d'eau et le point sur la courbe de récession extrapolée jusqu'au moment du pic (adapté de Healy, 2010).

La recharge peut également être estimée à partir de mesures quotidiennes de la température de l'air et des précipitations totales avec un bilan hydrologique de surface (SMB: Soil Moisture Balance) (ex.: Rushton, 2003; Rushton *et al.*, 2006). Puisque de nombreux pays maintiennent des

bases de données météorologiques depuis plusieurs décennies, cette technique est largement utilisée et peut facilement être appliquée en début de projet, ce qui représente un avantage considérable de la méthode. Cependant, l'application de cette technique pour l'estimation précise de la recharge n'est pas sans difficulté. Premièrement, les séries temporelles de données météorologiques sont, la plupart du temps, incomplètes. Combler les lacunes dans les jeux de données météorologiques est une tâche complexe qui peut nécessiter beaucoup de temps. Cette tâche est particulièrement difficile pour les précipitations quotidiennes en raison de leur grande variabilité spatiale et temporelle ([Simolo et al., 2010](#)). Cette problématique est abordée en détail à l'[article 4](#) de la thèse qui présente un algorithme qui a été développé dans le cadre de ce doctorat pour estimer et combler automatiquement les valeurs manquantes dans les séries temporelles de données météorologiques. Deuxièmement, bien que le calcul de la recharge à partir d'un bilan hydrologique de surface soit plutôt simple, une incertitude relativement importante est généralement associée aux divers paramètres du modèle (comme le coefficient de ruissellement, la capacité au champ du sol, la profondeur racinaire, le coefficient de fonte de la neige), de sorte que les taux de recharge estimés peuvent être aussi très incertains.

Un des problèmes majeurs qui est commun aux deux approches présentées ci-dessus est qu'il est très difficile de contraindre les méthodes avec des données observées et de quantifier l'incertitude sur les estimations de la recharge. Dans le cas de la méthode WTF, la recharge est estimée à partir des mesures de niveaux d'eau et il est très difficile de valider les résultats obtenus. La recharge potentielle peut être mesurée directement avec différents types de lysimètres, mais ces mesures sont le plus souvent représentatives de l'échelle locale et ne sont pas toujours comparables aux estimations obtenues avec la méthode WTF qui donne des valeurs de recharge représentatives de superficies pouvant aller jusqu'à plusieurs centaines de mètres carrés (voir [figure 1.3b](#)). La situation est similaire avec la méthode des bilans hydrologiques de surface. Par exemple, des mesures de teneur en humidité du sol peuvent être utilisées pour contraindre les paramètres du bilan hydrologique de surface. Cependant, ces mesures acquises dans la zone non saturée sont généralement représentatives de l'échelle locale ([Healy, 2010](#)) et ne sont donc pas idéales pour l'estimation de la recharge à de plus grandes échelles, ce qui est souvent requis dans les études de caractérisation des eaux souterraines.

Pour répondre à cette problématique, il a été proposé dans la littérature scientifique de combiner les méthodes WTF et SMB. [Baalousha \(2005\)](#) a appliqué la méthode proposée par [Bredenkamp et al. \(1995\)](#) pour estimer la recharge dans la bande de Gaza en combinant des données météorologiques à des mesures de niveau d'eau. [Lefebvre et al. \(2011\)](#) ont par la suite adapté la méthode à des

conditions climatiques tempérées continentales. Le principe de la méthode est 1) d'estimer des taux quotidiens de recharge avec la méthode SMB et 2) calculer les variations du niveau des eaux souterraines correspondantes en utilisant la porosité de drainage de l'aquifère libre. La méthode tient également compte de la récession du niveau des eaux souterraines pendant les périodes où la recharge est négligeable. Les paramètres hydrologiques sont par la suite optimisés par le calage des niveaux d'eau simulés à ceux mesurés dans le puits. Similairement, [Mackay et al. \(2014b\)](#) ont présenté le modèle AquiMod ([Mackay et al., 2014a](#)) permettant de reproduire les variations des eaux souterraines à partir de données météorologiques. Ils ont également utilisé leur modèle pour faire la prévision saisonnière du niveau de l'eau souterraine ([Mackay et al., 2015](#)). Bien que leur étude ne visait pas à estimer la recharge, celle-ci aurait pu être évaluée à partir de leur modèle, car elle est calculée comme variable interne. L'[article 3](#) de cette thèse s'appuie sur les études mentionnées ci-dessus et présente une approche originale permettant de combiner les méthodes WTF et SMB pour estimer la recharge et également quantifier l'incertitude sur les valeurs obtenues.

1.7 Objectifs du doctorat

Dans la perspective décrite à la [section 1.4](#), cette thèse de doctorat traite de deux méthodes d'estimation de la recharge qui sont simples d'application et basées sur des données facilement disponibles ou faciles à acquérir. Les objectifs des travaux de recherche sont 1) de mieux caractériser l'incertitude et les limites d'application de chacune des méthodes, 2) d'incorporer des techniques modernes d'assimilation des données et 3) d'adapter les méthodes aux contextes climatiques et hydrogéologiques retrouvés au Canada.

1.7.1 Sous objectifs du volet sur le traçage thermique

Les objectifs spécifiques à la méthode d'estimation de la recharge basée sur le *traçage thermique* dans le sol étaient de:

1. Développer une approche adaptée à la zone non saturée et à un climat froid et humide;
2. Évaluer l'incertitude de la méthode à partir de données synthétiques de température et d'humidité du sol représentatives d'un climat froid et humide.

1.7.2 Sous objectifs du volet sur les bilans hydrologiques combinés

Les objectifs spécifiques à la méthode des *bilans hydrologiques combinés* étaient de:

1. Développer un algorithme de programmation permettant de combler les données manquantes de façon automatisée dans les séries journalières de données météorologiques;
2. Améliorer le modèle conceptuel présenté par [Lefebvre et al. \(2011\)](#) et adapter la méthode de façon à ce que le calage des niveaux d'eau simulés aux valeurs mesurées soit automatisé;
3. Intégrer une méthode automatisée pour définir la courbe maîtresse de récession à partir de l'hydrogramme de puits;
4. Développer une méthodologie permettant de quantifier l'incertitude sur les estimations;
5. Implémenter la méthode dans le langage de programmation Python;
6. Développer une interface graphique couvrant toutes les étapes pour l'application de la méthode, incluant: a) le téléchargement et la mise en forme des données météorologiques disponibles sur le site internet du gouvernement du Canada, b) l'estimation automatisée des données manquantes dans les séries journalières de données météorologiques, c) le traçage des hydrogrammes de puits avec les données météorologiques dans un format facilitant l'interprétation visuelle des données, d) l'estimation de la courbe maîtresse de récession à partir des données de niveaux d'eau, e) l'estimation de la recharge en combinant les données météorologiques et les données de niveau d'eau et f) l'estimation de l'incertitude avec la méthode GLUE (Generalized Likelihood Uncertainty Estimation).

Chapitre 2

Traçage thermique

Le travail pour ce volet de la thèse a été réalisé en deux étapes. La première étape a consisté en une étude préliminaire pour estimer la sensibilité des températures de sous-surface à l'écoulement vertical de l'eau à travers la zone non saturée pour trois cas théoriques simples. Les travaux réalisés au cours de cette étape ont été publiés dans le compte-rendu de la conférence *GeoHydro2011* qui s'est tenue à Québec en 2011 ([Gosselin et al., 2011](#)). Une version révisée de ce compte-rendu de conférence est présentée à l'[article 1](#) de la thèse. Un survol de ces travaux est présenté à la [section 2.1](#) ci-dessous.

La seconde étape s'est appuyée sur les conclusions de l'étape 1 afin de développer une approche, adaptée à un climat froid et humide, pour estimer la recharge à partir de séries temporelles de température mesurées dans la zone non saturée. La méthode a été testée avec plusieurs jeux de données synthétiques réalistes de la température et de l'humidité du sol et l'incertitude de la méthode a été estimée par une étude de sensibilité. Les travaux réalisés dans le cadre de cette étape de l'étude ont fait l'objet d'un article scientifique qui a été publié dans la revue *Journal of Hydrology* ([Gosselin et al., 2016b](#)). Une version de cet article, tel que soumis à la revue, est présentée à l'[article 2](#) de la thèse et un survol des travaux est présenté à la [section 2.2](#) de ce chapitre.

2.1 Travaux préliminaires

Cette étude préliminaire a été réalisée suite à un travail pratique sur des séries temporelles de températures du sol acquises dans la zone non saturée d'un aquifère sableux deltique de la région

de Portneuf lors d'une étude de caractérisation hydrogéologique de [Fagnan et al. \(1999\)](#). L'approche analytique de [Stallman \(1965\)](#) avait alors été utilisée pour interpréter les données de température dans le but d'estimer des valeurs de la recharge annuelle. Les résultats obtenus étaient peu probants et n'étaient pas constants d'une année à l'autre. Il a alors été décidé de faire une étude de sensibilité afin de mieux comprendre l'impact réel de la recharge diffuse sur les températures de sous-surface avec des cas théoriques simples.

2.1.1 Méthodologie

Dans un premier temps, le simulateur numérique du transport vertical de la chaleur par advection et conduction présenté par [Keshari & Koo \(2007\)](#) a été implémenté dans le langage de programmation *Scilab* (www.scilab.org). Le simulateur numérique a ensuite été validé par rapport à la solution analytique de [Stallman \(1965\)](#).

Un modèle de transport de la chaleur pour une colonne de sol homogène a par la suite été développé dans le simulateur. Le modèle a été contraint à sa limite supérieure par une variation sinusoïdale de la température caractérisée par une période de 365 jours, une amplitude de 8 °C et une valeur moyenne de 12 °C. À la base de la colonne, la température a été fixée à une valeur constante de 12 °C. Ces valeurs ont été établies d'après le relevé de température atmosphérique présenté par [Bendjoudi et al. \(2005\)](#) pour une station météorologique située en France. La limite supérieure du modèle a été fixée à une profondeur de 0.5 m sous la surface de façon à être sous la zone racinaire et à pouvoir négliger les effets de chaleur latente dus à l'évaporation dans la couche superficielle du sol. La limite inférieure du modèle a été établie à une profondeur de 15 m sous la surface, où les variations annuelles de température à la surface du sol n'ont plus d'effet sur la température du sol.

Trois scénarios théoriques ont par la suite été définis permettant de représenter différentes distributions de la recharge mensuelle au cours d'une année. La distribution de la recharge mensuelle pour chacun de ces trois scénarios est présentée à la [figure 2.1](#). Chacun des trois scénarios était caractérisé par une recharge annuelle totale de 400 mm/a, répartie différemment entre les mois de l'année. Le premier scénario était caractérisé par une recharge mensuelle constante, le second par une recharge nulle durant l'été et l'hiver et le troisième par une recharge importante au printemps, modérée à l'automne et nulle durant l'été et l'hiver. Les scénarios de recharge mensuelle sont décrits plus en détail à la [section 3.2](#) de l'[article 1](#).

Des simulations du transport advectif et conductif de la chaleur ont ensuite été réalisées sur une période de 365 jours pour chacun des scénarios. Une simulation additionnelle a également été réalisée pour un cas où la recharge avait été fixée à zéro dans le modèle. Les températures simulées pour chacun des scénarios ont par la suite été comparées avec celles du scénario avec un flux de recharge nul afin d'évaluer l'impact de la recharge sur les températures du sol. Les résultats sont présentés aux figures 2.2 à 2.4

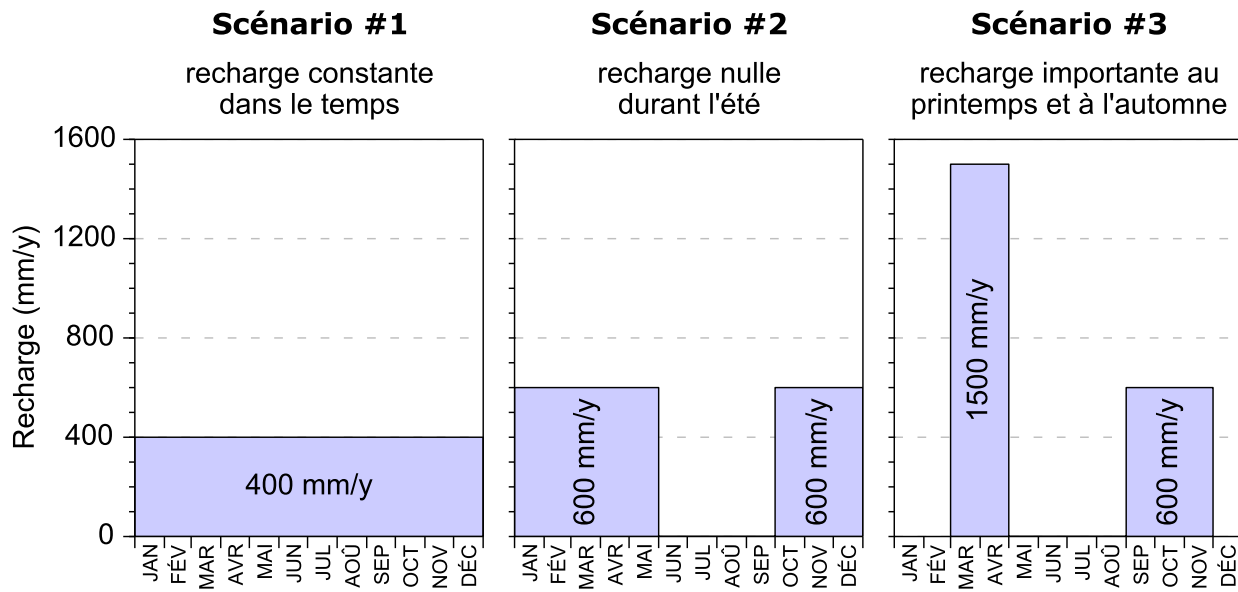


Figure 2.1 – Répartitions mensuelles de la recharge imposées pour les scénarios #1 à #3. Les 3 scénarios ont une recharge annuelle équivalente à 400 mm/a.

2.1.2 Discussion des résultats

Les résultats de ces travaux préliminaires ont d'abord permis d'établir que l'approche analytique de Stallman (1965) n'était pas bien adaptée pour l'estimation de la recharge dans la zone non saturée. Pour le premier scénario (recharge mensuelle constante), la déformation du signal thermique par la recharge correspond à une parfaite sinusoïde. À l'opposé, les résultats pour les deux autres cas (recharges mensuelles non uniformes) montrent une déformation non symétrique du cycle annuel des températures de sous-surface.

Or, la solution analytique de Stallman (1965) permet de simuler seulement des variations sinusoïdales de température, en conditions d'écoulement permanent, sur une base annuelle. Ces résultats suggèrent donc que cette approche n'est pas appropriée pour des applications en zone non saturée pour un climat froid et humide, où le flux d'écoulement mensuel et même hebdomadaire peut varier de façon importante au courant de l'année. L'utilisation d'un modèle numérique serait alors plus adéquate pour l'application de la méthode dans ces conditions et ne serait pas limitée à la résolution du flux de recharge potentielle sur une base annuelle.

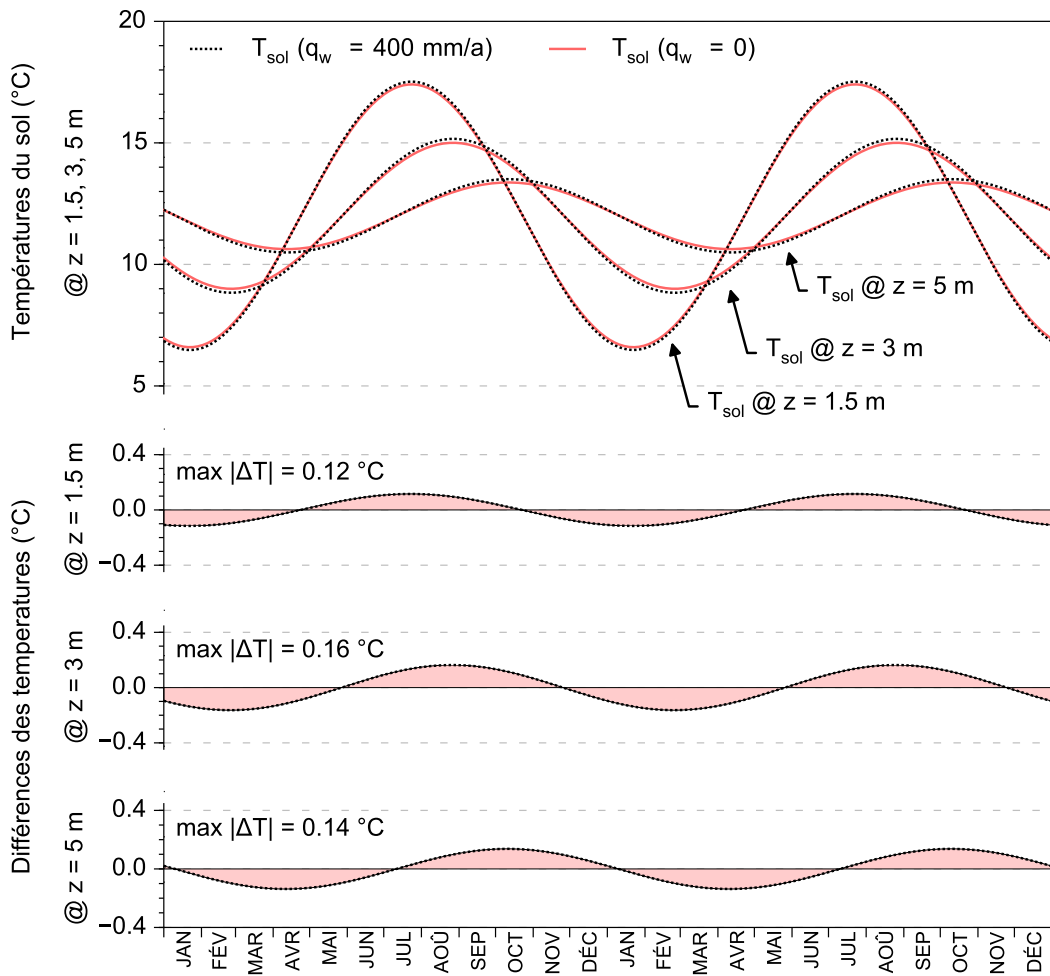


Figure 2.2 – Résultats pour le scénario #1: recharge constante dans le temps. [HAUT] Températures modélisées à des profondeurs de 1.5, 3 et 5 m pour le scénario #1 (pointillés noirs) et pour le scénario avec une recharge nulle (lignes rouges pleines). **[BAS]** Différences entre les températures simulées pour le scénario #1 et le scénario avec une recharge nulle.

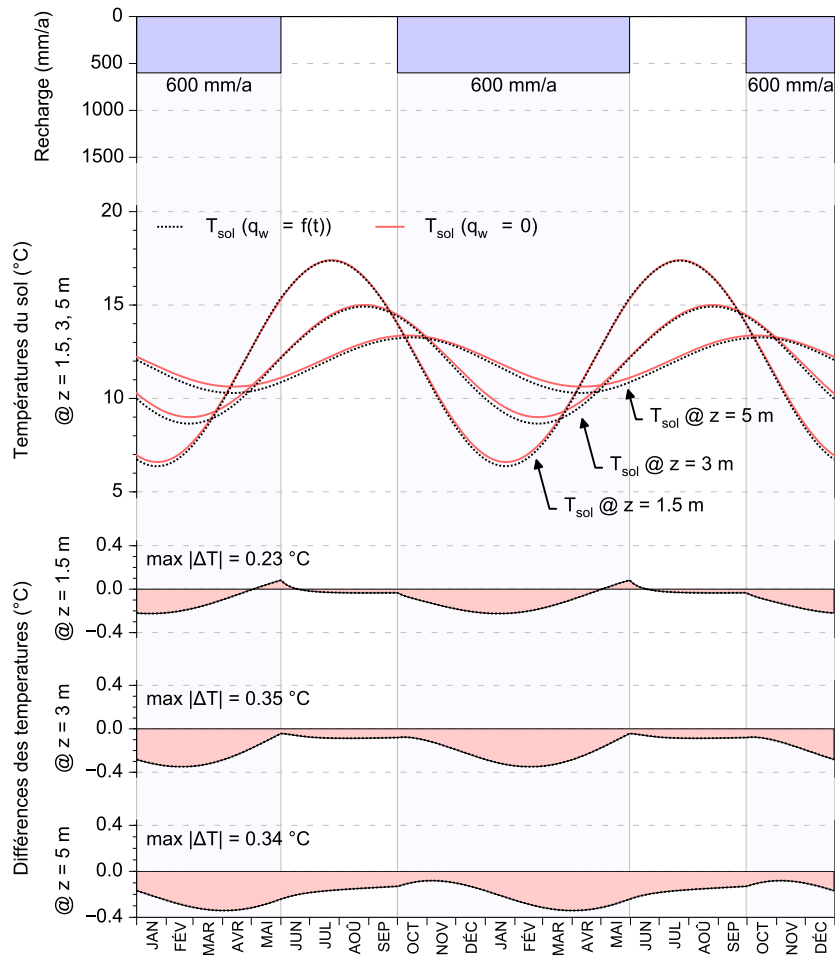


Figure 2.3 – Résultats pour le scénario #2: recharge nulle durant l’été. [HAUT] Distribution mensuelle de la recharge pour le scénario #2. [MILIEU] Températures modélisées à des profondeurs de 1.5, 3 et 5 m pour le scénario #2 (pointillés noirs) et pour le scénario avec une recharge nulle (lignes rouges pleines). [BAS] Différences entre les températures simulées pour le scénario #2 et le scénario avec une recharge nulle.

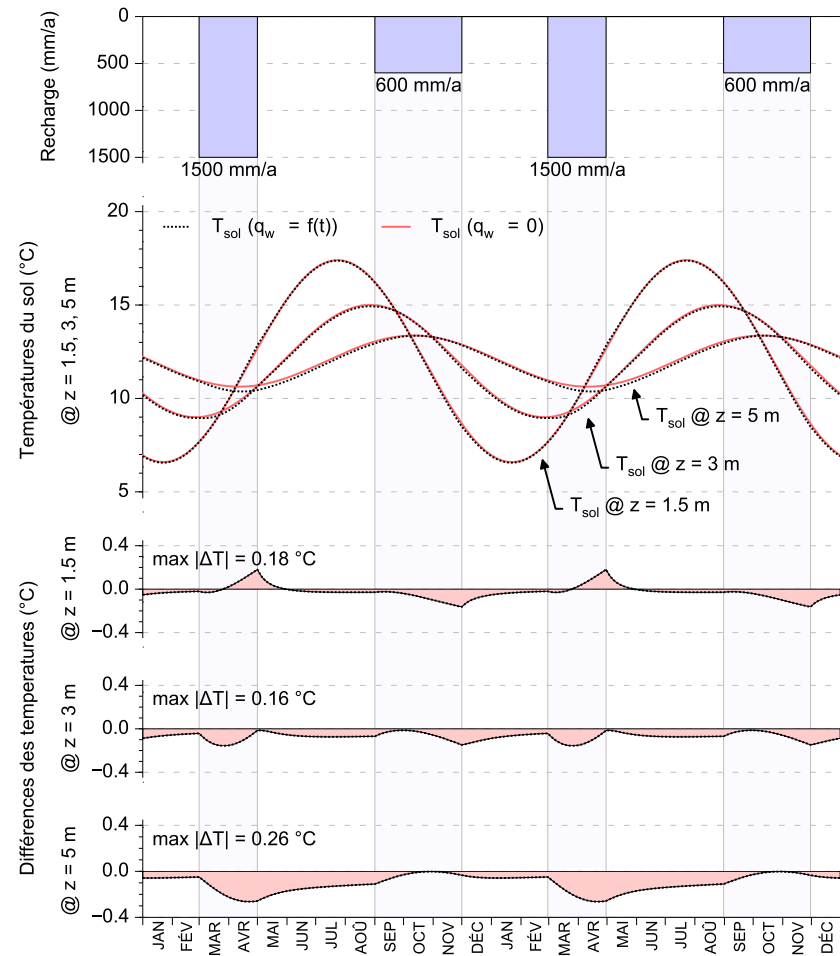


Figure 2.4 – Résultats pour le scénario #3: recharge importante au printemps et à l’automne. [HAUT] Distribution mensuelle de la recharge pour le scénario #3. [MILIEU] Températures modélisées à des profondeurs de 1.5, 3 et 5 m pour le scénario #3 (pointillés noirs) et pour le scénario avec une recharge nulle (lignes rouges pleines). [BAS] Différences entre les températures simulées pour le scénario #3 et le scénario avec une recharge nulle.

De plus, les résultats ont permis de souligner que l'impact du flux d'écoulement de l'eau en conditions de recharge naturelle diffuse sur les températures de sous-surface est peu important, et ce malgré une recharge annuelle importante de 400 mm/a. Pour l'ensemble des trois cas théoriques étudiés, l'écart entre les températures simulées avec et sans écoulement d'eau était inférieur à 0.35 °C. Considérant les nombreuses sources potentielles d'erreurs provenant des mesures et des paramètres du modèle, les résultats suggèrent donc aussi qu'une incertitude importante pourrait être associée aux estimations de recharge obtenues avec cette technique pour les conditions étudiées.

2.2 Développement méthodologique et analyse d'incertitude

L'étude préliminaire discutée à la section précédente et présentée à l'[article 1](#) a permis de faire des observations très utiles pour guider la suite des travaux de ce volet du doctorat. Toutefois, le fait que l'étude de sensibilité ait été réalisée en supposant que l'écoulement de l'eau et le taux d'humidité du sol étaient homogènes dans l'espace et constants sur une base mensuelle constituait une limitation majeure de l'étude. En effet, ces hypothèses ne permettent pas de bien représenter les conditions d'écoulement en zone non saturée dans des sols granulaires grossiers très perméables qui sont généralement caractéristiques des zones de recharge des aquifères. De plus, les processus de gel/dégel du sol et le stockage/fonte de la neige n'avaient pas été pris en considération dans les travaux préliminaires. Cela constituait une lacune majeure puisque l'un des objectifs de la thèse était de développer une méthode adaptée aux conditions climatiques et hydrogéologiques retrouvées au Canada. Enfin, bien que les résultats aient suggéré que l'incertitude sur les valeurs estimées de recharge puisse être importante, aucune estimation quantitative de cette incertitude n'avait été faite.

Dans le but de répondre aux limitations des travaux précédents, une seconde étude, basée sur des données synthétiques réalistes, a donc été réalisée. Une approche basée sur des données synthétiques offre plusieurs avantages. Premièrement, les taux de recharge "vrais" peuvent alors être connus, ce qui permet d'évaluer directement l'erreur sur les valeurs estimées. Ceci n'aurait pas été possible avec un cas réel puisque les taux de recharge ne sont jamais connus avec certitude. Deuxièmement, cette approche permet de contrôler les diverses sources d'erreur, ce qui permet de faire des analyses de sensibilité et d'évaluer l'incertitude de la méthode.

2.2.1 Méthodologie

Le simulateur numérique couplé de transport de la chaleur et de l'eau SHAW (Simultaneous Heat and Water model; [Flerchinger & Saxton, 1987](#); [Flerchinger, 2000](#)) a été utilisé pour produire 12 ensembles de données synthétiques sur une base horaire, incluant la température et l'humidité du sol. En plus de simuler le transport de l'eau et de la chaleur dans le sol, SHAW permet également de simuler le gel/dégel du sol et l'accumulation/fonte de la neige à la surface du sol. Les ensembles de données synthétiques ont été produits en utilisant deux séries de données météorologiques différentes (précipitation quotidienne, vitesse du vent, humidité relative, température de l'air et rayonnement solaire), deux conditions de couverture de la surface (sol nu et couvert d'herbes courtes) et trois textures de sol (sable, sable limoneux et loam sableux). Pour chacun des cas simulés, des taux de la recharge (potentielle) annuelle ont été calculés à partir du flux d'eau horaire simulé avec SHAW au bas du profil du sol. Un large éventail de valeurs de recharge des eaux souterraines pour un climat froid et humide a ainsi été obtenu. Une description détaillée des modèles développés avec SHAW pour produire les ensembles de données synthétiques est présentée à la [section 2.2](#) de l'[article 2](#) de la thèse.

L'idée de base était d'utiliser ces températures simulées réalistes comme des mesures synthétiques pour estimer des valeurs de recharge par l'inversion d'un modèle numérique et de comparer les estimations avec les valeurs "vraies" de recharge calculées avec SHAW. Pour ce faire, un simulateur numérique simple et unidimensionnel du transport vertical de la chaleur par advection et conduction dans la zone non saturée a été développé dans le langage de programmation Python avec la méthode numérique des volumes finis. Une description détaillée de ce simulateur numérique, ci-après nommé *HeatFlow1Dz*, est présentée à la [section 2.3](#) de l'[article 2](#) de la thèse.

La méthode consiste à diviser dans le temps les mesures synthétiques de températures en segments consécutifs, mutuellement exclusifs et englobant toutes les données disponibles. Dans le cadre de cette étude, les données ont été successivement divisées en segments égaux sur une base hebdomadaire, mensuelle, semestrielle et annuelle. Les températures synthétiques produites avec SHAW aux profondeurs de 1 et 5 m ont ensuite été utilisées pour contraindre (avec des conditions de Dirichlet) les limites inférieure et supérieure d'un modèle développé avec *HeatFlow1Dz*. Pour chacun des segments de données définis précédemment, un flux d'écoulement vertical moyen a été estimé

par le calage des températures simulées avec HeatFlow1Dz aux mesures synthétiques produites avec SHAW à une profondeur de 3 m sous la surface.

La méthode est donc basée sur le principe qu'à l'intérieur de chaque segment de données, le flux d'écoulement vertical de l'eau est considéré homogène dans l'espace et constant dans le temps. Bien que ces hypothèses simplificatrices ne soient pas représentatives des conditions d'écoulement en zone non saturée, elles sont nécessaires pour que la méthode soit applicable. Cela est discuté plus en détail à la [section 2.3.4](#) de l'[article 2](#). Le point important de la méthodologie proposée est que les données synthétiques, utilisées pour tester la méthode, n'aient pas été générées avec ces hypothèses dans SHAW (contrairement à ce qu'il avait été fait pour les travaux préliminaires présentés à la [section 2.1](#) ci-dessus).

Les taux de recharge potentielle estimés sur une base hebdomadaire, mensuelle et semestrielle ont ensuite été compilés pour calculer des taux annuels. Les résultats ont ensuite été comparés avec les valeurs "vraies" de recharge calculées avec SHAW pour estimer la précision de la méthode pour les différents cas étudiés.

Lors de l'inversion du modèle HeatFlow1Dz, tous les autres paramètres du modèle étaient supposés connus avec certitude (erreur nulle). Or, une incertitude parfois importante est souvent associée aux valeurs attribuées à ces paramètres. Cela peut avoir un impact important sur la précision des taux de recharge estimés avec la méthode. L'impact de ces sources d'incertitude sur la précision de la méthode a donc été évalué avec des études de sensibilité pour trois paramètres jugés importants dans le transport de chaleur en zone non saturée. Ces paramètres sont: la porosité totale, la conductivité thermique et la teneur en eau volumétrique du sol. De plus, l'impact des erreurs de mesure de la température du sol sur la précision de la méthode a également été évalué. Cela a été fait en introduisant alternativement des erreurs aléatoires et un biais dans les températures simulées avec SHAW avant de les utiliser comme mesures synthétiques pour estimer la recharge.

2.2.2 Discussion des résultats

Comme supposé dans l'étude préliminaire présentée à la [section 2.1](#) ci-dessus et dans l'[article 1](#) de la thèse, les résultats de cette étude ont tout d'abord permis de démontrer que la résolution du flux d'écoulement sur des périodes plus courtes permet d'améliorer la précision des estimations de la

recharge annuelle. La figure 2.5 montre en effet que l'erreur sur les taux annuels de recharge est beaucoup plus petite lorsque l'inversion du modèle HeatFlow1Dz est faite sur une base hebdomadaire ou mensuelle.

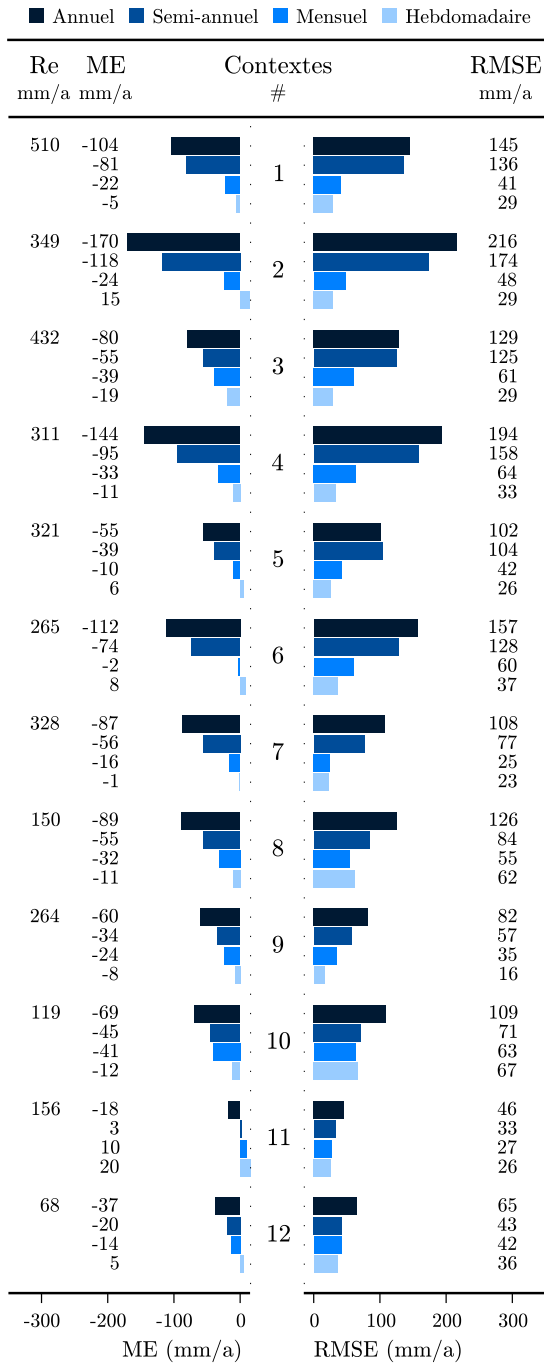


Figure 2.5
 Erreurs moyennes (ME) et erreurs quadratiques moyennes (RMSE) calculées entre les estimations annuelles de recharge (compilées à partir des flux d'eau résolus sur une base annuelle, semi-annuelle, mensuelle et hebdomadaire) et les valeurs simulées avec SHAW pour chacun des 12 contextes étudiés. Les valeurs moyennes de la recharge annuelle simulée avec SHAW (Re) sont également présentées.

Les erreurs les plus importantes sont obtenues lorsque le flux d'eau est résolu sur une base annuelle. Ces erreurs sont principalement dues au fait que le flux d'eau est supposé homogène dans l'espace et constant sur la période de temps sur laquelle le modèle est inversé. Comme présenté aux figures 2.3 et 2.4, le cycle de température est déformé de façon très irrégulière et non symétrique lorsque l'écoulement de l'eau dans la zone non saturée n'est pas constant sur une base annuelle. Ces déformations ne peuvent pas être adéquatement reproduites lorsque le flux est supposé constant sur une base annuelle. En réduisant la fenêtre temporelle sur laquelle les flux d'écoulement de l'eau sont supposés constants, les perturbations du cycle de la température peuvent alors être mieux reproduites par le modèle inverse, ce qui permet de réduire l'erreur sur l'estimation des taux de recharge.

Lorsque l'inversion est réalisée sur une base hebdomadaire, il est possible d'estimer la recharge annuelle lorsque celle-ci est supérieure à 200 mm/a avec une erreur de moins de 20 %. Toutefois, l'erreur relative sur les estimations de la recharge pour des taux annuels inférieurs à 200 mm/a augmente rapidement. La figure 2.6 montre que la relation entre l'erreur relative et les taux annuels estimés de recharge est inversement proportionnelle.

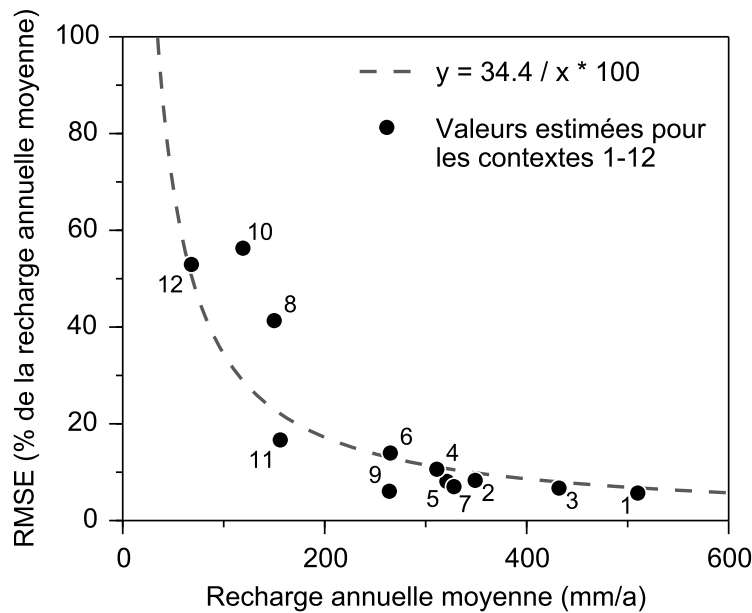


Figure 2.6 – Erreur quadratique moyenne (exprimée en % de la recharge annuelle moyenne) pour les valeurs estimées de recharge obtenues par inversion sur une base hebdomadaire par rapport à la recharge annuelle moyenne simulée pour chaque contexte avec SHAW.

Les résultats discutés ci-dessus ont toutefois été obtenus en conditions idéales. Lorsque l'incertitude sur les paramètres du modèle HeatFlow1Dz et les erreurs de mesure de la température du sol sont prises en considération, les taux de recharge estimés avec la méthode deviennent beaucoup plus incertains. Cela est bien illustré sur les graphiques a, b, et c de la [figure 2.7](#) qui présentent les erreurs obtenues sur les taux annuels de recharge estimés lorsqu'une incertitude est considérée sur la conductivité thermique du sable, sur la porosité totale et sur la teneur volumétrique en eau du sol. Ces résultats regroupent les erreurs calculées sur les valeurs de la recharge annuelle estimées sur une période de 20 ans pour les 12 contextes étudiés. Les résultats varient très peu d'un contexte à l'autre.

Ainsi, lorsqu'une incertitude de $\pm 10\%$ est considérée sur la porosité du sol par exemple, la médiane des erreurs sur les taux annuels de recharge est en moyenne de $\pm 373 \text{ mm/a}$ avec un écart interquartile supérieur à 120 mm/a . Les résultats sont similaires lorsqu'une incertitude de $\pm 30\%$ est considérée sur la conductivité thermique du sable. La médiane des erreurs est alors en moyenne de $\pm 507 \text{ mm/a}$ avec un écart interquartile supérieur à 140 mm/a . L'erreur sur les estimations de la recharge annuelle est toutefois beaucoup moins affectée par la teneur volumétrique du sol en eau. Cela est dû au fait que la teneur en eau a un effet limité sur la diffusivité thermique du sol, qui correspond au ratio entre la conductivité thermique du sol et sa chaleur massique volumétrique. La diffusivité du sol est le paramètre le plus important pour le transport de la chaleur dans le sol lorsque l'écoulement de l'eau est faible puisque le régime thermique est alors contrôlé principalement par le processus de conduction de la chaleur. Cela est discuté en détail à la [section 3.3](#) de l'[article 2](#) de la thèse.

De façon similaire, les résultats présentés sur les graphiques d et e de la [figure 2.7](#) montrent que les erreurs sur les mesures de la température du sol ont un impact important sur la précision de la méthode. La situation est particulièrement critique lorsqu'un biais est introduit dans l'une des séries de mesures utilisées pour estimer la recharge. Pour un biais de $\pm 0.1^\circ\text{C}$ (correspondant à la précision typique des sondes commerciales), l'erreur sur les taux annuels de recharge peut parfois être supérieure à 1000 mm/a . L'impact est un peu moins important lorsque les erreurs de mesure sont aléatoires. Lorsque des erreurs aléatoires non biaisées avec un écart-type de 0.1°C sont ajoutées aux mesures synthétiques de température à 3 m , l'erreur sur la recharge est toujours inférieure $\pm 300 \text{ mm/a}$ pour les conditions testées dans cette étude.

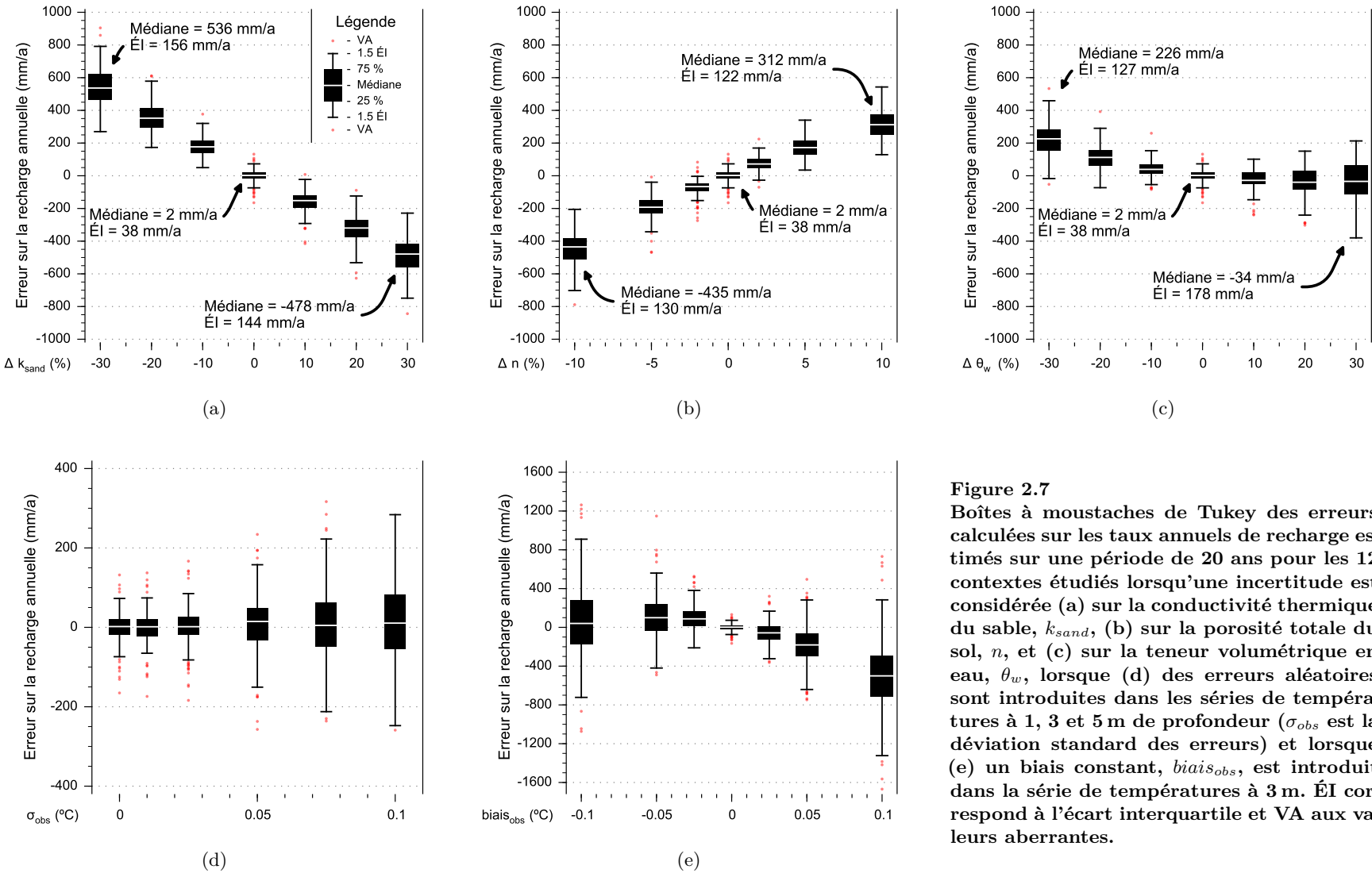


Figure 2.7
 Boîtes à moustaches de Tukey des erreurs calculées sur les taux annuels de recharge estimés sur une période de 20 ans pour les 12 contextes étudiés lorsqu'une incertitude est considérée (a) sur la conductivité thermique du sable, k_{sand} , (b) sur la porosité totale du sol, n , et (c) sur la teneur volumétrique en eau, θ_w , lorsque (d) des erreurs aléatoires sont introduites dans les séries de températures à 1, 3 et 5 m de profondeur (σ_{obs} est la déviation standard des erreurs) et lorsque (e) un biais constant, $biais_{obs}$, est introduit dans la série de températures à 3 m. ÉI correspond à l'écart interquartile et VA aux valeurs aberrantes.

Les analyses de sensibilité présentées ci-dessus ont montré qu'une incertitude considérable pouvait être associée aux taux annuels de la recharge diffuse estimés à partir de séries temporelles de la température mesurées dans la zone non saturée. De plus, comme discuté plus en détail dans l'[article 2](#) de la thèse, d'autres sources d'erreurs, non considérées dans cette étude, peuvent réduire davantage la précision de la méthode. Ces résultats suggèrent que les techniques utilisant la chaleur comme traceur ne sont pas bien adaptées pour l'estimation des taux de la recharge diffuse à partir de mesures temporelles de la température acquises près de la surface et dans la zone non saturée. Cela est dû principalement au faible impact de l'écoulement de l'eau sur les variations des températures du sol proches de la surface lorsque le flux d'écoulement est faible ($<600 \text{ mm/a}$). Le système thermique de sous-surface dans la zone superficielle est alors principalement contrôlé par la conduction de la chaleur. Ces conclusions permettent de mieux comprendre pourquoi les résultats obtenus pour le cas pratique à Portneuf, discuté en début de chapitre, étaient peu concluants. Il faut donc être très prudent si l'on veut estimer un taux de recharge à partir de données thermiques en raison des divers facteurs qui peuvent influencer significativement la précision de la méthode.

Chapitre 3

Bilans hydrologiques combinés

Ce volet de la thèse porte sur le développement méthodologique et l'évaluation de l'incertitude d'une méthode d'estimation de la recharge basée sur des mesures journalières de la température de l'air, des précipitations totales et du niveau des eaux souterraines. La méthode, de même qu'un exemple d'application pour un puits d'observation situé dans la région de Portneuf, Québec, sont présentés à l'[article 3](#) de la thèse et un survol de ces travaux est présenté à la [section 3.1](#).

Un algorithme, ci-après nommé PyGWD (Python Gap-filling Weather Data algorithm), a également été développé dans le cadre de ces travaux pour estimer et combler automatiquement les valeurs manquantes dans les séries de données météorologiques journalières. Ces données sont nécessaires pour l'application de la méthode d'estimation de la recharge mentionnée ci-dessus. L'algorithme, de même qu'un exemple d'application en Montérégie Est, Québec, sont présentés à l'[article 4](#) de la thèse et un survol de ces travaux est présenté à la [section 3.2](#).

Outre les contributions scientifiques mentionnées ci-dessus, des efforts importants ont également été consacrés au développement du logiciel WHAT (Well Hydrograph Analysis Toolbox; [Gosselin et al., 2016a](#)). Ce dernier permet de télécharger et mettre en forme automatiquement les données météorologiques journalières de la banque de données en ligne du gouvernement du Canada (<http://climate.weather.gc.ca>). Une interface graphique pour l'algorithme PyGWD a aussi été développée et incorporée dans WHAT. De plus, le logiciel comprend un module de visualisation permettant de produire des hydrogrammes de puits mettant en relation les données météorologiques et les mesures de niveaux d'eau. Un exemple est présenté à la [figure 3.1](#). Les données peuvent en plus être visualisées

et interprétées dans un environnement dynamique directement à partir de l'interface graphique de WHAT. À noter que le développement du logiciel n'est pas complété en date de la rédaction de cette thèse. À terme, le logiciel permettra également d'appliquer la méthode d'estimation de la recharge qui a été développée dans le cadre de ce volet de la thèse et dont un survol est présenté à la section 3.1.

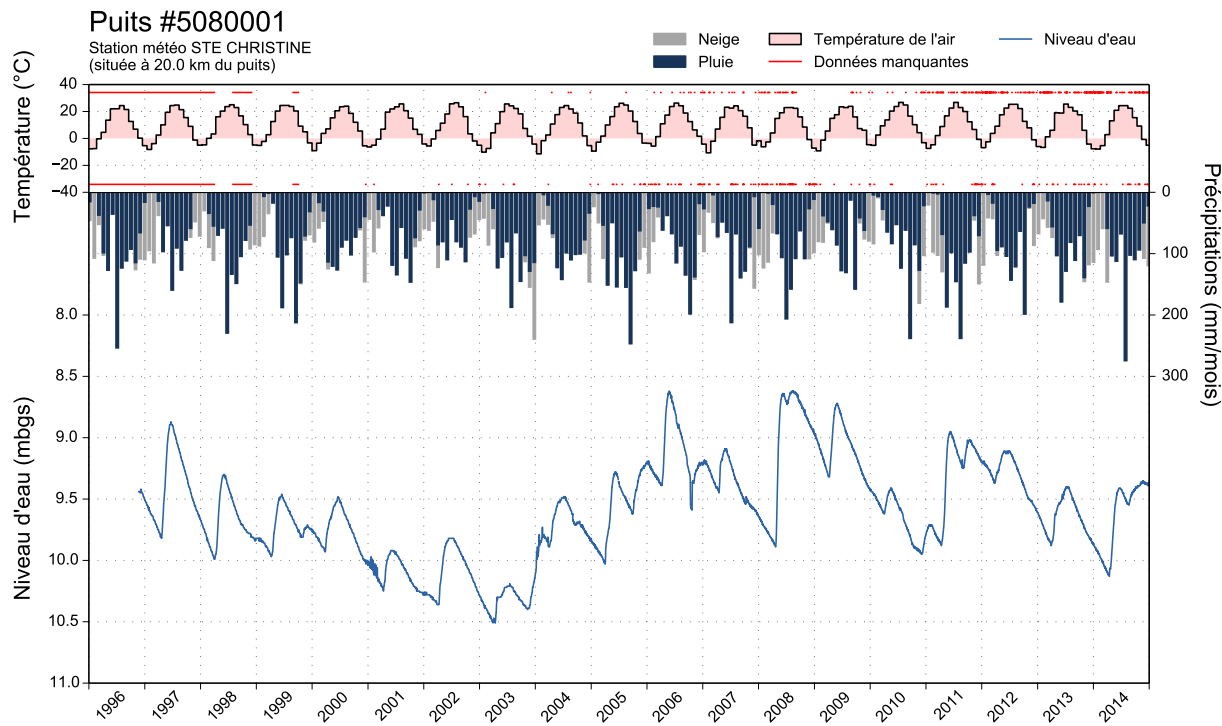


Figure 3.1 – Exemple d'un hydrogramme de puits produit avec le logiciel WHAT pour une série temporelle s'étalant sur 18 ans. Le graphique montre le niveau d'eau journalier mesuré dans un puits d'observation et les données météorologiques mensuelles (températures de l'air et précipitations) à la station météorologique STE CHRISTINE. Le puits et la station météorologique sont tous les deux situés dans la région de Portneuf, Québec. Les dates pour lesquelles des valeurs manquantes ont été estimées et comblées avec l'algorithme PyGWD sont indiquées avec un trait rouge au-dessus de chacune des séries de données.

En plus d'avoir servi à la production de deux articles scientifiques ([articles 3 et 4](#) de la thèse), WHAT a été utilisé dans plusieurs autres projets pour le traitement des données météorologiques, la production de figures et l'estimation de la recharge (sans l'interface graphique). Par exemple, il a été utilisé dans les projets de caractérisation hydrogéologique du PACES (Programme d'acquisition et de connaissances sur les eaux souterraines) Montérégie Est ([Carrier et al., 2013](#)), de Saint-Édouard-de-Lotbinière ([Ladevèze et al., 2016](#)) et de plusieurs bases militaires canadiennes (Valcartier et Farnham,

Québec, et Durndun, Saskatchewan). La dernière version du logiciel est disponible gratuitement sur GitHub (<https://github.com/jnsebgosselin/WHAT>). Les travaux étant toujours en cours, une version préliminaire du guide d'utilisateur de WHAT est présentée à l'[annexe A](#) de la thèse. Ce guide, une fois terminé, sera publié sous forme de Dossier public de la CGC.

3.1 Estimation de la recharge

[Lefebvre et al. \(2011\)](#) ont présenté une méthode d'estimation de la recharge consistant à simuler le niveau de la nappe à l'aide d'un modèle mathématique combinant un bilan hydrologique de surface (SMB: Soil Moisture Balance) journalier et un bilan en eau d'un aquifère à nappe libre. La méthode requiert des mesures journalières de la température de l'air, des précipitations totales et du niveau des eaux souterraines mesuré dans un aquifère en conditions de nappe libre. Idéalement, des mesures de niveaux d'eau sur une base journalière sur une durée d'au moins un an sont requises. Il n'est pas nécessaire que la série temporelle des niveaux d'eau soit continue dans le temps, bien que cela soit préférable.

Les paramètres hydrologiques du modèle (ex.: coefficient de ruissellement, porosité de drainage, réserve en eau utile maximale) sont ensuite estimés en ajustant les niveaux d'eau simulés aux mesures acquises dans un puits d'observation. Le modèle ainsi calé est ensuite utilisé pour estimer la recharge sur une base journalière, puis les résultats sont compilés pour donner des valeurs annuelles de recharge. [Lefebvre et al. \(2011\)](#) ont développé un tableur Excel pour l'application de la méthode et ont présenté un exemple d'application pour quatre puits d'observation situés dans la région de Portneuf, à environ 55 km au sud-ouest de la ville de Québec, sur la rive nord du fleuve St-Laurent. Les résultats présentés par [Lefebvre et al. \(2011\)](#) ont montré que leur approche était valide pour évaluer la recharge des aquifères à nappe libre pour des climats continentaux tempérés. En outre, elle permet de contourner plusieurs des limitations inhérentes aux méthodes conventionnelles basées sur un bilan hydrologique de surface et sur les fluctuations de la nappe (mentionnées à la [section 1.6](#)) lorsque ces dernières sont appliquées séparément.

Toutefois, dans leur application de la méthode, [Lefebvre et al. \(2011\)](#) ont utilisé une approche d'optimisation locale, qui consistait à rechercher un ensemble unique de paramètres optimaux, basée sur une comparaison visuelle (qualitative) entre les niveaux d'eau simulés et mesurés. L'incertitude

sur les valeurs estimées des paramètres était ensuite évaluée qualitativement sur la base d'une analyse de sensibilité réalisée autour de la solution jugée optimale.

Or, cela constitue une limitation majeure au niveau du potentiel d'application de la méthode et au niveau de l'objectivité des valeurs de recharge estimées, car le calage visuel par essais et erreurs des niveaux d'eau simulés aux valeurs observées n'est pas aisé et laisse beaucoup de place à la subjectivité. Cela est dû au fait que le problème d'optimisation à résoudre est mal posé. En effet, il n'existe pas de solution unique au problème d'optimisation et un ensemble de combinaisons de valeurs des paramètres permet de reproduire les niveaux d'eau mesurés de façon équiprobable. Ceci est bien illustré sur les trois graphiques de la [figure 3.2](#) qui présentent des niveaux d'eau simulés avec l'approche de [Lefebvre et al. \(2011\)](#) pour différentes combinaisons de paramètres. Ces paramètres, de même que les valeurs annuelles moyennes de recharge estimées pour la période 2007-2012 avec chaque modèle, sont présentés dans le [tableau 3.1](#).

Les résultats de la [figure 3.2](#) montrent bien que chacune des trois solutions permet de reproduire de façon très similaire les niveaux d'eau observés dans le puits d'observation. Les valeurs de recharge pour les trois modèles couvrent toutefois une plage assez large, allant de 363 à 591 mm/a. Pour un tel problème d'optimisation, le choix d'une solution "optimale" pour caractériser la recharge est alors arbitraire. Cette approche surestime donc l'information réellement contenue dans les données et entraîne des marges d'incertitude trop étroites sur les valeurs de recharge estimées. Pour la résolution d'un tel problème, il est nécessaire d'utiliser plutôt une méthode d'optimisation globale permettant de reconnaître qu'il n'existe pas une, mais bien un ensemble de solutions pouvant reproduire les valeurs observées de façon équiprobable et qui permette d'établir des contraintes *a priori* sur la plage de valeurs plausibles des paramètres hydrologiques.

Ce volet de la thèse s'est penché sur la problématique discutée ci-dessus et au développement d'outils (codes et logiciel) pour faciliter l'application de l'approche présentée par [Lefebvre et al. \(2011\)](#) et l'améliorer par l'incorporation d'une méthode d'optimisation adaptée au problème et permettant d'évaluer correctement l'incertitude.

Figures	S_y m^3/m^3	C_{RO} -	RAS_{max} mm	Recharge mm/a
Figure 3.2a	0.10	0.11	13	591
Figure 3.2b	0.08	0.32	7	478
Figure 3.2c	0.06	0.46	6	363

Tableau 3.1

Valeurs des paramètres hydrologiques utilisés pour la simulation des niveaux d'eau présentés dans les graphiques de la figure 3.2. La recharge moyenne annuelle pour la période 2007-2012 est donnée dans la dernière colonne pour chacune des solutions.

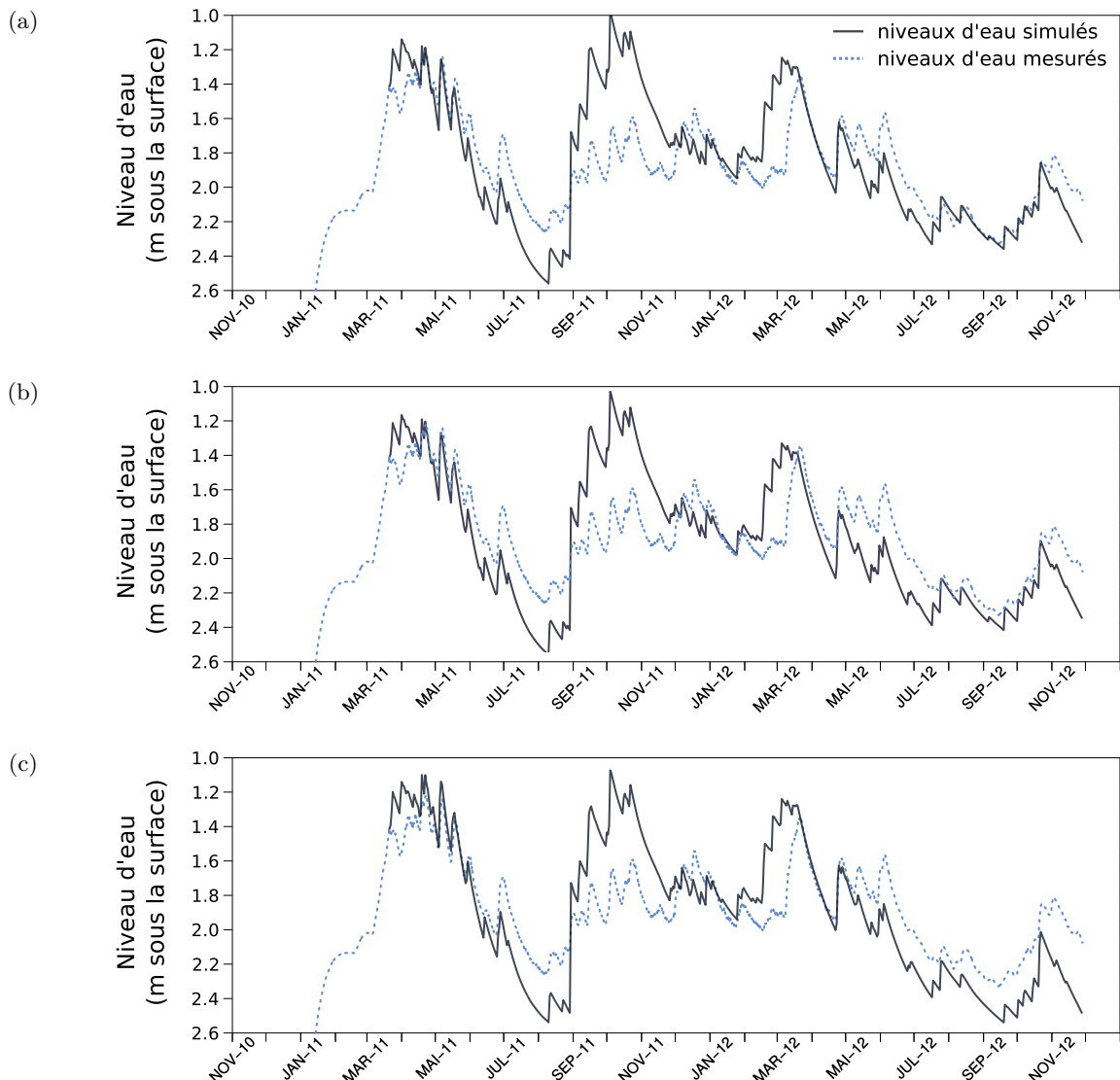


Figure 3.2 – Simulations équiprobables des niveaux d'eau mesurés dans un puits d'observation en Montérégie Est, Québec avec la méthode présentée par Lefebvre *et al.* (2011). Les valeurs des paramètres utilisées dans les simulations sont montrées dans le tableau 3.1 (adaptée de Gosselin *et al.*, 2013).

3.1.1 Méthodologie

La première étape des travaux a consisté à implémenter la méthode de Lefebvre *et al.* (2011) dans un code fonctionnel rédigé dans le langage de programmation Python qui offre plus de flexibilité qu'un tableauur Excel. Quelques améliorations ont été apportées à la formulation du modèle, mais en général, l'approche de Lefebvre *et al.* (2011) a été conservée. Entre autres, un module pour la fonte de la neige a été ajouté. Dans la version de Lefebvre *et al.* (2011), la neige accumulée sur le sol fondait en une seule journée lorsque la température de l'air atteignait une valeur seuil donnée. Le calcul du bilan hydrologique de surface a également été légèrement modifié pour faciliter la résolution du problème inverse. Une description détaillée de la formulation du modèle est présentée dans l'[article 3](#).

Par la suite, différents outils ont été développés pour faciliter l'application de la méthode. Un algorithme (PyGWD: Python Gap-filling Weather Data algorithm) a été développé pour estimer et combler les valeurs manquantes dans les séries de données météorologiques journalières qui sont nécessaires pour l'estimation de la recharge. Ce volet des travaux est présenté en détail à la [section 3.2](#) et dans l'[article 4](#) de la thèse. Un code a également été développé et inclus dans WHAT pour calculer automatiquement l'évapotranspiration potentielle à partir des données météorologiques avec la méthode de Thornthwaite (1948). Un algorithme et une interface graphique, incluse dans le logiciel WHAT, ont été développés pour l'estimation de la courbe maîtresse de récession (MRC: Master Recession Curve) à partir des séries temporelles de niveaux d'eau. Le développement mathématique de l'approche utilisée pour le calcul de la MRC est présenté dans l'[article 3](#) de la thèse et une capture d'écran de l'interface graphique est montrée à la [figure 3.3](#).

Afin d'améliorer la résolution du problème d'optimisation et pour évaluer l'incertitude de la méthode, la méthode GLUE (Generalized Likelihood Uncertainty Estimation; Beven & Binley, 1992, 2014) a été utilisée. Les détails de l'approche sont fournis dans l'[article 3](#) de la thèse. En résumé, le principe de l'approche de résolution consiste d'abord à définir des plages de valeurs plausibles pour les paramètres hydrologiques du modèle, c'est-à-dire pour le coefficient de ruissellement (C_{RO}), la porosité de drainage du sol (S_y) et la réserve en eau utile maximale (RAS_{max}). La méthode consiste ensuite à produire une grande quantité de réalisations (hydrogrammes de puits synthétiques) à partir de plusieurs combinaisons de valeurs des paramètres tirées des plages définies *a priori*. Une mesure de vraisemblance aux valeurs observées est ensuite calculée pour chaque hydrogramme synthétique ainsi simulé. Dans cette étude, l'inverse de la somme des résidus au carré a été utilisé comme mesure de

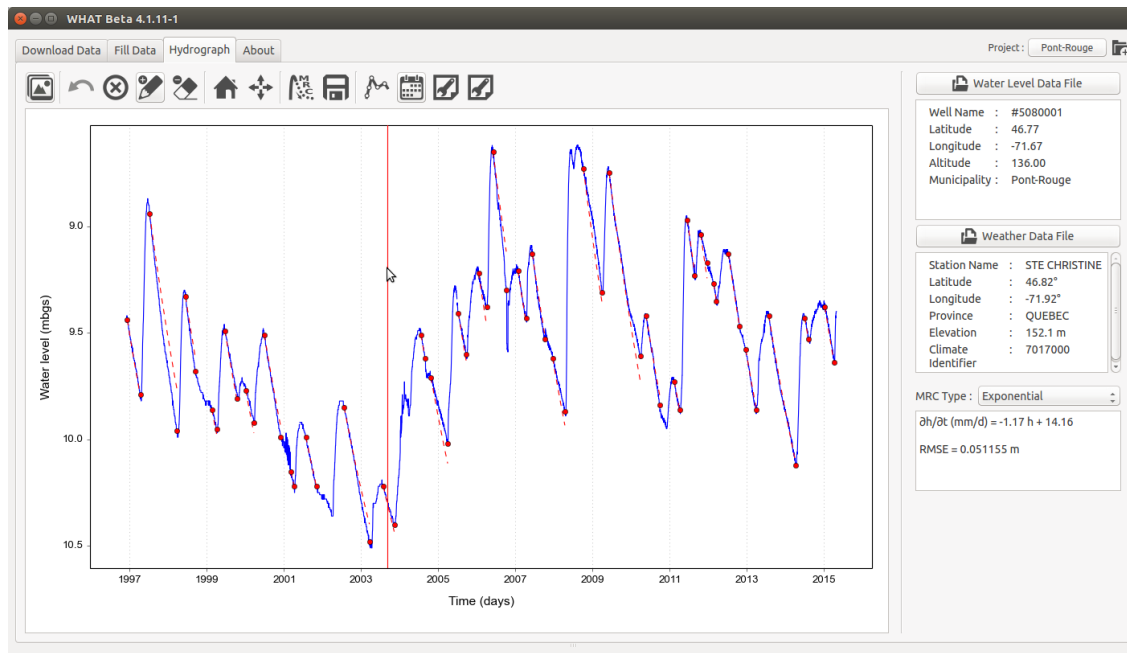


Figure 3.3 – Capture d'écran du logiciel WHAT montrant l'interface qui a été développée pour l'estimation de la courbe maîtresse de récession (MRC). Les points rouges correspondent aux endroits sélectionnés par l'utilisateur pour indiquer les segments dans la courbe qui seront utilisés pour l'estimation de la MRC. Les niveaux d'eau simulés avec la MRC sont ensuite tracés avec des lignes pointillées rouges sur l'hydrogramme.

vraisemblance comme suggéré par [Beven & Binley \(1992\)](#). Les mesures de vraisemblance sont ensuite utilisées pour établir une fonction de répartition de la recharge (CDF: Cumulative Distribution Function) sur une base journalière, puis les CDFs sont utilisées pour établir l'incertitude et les valeurs modales de la recharge.

La méthode a été testée avec des mesures de niveaux d'eau dans un puits d'observation situé à Pont-Rouge, dans l'aquifère deltaïque de la région de Portneuf où plusieurs études ont été réalisées au cours des dernières années, dont celle de [Larose-Charette et al. \(2000\)](#) et [Lefebvre et al. \(2011\)](#). La figure 3.1 montre l'hydrogramme mesuré dans le puits pour les années 1996-2014. La profondeur moyenne de la nappe durant cette période était de 9.6 m sous la surface du sol. Les précipitations et la température moyenne mensuelle de l'air à la station météorologique la plus proche sont également tracées dans la partie supérieure du graphique. Les fluctuations du niveau d'eau montrées sur la figure 3.1 indiquent que la recharge se produit principalement suivant la fonte des neiges au printemps, vers la fin du mois de mars. Les précipitations importantes à la fin de l'été et au début de l'automne (parfois plus de 200 mm/mois en août et septembre) ne semblent pas causer d'importantes remontées

du niveau des eaux souterraines, ce qui suggère que la recharge n'est pas importante pendant cette période où l'évapotranspiration est encore active.

Les plages de valeurs des paramètres utilisées pour la résolution du problème inverse avec GLUE sont présentées au [tableau 3.2](#). Les plages de valeurs pour RAS_{max} et C_{RO} qui ont été utilisées ont été basées sur celles de [Larose-Charette et al. \(2000\)](#) afin d'obtenir des résultats comparables à ceux des études précédentes. La plage de valeurs pour S_y a été établie en imposant une incertitude de $\pm 20\%$ sur la valeur nominale de 0.25 utilisée par [Larose-Charette et al. \(2000\)](#) et [Lefebvre et al. \(2011\)](#). Un survol des résultats obtenus est présenté à la section suivante.

Tableau 3.2 – Plage de valeurs des paramètres hydrologiques utilisées pour l'estimation de la recharge.

Paramètres	Descriptions	Plages de valeurs plausibles
S_y	Porosité de drainage de l'aquifère	0.2 à 0.3
RAS_{max}	Réserve en eau utile maximale	0 à 150 mm
C_{RO}	Coefficient de ruissellement	0.2 à 0.4

3.1.2 Discussion des résultats

Un total de 1195 modèles reproduisant adéquatement les mesures des niveaux d'eau ont été produits. La [figure 3.4](#) montre les valeurs modales de la recharge annuelle calculées avec la méthode GLUE pour la période 1997-2014 à partir de ces 1195 modèles. Les moustaches correspondent à l'incertitude calculée avec l'intervalle de confiance de GLUE de 5 à 95 %. Pour tenir compte de la neige qui s'accumule sur le sol durant l'hiver, la recharge a été estimée pour des années hydrologiques s'étendant du 1^{er} Octobre d'une année au 30 septembre de l'année suivante. Les valeurs modales de recharge varient entre 150 mm/a pour l'année 2009-2010 et 470 mm/a pour l'année 2010-2011. L'incertitude varie de 77 mm/a pour l'année 2005-2006 à 253 mm/a pour l'année 2004-2005.

La valeur moyenne de la recharge annuelle pour toute la période est de 286 mm/a. Les valeurs limites pour l'intervalle de confiance de 5 à 95 % sont, respectivement, de 223 et 384 mm/a (78 % et 134 % de la recharge moyenne). L'étendue de l'incertitude moyenne est donc de 161 mm/a, ce qui correspond à une réduction de l'incertitude de plus de 40 mm/a par rapport aux travaux de [Larose-Charette et al. \(2000\)](#). Par ailleurs, parmi la population de modèles produits, S_y varie entre

0.2 à 0.3, RAS_{max} entre 24 à 150 mm, et C_{RO} entre 0.26 à 0.4. La méthode a également permis de réduire les plages des paramètres qui avaient été établies *a priori* pour RAS_{max} et C_{RO} .

L'incertitude sur la recharge pourrait être réduite davantage par une meilleure connaissance préalable des plages de valeurs plausibles des paramètres hydrologiques du modèle. Par exemple, si une incertitude de 10 % était considérée sur la valeur nominale de S_y , au lieu de 20 %, la plage de valeurs plausibles pour S_y serait alors réduite à 0.225-0.275 (au lieu de 0.2-0.3 comme montré au tableau 3.2). L'étendue de l'incertitude sur la recharge annuelle moyenne pour l'intervalle de confiance 5 à 95 % serait alors de 124 mm/a.

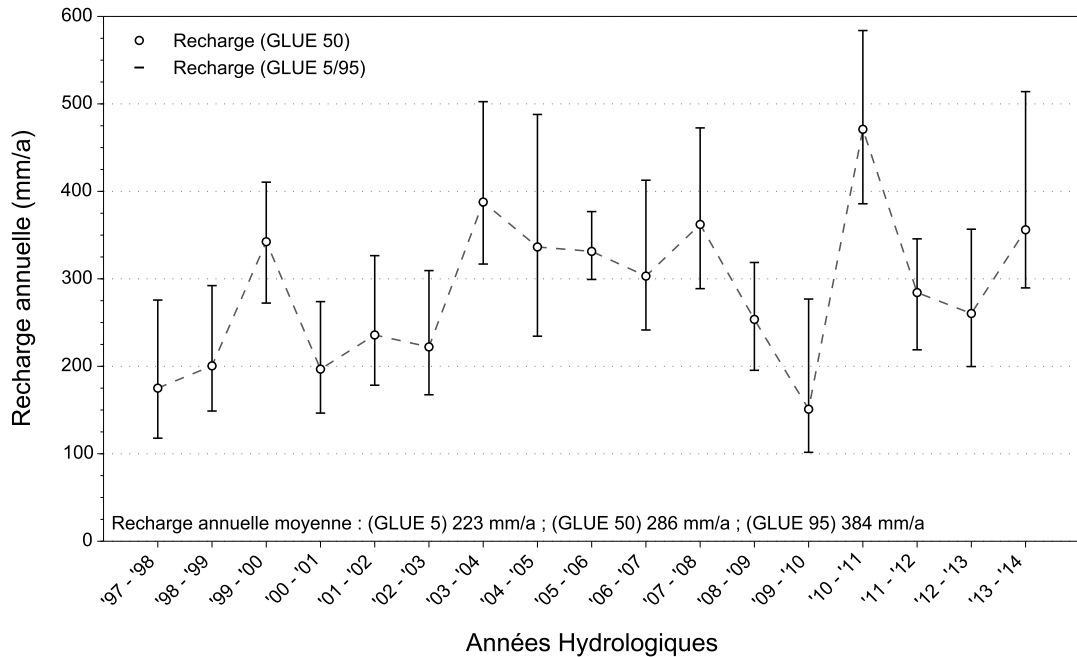


Figure 3.4 – Valeurs modales de recharge annuelle estimées avec la méthode GLUE. Les moustaches correspondent aux limites d'incertitude pour l'intervalle de confiance de GLUE entre 5 et 95 %. Les valeurs annuelles ont été calculées pour les années hydrologiques en additionnant les taux quotidiens de recharge à partir du 1^{er} octobre d'une année au 30 septembre de l'année suivante.

La figure 3.5 montre l'enveloppe des niveaux d'eau simulés pour l'intervalle de confiance de GLUE de 5 à 95 % pour la période 1996-2015. Ces résultats montrent que l'enveloppe des niveaux d'eau prédits ne permet pas d'englober toutes les mesures puisque les fluctuations à court terme ne sont pas bien représentées par le modèle. Plusieurs facteurs peuvent expliquer ce résultat, incluant le fait que les données météorologiques utilisées pour l'application de la méthode proviennent d'une station météorologique située à 20 km du puits.

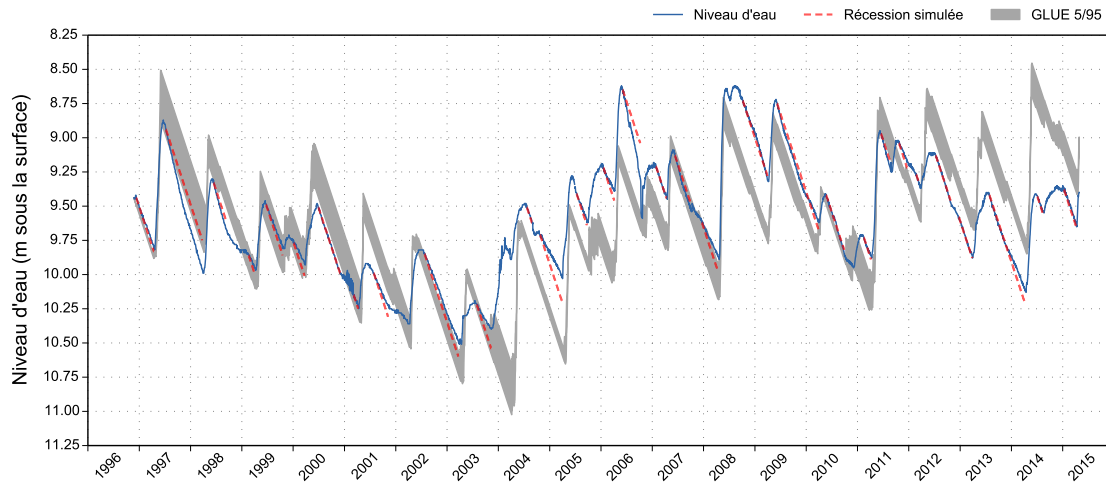


Figure 3.5 – Enveloppe des niveaux d'eau estimés (en gris) avec la méthode pour l'intervalle de confiance de GLUE de 5 à 95 %. Les mesures de niveaux d'eau dans le puits (ligne pleine bleue) et les niveaux d'eau simulés avec la courbe maîtresse de récession (lignes pointillées rouges) sont également montrés.

Des améliorations pourraient être apportées au modèle dans le futur afin de mieux représenter les fluctuations à court terme des niveaux d'eau. Par exemple, comme montrée sur la [figure 3.5](#) par les lignes pointillées rouges, la récession n'est pas toujours bien représentée par la courbe maîtresse de récession (MRC). Ainsi, cette dernière pourrait être définie sur une base annuelle ou saisonnière afin d'améliorer la représentation des niveaux d'eau par le modèle durant les périodes où la recharge est négligeable. L'incertitude des paramètres de la MRC pourrait également être évaluée et prise en considération dans l'application de la méthode GLUE. Quelques autres suggestions de travaux futurs pour améliorer la méthode sont discutées à la [section 3.3](#) de l'[article 3](#).

Même si le modèle n'a pas réussi à représenter avec précision les variations à court terme des niveaux d'eau, la tendance et le comportement général de l'hydrogramme observés sur toute la période de suivi de 18 ans sont bien représentés. La représentation de l'hydrogramme sur le long terme est certainement un des aspects les plus importants de cette méthode pour l'estimation des taux moyens annuels de la recharge. Cependant, étant donné que les événements de recharge individuels ne sont pas étroitement reproduits, il faut être prudent lorsque cette méthode est utilisée pour estimer des événements de recharge individuels, ou encore lorsque la méthode est appliquée avec une courte série de mesures de niveaux d'eau.

Tel qu'il a été discuté à la [section 1.4](#), il est impossible de valider les valeurs de la recharge estimées puisque des mesures réelles de cette dernière ne sont jamais disponibles. Lors de travaux futurs, la méthode pourrait être appliquée à un ensemble de données synthétiques produites avec un modèle couplé et complexe d'écoulement de l'eau souterraine comme le simulateur CATHY (CATchment HYdrogeological model; [Paniconi & Wood, 1993](#)). Cela devrait permettre de valider et d'évaluer pleinement les limites de l'approche, similairement à ce qui a été fait pour la méthode utilisant des mesures de la température du sol (présentée au [chapitre 2](#)).

3.2 Comblement des données météorologiques journalières manquantes

Les séries de données météorologiques quotidiennes sont utiles dans plusieurs domaines des sciences, y compris l'hydrologie, l'hydrogéologie et l'agronomie. Des séries journalières de la température de l'air et des précipitations totales sont entre autres nécessaires dans l'application de la méthode d'estimation de la recharge discutée ci-dessus à la [section 3.1](#).

Cependant, les jeux de données météorologiques sont, la plupart du temps, incomplets. Cela peut représenter un obstacle majeur dans diverses applications, comme pour l'utilisation de simulateurs hydrologiques et hydrogéologiques qui dépendent de ces données. Combler les valeurs manquantes dans les ensembles de données météorologiques peut rapidement devenir une tâche fastidieuse avec l'augmentation de la longueur et du nombre de séries de données. En outre, cette tâche peut devenir très complexe lorsque des aspects tels que le temps de calcul et la précision des valeurs manquantes estimées sont pris en compte. Cela est particulièrement vrai pour les précipitations quotidiennes en raison de leur grande variabilité spatiale et temporelle ([Simolo et al., 2010](#)) et de la complexité des processus physiques impliqués. Bien que diverses méthodes existent pour estimer les valeurs manquantes dans les séries quotidiennes de données météorologiques (ex.: [DeGaetano et al., 1995](#); [Eischeid et al., 2000](#); [Simolo et al., 2010](#)), peu d'outils sont disponibles pour effectuer cette tâche efficacement et automatiquement.

Afin de pallier ce manque de logiciel pouvant accomplir le comblement de données, l'algorithme PyGWD (Python Gap-filling Weather Data algorithm) a été développé dans le langage de programmation Python. Cet algorithme permet d'estimer et de combler automatiquement les données

manquantes dans les séries journalières de données météorologiques avec une approche robuste et efficace. PyGWD peut être utilisé en ligne de commande dans un interpréteur Python 2.7 (ou plus récent), tel que décrit à l'[article 4](#). De plus, une interface graphique a été développée et a été incorporée dans le logiciel WHAT, tel que décrit dans le guide d'utilisateur du logiciel ([Gosselin et al., 2016a](#)) dont une version préliminaire est présentée à l'[annexe A](#) de la thèse.

3.2.1 Méthodologie

L'estimation des données manquantes est faite dans PyGWD à l'aide de la méthode des modèles de régression linéaire multiple (MLR: Multiple Linear Regression). Les modèles de régression sont générés à partir des données météorologiques collectées à la même date aux stations voisines. Cette approche est robuste et couramment utilisée en pratique ([Eischeid et al., 1995, 2000](#)). Une brève description de l'approche utilisée pour implémenter la méthode est donnée ci-dessous et une description détaillée est présentée à l'[article 4](#) de la thèse.

La première étape consiste à calculer les coefficients de corrélation (CC) pour chaque variable climatologique (c'est-à-dire les températures journalières minimales, moyennes et maximales et les précipitations totales journalières) entre toutes les données mesurées à la station cible (station dont les données manquantes sont à combler) et aux stations voisines. Les stations voisines avec moins de 182 jours (une demi-année) de données simultanées avec la station cible ou avec un CC inférieur à 0.35 pour une variable climatologique donnée, ne sont pas utilisées pour l'estimation des données manquantes. Les stations voisines peuvent également être écartées en fonction d'une trop grande distance horizontale et/ou différence d'altitude avec la station cible. Les stations voisines n'ayant pas été rejetées sont ensuite classées en ordre décroissant de leur CC pour chaque variable climatologique.

La sélection des stations voisines est une étape cruciale pour l'estimation précise des données météorologiques manquantes avec cette méthode. Puisque les séries de données aux stations voisines contiennent généralement un certain nombre de valeurs manquantes, la liste des stations avec des données disponibles peut varier d'un jour à l'autre. Ainsi, la sélection des stations météorologiques doit être faite indépendamment pour chaque journée où une valeur est manquante. Pour un jour donné avec une valeur manquante, les stations voisines avec des données disponibles pour cette journée sont sélectionnées en ordre décroissant de leur CC, jusqu'à un nombre maximal de stations spécifié par l'utilisateur. Les données des stations voisines sélectionnées sont ensuite utilisées pour

générer un modèle de RLM (Régression Linéaire Multiple) qui est par la suite utilisé pour estimer la donnée manquante. Il n'est pas possible d'estimer une valeur pour une donnée manquante dans le cas où aucune station voisine n'a de donnée mesurée pour cette journée.

PyGWD comprend également une routine permettant de valider et estimer l'incertitude de la méthode grâce à de la validation croisée. Le principe consiste à retirer une valeur mesurée dans la série de données de la station cible et d'estimer une valeur avec la méthode décrite ci-dessus. Le processus est alors répété successivement pour chaque jour des séries de données de la station cible où une valeur mesurée est disponible. La routine de validation croisée a été utilisée pour tester l'algorithme PyGWD pour un réseau de 19 stations météorologiques situées en Montérégie Est, Québec. Un survol des résultats obtenus est présenté à la [section 3.2.2](#) ci-dessous.

3.2.2 Discussion des résultats

Un résumé des résultats de la validation croisée pour l'ensemble des 19 stations en Montérégie Est est présenté au [tableau 3.3](#). Les résultats détaillés pour chaque station sont présentés au tableau [tableau 2](#) de l'[article 4](#). Ces résultats montrent que la méthode permet d'estimer de façon cohérente les valeurs manquantes pour la température de l'air et les précipitations journalières pour les 19 stations météorologiques testées.

Tableau 3.3 – Résumé des résultats de la validation croisée pour les 19 stations météorologiques situées en Montérégie Est pour la période 1980-2009. Les valeurs minimales, moyennes et maximales, calculées d'après les résultats obtenus pour l'ensemble des 19 stations, sont présentées pour la racine carrée de l'erreur quadratique (RMSE), l'erreur moyenne absolue (MAE), l'erreur moyenne (ME) et le coefficient de corrélation (r). Les quatre variables météorologiques sont la température de l'air minimum, moyenne et maximum (T_{\min} , T_{moy} , T_{\max}) et les précipitations totales (P_{tot}).

	T_{\max}				T_{\min}				T_{moy}				P_{tot}			
	RMSE °C	MAE °C	ME °C	r	RMSE °C	MAE °C	ME °C	r	RMSE °C	MAE °C	ME °C	r	RMSE* mm	MAE* mm	ME* mm	r
Min	0.9	0.6	-0.07	0.993	1.2	0.8	-0.11	0.987	0.8	0.5	-0.08	0.995	2.3	1.0	-0.20	0.847
Mean	1.1	0.7	0.00	0.996	1.4	1.0	0.01	0.993	0.9	0.7	0.00	0.997	2.8	1.1	-0.06	0.901
Max	1.5	1.0	0.03	0.997	2.0	1.4	0.15	0.995	1.2	0.9	0.07	0.998	3.4	1.4	0.03	0.928

Plus spécifiquement, pour la température de l'air, la racine carrée de l'erreur quadratique (RMSE: Root-Mean-Square Error) et l'erreur absolue moyenne (MAE: Mean Absolute Error) sont dans les deux cas inférieures à 2.0 et 1.4 °C pour les températures journalières minimales, moyennes et maximales de l'air. Pour ces trois variables météorologiques, il n'y a pas non plus de biais au niveau

des estimations puisque la moyenne des erreurs est dans tous les cas inférieure à 0.01 °C. Le coefficient de corrélation entre les valeurs estimées et mesurées est supérieur à 0.987 pour toutes les stations, pour les trois variables de températures. Les graphiques a, b et c de la [figure 3.6](#) montrent un exemple de corrélation entre les valeurs mesurées et prédictes des températures journalières minimales, moyennes et maximales à la station *Granby*, située au centre de la région d'étude Montérégie Est.

Contrairement à la température de l'air, les précipitations sont caractérisées par une grande variabilité spatiale et temporelle et sont donc plus difficiles à estimer avec précision sur une base journalière. Néanmoins, les résultats obtenus en Montérégie Est avec la méthode sont satisfaisants. La RMSE et la MAE sont, respectivement, inférieures à 3.4 et 1.4 mm pour toutes les stations, alors que l'intensité des précipitations moyennes varie entre 6.4 à 7.6 mm/jour. Le coefficient de corrélation entre les valeurs estimées et mesurées est supérieur à 0.847 pour toutes les stations. Finalement, les valeurs estimées présentent un léger biais négatif, avec des erreurs moyennes qui varient entre –0.20 à 0.03 mm. Le graphique d de la [figure 3.6](#) montre un exemple de corrélation entre les valeurs mesurées et prédictes des précipitations totales journalières à la station *Granby*.

La tendance observée de la méthode à générer un biais négatif dans les estimations des précipitations totales (15 des 19 stations sont caractérisées par une ME légèrement négative) est une indication de l'asymétrie positive dans la distribution des événements de précipitations. Les valeurs estimées ont alors tendance à se regrouper autour de l'erreur médiane plutôt que l'erreur moyenne. La [figure 3.7](#) montre un exemple de la distribution des précipitations quotidiennes à la station *Granby* qui illustre bien cette asymétrie positive (aire bleue claire). C'est pour cette raison que les techniques basées sur la régression linéaire, qui permettent de préserver la moyenne, ont tendance à sous-estimer systématiquement l'amplitude des événements de forte intensité. Ceci est également illustré sur la [figure 3.7](#) qui compare les fonctions de répartition gamma entre les précipitations estimées (ligne rouge pointillée) et mesurées (ligne bleue continue) à la station *Granby*. Concrètement, ceci implique que des erreurs importantes peuvent être associées à des événements de fortes précipitations estimés avec la méthode. Toutefois, ceux-ci sont habituellement peu fréquents.

Pour les mêmes raisons, le nombre de jours pluvieux (jours avec des précipitations) est également surestimé par la méthode. Les résultats obtenus par la validation croisée ont montré qu'en moyenne, le nombre de jours pluvieux est surestimé de 29 % (+43 jours par année), avec une valeur minimale de 13 % (+26 jours par année) et maximale de 53 % (+72 jours par année). Ces résultats ont été

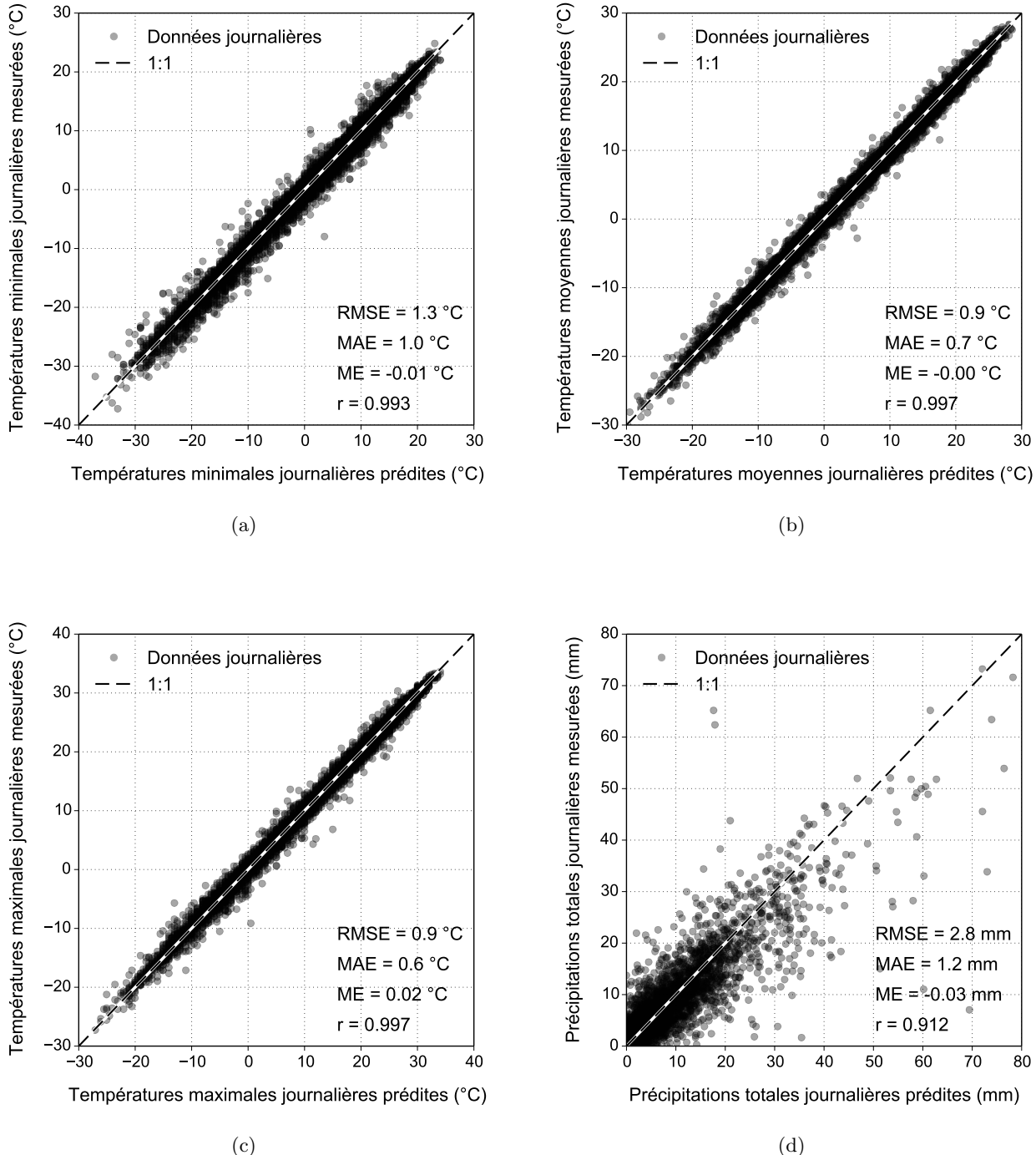
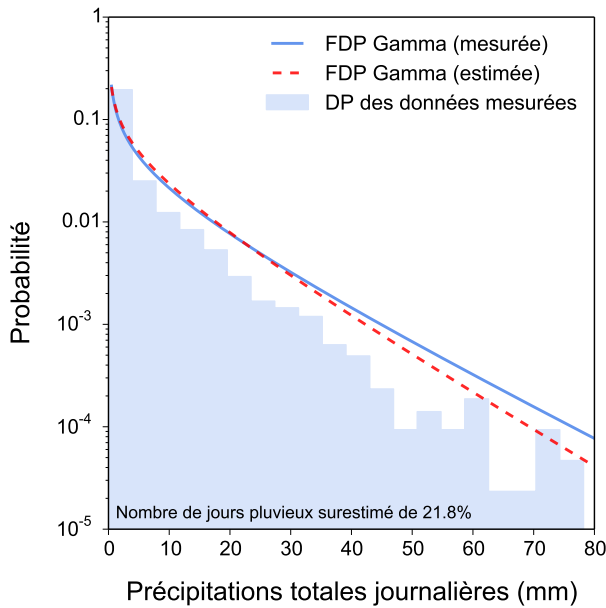


Figure 3.6 – Nuages de points comparant les valeurs estimées et mesurées des températures de l'air (a) minimales, (b) moyennes, (c) maximales et des (d) précipitations journalières à la station *Granby* située au centre de la région d'étude.

**Figure 3.7**

Fonctions de densité de probabilité (FDP) gamma obtenues à partir des précipitations journalières estimées (ligne pointillée rouge) et mesurées (ligne pleine bleue) à la station météorologique *Granby*. L'histogramme de la densité de probabilité (DP) des événements mesurés de précipitations est également représenté en bleu clair.

obtenus en considérant qu'un jour était dit “pluvieux” lorsque les précipitations pour ce jour étaient supérieures à 0 mm/jour. Bien que cela se traduise par de petites erreurs sur les précipitations totales d'une année, cela peut avoir des implications importantes pour les modèles de bilan en eau de surface qui, parfois, ne permettent pas l'évapotranspiration pendant les jours pluvieux. Pour limiter l'impact de cette surestimation, une valeur seuil de 0.5 mm/jour (au lieu de 0 mm/jour) peut être utilisée pour partitionner les jours secs et pluvieux. La surestimation des jours pluvieux devient alors en moyenne de 9 % (+12 jours par année) et varie entre 0.7 % (+1 jours par année) à 18.2 % (+20 jours par année) d'une station à l'autre.

[Simolo et al. \(2010\)](#) ont proposé une procédure en deux étapes pour limiter la surestimation du nombre de jours pluvieux et la sous-estimation de l'amplitude des événements de précipitations de forte intensité avec la méthode MLR. Toutefois, ces derniers n'ont pas comparé leur méthode améliorée avec l'approche conventionnelle. Les résultats présentés dans cette étude soulignent bien les limites de la méthode MLR et suggèrent que l'approche proposée par [Simolo et al. \(2010\)](#) soit intégrée et testée dans une future version de PyGWD. Par ailleurs, la routine de validation croisée intégrée dans PyGWD devrait faciliter la comparaison des résultats avec et sans les modifications proposées par [Simolo et al. \(2010\)](#).

De plus, selon [Xia et al. \(1999\)](#), les deux facteurs les plus importants pour l'estimation des valeurs météorologiques journalières sont les intercorrélations entre les stations et les variations saisonnières

dans les relations entre les stations. Le dernier point n'a pas été abordé dans ce travail puisque les modèles de régression sont générés dans PyGWD en utilisant toutes les données disponibles. Une autre approche, qui devrait être considérée dans une future version de PyGWD, consisterait à partitionner les données sur une base saisonnière pour calculer les coefficients de corrélation et les modèles de régression. Cela permettrait une meilleure représentation des variations saisonnières dans les relations entre les stations. Les inconvénients comprennent un algorithme plus complexe à mettre en oeuvre, une réduction de la robustesse de la méthode et de plus longs temps de calcul.

Chapitre 4

Conclusion

Cette thèse de doctorat propose des développements méthodologiques et de logiciels pour l'estimation de la recharge et de son incertitude à partir de séries de données temporelles. Deux méthodes d'estimation de la recharge ont été traitées dans deux volets distincts de la thèse. La première méthode permet d'estimer des taux de recharge potentielle à partir de mesures temporelles de la température dans la zone thermique superficielle et non saturée du sol. La seconde consiste à combiner un bilan hydrologique de surface avec un bilan en eau d'un aquifère libre pour estimer des taux de recharge quotidiens à partir de mesures journalières des précipitations totales, de la température de l'air et des niveaux d'eau mesurés dans un puits d'observation. Les travaux réalisés dans le cadre de la thèse ont permis de mieux caractériser l'incertitude et les limites d'applicabilité de chacune des méthodes, d'incorporer des techniques modernes d'assimilation des données et d'adapter les méthodes aux contextes climatiques et hydrogéologiques retrouvés au Canada.

4.1 Traçage thermique

Les travaux du volet portant sur le traçage thermique ont été initiés par des résultats peu concluants obtenus dans le cadre d'un travail appliqué qui consistait à estimer des taux annuels de la recharge diffuse à partir de séries temporelles de la température du sol. Une revue exhaustive des travaux publiés sur ce sujet a par la suite permis de constater que peu d'études avaient été réalisées sur

l'estimation de la recharge diffuse à partir de mesures de températures dans la zone thermique superficielle du sol pour les climats froids et humides.

Une étude de sensibilité préliminaire réalisée sur des cas théoriques simples a par la suite permis de mieux comprendre l'impact de la recharge diffuse sur les températures de sous-surface. Les résultats obtenus lors de cette étude ont démontré que l'approche analytique de [Stallman \(1965\)](#) permettant d'estimer des taux annuels de la recharge n'était pas bien adaptée pour l'estimation de la recharge dans la zone non saturée. Il a alors été suggéré que la résolution du flux d'écoulement devrait être faite par l'inversion d'un modèle numérique de transport advectif et conductif de la chaleur sur des périodes de temps plus courtes permettant de mieux représenter le patron d'écoulement dans la zone non saturée. De plus, les résultats ont démontré que l'impact du flux d'eau en conditions de recharge diffuse sur les températures de sous-surface était très faible. Considérant les nombreuses sources potentielles d'erreurs provenant des mesures et des paramètres du modèle inverse de transport de la chaleur, ces résultats suggéraient qu'une incertitude importante pouvait être associée à l'estimation de la recharge avec cette approche.

Dans le but de tester ces hypothèses, un modèle inverse du transport vertical de la chaleur par advection et conduction, adapté à la zone non saturée et aux climats froids et humides, a été développé. Ce dernier a ensuite été utilisé pour estimer la recharge à partir de données synthétiques réalistes produites avec le simulateur SHAW (Simultaneous Heat and Water model) sur une base hebdomadaire, mensuelle, semi-annuelle et annuelle. Ceci correspond à une amélioration importante de la méthode par rapport à l'approche analytique de [Stallman \(1965\)](#) généralement utilisée pour ce genre d'analyse qui ne permet l'estimation de la recharge que sur une base annuelle. Les résultats de cette étude ont confirmé que la résolution du flux d'écoulement sur une base hebdomadaire par l'inversion d'un modèle numérique de transport advectif-conductif de la chaleur permettait d'améliorer la précision des valeurs de recharge estimées. La méthode présentée dans cette thèse permet d'estimer la recharge avec une incertitude raisonnable (moins de 20 %) lorsque les taux annuels sont supérieurs à 200 mm/a. Toutefois, ces résultats ne sont valides qu'en conditions idéales, c'est-à-dire en considérant les valeurs des paramètres du modèle comme connues *a priori* et en supposant qu'il n'y ait aucune incertitude sur les températures mesurées. Toutefois, des analyses de sensibilité ont démontré qu'une incertitude considérable pouvait être associée aux taux de recharge estimés lorsque l'incertitude sur les paramètres du modèle inverse et les erreurs de mesure des séries de températures étaient prises en compte. Ces résultats suggèrent que cette méthode n'est pas

applicable dans la grande majorité des cas pour évaluer des taux de recharge diffuse, à moins que les propriétés et la température du sol soient connues avec précision. Cela est dû principalement au faible impact de l'écoulement de l'eau sur les variations des températures du sol lorsque le flux d'écoulement est inférieur à 1000 mm/a. Le système thermique de sous-surface dans la zone superficielle est dans ces conditions principalement contrôlé par la conduction de la chaleur.

Dans de futurs travaux, il serait intéressant de tester la méthode en laboratoire sur des colonnes de sol dont les propriétés hydrogéologiques et thermiques auraient été caractérisées de façon indépendante. Une autre approche qui pourrait être testée sur le terrain consisterait à soumettre un système de mesure thermique, constitué de sondes de température enfouies à différentes profondeurs dans le sol, à un flux d'écoulement d'eau artificiel et connu. Connaissant le flux d'écoulement, il serait alors possible de déduire les propriétés du sol. Le système de mesure ainsi étalonné pourrait ensuite permettre d'estimer la recharge avec la méthode présentée dans cette thèse.

4.2 Bilans hydrologiques combinés

4.2.1 Estimation de la recharge

Ce deuxième volet de la thèse a porté sur le développement méthodologique et d'outils logiciels pour l'application et l'amélioration d'une méthode d'estimation de la recharge présentée par [Lefebvre et al. \(2011\)](#). Cette méthode est basée sur le calage d'un bilan hydrologique de surface couplé à un bilan en eau d'un aquifère libre à des mesures du niveau d'eau dans un puits d'observation et requiert également des mesures journalières continues de la température de l'air et des précipitations totales.

Dans le cadre de ces travaux, le tableur Excel développé par [Lefebvre et al. \(2011\)](#) pour l'application de la méthode a d'abord été converti dans le langage de programmation Python. Ceci a permis de faciliter l'automatisation de la méthode et l'ajout de modifications basées sur des techniques de calcul plus complexe dont l'implémentation dans Excel aurait été plus difficile. Par la suite, un modèle pour simuler la fonte de la neige accumulée à la surface du sol a été ajouté au bilan hydrologique de surface. Ceci est une amélioration importante par rapport à la méthode présentée dans [Lefebvre et al. \(2011\)](#) où toute la neige accumulée en surface était fondue instantanément dès que la température de l'air dépassait un certain seuil. Cela ne permettait pas de bien représenter

la fonte au printemps, ni les redoux de la température durant la période hivernale. Ensuite, un algorithme a été développé dans Python pour estimer de façon précise et automatisée la courbe maîtresse de récession à partir des hydrogrammes de puits observés. Ceci constitue une contribution majeure puisque la courbe maîtresse de récession était auparavant estimée graphiquement. Enfin, la méthode d'optimisation GLUE (*Generalized Likelihood Uncertainty Estimation*) a été utilisée pour automatiser l'estimation de la recharge et évaluer son incertitude. Ceci constitue une contribution majeure par rapport à la méthode originale où l'optimisation de la recharge était faite manuellement par essai et erreur et où l'incertitude était estimée de façon plus ou moins arbitraire.

La méthode ainsi améliorée a été testée avec des mesures de niveaux d'eau dans un puits d'observation situé à Pont-Rouge, dans l'aquifère deltaïque de la région de Portneuf, près de Québec, où plusieurs études ont été réalisées au cours des dernières années, dont celle de [Larose-Charette et al. \(2000\)](#) et [Lefebvre et al. \(2011\)](#). La recharge annuelle moyenne a été estimée à 286 mm/a et des valeurs limites pour l'intervalle de confiance de 5 à 95 % de 223 et 384 mm/a ont été établies. Cela correspond à une plage de l'incertitude moyenne de 161 mm/a, ce qui représente une réduction de l'incertitude de plus de 40 mm/a par rapport à celle estimée par [Larose-Charette et al. \(2000\)](#). De plus, l'application de la méthode a permis de réduire les plages des paramètres qui avaient été établies *a priori* pour RAS_{max} et C_{RO} par [Larose-Charette et al. \(2000\)](#). L'incertitude sur la recharge pourrait même être réduite davantage par une meilleure connaissance préalable des plages de valeurs plausibles des paramètres hydrologiques du modèle, à l'aide de travaux en laboratoire ou sur le terrain. Les résultats ont également montré que l'enveloppe des niveaux d'eau estimée avec GLUE pour l'intervalle de confiance de 5 à 95 % ne permet pas d'englober toutes les mesures puisque les fluctuations à court terme ne sont pas toujours bien représentées par le modèle.

Plusieurs pistes ont été proposées pour améliorer la méthode dans de futurs travaux. Entre autres, l'incertitude sur la définition de la courbe maîtresse de récession devrait être prise en compte dans la résolution du problème d'optimisation avec la méthode GLUE. Le modèle de fonte de la neige, qui a été ajouté pour améliorer le modèle de [Lefebvre et al. \(2011\)](#), pourrait être complexifié davantage de façon à mieux caractériser les paramètres de ce dernier à partir des données météorologiques déjà requises pour l'application de la méthode. Des travaux pourraient également être réalisés pour développer une méthodologie permettant de mieux définir les plages de valeurs plausibles des paramètres hydrologiques du modèle. Finalement, il serait bénéfique de tester l'approche avec des

données de niveaux d'eau synthétiques produites avec un modèle couplé complexe comme CATHY (CATchment HYdrogeological model).

4.2.2 Comblement des données météorologiques journalières manquantes

Outre l'estimation de la recharge, une partie importante des travaux présentés dans ce volet de la thèse a porté sur le comblement automatisé des valeurs manquantes dans les séries de données météorologiques quotidiennes. Cela était d'intérêt dans le cadre de ce projet, car des données journalières continues de précipitations et de la température du sol sont nécessaires pour l'application de la méthode discutée à la section précédente.

Un algorithme nommé PyGWD (Python Gap-filling Weather Data algorithm) a donc été développé dans le langage de programmation Python. L'algorithme a été testé sur un réseau de 19 stations météorologiques situées en Montérégie Est et validé avec de la validation croisée. Les résultats obtenus ont montré que la méthode permet d'estimer de façon adéquate les valeurs manquantes pour les températures minimales, moyennes et maximales de l'air et les précipitations totales pour les 19 stations testées. Cet algorithme permet de faciliter grandement l'application de la méthode d'estimation de la recharge discutée précédemment. De plus, une fois publié, il pourra être utile à des applications dans des domaines autres que l'hydrogéologie, tels que l'agronomie et l'hydrologie.

Toutefois, les travaux de validation de l'algorithme ont souligné certaines limitations de l'approche pour l'estimation des précipitations quotidiennes. La méthode de régression linéaire multiple utilisée dans l'algorithme a tendance à sous-estimer systématiquement l'amplitude des événements de forte intensité. Concrètement, ceci implique que des erreurs importantes peuvent être associées à des événements de fortes précipitations estimés avec la méthode, qui sont toutefois peu fréquents. Le nombre de jours pluvieux (jours avec des précipitations) est également surestimé par la méthode. Bien que cela ne se traduise que par de petites erreurs sur les précipitations totales d'une année, cela peut avoir des implications importantes pour les modèles de bilan en eau de surface qui, parfois, ne permettent pas l'évapotranspiration pendant les jours pluvieux.

Des travaux futurs ont été proposés pour améliorer l'approche et pallier les limitations qui ont été mises en évidence par ces travaux. Entre autres, l'approche en deux étapes proposée par Simolo

et al. (2010) pour limiter les problèmes discutés ci-dessus pourraient être intégrée et testée dans une future version de PyGWD.

4.2.3 Logiciel WHAT

Enfin, un logiciel nommé WHAT (*Well Hydrograph Analysis Toolbox*) a également été développé pour faciliter l'application des différentes étapes de la méthode d'estimation de la recharge discutée à la [section 4.2.1](#).

Notamment, le logiciel comprend une interface graphique pour: a) le téléchargement et la mise en forme des données météorologiques disponibles sur le site internet du gouvernement du Canada, b) l'estimation automatisée des données manquantes dans les séries journalières de données météorologiques avec la méthode discutée à la [section 4.2.2](#), c) le traçage des hydrogrammes de puits avec les données météorologiques dans un format facilitant l'interprétation visuelle des données, d) l'estimation de la courbe maîtresse de récession à partir des données de niveaux d'eau et e) l'estimation de la recharge en combinant les données météorologiques et les données de niveau d'eau.

Un des objectifs des travaux de ce volet du doctorat était de faciliter l'estimation de la recharge à partir de données météorologiques et de niveaux d'eau dans les puits d'observation, qui sont désormais de plus en plus facilement accessibles. Les innovations apportées par les travaux de ce volet de la thèse permettent d'estimer facilement et rapidement des taux de recharge et leur incertitude, ce qui constitue une contribution majeure par rapport à la majorité des approches existantes. En effet, l'évaluation de l'incertitude est souvent une étape négligée ou complètement omise dans les travaux de caractérisation des eaux souterraines même s'il est généralement reconnu que la recharge peut varier grandement dans le temps et l'espace.

Pour le futur, le logiciel WHAT devra être complété. D'autres outils pourraient être également être ajoutés à ce dernier, tel qu'un outil pour faire l'interprétation de la réponse barométrique des puits. Le logiciel devra ensuite être testé dans plusieurs contextes hydrogéologiques et le guide de l'utilisateur devra être terminé.

Deuxième partie

Articles

Article 1

Applicability of temperature profile techniques for estimating recharge fluxes through the vadose zone

Titre traduit

Applicabilité des techniques d'estimation de la recharge basées sur des profils de températures dans la zone non saturée.

Auteurs

Jean-Sébastien Gosselin¹, Christine Rivard², Richard Martel¹ et Claudio Paniconi¹

¹ Institut national de la recherche scientifique, Centre Eau Terre Environnement, 490 rue de la Couronne, Québec, QC, Canada

² Commission Géologique du Canada, Division Québec, 490 rue de la Couronne, Québec, QC, Canada

Publié

GeoHydro2011, Joint IAH-CNC, CANQUA and AHQ conference proceedings
août 2011

Résumé

La recharge des eaux souterraine est difficile à quantifier. Pour cette raison, l'application de plusieurs méthodes est généralement recommandée. La température du sol peut être mesurée facilement et à faibles coûts. Ces mesures pourraient ainsi représenter un outil utile pour l'estimation de la recharge. Dans cet article, l'applicabilité d'une approche pour calculer les flux d'eau verticaux dans la zone non saturée (recharge potentielle) à partir de séries temporelles de températures a été étudiée avec un modèle numérique simple du transport vertical conductif et advectif de la chaleur. Les résultats suggèrent que l'impact du flux d'écoulement de l'eau est petit dans un contexte de recharge diffuse et difficile à distinguer des autres influences potentielles. De plus, il a été démontré que les modèles analytiques ne sont pas appropriés pour estimer des taux de la recharge diffuse à partir de mesures de la température du sol dans la zone non saturée.

Abstract

Groundwater recharge is difficult to assess. For this reason, the use of multiple methods is generally recommended. Temperature can easily and cheaply be measured in soils and could represent a valuable tool for the estimation of groundwater recharge. In this paper, the applicability of using near-surface temperature time series for deriving vertical water fluxes in the vadose zone (potential recharge) was investigated using a simple numerical model of 1Dz advective-conductive heat transport. The results suggest that the impact of the vertical water flux, in a context characterized by 400 mm/y of diffuse recharge, is small and difficult to distinguish from all the other potential sources of errors (modeling and measurement). Moreover, it was demonstrated that the current existing analytical approaches are not well suited for the estimation of diffuse recharge rates from temperature measurements in most cases.

1 Introduction

It is, nowadays, general knowledge in hydrogeology that heat is transported in the subsurface not only by conduction, but also by advection with groundwater movement. More specifically, the heat carried downward by the groundwater flux modifies the soil vertical temperature profile and its variation with

time. Therefore, there is a direct relationship between the transient temperature distribution and the vertical flow of water in the subsurface. From a theoretical point of view, potential groundwater recharge rates can thus be deduced from subsurface temperature measurements. Heat could indeed be a tracer well suited for this purpose because it has a natural dynamic signal and also because temperature can be cheaply and easily monitored in soil, in contrast to most other environmental or applied tracers used in these kinds of studies.

Estimation of the vertical groundwater flux from the analysis of transient subsurface temperature measurements was introduced in the literature by [Suzuki \(1960\)](#) who presented an approximate analytical solution of the transient 1Dz advective-conductive heat transport equation in soil constrained with an idealized sinusoidal temperature condition at the surface. The method he developed was meant to be used for estimating in situ percolation rates from near surface temperature measurements under irrigated rice paddy fields. [Stallman \(1963, 1965\)](#) subsequently extended Suzuki's work by developing the exact analytical solution for Suzuki's case and by presenting a method to estimate vertical groundwater flux from transient temperature measurements with the new equation he developed. Concurrently, [Bredehoeft & Papadopoulos \(1965\)](#) introduced a method to estimate steady-state vertical percolation rates across an aquitard using a time-point temperature-depth profile measured in the geothermal zone, where the soil's temperature is mostly isolated from the influence of climate. These pioneering theoretical works were the foundation on which subsequent groundwater studies using heat as a tracer were based. Thereafter, the use of heat as a tracer for groundwater flux estimation has been extended to a wide variety of hydrogeological settings. Among others, this approach has been increasingly used to assess groundwater-surface water interactions beneath streams and large surface water bodies (e.g. [Stonestrom & Constantz, 2003](#)).

In contrast, methods based on heat transport analysis have not been commonly used to estimate diffuse groundwater recharge rates, and the literature on this specific subject is scarce. [Taniguchi \(1993\)](#) was among the first to present a practical application of vertical groundwater flux estimation from transient temperature-depth profiles, following the theoretical studies presented by [Suzuki \(1960\)](#) and [Stallman \(1965\)](#) nearly 30 years before. Works prior to [Taniguchi \(1993\)](#) focused mainly on the estimation of groundwater flux from steady-state temperature-depth profiles in relatively deep aquifers located in the geothermal zone as introduced by [Bredehoeft & Papadopoulos \(1965\)](#) (e.g. [Sorey, 1971](#); [Boyle & Saleem, 1979](#)). In contrast, [Taniguchi \(1993\)](#) calculated steady upward and downward groundwater fluxes in a relatively shallow aquifer in Japan by fitting transient

temperature-depth profiles measured in boreholes to type curves he had derived from the analytical solution developed by [Stallman \(1965\)](#). Annual steady groundwater fluxes estimated at two point locations with this type-curve fitting technique showed good agreement in magnitude with values obtained from hydraulic gradient calculations.

Using an approach similar to the one presented by [Taniguchi \(1993\)](#), [Tabbagh *et al.* \(1999\)](#) estimated steady water infiltration rates in the vadose zone on a yearly basis, from temperature data collected at meteorological stations in France. Other studies have been carried out since, using either an analytical (e.g., [Cheviron *et al.*, 2005](#); [Bendjoudi *et al.*, 2005](#); [Tabbagh *et al.*, 2009](#)) or a numerical solution (e.g., [Koo & Kim, 2008](#)). However, quantification of recharge using temperature measurements in the vadose zone have shown mixed success. Although the approaches presented in the aforementioned studies are theoretically rigorous and appealing, none have been able yet to derive systematic recharge estimates that agree well with observed precipitation or/and values obtained from other methods in a similar environment. These inconsistent results highlight the difficulties arising from the use of transient temperature measurements in the vadose zone to estimate diffuse recharge rates.

The objective of this paper is to examine if and how near-surface temperature time series could better be used to estimate vertical water fluxes in the unsaturated zone for the assessment of (potential) groundwater recharge. For this purpose, subsurface temperatures were simulated with a simple numerical model of 1Dz advective-conductive heat transport for three theoretical cases characterized by increasing variability, both in time and in magnitude, of the groundwater recharge monthly fluxes over a year. All of the three cases were developed with an annual groundwater recharge of 400 mm/y. The impact of percolating water on the simulated temperatures was then assessed by comparing the results for each case with that of a conduction-case solution, for which the water flux was set to zero in the model. The results showed that the subsurface temperatures were not significantly affected by the downward flow of water for each of the three cases tested. This indicates that the uncertainty on groundwater recharge estimates derived from near-surface temperature time series could potentially be very large. Moreover, the results suggest that the use of a numerical model is better suited for the application of the method than the analytical model of [Stallman \(1965\)](#) when the water flux is variable over time, which is often the case in the vadose zone.

2 Theoretical basis and literature review

In this paper, the word “soil” is used to denote an unsaturated porous medium formed by a rigid matrix of solid particles filled with air and water. The transient 1Dz advective-conductive heat transport equation in soil can be written as follows ([Bear, 1972](#)):

$$C_{soil} \frac{\partial T_{soil}}{\partial t} = \frac{\partial}{\partial z} \left(k_{soil} \frac{\partial T_{soil}}{\partial z} \right) - q_w C_w \frac{\partial T_{soil}}{\partial z} \quad (1)$$

where q_w is the vertical volumetric flux water (m/s) taken as positive downward, k_{soil} and C_{soil} are, respectively, the bulk thermal conductivity (W/m °C) and the volumetric heat capacity (J/m³ °C) of the soil, C_w is the volumetric heat capacity (J/m³ °C) of pure water and T_{soil} is the soil temperature (°C). The soil is assumed to be in local thermodynamic equilibrium, meaning that the temperature of adjoining water, air, and solid particles are assumed equal at all times.

The soil volumetric heat capacity can be expressed as a simple additive mixing law ([Farouki, 1981](#)):

$$C_{soil} = (1 - n)C_s + \theta_w C_w \quad (2)$$

where n is the soil’s total porosity, θ_w is the volumetric water content, and C_s is the volumetric heat capacity (J/m³ °C) of the soil’s solid particles. The soil bulk thermal conductivity can be approximated by a geometric mixing law ([Farouki, 1981](#)):

$$k_{soil} = k_s^{1-n} \cdot k_w^{\theta_w} \cdot k_a^{n-\theta_w} \quad (3)$$

where k_s , k_w , and k_a refer, respectively, to the thermal conductivities of the solid particles, water, and air.

In order to solve the heat transport in unsaturated soils, a time- and space-dependent definition of q_w and θ_w is required. This can be done by coupling [equation \(1\)](#) to Richards equation. However, as highlighted by [Koo & Kim \(2008\)](#), solving the coupled process of heat and water flow in the vadose zone makes the inverse problem computation much more complex and difficult and adds input parameters along with their inherent uncertainties. Therefore, the heat transport equation is generally simplified by assuming that the soil thermophysical properties are homogeneous in space

and constant during a certain period of time. This reduces [equation \(1\)](#) to the form originally presented in [Suzuki \(1960\)](#):

$$\frac{\partial T_{soil}}{\partial t} = \frac{k_{soil}}{C_{soil}} \frac{\partial^2 T_{soil}}{\partial z^2} - q_w \frac{C_w}{C_{soil}} \frac{\partial T_{soil}}{\partial z} \quad (4)$$

As presented in [Stallman \(1965\)](#), by assuming a sinusoidal temperature fluctuation at the model's uppermost boundary, it is possible to derive an exact analytical solution for [equation \(4\)](#). This solution can be afterwards directly used for computing vertical water fluxes from transient-temperature measurements taken at two different depths as done by [Taniguchi \(1993\)](#). However, a perfect sinusoidal temperature variation is a condition that is never encountered in natural conditions on a daily or annual cycle. This alone, as explained further below, limits greatly the applicability of analytical approaches for water flux estimation from temperature measurements in the vadose zone.

First of all, the daily atmospheric temperature oscillation is only measurable down to a depth of 0.1 to 0.3 m. At this depth, other heat transfer mechanisms, such as radiation, and processes involving latent heat consumption or liberation, such as freezing, thawing, or evaporation, are likely present and may have an impact on heat transfer of the same magnitude as the one by advection of water. Also, plant water uptake can be an important component of the water flow balance that would thus need to be accounted for. Hence, estimation of water flow rates from daily temperature variations measured in the first 0.3 m of the subsurface is a quite complex exercise that would be difficult to perform within a reasonable uncertainty range given all the processes involved.

Thus, for these reasons, analytical approaches are mostly limited to the estimation of steady-state vertical water fluxes on a yearly basis. This assumption is likely acceptable for groundwater-surface water interactions assessment where there is a continuous overlying source of water feeding the aquifer and is also probably correct for vertical groundwater flux estimation in the saturated zone. In these contexts, it is assumed that the fluctuations of the vertical flux of water over time do not depart too much from the annual mean, and therefore, recharge rates may be considered uniform throughout the year. However, this assumption is arguable for the vadose zone because water infiltration is more of a pulse-like flux, strongly related to short time-scale precipitation events compared to a uniform time-distributed flux. In addition, recharge is known to vary significantly from one season to another throughout the year. This could be the cause of errors, as will be shown later, when computing water fluxes with an analytical model.

Numerical models do not have the limitations discussed above and represent a way to address some of the problems encountered with the analytical approaches. For this purpose, [Keshari & Koo \(2007\)](#) introduced a simple numerical model based on [equation \(4\)](#) that can be used to simulate conductive-advection heat transport in the subsurface with any temperature condition at the surface. Although groundwater flow through the vadose zone is still considered in steady-state during a certain period of time, the length of this period is not restricted to the annual temperature cycle. This allows the computation of the inverse problem over periods of time that match more closely the infiltration events resulting from precipitation.

In this regard, [Koo & Kim \(2008\)](#) used [Keshari & Koo \(2007\)](#)'s model to solve the inverse problem from temperature measurements taken in the vadose zone of a site located in Korea. In order to take into account the seasonal weather patterns of their study area, they partitioned their analysis into three periods per year, based on the intensity of the observed precipitation. Afterwards, they calibrated their model output to the measured temperatures over each segment by optimizing two lumped parameters defined as k_{soil}/C_{soil} and $q_z C_w/C_{soil}$. They were able to successfully demonstrate a linear relationship between the lumped parameters and precipitation intensity, thus demonstrating the importance of considering the temporal variability of the water flux when dealing with the unsaturated zone. However, no value of groundwater recharge was actually computed in their study, since only the lumped parameters were evaluated. Therefore, they were not able to validate their approach or compared it with results obtained from other groundwater recharge assessment techniques.

A numerical inverse heat transport model is usually constrained at its uppermost boundary with a Dirichlet condition using a measured temperature time series. As discussed earlier, the depth of this boundary should be located below the root zone to exclude other transport mechanism effects from the computations. A second set of temperature measurements is also needed to constrain the model at its lowermost boundary with a Dirichlet condition. Alternatively, a no-heat-flux condition could be used if the lower boundary is located sufficiently deep, i.e. in the geothermal zone (>10 m below the ground surface). Finally, at least one additional temperature time series must be acquired between the model's boundaries for optimization purposes. Solving the inverse problem consists of best-fitting the temperatures simulated with the model to the ones measured in-between the model boundaries by searching for the optimal value of the water flux (thus considered a constant model parameter) over a given period of time. The length of the period over which the water flux

is resolved must be chosen carefully. On one hand, it must be sufficiently large to contain enough measurement points, so that the computation is not too sensitive to measurement errors ([Zhang & Osterkamp, 1995](#)). On the other hand, it must be sufficiently small so that it is representative of the observed seasonal recharge pattern.

Despite the fact that [Koo & Kim \(2008\)](#)'s results suggest an improvement of the numerical approach over the analytical one, the use of a numerical model for water flux estimation in the vadose zone is still challenging for real-life applications. In the following sections, we present simulation results from a simple subsurface heat transport model that highlight some of the difficulties related to the interpretation of near-surface temperature time series in the vadose zone for the assessment of groundwater recharge.

3 Methodology

3.1 Description of the numerical model

The advective-conductive heat transport numerical model of [Keshari & Koo \(2007\)](#) was implemented in the Scilab programming language. The model is based on a finite difference discretization of [equation \(4\)](#) with an explicit MacCormack scheme ([Hoffman, 2001](#)). The numerical code was verified against the analytical equation of [Stallman \(1965\)](#).

The soil volumetric heat capacity, C_{soil} and thermal conductivity, k_{soil} were considered time-independent in the model. In reality, it is well known that these properties depend on the soil water content, θ_w , which varies throughout the year in a similar way as the recharge flux in the unsaturated zone ([Farouki, 1981](#)). In a case study, the value of θ_w should be defined in the model from in-situ measurements, or should be considered as a parameter to be optimized in the resolution of the inverse problem, in addition to the water flux. However, since this is not the goal pursued here, it is supposed, for the sake of simplicity, that θ_w is time-independent and equal to the soil residual saturation at all times. The values of C_{soil} and k_{soil} were then computed with [equations \(2\)](#) and [\(3\)](#) respectively using values taken from the literature for n , C_s , k_s , and θ_w that were representative of a fine to medium sand composed mainly of quartz minerals. The values of all the properties used for these calculations, as well as the resulting values of C_{soil} and k_{soil} , are presented in [table 1](#).

Note that the values of C_{soil} and k_{soil} presented in [table 1](#) are comparable to the ones used in the published studies that were cited in [sections 1](#) and [2](#) (e.g. [Taniguchi, 1993](#); [Tabbagh *et al.*, 1999](#); [Keshari & Koo, 2007](#)).

The model was constrained at its uppermost boundary ($z = 0.5$ m) using a temperature time series produced with an idealized sinusoidal function with a period of 365 days, an amplitude of 8 °C and a mean temperature of 12 °C. At the lowermost boundary of the model ($z = 15$ m), a constant temperature condition of 12 °C was imposed. These values were inspired by the atmospheric temperature record presented in [Bendjoudi *et al.* \(2005\)](#) for a meteorological station located in France.

The time and vertical numerical resolutions of the model were set, respectively, to 1 h and 0.25 m. The initial vertical temperature profile was determined using a spin-up procedure, i.e. by running the model for several year-cycles, using the final temperature vertical profile of a given run as the initial conditions of the next run.

Table 1 – Published values for the properties used for the calculation of C_{soil} and k_{soil} with [equations \(2\)](#) and [\(3\)](#). Values of n , C_s , k_s , and θ_w are representative of a fine to medium sand composed mainly of quartz minerals. The value given for θ_w corresponds to the soil residual saturation.

Soil Properties	Value	Reference
Volumetric water content, θ_w	0.16	Todd & Mays (2005)
Total porosity, n	0.42	Todd & Mays (2005)
Thermal conductivity (W/m °C)	Value	Reference
of soil solid particles, k_s	8.8	Williams & Smith (1991)
of water, k_w	0.6	de Vries (1966)
of air, k_a	0.024	de Vries (1966)
of soil, k_{soil}	1.2	equation (3)
Volumetric heat capacity (J/m ³ °C)	Value	Reference
of soil solid particles, C_s	2.1×10^6	Williams & Smith (1991)
of water, C_w	4.3×10^6	de Vries (1966)
of soil, C_{soil}	1.9×10^6	equation (2)

3.2 Description of the simulations

With the developed numerical model of heat transport described in [section 3.1](#), subsurface temperatures were simulated on an hourly basis, for three theoretical cases, over a period of 365 days between 0.5 to 15 m below the ground surface. Each case was characterized by a different monthly distribution of groundwater recharge, which were each equivalent to an annual groundwater recharge of 400 mm/y (see [figure 1](#)).

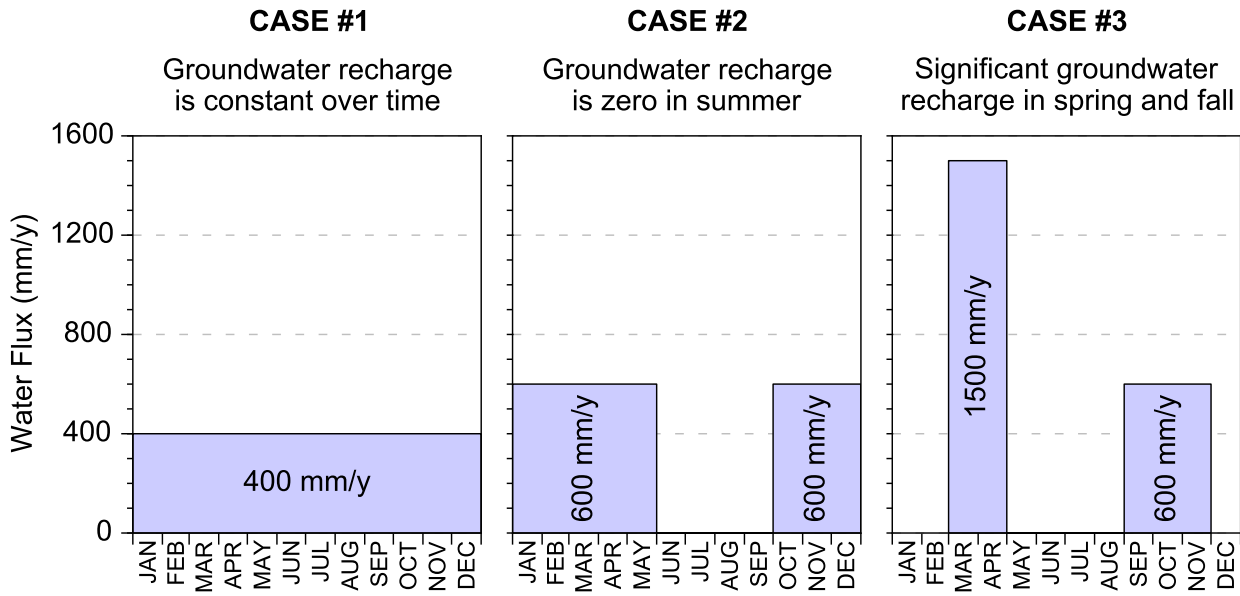


Figure 1 – Monthly distribution of groundwater recharge that were used as input to run forward simulations of advective-conductive heat transport with the model developed in [section 3.1](#). The monthly distribution for each of the three cases is equivalent to an annual groundwater recharge 400 mm/y

Case #1 was computed with a constant recharge flux of 400 mm/y. For Case #2, an annual recharge amount of 400 mm was uniformly distributed over the period going from October to May. A zero recharge flux was set for the months of June to September, simulating the limited amount of recharge that is usually observed during the summer. The Case #3 consisted of an annual recharge amount of 400 mm unevenly distributed over the spring and fall. A total amount of 250 mm was uniformly distributed over the months of March and April to represent the important recharge event that occurs during snow melt in cold climate. Similarly, a smaller recharge amount of 150 mm was

uniformly distributed over the months of September, October, and November to mimic recharge from significant rain events that frequently occur in the fall combined with the reduced evapotranspiration during this same period. For the other months, i.e. from December to February, and from May to August, a zero recharge flux was assigned in the model.

The purpose of these three sets of simulation was to better understand and illustrate the impact of a distinct seasonal recharge pattern on the transient subsurface temperature time series compared to a constant annual recharge flux case. To isolate the effect that the vertical groundwater flux had on the subsurface temperature variations, each simulation was compared with results from a conduction-case solution, for which q_w was set to 0 in the model. These results are presented and discussed in sections 4.1 and 4.2.

4 Results and Discussion

4.1 Case #1: constant recharge

The temperatures time series computed for the Case #1 ($q_w = Cte = 400 \text{ mm/y}$) are shown in the top graph of figure 2 (dotted black lines) for two annual cycles of 365 days at depths of 1.5, 3 and 5 m. The temperatures simulated for the conduction-case ($q_w = 0$) are also given for the same period (solid red lines).

The three graphs in the lower part of figure 2 present the temperature differences that were calculated between the temperature time series simulated for the Case #1 and those of the conduction-case scenario. These results show that for a given depth, the sensitivity of the subsurface temperatures to the water flux varies over time, and is even close to zero during certain periods of the year. Solving the water flux, by the inversion of the heat transport model, over these low sensitivity periods, can potentially result into large estimation errors due to the uncertainty on the observed temperatures and on the other input model parameters as well, such as the soil thermal conductivity, k_{soil} and its heat volumetric capacity, C_{soil} . Since the periods when the temperatures are insensitive to the water flux are not synchronous with depth, these results suggest that there may be a benefit to use multiple temperature time series acquired at various depths for the inversion of the heat transport model.

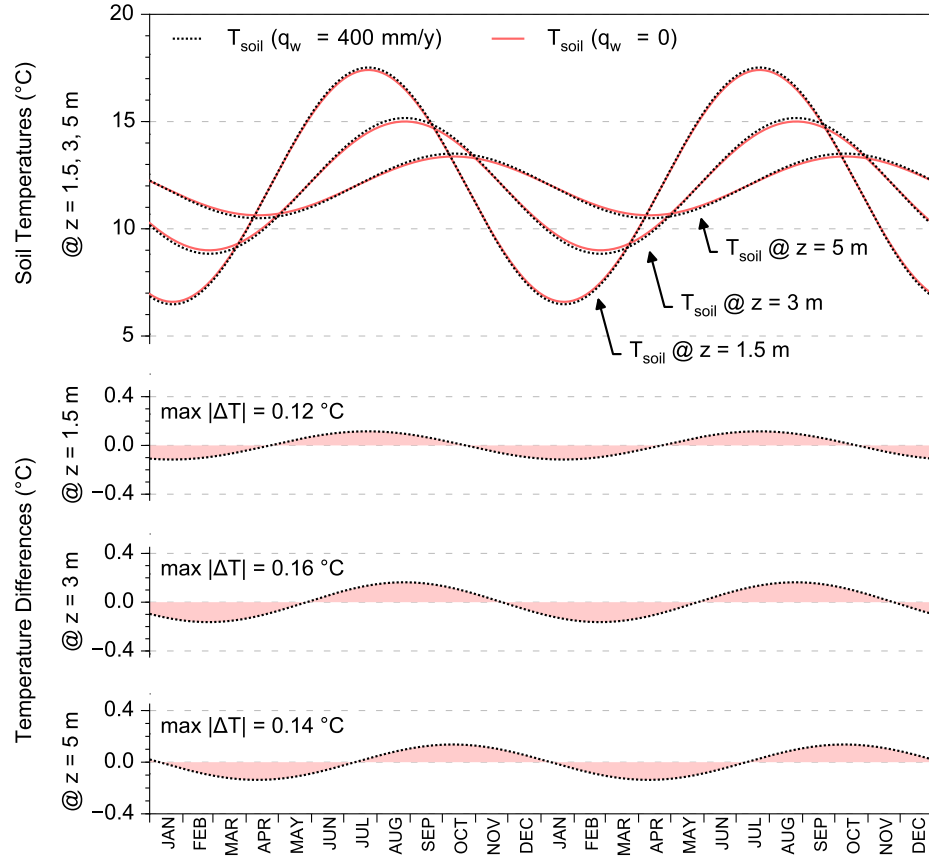


Figure 2 – Results for Case #1: constant recharge case. [TOP] Modeled temperatures at depths of 1.5, 3 and 5 m (dotted black lines), as well as the simulated temperatures for the conduction case (solid red lines). [Bottom] Temperature differences between the temperatures simulated for Case #1 and those of the conduction-case.

The results of figure 2 also highlight that the overall impact that the percolating water has on the subsurface temperatures is small, despite the relatively large annual recharge rate used for the simulation (400 mm/y). Indeed, the differences between the temperatures simulated for the Case #1 and that of the conduction-case are less than 0.2 °C, a value that is slightly above the 0.1 °C resolution of standard temperature probes available on the market. This observation was also made by Goto *et al.* (2005), who performed a sensitivity analysis of sea floor temperatures on the Mid-Atlantic Ridge to seepage fluxes. They found that the thermal response of the sediments to a constant vertical groundwater flux of about 1×10^8 m/s (~ 315 mm/y) was almost the same as the results obtained under pure heat conduction. As it will be further discussed in section 4.2, this represents an important limitation for the estimation of diffuse groundwater recharge rates from near-surface temperature time series, whether it is applied to the saturated or the vadose zone.

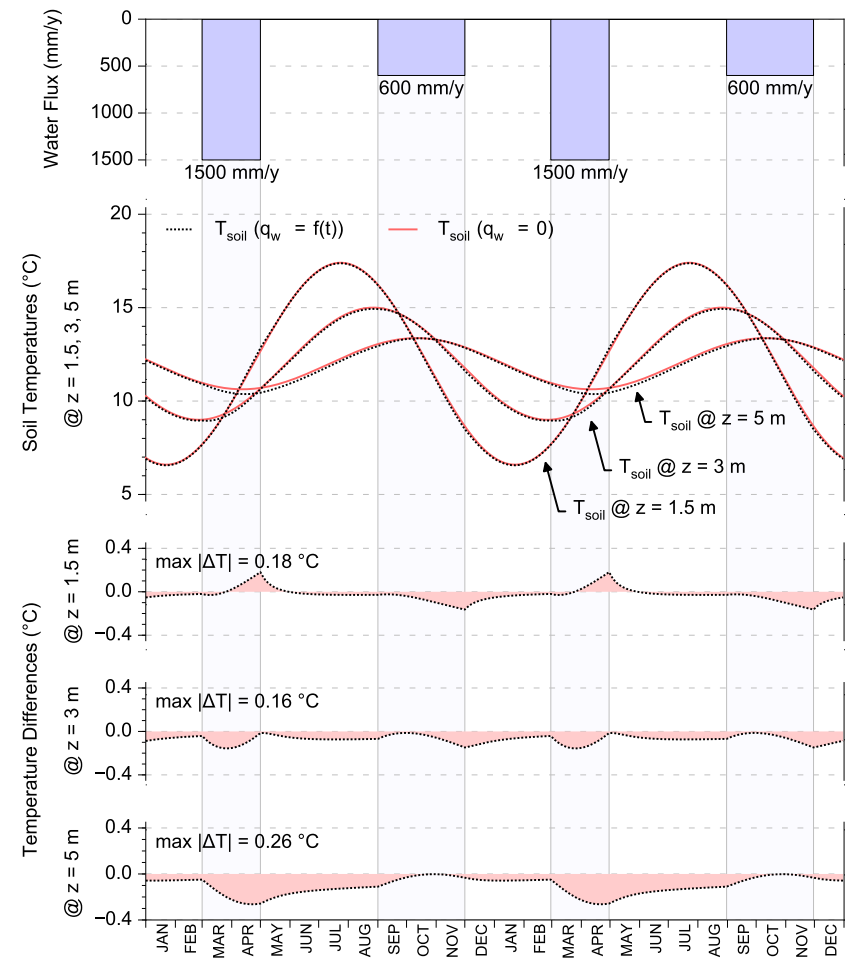
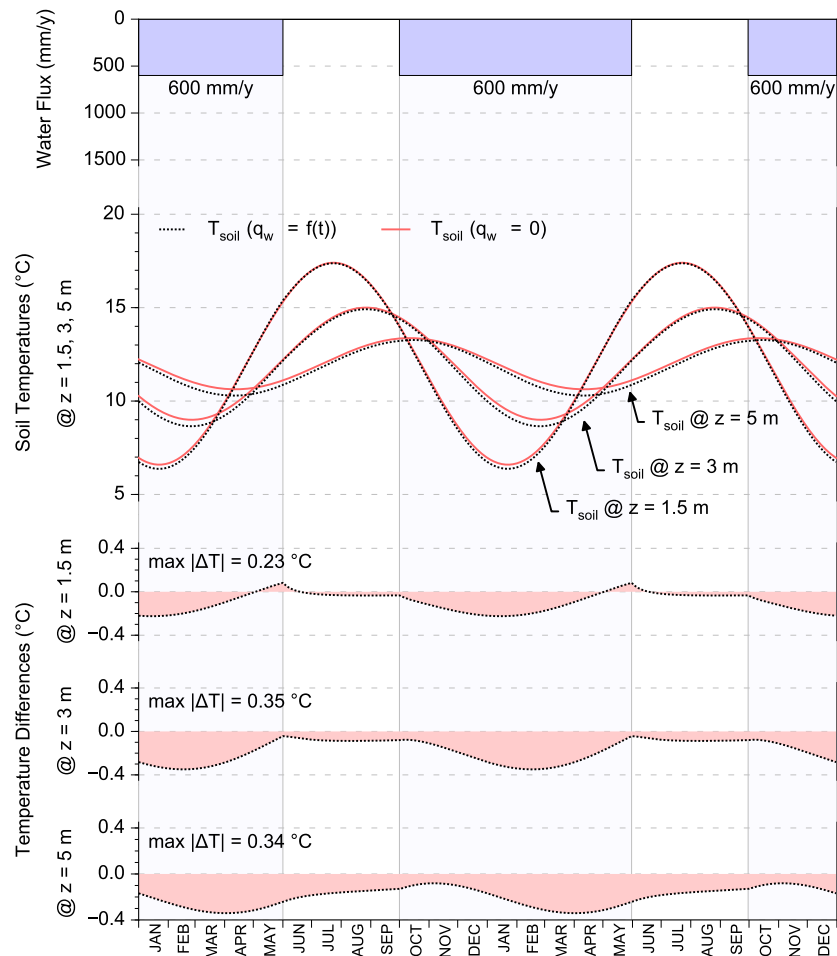
4.2 Case #2 and #3: variable monthly recharge

The results for Cases #2 and #3 are presented in [figures 3](#) and [4](#), respectively. The monthly groundwater vertical flux distribution is shown in the upper graph of both figures, while the simulated temperature times series are plotted in the middle graphs for the depths of 1.5, 3 and 5 m (dotted black lines), along with the results obtained for the conduction-case (solid red lines). The three graphs in the lower part of each figure show the temperature differences between the temperatures computed for each case and those of the conduction-case.

For Case #2, it can be seen that the deformation of the subsurface temperature annual cycle by the water flux is not anymore an ideal sinusoidal curve (see bottom graphs of [figure 3](#)), in contrast to the results presented for the Case #1 (see bottom graphs of [figure 2](#)). This is even more apparent when the seasonal variability of recharge becomes more important as it is illustrated in the bottom graphs of [figure 4](#) for the Case #3. These results suggest that the use of the analytical model of [Stallman \(1965\)](#) is likely not appropriate for the estimation of recharge from temperature time series measured in the vadose zone, where a seasonal variability of the vertical water flux is often present. This is due to the fact that the analytical model is limited to the estimation of steady states vertical fluxes on an annual basis, which limits the output to idealized sinusoidal annual temperature cycles. When comparing results of Case #1 with those of Cases #2 and #3, it is clearly evident that such an approach cannot reproduce appropriately the temperature perturbations that are caused by a water flux that is not in steady-state on a yearly basis. This suggests that the resolution of the inverse problem for the unsaturated zone should be done instead with a numerical model, over periods that match more closely the recharge pattern that is expected on the field.

Furthermore, similarly to what was observed for Case #1, the overall impact of the water flux on the temperature variations remains small, even with the significant recharge events of Case #3 during the 2-month period that simulates snowmelt (March and April). The maximal temperature differences computed are 0.35 °C and 0.26 °C, respectively for Case #2 and Case #3. The temperature differences are smaller for Case #3 than for Case #2 because groundwater recharge for Case #3 occurs mainly during periods of time where the subsurface temperatures are less sensitive to the water flux, as discussed previously in [section 4.1](#).

The small influence that the downward water flux has on the simulated temperatures can be explained by the small volumetric fluxes that occurs in a natural context of diffuse recharge. Under



these conditions, the conductive heat flux is more than 2 orders of magnitude higher than the advective heat flux. Hence, for this method to be fully functional for the assessment of diffuse recharge rates, temperature measurements with a resolution of more than 0.1 °C would be required. However, even then, reliable estimates are not guaranteed because of the likely possibility that other external or internal physical, chemical, and biological processes, not taken into account in the inverse model, have an influence of a similar order of magnitude than the water flux on the subsurface temperatures. In addition, the uncertainty of the temperature measurements and of the soil thermophysical properties (e.g. k_{soil} and C_{soil}), could also cause important errors on the estimation of the vertical water flux by the inversion of the heat transport model. All of these uncertainties (modeling, measurements, input model parameters), combined with the small impact that the vertical water flux has on the subsurface temperatures, strongly suggest that one must be careful when interpreting diffuse recharge estimates obtained by the interpretation of near-surface temperature time series because of the large uncertainty that can be associated with those values.

5 Conclusion

The objective of this work was to study the applicability of a diffuse recharge estimation method using near-surface temperature time series measured in the vadose zone. This study has first shown that analytical methods are likely not appropriate for applications to the vadose zone. This is due to the fact that these analytical approaches are limited to the estimation of a constant recharge flux on a yearly basis by fitting an idealized sinusoidal function to measured temperature time series at one or more depths. As demonstrated in this study, the subsurface temperatures are deformed in a non-sinusoidal manner when variability of recharge patterns increases, both in time and in magnitude. For this reason and due to other inherent limitations of these analytical methods, the results suggest that the inversion of a numerical model of heat transport over periods of time that match more closely the time-distribution of the vertical groundwater flux would be a more appropriate approach for the vadose zone.

Moreover, the numerical simulations performed for this study also pointed out the very limited sensitivity of the subsurface temperatures to the water flux in a context of diffuse recharge. Temperature differences, computed by comparing the simulated temperatures for each Case with those of a conduction-case solution (zero recharge), were less than 0.35 °C for all three cases tested,

despite an important annual groundwater recharge of 400 mm/y. Considering the uncertainty of the temperature measurements and the soil thermal properties, this low sensitivity can result in large estimation errors on groundwater recharge rates estimated with the heat-based technique that was investigated in this study.

This work has shown that further research efforts are needed to validate and improve diffuse recharge assessment methods based on near-surface temperature time series measured in the unsaturated zone. The next step would probably consist in validating the method introduced by [Koo & Kim \(2008\)](#), who solved the inverse problem using a numerical model over periods of time that match more closely the pattern of the observed recharge. This method could therefore be applied to a cold climate, such as that of Quebec, Canada, which includes an annual freezing and thawing cycle, as well as snow accumulation during winter. The time-distribution of recharge for such a region is characterized by an intense recharge in the spring following snow melt, a significant recharge in the fall due to important rain events and reduced evapotranspiration, and very limited recharge during the winter and summer. Results could then be compared to recharge estimates obtained from other approaches.

6 Acknowledgments

This research was supported by the NSERC Scholarship of Jean-Sébastien Gosselin, the NSERC-discovery grant (326975-2011) of Dr. Richard Martel, by funds from the Groundwater Geoscience Program of the Geological Survey of Canada, and the Projet Montérégie Est of the PACES program of the Ministère du Développement durable, de l'Environnement et de la Lutte contre le changement climatique. The authors would like to thank Dr. René Lefebvre (INRS-ETE) and Dr. John Molson (Université Laval) for their contribution to and interest in this work.

Article 2

Application limits of the interpretation of near-surface temperature time series to assess groundwater recharge

Titre traduit

Limites d'application de l'interprétation des séries temporelles de températures dans la zone superficielle du sol pour l'estimation de la recharge.

Auteurs

Jean-Sébastien Gosselin¹, Christine Rivard², Richard Martel¹ et René Lefebvre¹

¹ Institut national de la recherche scientifique, Centre Eau Terre Environnement, 490 rue de la Couronne, Québec, Qc, Canada

² Commission Géologique du Canada, Division Québec, 490 rue de la Couronne, Québec, Qc, Canada

Publié

Journal of Hydrology

2 avril 2016

Résumé

L'objectif principal de cette étude était de tester les limites d'application d'une technique d'estimation de la recharge des eaux souterraines basée sur l'inversion d'un modèle numérique du transport vertical de la chaleur par advection et conduction, en utilisant des séries temporelles de températures à trois profondeurs différentes (1, 3 et 5 m) dans la zone non saturée. À cet effet, plusieurs jeux de données synthétiques horaires des températures du sol, représentatives de diverses conditions météorologiques, de conditions de couverture du sol et de textures du sol, ont été produites avec le simulateur SHAW (Simultaneous Heat and Water Model). Ces simulations ont permis de produire un large éventail de valeurs de recharge. Le flux vertical de l'eau dans le sol a ensuite été estimé à partir de ces valeurs de températures réalistes par l'inversion d'un simple simulateur numérique unidimensionnel du transport de chaleur par advection et conduction dans la zone non saturée. Ce simulateur a été développé dans le cadre de cette étude. Le flux d'eau a été estimé sur une base hebdomadaire, mensuelle, semi-annuelle et annuelle. À partir de ces estimations de flux d'eau vertical, des taux annuels de la recharge (potentielle) ont ensuite été calculés. Les résultats ont ensuite été comparés à ceux simulés précédemment avec SHAW pour évaluer la précision de la méthode. Les résultats ont montré que, dans des conditions idéales, il serait possible d'estimer les taux de recharge annuels qui sont au-dessus 200 mm/a avec une erreur acceptable de moins de 20 %. Ces conditions "idéale" incluent la résolution du flux d'écoulement de l'eau sur une base hebdomadaire, des températures mesurées sans erreur sous la zone maximale de gel du sol et une connaissance très précise *a priori* des propriétés de la colonne de sol (conductivité thermique et chaleur massique volumétrique). Cependant, ce travail a démontré que la précision de la méthode est très sensible à l'incertitude des paramètres d'entrée du modèle utilisé pour réaliser l'inversion et aux erreurs de mesure sur les séries temporelles de températures. Pour les conditions représentées dans cette étude, ces résultats suggèrent que, malgré les meilleures pratiques de modélisation et d'instrumentation actuelle, les techniques basées sur la chaleur pour l'évaluation des taux de la recharge diffuse des eaux souterraines ne sont probablement pas bien adaptées aux conditions réelles. Elles pourraient toutefois représenter une approche viable pour les applications réalisées dans des matériaux d'ingénierie et dans des conditions contrôlées.

Abstract

The main objective of this study was to test the application limits of a groundwater recharge assessment technique based on the inversion of a vertical one-dimensional numerical model of advective-conductive heat transport, using temperature time series at three different depths (1, 3 and 5 m) in the unsaturated zone. For this purpose, several synthetic hourly datasets of subsurface temperatures, representing various weather, ground cover, and soil texture conditions, thus covering a wide range of groundwater recharge values, were produced with the vertical one-dimensional coupled heat and moisture transport simulator SHAW (Simultaneous Heat and Water Model). Estimates of the vertical flux of water in the soil were then retrieved from these realistic temperature profiles using a simple one-dimensional numerical simulator of advective and conductive heat transport in the unsaturated zone that was developed as part of this study. The water flux was assumed constant on a weekly, monthly, semiannual, and annual basis. From these vertical water flux estimates, annual (potential) groundwater recharge rates were then computed and results were compared to those calculated previously with SHAW to assess the accuracy of the method. Results showed that, under ideal conditions, it would be possible to estimate annual recharge rates that are above 200 mm/y, with an acceptable error of less than 20 %. These “ideal” conditions include the resolution of the water flux on a weekly basis, error-free temperature measurements below the soil freezing zone, and model parameter values (thermal conductivity and heat capacity of the soil) known a priori with no uncertainty. However, this work demonstrates that the accuracy of the method is highly sensitive to the uncertainty of the input model parameters of the numerical model used to carry out the inversion and to measurement errors of temperature time series. For the conditions represented in this study, these findings suggest that, despite the best modeling and field instrumentation practices, heat-based techniques for the assessment of diffuse groundwater recharge rates are likely not well suited for real field conditions, but could still represent a viable approach for applications carried out in engineered materials and under controlled conditions.

1 Introduction

1.1 Background

It has long been recognized in the field of hydrogeology that water flowing in the soil carries sensible heat affecting subsurface temperatures (Anderson, 2005; Healy, 2010; Rau *et al.*, 2014). Therefore, hydrogeologists have been interested since the 1960s in using heat as a tracer to monitor qualitatively and quantitatively the movement of groundwater (e.g. Suzuki, 1960; Stallman, 1963, 1965; Bredehoeft & Papadopoulos, 1965). Heat is an attractive tracer for groundwater studies because soil temperature has a natural dynamic signal that can be measured accurately, cheaply, and at high frequencies (Stonestrom & Blasch, 2003). Arrays of sensors can be easily deployed, with minimal soil disturbance, to monitor temperature at various depths below the ground surface. Moreover, unlike methods based on chemical and isotopic tracers, no sample of water or soil is required (Healy, 2010).

Assessment of the vertical flow of groundwater by the analysis of transient subsurface temperature measurements was introduced by Suzuki (1960) and Stallman (1963, 1965). They estimated the downward flow of water in irrigated rice paddy fields by fitting an analytical solution of the transient vertical one-dimensional (1Dz) advective-conductive heat transport equation in homogeneous soils to near-surface temperature measurements. Several years later, Taniguchi (1993) calculated the steady upward and downward flow of groundwater in a shallow irrigated aquifer in Japan using transient vertical temperature profiles measured in boreholes, with a method based on the analytical solution of Stallman (1965). These results were later validated by Vandenbohede & Lebbe (2010a) who used inverse numerical modeling to estimate the vertical flow of water with the dataset published by Taniguchi (1993). All the aforementioned studies used transient near-surface (0 to 15 m) temperature measurements to estimate the steady vertical flow of water in the saturated zone and involved irrigated conditions at the ground surface. Stallman's approach has also been extensively and successfully employed in the last decades to assess interactions beneath streams and large bodies of water (e.g. Lapham, 1989; Silliman *et al.*, 1995; Stonestrom & Constantz, 2003; Baskaran *et al.*, 2009). In contrast, studies on the use of heat for the estimation of the vertical flow of water in the context of natural diffuse recharge are very scarce. Diffuse recharge is defined by Healy (2010) as “recharge that is distributed over large areas in response to precipitation infiltrating the soil surface and percolating through the unsaturated zone to the water table”.

Published studies on this topic include the work of [Taniguchi \(1994\)](#) who used the method he had published the previous year ([Taniguchi, 1993](#)) to estimate the steady vertical flow of water in the saturated zone from vertical temperature profiles measured in 10 observation wells located in a sandy aquifer in the Nara Basin, Japan. [Tabbagh *et al.* \(1999\)](#) estimated steady percolation rates in the vadose zone on an annual basis, from transient temperature time series measured in the upper first meter of soil at weather stations located in metropolitan and northern France, with a method based on the analytical solution of [Stallman \(1965\)](#). [Koo & Kim \(2008\)](#) fitted a numerical heat transport model to temperature time series measured in the unsaturated zone of a site located in Korea, by optimizing the value of two lumped parameters of the heat transport equation on a seasonal basis. However, no quantification of recharge was achieved in their study, as only the lumped parameters were estimated (one of which included the vertical water flux).

1.2 Rationale and Objectives

One of the main issues that is common to most of the studies using heat as a tracer to estimate groundwater recharge is the difficulty to properly assess the uncertainty associated to the estimated values. This topic was addressed by [Vandenbohede & Lebbe \(2010a,b\)](#) for applications to the saturated zone and its relevance was stressed by [Rau *et al.* \(2014\)](#). The uncertainty of seepage fluxes estimated beneath streams with a heat-based approach has also been studied (e.g. [Shanafield *et al.*, 2011](#); [Soto-López *et al.*, 2011](#)). However, no substantial work has been carried out to validate the application and assess the uncertainty of heat-based methods in the vadose zone in a context of natural diffuse recharge, moreover for a snow climate with seasonally frozen ground.

Estimation of the vertical flow of water with a heat-based approach in a shallow unsaturated zone is complex. In contrast to the saturated zone, water fluxes in the near-surface vadose zone can be very irregular over time, being strongly related to short time-scale precipitation events. Furthermore, thermal properties of unsaturated sediments vary over time, following the fluctuations of their moisture content ([Farouki, 1981](#)). The application of the method becomes even more complex for cold environments, due to the combined effect of the snow cover insulation during winter and the annual cycle of freezing and thawing of the soil, which involve large latent heat effects. These elements play a significant role in heat transfer within the near-surface soil and cause asymmetrical annual subsurface temperature cycles, which make the use of analytical models difficult ([Williams &](#)

Smith, 1991). For these reasons, Gosselin *et al.* (2011) suggested that the assessment of the vertical flow of water from temperature time series in the unsaturated zone should be carried out through the inversion of a numerical model of heat transport over periods that match the expected recharge pattern.

The purpose of the present work was to use synthetic data to test and assess the accuracy of the above approach for the estimation of annual groundwater recharge rates. For this purpose, several long-term (20 years) synthetic hourly datasets of subsurface temperatures, representative of a range of weather under cool humid climate, ground covers, and soil texture conditions, were generated with the coupled simulator of heat and water transport SHAW (Simultaneous Heat and Water). Annual groundwater recharge rates were inferred from these synthetic datasets and compared with the “true” values simulated with SHAW. The influence of input model parameter uncertainty and of subsurface temperature measurement errors on the accuracy of the method was also assessed with a sensitivity analysis.

A unique aspect of this study is that the method was tested for conditions beyond the traditional assumption of quasi steady-state water flux. Contributions of this work include a better definition of the applicability limits of heat-based approach for the unsaturated zone and of the magnitude of the uncertainty on predicted annual groundwater recharge values that can be expected in real-life applications. Furthermore, this paper presents a functional and simple inverse numerical simulator of heat transport for the unsaturated zone that was validated against the more complex and proven numerical simulator SHAW.

2 Materials and Methods

2.1 Overview of the Methodology

The methodology that was followed to assess the uncertainty of annual groundwater recharge rates derived from temperature time series is illustrated in [figure 1](#) and briefly summarized below.

First, the coupled numerical simulator of heat and moisture transport SHAW (Simultaneous Heat and Water, version 3.0; Flerchinger & Saxton, 1987; Flerchinger *et al.*, 1996) was used to produce 12 synthetic datasets of hourly subsurface temperatures. This was done using, as inputs,

two different weather datasets (daily precipitation, wind speed, relative humidity, air temperature, and solar radiation), two ground covers (bare soil and short grass), and three soil textures (sand, loamy sand, and sandy loam). Annual (potential) groundwater recharge rates were computed from the hourly water flux simulated with SHAW (q_{SHAW}) at the bottom of the soil profile. A wide range of realistic recharge values that can occur under a cool humid climate were thus obtained. A detailed description of the models developed with SHAW to produce the synthetic datasets is presented in section 2.2.

SHAW heat and water unsaturated transport

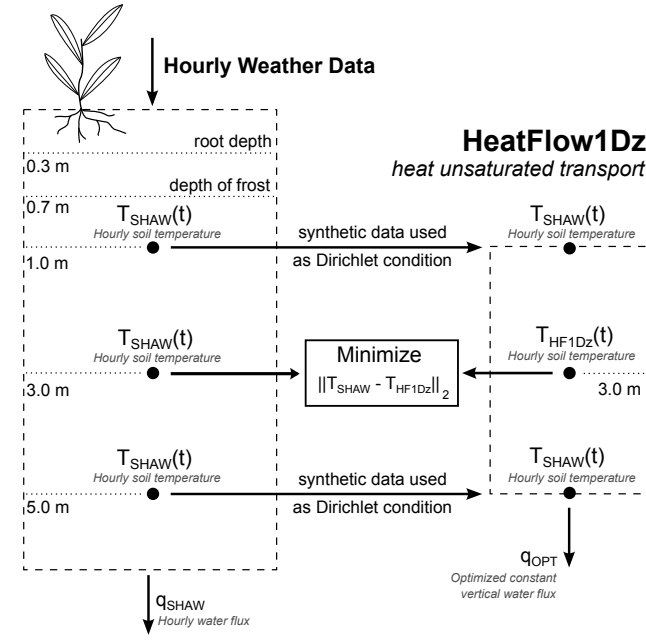


Figure 1
 Diagram showing the methodology followed for assessing the estimation error of annual groundwater recharge rates. Hourly synthetic temperature time series (T_{SHAW}) were produced at three different depths with the SHAW model and used in the inversion of a numerical model (HeatFlow1Dz) of heat transport in the unsaturated zone. In the diagram, q_{SHAW} is the hourly flux of water simulated with SHAW at the bottom of the soil profile, q_{OPT} is the time- and space-averaged water flux optimized by the inversion of HeatFlow1Dz, and T_{HF1Dz} are the temperatures simulated with HeatFlow1Dz.

The basic idea was then to use these realistic simulated temperatures as synthetic measurements to retrieve groundwater recharge values through the inversion of a simple numerical model and to compare the recharge estimates with those computed previously with SHAW. For this purpose, a simple vertical one-dimensional numerical simulator of advective and conductive heat transport in the unsaturated zone was developed as part of this study. A detailed description of this numerical simulator, hereafter referred to as *HeatFlow1Dz*, is presented in section 2.3.

The temperature time series simulated at the depths of 1 and 5 m below the ground surface with SHAW were first used as synthetic measurements to constrain (with Dirichlet conditions) a

model developed in HeatFlow1Dz. Then, the method consisted in assuming that the vertical water flux in HeatFlow1Dz (q_{OPT}), associated to the advective transport of sensible heat in the soil, was homogeneous in space and remained constant over a given period of time. Weekly, monthly, semiannual, and annual time- and space-averaged values of the vertical water flux were then computed through the inversion of the HeatFlow1Dz model using the temperatures simulated with SHAW at a depth of 3 m as observations. All the other parameters of HeatFlow1Dz (e.g., porosity, thermal conductivity) were assumed to be known *a priori* for the inversion. The inversion process is discussed in more detail in [section 2.3.4](#).

The time- and space-averaged water fluxes thus computed for four different time scales were used to compute annual rates of potential groundwater recharge. Results were compared with the actual values of recharge previously simulated with SHAW to evaluate the accuracy of the method under various contexts and lengths of the inversion period.

Sensitivity analyses were also done to assess the influence of the uncertainty of the model input parameters on the accuracy of the method. This was done by alternately introducing errors in the total porosity, thermal conductivity of the sand fraction, and volumetric water content of the soil before solving the water flux by the inversion of HeatFlow1Dz. Finally, the impact of subsurface temperature measurement errors on the accuracy of the derived annual groundwater recharge rates was assessed by alternately introducing random errors and bias in the soil temperature simulated with SHAW before using them as synthetic measurements to solve the water flux with HeatFlow1Dz.

2.2 Generation of the Synthetic Datasets

2.2.1 SHAW simulator overview

There are numerous well-known and documented numerical simulators that can represent the vertical flow of water in the unsaturated zone in response to precipitation and snow melt events. For instance, [Scanlon *et al.* \(2002\)](#) compared results from seven different models (HELP, HYDRUS-1D, SHAW, SoilCover, SWIM, UNSAT-H, and VS2DTI) using monitoring data from non-vegetated engineered covers. However, few of them can simulate the coupled processes of heat and water transport in the unsaturated zone and even fewer can handle the accumulation of snow and freeze-thaw cycles of the soil upper layer.

SHAW (Simultaneous Heat and Water, version 3.0; [Flerchinger & Saxton, 1987](#); [Flerchinger et al., 1996](#)) is one of the most detailed 1Dz numerical simulators of heat and moisture transport in the unsaturated zone that can take into account snow accumulation on the ground surface, snow melt and soil freezing and thawing. It uses as inputs basic meteorological data (precipitation, wind speed, relative humidity, temperature, and solar radiation), either on an hourly or daily basis. Transfer of heat and moisture within the soil profile is solved concurrently with the surface energy and mass balance. Actual evaporation is solved directly within the energy budget equation (i.e. potential evaporation is not used). Infiltration is simulated with the [Green & Ampt \(1911\)](#) approach, while Richards equation is used for the transport of moisture within the soil vertical profile. Runoff occurs when precipitation intensity exceeds the infiltration capacity of the soil. The soil hydraulic and capillary properties were represented with the [Brooks & Corey \(1966\)](#) conductivity model, which is defined as:

$$K_{unsat} = K_{sat} \frac{\psi_e}{\psi}^{2+3\lambda} = K_{sat} \left(\frac{\theta_w - \theta_r}{n - \theta_r} \right)^{2/\lambda+3} \quad (1)$$

where K_{unsat} and K_{sat} are, respectively, the unsaturated and saturated hydraulic conductivity, n is the total porosity, θ_r and θ_w are, respectively, the residual and total volumetric moisture content, λ is the Brooks-Corey pore-size distribution parameter, ψ_e is the air-entry potential, and ψ is the soil matric potential.

Heat transport considers advected water and vapor, conduction, latent heat of fusion during snow melt and soil thawing, as well as latent heat of evaporation. The volumetric heat capacity of the soil (C_{soil}) is expressed as a standard additive mixing law ([Farouki, 1981](#)):

$$C_{soil} = \sum C_j \theta_j \quad (2)$$

where C_j and θ_j are respectively the volumetric heat capacity ($J/m^3 \text{ } ^\circ\text{C}$) and volumetric fraction (m^3/m^3) of the jth constituent of the soil, i.e. minerals, water, ice, and air.

The soil thermal conductivity is calculated with a modified version of the [de Vries \(1966\)](#) method:

$$k_{soil} = \frac{\sum f_j k_j \theta_j}{\sum f_j \theta_j} \quad (3)$$

where f_j , k_j , and θ_j are respectively the weighting factor, thermal conductivity, and volumetric fraction of the jth constituent of the soil, i.e. sand, silt, clay, water, ice, and dry air. The thermal

conductivity of sand is supposed equal to that of quartz in the SHAW simulator ($8.4 \text{ W/m } ^\circ\text{C}$), while the thermal conductivities of silt and clay are equal to $2.9 \text{ W/m } ^\circ\text{C}$. This approach overestimates the thermal conductivity of sands having low quartz content, unlike the original formulation of the [de Vries \(1966\)](#) method that calculates the soil thermal conductivity directly from the soil total fraction of quartz. Due to the high degree of mechanical and chemical stability of quartz compared to that of other minerals, older (pre-Quaternary) sands generally show significant quartz enrichment compared to young Late Quaternary sands derived from glaciated terrains. For example, sands derived from Late Quaternary sediments in glaciated North American terrains, have a quartz content estimated to be from 10 to 30 % ([Dell, 1959, 1963](#)), whereas pre-Quaternary sands derived from felsic igneous rocks (12 to 20 % of quartz) typically contain between 67 and 70 % of quartz ([Pettijohn, 1975](#)). For this reason, the source code of SHAW was modified for this study to better represent the thermal conductivity of sands with quartz content of 30 %. This is likely to be more representative of sands found in the two regions of Canada from which the weather datasets used to carry this study were taken from (see [section 2.2.2](#)).

2.2.2 Synthetic SHAW models description

The developed soil profile in SHAW extended from the ground surface down to a depth of 30 m, where the temperature variation in time is considered to be negligible ([Parsons, 1970](#)). The lower boundary was assigned a no-heat flux condition for temperature and a unit gradient for water flow. The latter boundary condition allowed the entire column of homogeneous and coarse soil to remain unsaturated at all times under the conditions tested in this study. The objective here was not so much to represent a site with a very deep unsaturated zone, but rather to intentionally exclude the water table dynamics from this already complex analysis. This limitation of this study is discussed in more detail in [section 4](#).

The soil profile was assumed homogeneous and was discretized vertically with a total of 50 nodes. Nodal spacing varied from 0.1 m close to the ground surface to a maximum of 5 m at the bottom of the profile. The vertical discretization between the depths of 1 and 5 m, which corresponds, respectively, to the upper and lower limits of the HeatFlow1Dz numerical model, was kept to a constant value of 0.2 m. This was done to have the numerical grids of the SHAW and HeatFlow1Dz models aligned.

Simulations were run using three different soil texture classes (sand, loamy sand, and sandy loam) that were selected because they represent the most common types of sediments associated with recharge area. The property values that were used for the calculation of the soil thermal and hydraulic properties are presented for each soil texture class in [table 1](#). The soil mass fraction of sand and clay were determined graphically from the soil textural triangle of the USDA classification ([Todd & Mays, 2005](#)). The hydraulic parameters for the Brooks-Corey model were defined according to the values provided in [Rawls *et al.* \(1982\)](#). The soil water retention, unsaturated hydraulic conductivity, and thermal property curves for the three soil texture classes of [table 1](#) are shown in [figures 11](#) and [12](#) in [appendix 7](#).

Two different types of ground cover conditions were used at the soil surface for the simulations: bare soil and a uniform cover of short grass. The height of the plants, their effective rooting depth, and the leaf area index were specified to, respectively, 0.2 m, 0.3 m, and 1.

Hourly weather data (precipitation, wind speed, relative humidity, air temperature, and solar radiation) from the Quebec and Toronto city airport stations (see [figure 2](#)) were used as inputs in the model for the 1985-2005 period. This 20-year period was selected due to the availability of daily solar radiation from the Canadian Weather and Energy and Engineering Data Sets ([Environment Canada, 2011](#)). The Quebec and Toronto city airport weather stations were chosen to study the performance of the groundwater recharge estimation method under a range of weather conditions (precipitation and air temperature) representative of a cool and humid climate. Hourly wind speed, relative humidity, and air temperature were obtained from the online climate Canadian database ([Environment Canada, 2011](#)). Hourly precipitation was derived from daily precipitation records: the

Table 1 – Soil mass fraction of grain sizes (sand, silt, and clay) and Brooks-Corey model parameters for the 3 soil texture classes that were defined in SHAW for the production of synthetic temperature datasets.

Texture Class	mass fraction			Brooks-Corey model parameters				
	Sand (%)	Silt (%)	Clay (%)	λ (-)	ψ_e (cm)	θ_r (m^3/m^3)	n (m^3/m^3)	K_{sat} (cm/h)
Sand	100	0	0	0.592	-7.26	0.020	0.437	21.00
Loamy Sand	85	10	5	0.474	-8.69	0.035	0.437	6.11
Sandy Loam	65	25	10	0.322	-14.66	0.041	0.453	2.59

**Figure 2**

Location of the two weather stations used for this study. Hourly records of precipitation, wind speed, relative humidity, air temperature, and solar radiation were used as inputs in the simulator SHAW for the production of the synthetic datasets of subsurface temperature.

total amount of precipitation recorded each day was evenly distributed among hours of the day for which an occurrence of precipitation (e.g. rain, snow, grizzle) was observed at the weather station. Missing data in the original daily precipitation records were estimated with the software WHAT ([Gosselin et al., 2016a](#)) using the single best estimator method ([Eischeid et al., 1995](#)). Yearly and monthly normals for precipitation and air temperature for each weather station are presented in [figures 3a](#) and [3b](#).

The conditions described above were used to define a total of 12 contexts (weather station, soil texture, and ground cover), for which 20-year simulations of the coupled transport of heat and water in the unsaturated zone were run, on an hourly basis, with the developed models in SHAW. [Table 2](#) presents a summary of modeling results for the 12 contexts, including mean and range of the soil moisture saturation at the depth of 1 m, the maximum soil frost depth during the 20-year simulation and the groundwater recharge calculated from the hourly water fluxes at the bottom of the soil profile. Annual groundwater recharge varied widely among the various contexts, ranging from 69 mm/y for the grass covered sandy loam in the Toronto area to 510 mm/y for the bare sand in the Quebec City area.

For each context, the initial temperature and soil moisture vertical profiles were obtained using a spin-up procedure, i.e. by running each 20-year simulation several times using the final conditions of a given run as the initial conditions of the next run. It generally required less than 3 cycles before the impact of initial conditions on the simulation became negligible.

Table 2 – Summary of SHAW modeling results for the 12 contexts considered. These contexts comprise two groups with weather conditions of Quebec and Toronto, respectively, each comprising three soil types (sand, loamy sand and sandy loam) and two land covers for each soil type (bare soil and grass). The table shows mean and range of the soil moisture saturation at the depth of 1 m, the maximum soil frost depth during the 20-year simulation, as well as annual groundwater recharge calculated from the hourly water fluxes at the bottom of the soil profile.

Context	simulated conditions			moisture saturation		max depth	Average
	Weather #	Station	Soil Texture	Ground Cover	min-max (%)	mean (%)	of frost (cm)
1	Quebec	Sand	Bare	19 - 61	29	63	510
2	Quebec	Sand	Grass	20 - 62	27	61	349
3	Quebec	Loamy Sand	Bare	30 - 75	40	52	433
4	Quebec	Loamy Sand	Grass	34 - 74	38	51	312
5	Quebec	Sandy Loam	Bare	42 - 80	52	50	321
6	Quebec	Sandy Loam	Grass	41 - 77	50	42	265
7	Toronto	Sand	Bare	20 - 47	28	78	328
8	Toronto	Sand	Grass	19 - 47	25	79	151
9	Toronto	Loamy Sand	Bare	30 - 59	39	71	264
10	Toronto	Loamy Sand	Grass	28 - 61	35	71	119
11	Toronto	Sandy Loam	Bare	40 - 71	49	70	157
12	Toronto	Sandy Loam	Grass	38 - 65	45	69	69

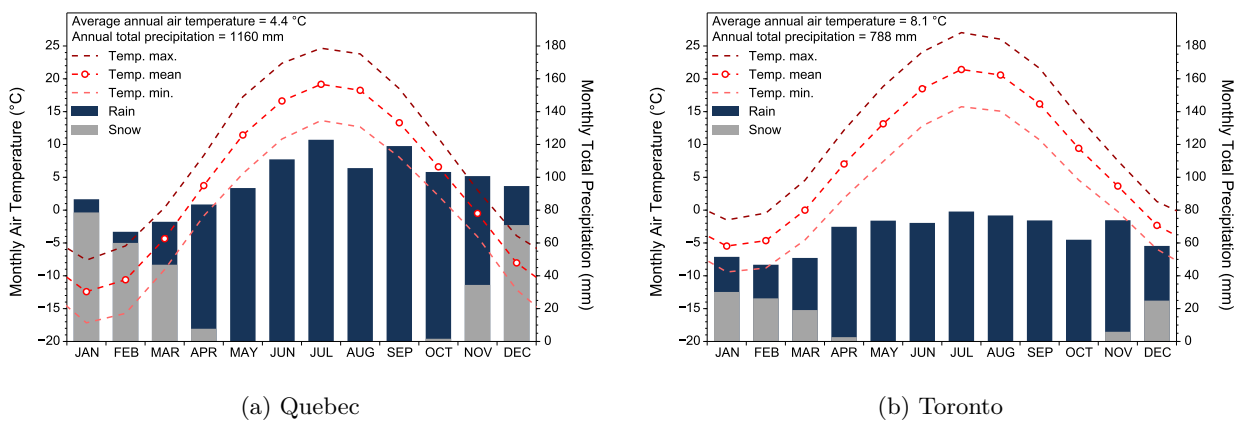


Figure 3 – Yearly and monthly averages for total precipitation and mean air temperature calculated at the Quebec (a) and Toronto (b) airport weather stations for the 1985-2005 period.

2.3 Inverse Numerical Model of Heat Transport

2.3.1 HeatFlow1Dz simulator description

HeatFlow1Dz is a simple finite volume numerical simulator of vertical one-dimensional (1Dz) advective and conductive heat transport in the subsurface that was developed as part of this study in the Python 2.7 programming language. The simulator is based on the transient 1Dz advective-conductive equation of heat transport in heterogeneous unsaturated soils, which can be expressed as follows (Bear, 1972):

$$C_{soil} \frac{\partial T_{soil}}{\partial t} = \frac{\partial}{\partial z} \left(k_{soil} \frac{\partial T_{soil}}{\partial z} \right) - q_w C_w \frac{\partial T_{soil}}{\partial z} \quad (4)$$

where k_{soil} and C_{soil} are respectively the thermal conductivity ($\text{W}/\text{m}^{\circ}\text{C}$) and the volumetric heat capacity ($\text{J}/\text{m}^3^{\circ}\text{C}$) of the soil, C_w is the volumetric heat capacity of water ($\text{J}/\text{m}^3^{\circ}\text{C}$), T_{soil} is the soil temperature ($^{\circ}\text{C}$), and q_w is the vertical flux of water (m/s).

The soil volumetric heat capacity (C_{soil}) and thermal conductivity (k_{soil}) are calculated as in SHAW with equations (2) and (3), respectively. However, unlike SHAW, the transfer of latent heat due to vapor movement across the pores in the soil is not explicitly taken into account in equation (4). This process was included in HeatFlow1Dz by computing equation (3) using an apparent thermal conductivity for air instead of the dry air conductivity. This was done using the two-parameter empirical model of Campbell (1974), which expresses the apparent thermal conductivity of air as a function of temperature and soil moisture.

Equation (4) is discretized spatially with respect to z using a finite volume method, while an implicit second-order Crank-Nicolson method is used to discretize the equation with regard to time.

2.3.2 HeatFlow1Dz model description

As shown in figure 1, the upper limit of the model was set to a depth of 1 m so as to remain below the maximum depth of ground frost (see table 2). To maximize the sensitivity of the HeatFlow1Dz model to the water flux, the lower boundary was set to a depth of 5 m. Sensitivity analyses showed that there was no substantial gain from simulating heat transport beyond this value for the estimation of groundwater recharge. Soil temperature was constrained at these two limits by a Dirichlet-type boundary condition using the synthetic temperature time series produced previously with SHAW.

The soil profile was assumed homogeneous and was discretized vertically with a total of 19 nodes with a constant nodal spacing of 0.2 m. Values for the soil porosity and mass fraction of grain sizes (sand, silt, and clay) were set according to [table 1](#) for each context.

Parameter values for the [Campbell \(1974\)](#) apparent thermal conductivity equation of air were obtained for each context of [table 2](#) by optimization of HeatFlow1Dz using the temperatures simulated with SHAW at a depth of 3 m. To do so, the vertical flux of water (q_w) and volumetric water content (θ_w) were defined at each node of the HeatFlow1Dz model on an hourly basis using the values simulated with SHAW.

This calibration was done to minimize the modeling errors of the HeatFlow1Dz models when the water flux and soil volumetric water content were known at any time and depth in the soil column. This allowed evaluation of the best possible accuracy of annual recharge rates estimated with the method when all model parameters are known exactly and when there is no uncertainty in the temperature measurements. Under these ideal conditions, errors on the estimated recharge rates are mainly due to the assumptions that have to be made in the inverse model regarding the spatial and temporal distribution of the water flux and soil volumetric water content. This is discussed further in [section 2.3.4](#).

2.3.3 HeatFlow1Dz model validation

Forward simulations were run with the calibrated HeatFlow1Dz model using, as inputs, the hourly vertical water flux and volumetric water content simulated with SHAW. Soil temperatures simulated with HeatFlow1Dz were then compared with those produced with SHAW.

Additional forward simulations with HeatFlow1Dz were carried out using a no-water flux scenario, i.e. by specifying a zero flux value ($q_w = 0$) at all times and depths of the model. Results were then compared with those of SHAW to assess the global impact of groundwater flow on the subsurface temperatures simulated with HeatFlow1Dz.

2.3.4 Resolution of the inverse problem with HeatFlow1Dz

The water flux (q_w) in [equation \(4\)](#) is, in fact, an unknown model parameter that varies both in space and in time. However, solving the inverse problem of heat transport for q_w at each time step ($\Delta t = 1$ h) and every node ($\Delta z = 0.2$ m) of the numerical model would make the method impracticable. Aside from the computational requirement considerations that this would imply, the temperature observations that are generally available for the application of the method would not support an independent estimation of the water flux at each node and time step of the model. The approach that was followed in this study to work around these issues consisted in assuming, for the resolution of the inverse problem, that the water flux was homogeneous in space and constant in time over a given period of time, similarly to the approach followed by [Koo & Kim \(2008\)](#).

The soil moisture saturation ($S_w = \theta_w/n$) was also considered constant in time and space for the resolution of the inverse problem with the HeatFlow1Dz model. For each context, the value of the soil moisture saturation was set equal to the mean of the simulated values with SHAW over a 20-year period at a depth of 1 m. These values are presented in [table 2](#), along with the range of variation of S_w for each context.

Alternative approaches could have been used for the representation of S_w in the inverse problem. For example, the simulated volumetric water contents with SHAW could have been used as synthetic measurements to define vertical profiles of S_w on an hourly basis. This is possible in practice considering that sensors now exist on the market that allow the combined measurement of soil temperature and moisture content (e.g., [Decagon Devices, 2010](#)). For this work however, it was chosen to study the case where only temperature measurements were available and where a best mean value of S_w had to be defined for the inversion. The implication of this simplifying assumption on the accuracy of the method for the assessment of groundwater recharge is discussed further in [section 3.3](#).

The method for the resolution of the time- and space-averaged values of the water flux consisted first in partitioning the temperature time series into a set of consecutive and mutually exclusive segments on a weekly, monthly, semiannual, and annual basis. For each segment, the temperatures simulated with SHAW at the depths of 1 and 5 m were used as imposed Dirichlet conditions at the upper and lower boundary of the HeatFlow1Dz model. A time and space-averaged value of the vertical water flux was then estimated consecutively for each segment through the minimization of

the sum of the square differences between the temperatures simulated with SHAW and HeatFlow1Dz at the depth of 3 m (referred to as T_{SHAW} and T_{HF1Dz} , respectively, in [figure 1](#)). The thermal properties of the soil computed with [equations \(2\)](#) and [\(3\)](#) were also assumed to be known *a priori*. The initial temperature profile for one segment was set equal to the last temperature profile simulated with HeatFlow1Dz for the previous segment. The optimization for each segment was done with a modified Gauss-Newton gradient method described, for instance, in [Hill & Tiedman \(2007\)](#).

Observed temperature time series at more than one point between 1 and 5 m depths could have been used for the inversion of the HeatFlow1Dz model to better explore the potential variability of the subsurface temperature profiles. However, preliminary analysis on this subject showed that the gain on the inverse model sensitivity to the water flux was marginal when using temperature data at more than one point. Besides, [Vandenbohede & Lebbe \(2010a\)](#) showed that gains when using vertical temperature profiles instead of time series at a single depth when the flow of water is small (250 mm/y) were not significant. Therefore, to avoid complicating further the presentation and discussion of the results, this paper only explores the case where the inversion is done using a single temperature time series at a depth of 3 m. This depth was chosen because it corresponds to where the temperatures are the most sensitive to water percolation, as simulated with HeatFlow1Dz.

2.3.5 Estimation error and sensitivity analyses

The inverse model of heat transport described above was used to assess the impact of modeling errors, input parameter uncertainty, and subsurface temperature measurement errors on the accuracy of the annual groundwater recharge values estimated on the basis of soil temperature time series.

In a first step, the water flux q_w in [equation \(4\)](#) was solved alternately on an annual, semiannual, monthly, and weekly basis over a 20-year period for each of the 12 contexts described in [table 2](#). The resulting water fluxes were used to compile annual groundwater recharge rates, which were then compared with the values simulated with SHAW to compute the estimation errors. As stated previously in [section 2.3.2](#), the errors obtained at this step are explained mainly by the assumptions that are made regarding the spatial and temporal distribution of the water flux in the inverse model.

For real life applications, it is expected that an important source of error comes from the uncertainty of the input parameters used in the inverse model to compute the thermal properties of

the soil. Therefore, sensitivity analyses were carried out for three different key parameters of the HeatFlow1Dz simulator, namely the thermal conductivity of the sand fraction (k_{sand}), the total porosity of the soil (n), and the soil volumetric water content (θ_w). Other parameters used in the HeatFlow1Dz simulator (k_{air} , k_w , C_m and C_w) do not vary significantly in the range of conditions tested in this study and were thus excluded from this sensitivity analysis. More specifically, the sensitivity analyses were done by alternately varying in [equations \(2\)](#) and [\(3\)](#) the value of k_{sand} , n , and θ_w by as much as $\pm 30\%$ before solving the water flux on a weekly basis for the 12 contexts defined in [table 2](#). Annual groundwater recharge rates were then compiled from the weekly water fluxes and were compared with the actual values produced with SHAW to assess the impact on the estimation errors.

Finally, to study the influence of measurement errors on the accuracy of the derived annual recharge rates, random errors were introduced in the synthetic datasets of soil temperatures generated with SHAW, similarly to the approach followed by [Vandenbohede & Lebbe \(2010b\)](#). This was done using random errors with a standard deviation (σ_{obs}), ranging from 0 to $0.1\text{ }^\circ\text{C}$ with no bias (the typical resolution of commercial temperature sensors is $\pm 0.1\text{ }^\circ\text{C}$). The synthetic temperature data were then interpreted on a weekly basis with the inverse model of heat transport and annual groundwater recharge rates were compiled from the results. These values were then compared with the actual values produced with SHAW to assess the impact on the estimation errors. The same procedure was repeated in a second step, but by adding a constant bias (-0.1 to $0.1\text{ }^\circ\text{C}$) to the synthetic temperature time series at the depth of 3 m instead of introducing random errors.

3 Results

3.1 Validation of the HeatFlow1Dz Simulator

[Figure 4](#) presents simulation results produced with HeatFlow1Dz and SHAW for Context #1 (Quebec weather station, bare soil and sand, see [table 2](#)) for the years 1999 to 2001. This figure shows that the two temperature time series (dotted black and solid blue lines) for the 3 m depth overlap almost perfectly, showing that the simple heat transport simulator developed as part of this study is able to adequately reproduce the temperatures simulated with the more complex and proven SHAW simulator below the ground freezing zone. The temperature time series simulated with SHAW at

depths of 1 and 5 m, used to constrain HeatFlow1Dz at its upper and lower boundaries, are also shown on the graph of figure 4 (solid blue lines). These results also show that the amplitude of the temperature annual cycle decreases with depth, while its phase lag increases. The asymmetry of the annual temperature cycle, which is typical of cold climates, is also well represented in the time series, especially for the 1 m depth.

The hourly water fluxes simulated with SHAW at depths of 1 and 5 m below the ground surface are also presented in the upper portion of figure 4. The water flux time series at the depth of 1 m is very irregular and strongly correlated with precipitation and snow melt events. This clearly suggests that the inverse problem of the advective-conductive heat transport in the near surface vadose zone should be resolved over periods that match more closely the expected vertical groundwater flow pattern, instead of only considering steady-state fluxes on a yearly basis like it has traditionally been done for the saturated zone. However, the steady-state assumption likely appears to be applicable deeper into the unsaturated zone, where the spikes in the water flux signal have been considerably smoothed, as illustrated for the results simulated at the depth of 5 m.

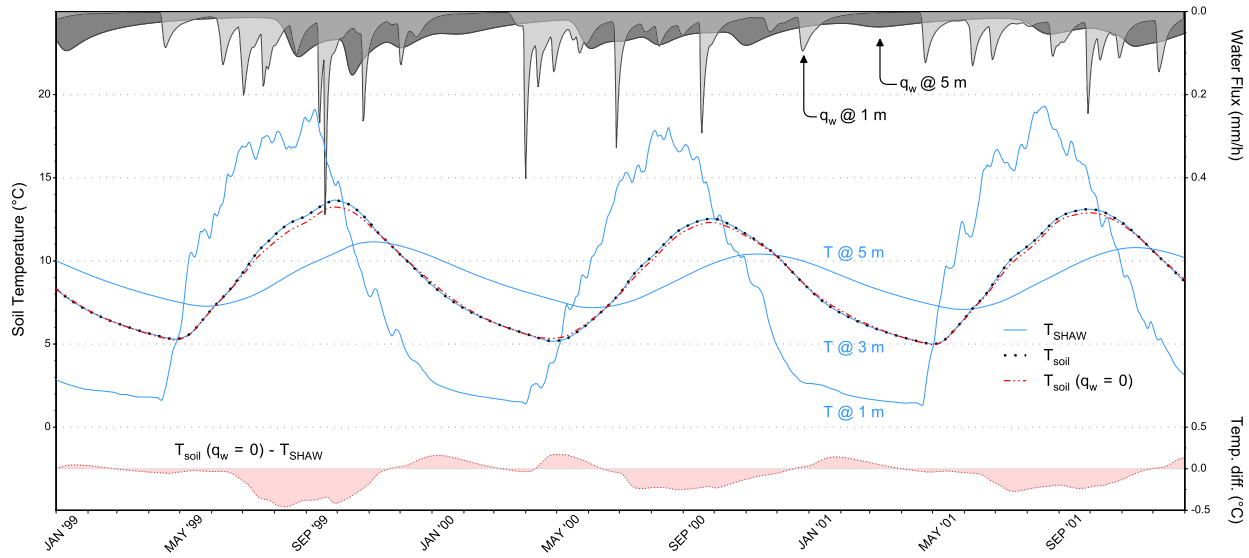


Figure 4 – Hourly simulation results for Context #1 (Quebec weather station, sand, bare soil) for the years 1999 to 2001. **TOP** – Vertical hourly water fluxes calculated with SHAW at depths of 1 and 5 m below the ground surface. **MIDDLE** – Temperature time series produced with SHAW (solid blue lines) at depths of 1, 3 and 5 m, as well as with the heat transport model at a depth of 3 m after the calibration (dotted black line) and for the no-water flux scenario (dash-dot red line). **BOTTOM** – Temperature differences calculated between the time series simulated with SHAW and with the heat transport model for the no-water flux scenario at a depth of 3 m.

Despite the important short-term infiltration events that occur in spring and fall (see water flux at a depth of 1 m in [figure 4](#)), the subsurface temperatures simulated at the depth of 3 m vary very smoothly throughout the entire simulation. To investigate further the cumulative impact of advective heat transport on subsurface temperatures, simulation results with HeatFlow1Dz for a no-water flow scenario ($q_w = 0$, i.e. water fluxes were assigned a value of zero at all times and depths in the model) are also plotted in [figure 4](#) for the depth of 3 m (dash-dotted red line). The temperature differences calculated between this time series and that obtained with SHAW are presented in the lower part of the graph. These results stress how small the impact of advective heat transport is on subsurface temperatures (always below 0.5 °C), even for a context characterized by significant natural diffuse recharge (510 mm/y in Context #1, shown in [figure 4](#)). This observation was also highlighted by [Goto et al. \(2005\)](#) who found that the thermal regime of sea floor sediments, in the Mid-Atlantic Ridge, was almost not affected by seepage fluxes equal or less than 10×10^{-8} m/s (about 315 mm/y). Considering the uncertainty of the temperature measurements and soil thermal properties, this suggests potential large errors on natural diffuse recharge rates estimated with an approach based on temperature measurements of the soil. This topic is further investigated in [sections 3.2 to 3.4](#).

3.2 Impact of Modeling Errors

[Figure 5](#) presents the Mean Errors (ME) and the Root Mean Square Errors (RMSE) calculated between the estimated annual groundwater recharge rates by inversion of the HeatFlow1Dz model and those produced with SHAW for each of the 12 contexts described in [table 2](#) and for the four different time scales (annual, semiannual, monthly, weekly) for which the vertical water fluxes were resolved with the inverse model. These results clearly demonstrate the importance of resolving the inverse problem of advective-conductive heat transport over a time scale that is consistent with the time variation of the vertical water flux in the soil. Both the RMSE and ME are lower when the water flux is solved on a weekly and monthly basis for the 12 contexts. This is explained by the fact that the water flux in the near-surface vadose zone is not uniformly distributed throughout the year (see top plot of [figure 4](#)). Therefore, the sensible heat carried by the percolating water through the soil causes an asymmetrical deformation of the temperature signal (see bottom plot of [figure 4](#)) that cannot be reproduced adequately if the water flux is considered in steady state on an annual or semiannual basis. This effect is even more important when the ground surface is covered with vegetation (see Contexts #2, 4, 6, 8, 10 and 12), especially when the mean annual recharge is large.

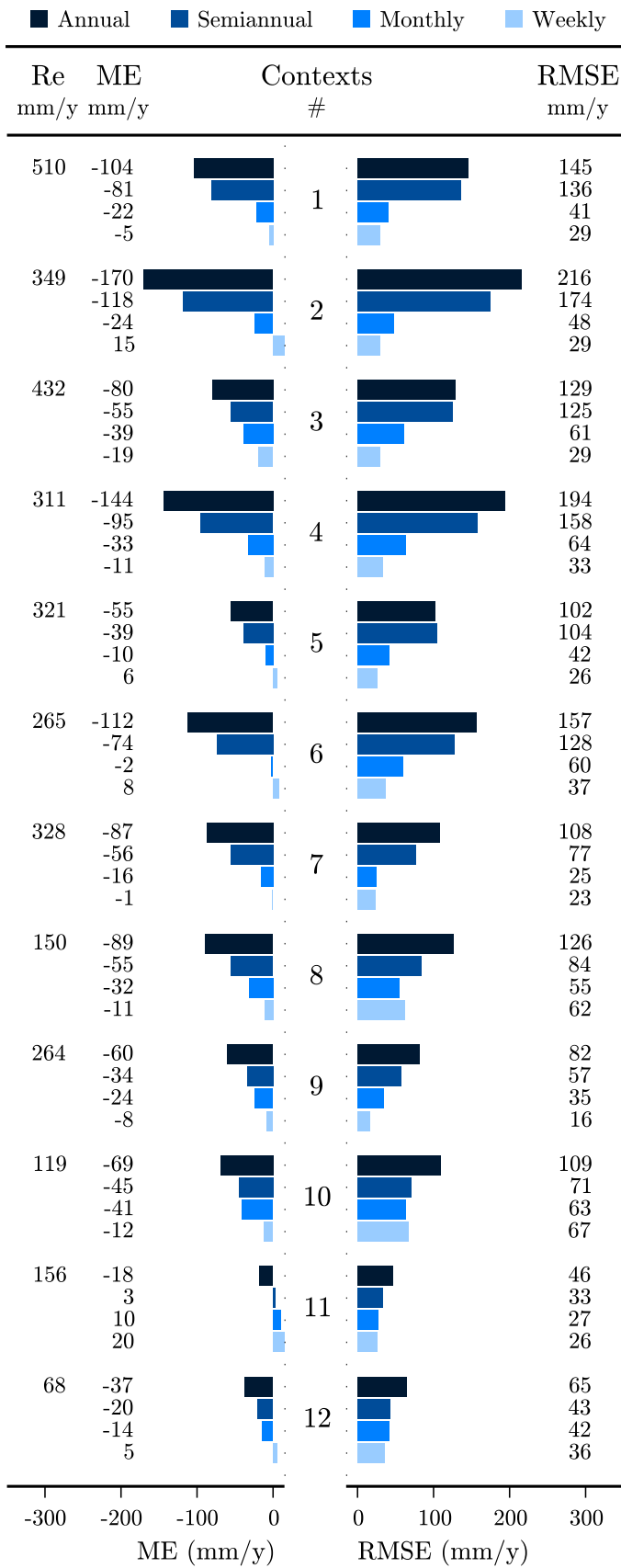


Figure 5
 Mean Errors (ME) and Root Mean Square Errors (RMSE) calculated between the annual recharge estimates (compiled from water fluxes solved on an annual, semiannual, monthly, and weekly basis) and those produced with SHAW for each of the 12 contexts studied. The mean value (Re) of the actual annual recharge produced with SHAW is also provided.

Vegetation limits the amount of water infiltrating in the soil during most of the summer, causing the time distribution of the water flux to be even more irregular than for the contexts with bare ground conditions. To illustrate this, figure 6 presents the mean monthly recharge amounts obtained with SHAW over the 20-year period for Contexts #1 and #2 for the sand texture class and weather from Quebec, with and without vegetation respectively.

When looking at the results of figure 5 for the cases for which the flux was solved on a weekly basis only, it can be seen that the magnitude of the errors is relatively insensitive to that of the annual groundwater recharge. As illustrated in figure 7, this translates in a relative estimation error (i.e. ratio of RMSE to annual recharge) that is almost inversely proportional to the annual groundwater recharge, ranging from a value of 5 % of the annual recharge for Context #1 (510 mm/y of recharge) up to a value of more than 50 % for Contexts #10 and #12 (119 and 68 mm/y of recharge).

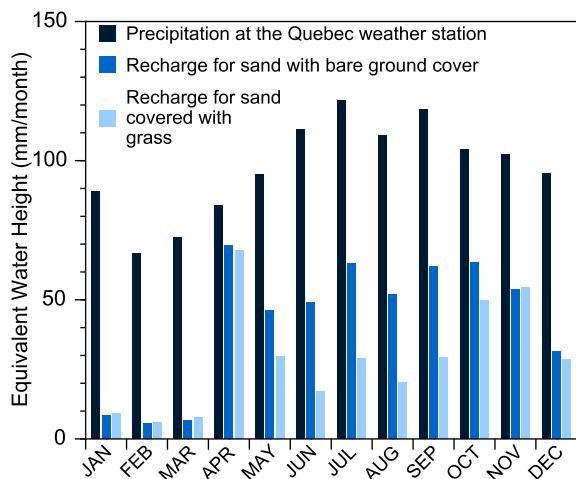


Figure 6 – Monthly averages of precipitation and recharge simulated with SHAW for the hydrogeological Contexts #1 and #2 to illustrate the impact of the vegetation cover on the time distribution of recharge over the year.

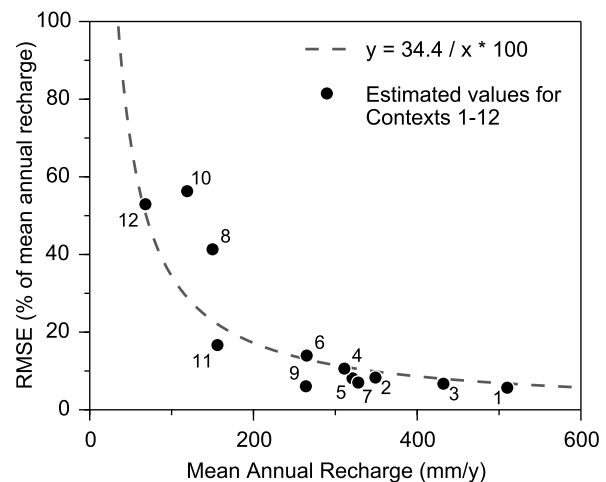


Figure 7 – Root Mean Square Error (RMSE), calculated between the annual groundwater recharge rates estimated with the inverse heat transport model (compiled from water fluxes solved on a weekly basis) and those produced with the SHAW model, expressed in % of the mean annual recharge obtained with SHAW for each hydrogeological context.

3.3 Impact of Input Parameter Uncertainty

The estimation error on the annual groundwater recharge rates that resulted from the sensitivity analyses, carried out for three different key parameters (k_{sand} , n , θ_w) of HeatFlow1Dz for each context, were pooled together and are presented in [figures 8a](#) to [8c](#). Though the results vary from one context to the other, these are presented together to show the overall impact that the input parameter uncertainty has on the accuracy of the estimated annual groundwater recharge rates. Note that the magnitude of the estimation error (in mm/y) is mainly unrelated to that of the groundwater recharge for the range of conditions tested and are principally influenced by the thermal properties of the soil as discussed further below.

The results presented in [figures 8a](#) and [8b](#) show that the estimation errors of the annual recharge rates are very sensitive to the uncertainty of the model parameters k_{sand} and n . Both the median and the interquartile range of the errors increase substantially when an uncertainty of $\pm 30\%$ and $\pm 10\%$ are introduced in the values of k_{sand} and n , respectively. For the model parameter θ_w , the introduction of an uncertainty of $\pm 30\%$ had less impact on the estimation error of annual groundwater recharge rates for the following reason. Due to the small magnitude of the downward flow of water that occurs under natural diffuse recharge conditions, the transport of heat in the subsurface is mostly controlled by conduction. Therefore, the influence that the uncertainty of the model input parameters has on the estimation error of groundwater recharge can be mostly related to the sensitivity of the soil thermal diffusivity to those input model parameters (k_{sand} , n , θ_w). The thermal diffusivity of the soil is defined as the ratio between the soil thermal conductivity (k_{soil}) and its heat capacity (C_{soil}). As can be seen in [figure 9](#), variations of the soil thermal diffusivity is more limited for the range over which the soil moisture saturation ($S_w = \theta_w/n$) varies, for the contexts simulated in this work (see [table 2](#) and [figure 9c](#)), than for k_{sand} and n ([figures 9a](#) and [9b](#)). This explains in part why θ_w is the parameter that has the smallest influence on the estimation error of annual groundwater recharge rates. The differences in the curves for each type of soil also mostly explains the variation in the results obtained for each context.

Further investigations also revealed that the resolution of the water flux on a weekly basis, when the volumetric water content (θ_w) was defined at every node and time step of the HeatFlow1Dz model from the synthetic data produced with SHAW (instead of being assumed constant), did not result in a significant improvement of the method accuracy for the majority of the contexts. This

is due to the fact that the volumetric water content varies following the annual cycle. Therefore, the error on the water fluxes estimated for each weekly period tends to cancel out when results are summed to compile an annual groundwater recharge value.

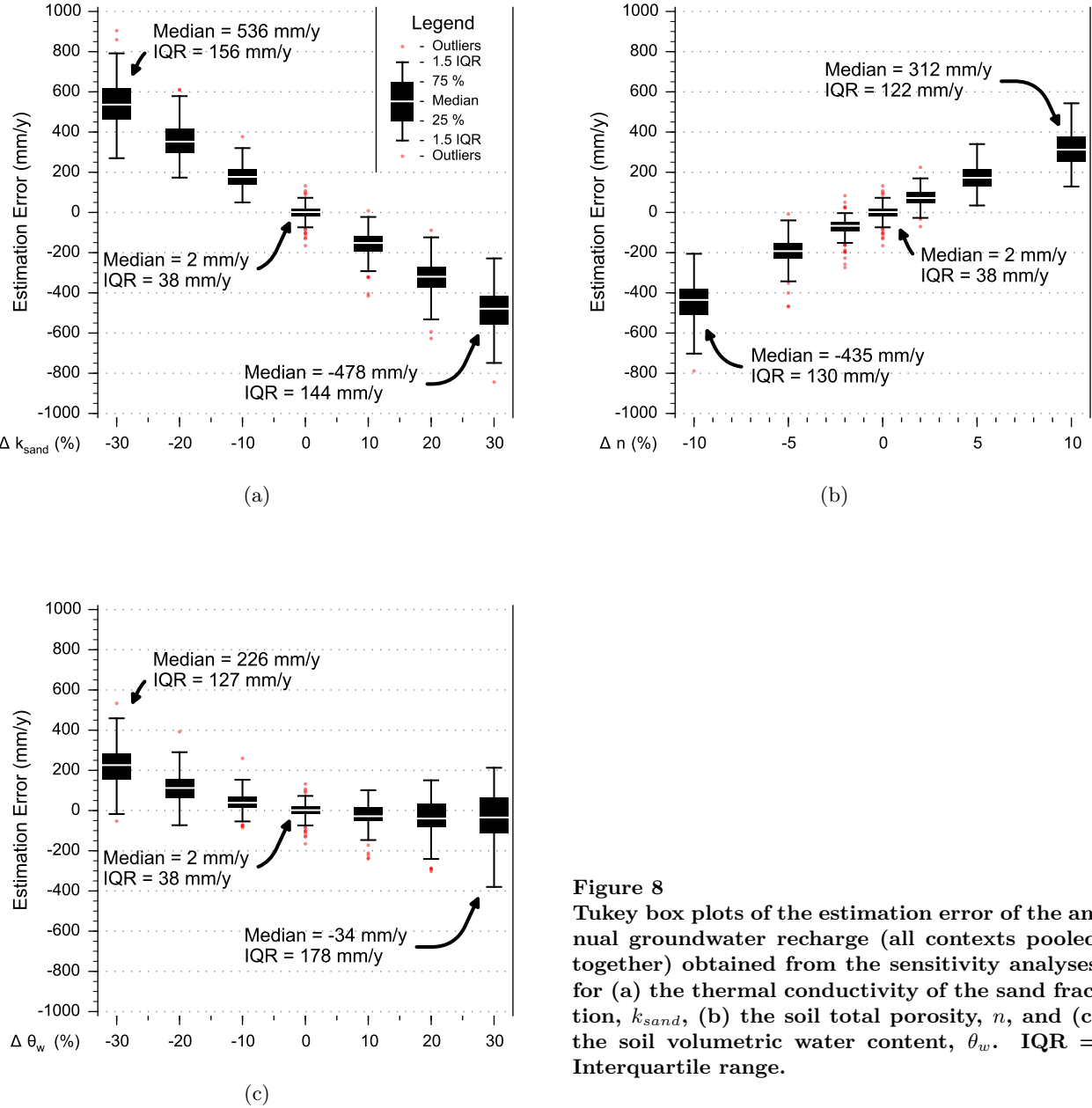


Figure 8
Tukey box plots of the estimation error of the annual groundwater recharge (all contexts pooled together) obtained from the sensitivity analyses for (a) the thermal conductivity of the sand fraction, k_{sand} , (b) the soil total porosity, n , and (c) the soil volumetric water content, θ_w . IQR = Interquartile range.

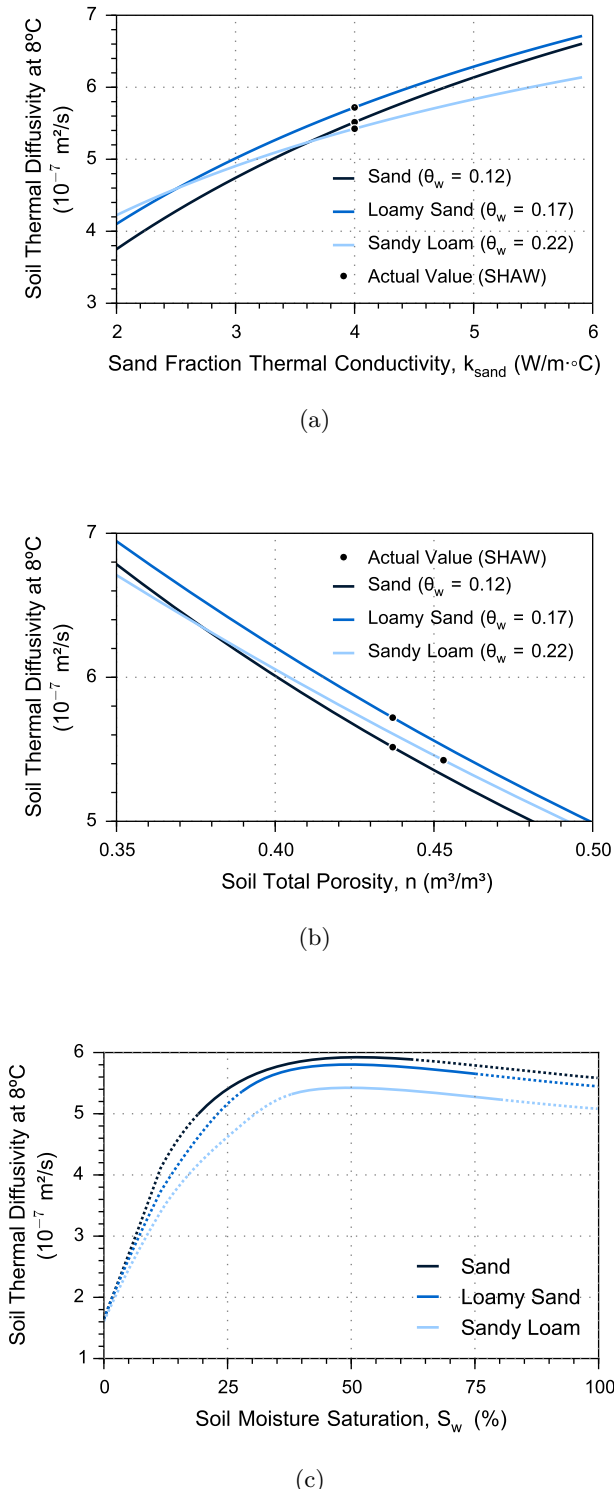


Figure 9
Soil thermal diffusivity as a function of (a) the soil total porosity, (b) the sand fraction thermal conductivity, and (c) the soil moisture saturation. The soil thermal diffusivity takes into account the transfer of latent heat of vaporization and was computed from the calibrated model described in section 2.3.1 at a constant temperature of 8 °C (mean value at 3 m). For (a) and (b), the curves were produced for a fixed value of θ_w that corresponds to the average value of θ_w simulated for each soil type at the depth of 1 m with SHAW (see table 2). The dots in (a) and (b) correspond to the soil thermal diffusivity at the actual value of n and k_{sand} used in SHAW in the simulations. In (c), the solid and dotted lines show, respectively, the value of the soil thermal diffusivity within and outside the range of S_w simulated with SHAW (see table 2).

3.4 Impact of Measurement Errors

The estimation errors of the annual recharge rates that were obtained after the introduction of measurement errors in the synthetic temperature time series for each context were pooled together (for the same reasons that were discussed in [section 3.3](#)) and are presented in the graphs of [figure 10](#). [Figure 10a](#) shows that the addition of random errors to the synthetic temperature time series results in estimation errors of the annual groundwater recharge rates with a median that is always less than 15 mm/y. The scatter of the errors, however, becomes larger as the standard deviation (σ_{obs}) of the measurement error increases. With a σ_{obs} of 0.1 °C, which corresponds to the typical precision limit of a temperature sensor, the interquartile range of the estimation errors corresponds to 130 mm/y, while it reduces to 46 mm/y when σ_{obs} equals 0.025 °C. The errors obtained with a σ_{obs} of 0 °C are explained by the modeling errors as discussed in [section 3.2](#).

Results presented in [figure 10b](#) show that a small bias in the measurements of subsurface temperatures causes a large estimation error of the annual groundwater recharge rates. For instance, a bias of 0.1 °C produces estimation errors with an interquartile of more than 400 mm/y compared to 39 mm/y for the case with no measurement error.

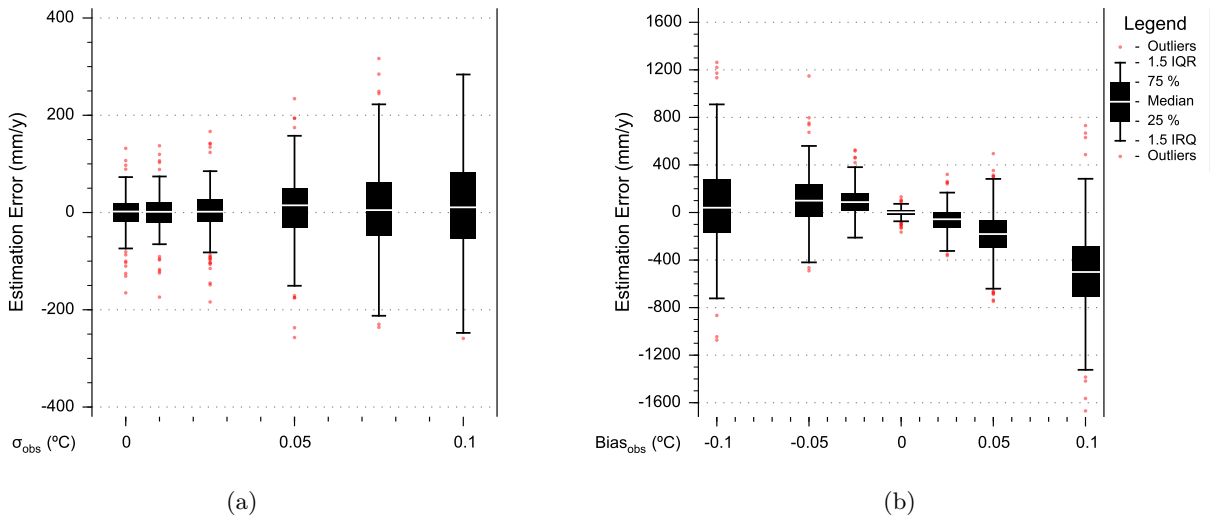


Figure 10 – Tukey box plots of the estimation error of the annual groundwater recharge (all contexts pooled together) obtained after the introduction of (a) random errors in the synthetic temperature time series at 1, 3 and 5 m and (b) a constant bias to the synthetic temperature time series at the depth of 3 m.

4 Discussion

The results presented in [section 3.2](#) showed that, under very controlled conditions, it is possible to estimate annual recharge rates of at least 200 mm/y with an uncertainty of less than 20 % with the method presented in this study. This is assuming, among other things, that the water flux is solved on a weekly basis, that the temperature measurements are taken below the soil freezing zone and are error free, and that the thermophysical properties of the soil are known perfectly *a priori*. The soil thermal conductivity and heat capacity cannot be estimated jointly with the water flux from temperature measurements alone because these parameters are too strongly correlated with the water flux in the advective-conductive heat transport model ([Vandenbohede & Lebbe, 2010a](#)).

When the ideal conditions listed above are not met, results presented in [sections 3.3](#) and [3.4](#) showed that errors on the input model parameters and soil temperature measurements can have a large impact on the accuracy of annual groundwater recharge rates estimated with this technique. For instance, an error of 10 % on the soil total porosity (n) can yield to an estimation error of more than 400 mm/y, regardless of the magnitude of the actual annual groundwater recharge rate. This represents a major limitation of the method for applications in hydrogeology, especially for contexts with low vertical flow rates (and thus where recharge is small). That is, an error of about 400 mm/y may be reasonable for the assessment of the vertical flow rates that are over 4000 mm/y, such as in irrigated fields (e.g. [Taniguchi, 1993](#); [Vandenbohede & Lebbe, 2010a](#)), but may be considered inadequate for diffuse recharge rates that are typically less than 600 mm/y. For instance, large variability and inconsistencies of estimated annual groundwater recharge rates obtained in previous published studies could probably have been explained by the large possible uncertainty of the method. This is the case of [Tabbagh et al. \(1999\)](#), for example, who obtained with a heat-based method at a single site in France, annual recharge to rainfall ratio varying between -0.9 to 2 over a 7 year period.

It is important to stress that the above results were obtained from a numerical exercise based on synthetic data. It is therefore important to discuss further the limits of the present study and to put the above results into perspective for real life applications. Given typical errors of soil thermal properties and temperatures that can be measured with various instruments and techniques ([Stonestrom & Blasch, 2003](#)), the sensitivity analysis presented above could be used to evaluate the magnitude of the possible uncertainty related to annual recharge rates inferred with the method

presented in this study. However, additional sources of error, which were not considered in this study, could also contribute to increase the uncertainty of the estimates in real life application.

The method was tested with synthetic data produced with a set of finite and known parameter values and mathematical expressions that are easily reproducible (see [figure 4](#)). In contrast, real data may be subject to significant epistemic uncertainties that are often hard to reproduce accurately with a mathematical model. The accuracy of the method is thus limited by the capability of the inverse model to faithfully reproduce heat transport and the resulting temperatures in the unsaturated zone. In particular, great care should be taken when calibrating the model of thermal properties (see [equations \(2\)](#) and [\(3\)](#)) as a function of the soil volumetric water content to real measurements in order to limit as much as possible errors on the predicted values of soil thermal diffusivity. According to [de Vries \(1966\)](#), if the mineral composition, porosity, and water content of the soil are known, the accuracy of the soil thermal conductivity computed with the method is within 10% in most cases. This was not a concern in this study since the parameters used to produce the synthetic data with the [de Vries \(1966\)](#) conductivity equation were already known.

Moreover, the synthetic data were produced assuming a soil column with homogeneous soil properties. Soil heterogeneity, which is intrinsic to field studies, would need to be taken into account when applying the method. This implies that measurements of soil properties and calibration of the [de Vries \(1966\)](#) thermal conductivity equation, as discussed above, would need to be done at various depths along the soil profile.

The presence of a shallow water table (excluded from this analysis) would also lead to large vertical variations of the soil volumetric water content, and consequently of the soil thermal properties, above the capillary fringe. Ideally, for environments where the water content varies significantly with time and depth, the soil volumetric water content should be monitored alongside temperature and used as input in the inverse model as was discussed in [section 2.3.4](#). In addition, all temperature time series must be acquired above or below (not a mix of both) the water table for the method to be applicable. Fluctuations of the water table implies the cyclic advection of large amount of sensible heat that cannot be represented properly in the inverse model since the water flux is assumed homogeneous with depth.

Finally, the depth of installation of the three thermal sensors in the ground (top, middle, bottom, see [figure 1](#)) must be determined carefully, because it has an impact on the sensitivity of the heat

transport model to the vertical flux of water in the ground. In this study, the installation depth of the top sensor was determined from the maximum soil frost depth simulated with SHAW, while the depth for the lower and middle sensors were determined from sensitivity analysis (not presented). The sensitivity of the HeatFlow1Dz model to the vertical water flux, and thus its accuracy to assess recharge, increases when the top sensor is installed closer to the surface ($<1\text{ m}$) and when the vertical distance between the top and bottom sensors is large ($>5\text{ m}$). In reality, the extent of frozen ground can be larger than the conditions investigated in this study and subsurface temperature measurements in the unsaturated zone at depths as deep as 5 m below the ground surface are not always available. These limitations would lead to a reduction in the sensitivity of the heat transport model to the vertical flow of water, which will likely cause the estimation errors on annual groundwater recharge rates to be larger. Moreover, uncertainty on the depth of installation of the thermal sensors themselves will also result in an increase of estimation errors (see [Shanafield *et al.*, 2011](#)).

5 Conclusion

The main objective of this study was to test the application limits of a groundwater recharge assessment technique based on the inversion of a numerical heat transport model using temperature time series at three different depths (1, 3 and 5 m) in the unsaturated zone. For this purpose, several synthetic hourly datasets of subsurface temperatures, representing various weather, ground cover, and soil texture conditions, thus covering a wide range of groundwater recharge values, were produced with the vertical one-dimensional coupled heat and moisture transport simulator SHAW ([Flerchinger & Saxton, 1987](#); [Flerchinger *et al.*, 1996](#)). Estimates of the vertical flux of water in the soil were then retrieved from these realistic temperature profiles using a simple one-dimensional numerical simulator of advective and conductive heat transport in the unsaturated zone that was developed as part of this study (HeatFlow1Dz). Unlike previous studies on this topic (e.g. [Suzuki, 1960](#); [Stallman, 1965](#); [Lapham, 1989](#); [Silliman *et al.*, 1995](#); [Taniguchi, 1994](#)), the water flux was not assumed constant on a yearly basis exclusively, but was solved instead on a weekly, monthly, semiannual, and annual basis. From these vertical water flux estimates, annual (potential) groundwater recharge rates were then computed and results were compared to those calculated previously with SHAW to assess the accuracy of the method.

Results showed that, as suggested in [Gosselin *et al.* \(2011\)](#), the water flux has to be solved on a time scale that matches the flow pattern in the ground in order to minimize the estimation error. For the flow conditions tested in this work, the inverse model had to be solved at least on a monthly basis, and weekly simulations worked best. Although simulations showed that it is possible to obtain acceptable estimation errors (e.g. $\pm 20\%$) in ideal conditions (i.e. when all kinds of errors are kept close to zero), they also indicated that this method can rarely be used in real conditions for aquifer recharge assessment. Indeed, sensitivity analyses clearly showed that the introduction of measurement errors and of parameter uncertainty both increase the estimation errors rapidly beyond the recharge value itself. Moreover, the method was tested in a cold and humid climate characterized with an important contrast of air temperature on an annual basis. A contrast reduction of the air temperature would be associated with smaller vertical gradients and smaller annual variation of the temperature in the subsurface, thus leading to a reduced sensitivity to the vertical flow of water and to a more important noise to signal ratio. The application of the method would then lead to even larger uncertainty on the estimated values of groundwater recharge than what was presented in this paper.

In summary, the assessment of groundwater recharge by inverse modeling of the heat transport in the unsaturated zone using temperature time series is complex and is applicable only under very limited conditions. Despite the best modeling and field instrumentation practices, this technique is best suited for engineering or laboratory applications that are carried out in a strictly controlled environment and is likely not well suited to real field conditions. This finding is likely also applicable to other similar methods using heat as a tracer for the estimation of diffuse groundwater recharge rates, either in unsaturated or saturated conditions. Caution is thus advisable when interpreting values of diffuse groundwater recharge predicted with this approach due to the large uncertainty that are likely to be present in the estimated values. Subsurface temperature time series would likely be more useful for the calibration of the thermal properties of a coupled heat and moisture transport model like SHAW, which could in turn be used to assess groundwater recharge, than for the direct estimation of the water flux through the inversion of a heat transport model.

6 Acknowledgments

This research was supported by the NSERC Grant of Jean-Sébastien Gosselin, the NSERC-discovery grant (326975-2011) of Dr. Richard Martel, by funds from the Groundwater Geoscience Program of the Geological Survey of Canada, and the Projet Montérégie Est of the PACES program of the Ministère du Développement durable, de l'Environnement et de la Lutte contre le changement climatique. We thank Dr. Gerald N. Flerchinger of the United States Department of Agriculture for its assistance in the understanding and setup of the SHAW simulator. We thank Dr. Anne-Marie Leblanc, as well as the anonymous reviewers for their very helpful comments on the paper. The climate data for this study were taken free of charge from the Government of Canada website (www.climate.weather.gc.ca).

7 Soil Hydraulic and Thermal Properties

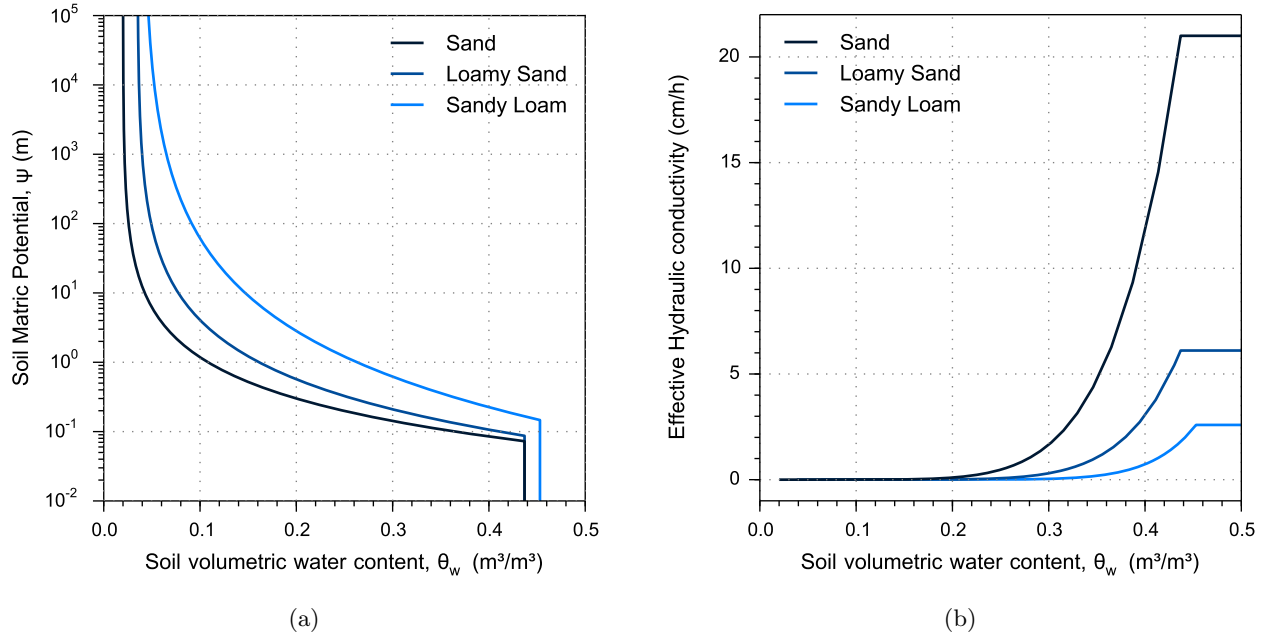


Figure 11 – Soil hydraulic characteristic curves for (a) the water retention and (b) the unsaturated hydraulic conductivity computed using the model of [Brooks & Corey \(1966\)](#) and the parameter values presented in [table 1](#).

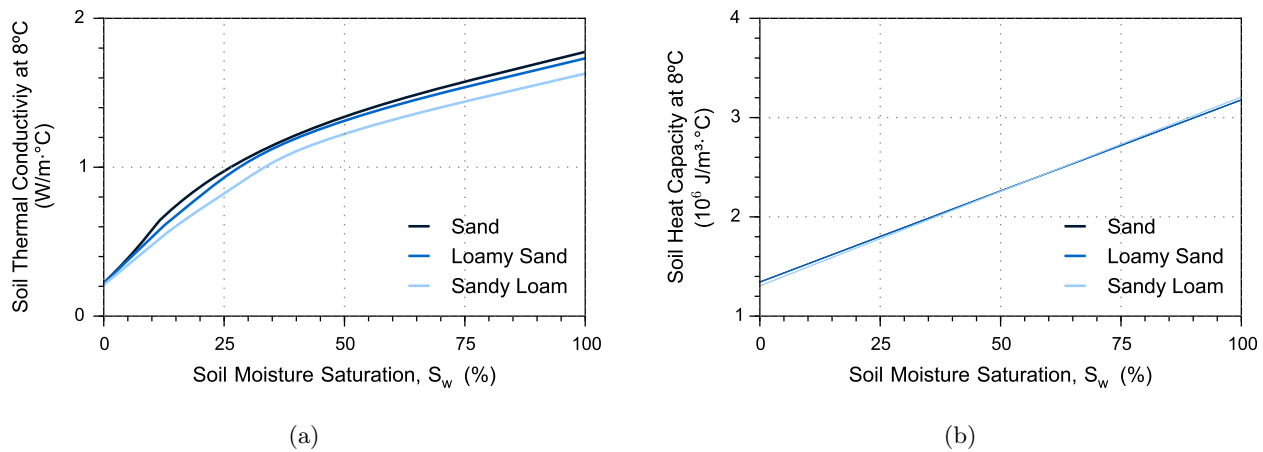


Figure 12 – Soil thermal characteristic curves for (a) the thermal conductivity of the soil computed with the model of [de Vries \(1966\)](#) compensated for the transport of the latent heat of vaporization with the model of [Campbell \(1974\)](#) and (b) the heat capacity of the soil computed with a standard additive mixing law.

Article 3

Combined soil moisture balance and unconfined aquifer water budget to assess recharge from daily weather data and well hydrographs

Titre traduit

Un méthode couplant un bilan hydrologique de surface à un bilan en eau d'un aquifère libre pour estimer la recharge à partir de données météorologiques quotidiennes et de mesures de niveaux d'eau dans un puits d'observation.

Auteurs

Jean-Sébastien Gosselin¹, René Lefebvre¹, Richard Martel¹ et Christine Rivard²

¹ Institut national de la recherche scientifique, Centre Eau Terre Environnement, 490 rue de la Couronne, Québec, QC, Canada

² Commission Géologique du Canada, Division Québec, 490 rue de la Couronne, Québec, QC, Canada

À soumettre

Water Resources Management

Résumé

Cet article décrit une méthode d'estimation de la recharge couplant un bilan hydrologique de surface (*SMB: Soil Moisture Balance*) à un bilan en eau (*AWB: Aquifer Water Budget*) d'un aquifère à nappe libre. La méthode a été testée dans des conditions climatiques continentales humides typiques de l'est du Canada dans un aquifère sableux deltaïque dans la région de Portneuf, près de Québec, où les niveaux des eaux souterraines ont été enregistrés dans un puits d'observation sur une période de plus de 17 ans. Le principe de la méthode consiste à convertir les flux de recharge potentielle calculés avec le bilan hydrologique de surface en un hydrogramme de puits synthétique via le bilan en eau de l'aquifère libre. Une optimisation du modèle couplé des bilans SMB et AWB est ensuite réalisée avec la méthode globale GLUE (*Generalized Likelihood Uncertainty Estimation*). Cette approche est efficace et permet d'estimer des valeurs représentatives de la recharge de même que leur incertitude. La méthode a été implémentée dans le langage de programmation Python et un logiciel informatique, incluant une interface graphique, a été développé pour faciliter l'application de la méthode.

Abstract

This paper describes a recharge assessment method combining a daily soil moisture balance (SMB) and an aquifer water budget (AWB) applicable to unconfined aquifers. Its applicability to continental humid climatic conditions typical of Eastern Canada was tested with the Portneuf region deltaic sand unconfined aquifers, where groundwater levels have been recorded in an observation well for more than 17 years. Daily potential recharge rates obtained from soil moisture balance are converted into changes in groundwater level using the aquifer specific yield and hydrograph recessions, thus producing a synthetic well hydrograph. Calibration of the SMB and AWB hydrologic parameters and uncertainty assessment on predicted water levels and recharge is done with the Generalized Likelihood Uncertainty Estimation (GLUE) method. This approach efficiently provides representative recharge estimates and uncertainty ranges for unconfined aquifers. The method was implemented in the Python programming language and a computer program with a graphical user interface was also developed to facilitate the application of the method.

1 Introduction

Accurate quantification of groundwater recharge rates is important for sustainable aquifer management, considering that recharge has effects on water quality, ecology, and socioeconomic factors (Devlin & Sophocleous, 2005). Recharge is defined in this study as in Healy (2010) as the “downward flow of water reaching the water table, adding to groundwater storage”. Multiple methods are available to estimate recharge and they encompass a wide range of complexity and expense (Scanlon *et al.*, 2002; Healy, 2010). Most of these methods are used to infer recharge rates from indirect measurements (e.g., groundwater level, soil temperature), based on various simplifying assumptions on the timing, spatial distribution, and processes that control recharge. Therefore, large epistemic uncertainties are generally associated with any assessment of groundwater recharge. Moreover, since actual recharge rates are generally unknown and are hardly measurable in-situ, there are no standards that can be used to assess the uncertainty related to recharge estimates (Healy, 2010). Since most of the errors associated with recharge assessments are not quantifiable, it is advised to apply multiple methods to estimate recharge (Lerner *et al.*, 1990; Scanlon *et al.*, 2002; de Vries & Simmers, 2002; Healy, 2010). This recommendation seems, in general, to have been accepted by the scientific community considering the large number of studies that have been carried out since the 2000s whose objective was to compare results from various existing recharge assessment techniques (e.g. Grismer *et al.*, 2000; Arnold *et al.*, 2000; Timlin *et al.*, 2003; Goodrich *et al.*, 2004; Coes *et al.*, 2007; Delin *et al.*, 2007; Heppner *et al.*, 2007; Risser *et al.*, 2009; Sibanda *et al.*, 2009; Croteau *et al.*, 2010; Obiefuna & Orazulike, 2011; Yin *et al.*, 2011; Aurand & Thamke, 2014; Rivard *et al.*, 2014; Huet *et al.*, 2015; Ringleb *et al.*, 2015).

However, application of multiple methods does not resolve all issues related to accurate assessment of groundwater recharge. Even though multiple methods may qualitatively increase confidence in the estimates, it does not reduce nor quantify uncertainty (Healy, 2010). Moreover, application of multiple methods is not always possible in all studies due, for instance, to financial, time or data availability constraints. Among the various existing methods to estimate recharge, those that are simple to apply and based on readily available data, such as basic weather data or groundwater level measurements, remain the most widely used techniques for aquifer assessment studies. Even if the available resources to carry out a study allow the use of a more complex and data-intensive methods to estimate recharge (e.g. in Croteau *et al.*, 2010), comparison of results with those obtained from

simpler approaches is always beneficial. So there are strong practical and scientific incentives for improving simple and data-friendly groundwater recharge assessment methods. These improvements can be in the application procedures, a better definition of application limits, the integration of modern data assimilation techniques, and the development of approaches to assess their uncertainty.

In that perspective, the Water Table Fluctuation (WTF) method is a simple recharge assessment technique, based on a water budget of an unconfined aquifer, that was introduced in the 1920s and has since then been extensively used in numerous studies ([Healy & Cook, 2002](#)). The WTF method requires knowledge of the aquifer specific yield (S_y) and the availability of groundwater level measurements over time. Typically, application of the method consists in manually interpreting the rises in water levels related to individual groundwater recharge events (e.g., [Rasmussen & Andreasen, 1959](#)). Recharge for the entire available water-level monitoring period is calculated by summing the values estimated for the individual events. However, this approach is prone to subjectivity, is time consuming, and is not adapted to the processing of data from large networks of observation wells that monitor groundwater levels on a daily basis or more with automatic pressure transducers. In recent years, efforts have been made to automate the method using a Master Recession Curve (MRC). The MRC is a mathematical description of the average behavior of the declining water-table during periods when groundwater recharge is negligible. Recharge rates are computed by doing a step-by-step comparison of the measured groundwater level fluctuations with those predicted with the MRC over the entire monitoring period. [Posavec et al. \(2006, 2010\)](#) presented a spreadsheet application to automatically construct a MRC from water level time series with a matching strip method. [Heppner & Nimmo \(2005\)](#) developed a computer program for predicting recharge with a MRC and the method was successfully applied in [Heppner et al. \(2007\)](#). These new automated adaptation of the WTF method will become very valuable for recharge assessment since monitoring groundwater levels on a daily, and even hourly basis, has become more accessible since the commercialization in the 1990s of affordable submersible pressure transducers combined with electronic data loggers ([Freeman et al., 2004](#)).

Recharge can also be estimated as the residual of a simple daily Soil Moiture Balance (SMB) (e.g., [Rushton, 2003](#); [Rushton et al., 2006](#)). The most basic SMB models typically require as inputs daily air temperature and total precipitation. Even the simplest SMB models represent most of the important processes controlling recharge. Potential evapotranspiration and surface runoff can be calculated from the input data using empirical models or functional relationships. Under cool humid climate,

precipitation falling as snow must be accumulated on the surface and melted when temperatures become warmer ([USDA NRCS, 2004](#)). Infiltration of water into the soil is calculated as the total amount of available water from precipitation and/or snow melt less any interception and/or runoff. The amount of water in excess of field capacity within the root zone, after (actual) evapotranspiration and infiltration have been resolved, is then simply compiled as potential groundwater recharge that is assumed to eventually reach the water table. More complex SMB models also simulate the downward movement of water through the unsaturated zone, either through a water routing procedure (bucket models), such as the HELP3 infiltration model ([Schroeder et al., 1994](#)), or through the resolution of Richards equation, such as the HYDRUS numerical simulator ([Šimůnek et al., 2013](#)). An alternate approach consists in representing the movement of water through the unsaturated zone with a transfer function, such as in the AquiMod model ([Mackay et al., 2014a](#)). Since SMB methods rely mostly on readily available data and are relatively straightforward to apply, they can easily be used at the onset of aquifer assessment studies or for routine recharge assessment and are, for these reasons, widely used in practice. Many countries maintain databases of measured daily weather data. For example, the Canadian Daily Climate Database (CDCD) contains daily data for air temperature and precipitation for about 8450 stations distributed across Canada. Some stations have data available dating back to 1840 to the present.

Uncertainty of recharge rates estimated with the WTF method relates to the limited accuracy with which specific yield of the aquifer can be determined ([Healy & Cook, 2002](#)). Similarly, SMB calculations are quite simple, but there is a relatively large uncertainty on input parameters (e.g. potential ET, runoff coefficient, water storage in soils), so that estimated recharge rates are uncertain as well ([Larose-Charette et al., 2000](#); [Lefebvre et al., 2011](#)). Large epistemic errors can also be expected in the WTF and SMB methods due to uncertainty in data inputs and validity of the simplifying assumptions that are inherent to both methods. For example, small or diffuse recharge events are hard to assess in the WTF method, as the competing effects of level recession and small infiltration do not lead to clear peaks in water level. The use of a MRC alleviates somewhat this issue, but there is an uncertainty associated with the definition of the MRC as well. Representation of the various processes controlling recharge in the SMB (e.g., evapotranspiration, runoff) is most likely not always representative of field conditions and is also a source of errors that is hard to quantify. For both of these methods, validation of results is difficult because they cannot be compared to accurate measurements of recharge.

For example, although the flux of water draining through the unsaturated zone can be directly measured with different types of lysimeters, these measurements are most often representative of local conditions. It is thus generally difficult to reconcile lysimeter data with estimates obtained from the WTF method that is generally used to evaluate recharge rates that are representative at the field scale. Similarly, measurements of moisture content in the saturated zone can be used to calibrate a SMB model. However, these unsaturated measurements are generally representative of the local scale ([Healy, 2010](#)) and are thus not optimal if estimation of recharge at a larger scale is needed.

In recent years, work has been done to combine the WTF and SMB approaches to circumvent some of limitations of these two methods. For instance, [Baalousha \(2005\)](#) applied the method initially proposed by [Bredenkamp *et al.* \(1995\)](#) called Cumulative Rainfall Departure (CRD) for the estimation of recharge in the Gaza Strip. [Lefebvre *et al.* \(2011\)](#) subsequently adapted the method to temperate continental climate conditions. The principle of the method is to 1) estimate recharge from daily SMB and 2) to calculate the change in groundwater level related to that daily recharge using the specific yield of the unconfined aquifer. The method also accounts for the recession of groundwater levels during periods without recharge. Hydrologic parameters are calibrated by matching SMB-derived water levels (synthetic hydrograph) to the observed well hydrographs. Similarly, [Mackay *et al.* \(2014b\)](#) presented the lumped conceptual model AquiMod to simulate groundwater level time-series. They subsequently presented an application in [Mackay *et al.* \(2015\)](#) to do seasonal forecasting of groundwater levels. Though their study was not aimed at groundwater recharge estimation, recharge could have been assessed from their model since it is calculated as an internal variable.

This paper builds on previous studies and presents another approach that combines a daily Soil Moisture Balance (SMB) with an Aquifer Water Budget (AWB) to estimate groundwater recharge, using as input basic daily weather data (air temperature and total precipitation) and daily groundwater level measurements. The method was kept as simple as possible and is thus straightforward to apply on the basis of readily available data. Original contributions of this work include 1) improvements of the conceptual SMB model described in [Lefebvre *et al.* \(2011\)](#) for cool humid climate, 2) integration of an automated procedure to define a Master Recession Curves (MRC), 3) development of an automated optimization approach, 4) assessment of uncertainty with the GLUE methodology (Generalized Likelihood Uncertainty Estimation; [Beven & Binley, 1992, 2014](#)), 5) implementation of the method in the Python programming language and 6) development

of a graphical user interface. The theoretical basis underlying the method is presented in the first part of this paper, followed by an application to a study site located in the unconfined deltaic aquifer system of the Portneuf area, located in southern Quebec, Canada ([Fagnan et al., 1999](#)).

2 Method

The proposed method is based on a daily Soil Moisture Balance (SMB), combined with an Aquifer Water Budget (AWB), as shown in [figure 1](#). Required input data are daily total precipitation, mean air temperature, and groundwater level measurements. The principle of the method is to first calculate the amount of water from liquid precipitation and/or snow melt that is available for surface runoff and soil infiltration. Daily potential recharge rates are then computed as the amount of water in excess of the field capacity in the root zone. Variation of moisture storage in the root zone is computed with a book keeping procedure as the net balance between infiltration (I), actual evapotranspiration (ET) and potential recharge rates (PR). The SMB-derived daily potential rates are then used as input in the AWB to compute variations in water level (Δh) considering the aquifer specific yield (S_y) and thus produce a synthetic well hydrograph that can be compared to actual measurements. The net lateral outflow from the aquifer ($Q_{net} = Q_{out} - Q_{in}$) is estimated using a Master Recession Curve MRC defined from the recession periods in the observed well hydrograph.

Calibration of the SMW-AWB model and assessment of the uncertainty of predicted water levels and recharge rates are done with the global optimization method GLUE (Generalized Likelihood Uncertainty Estimation; [Beven & Binley, 1992, 2014](#)). Briefly, this method consists in producing a large amount of realizations, using multiple sets of parameter values drawn from a distribution range of plausible values of the hydrologic parameters, namely the runoff coefficient (C_{RO}), maximum readily available water supply (RAS_{max}), and specific yield of the aquifer (S_y). An informal likelihood measure is calculated for each synthetic well hydrograph by comparison with observations, which are subsequently used to derive Cumulative Distribution Functions (CDF) of the predicted variables of interest (water level and recharge) at each time step of the simulation. The CDFs are finally used to specify uncertainty limits on the predicted water level and daily recharge rates.

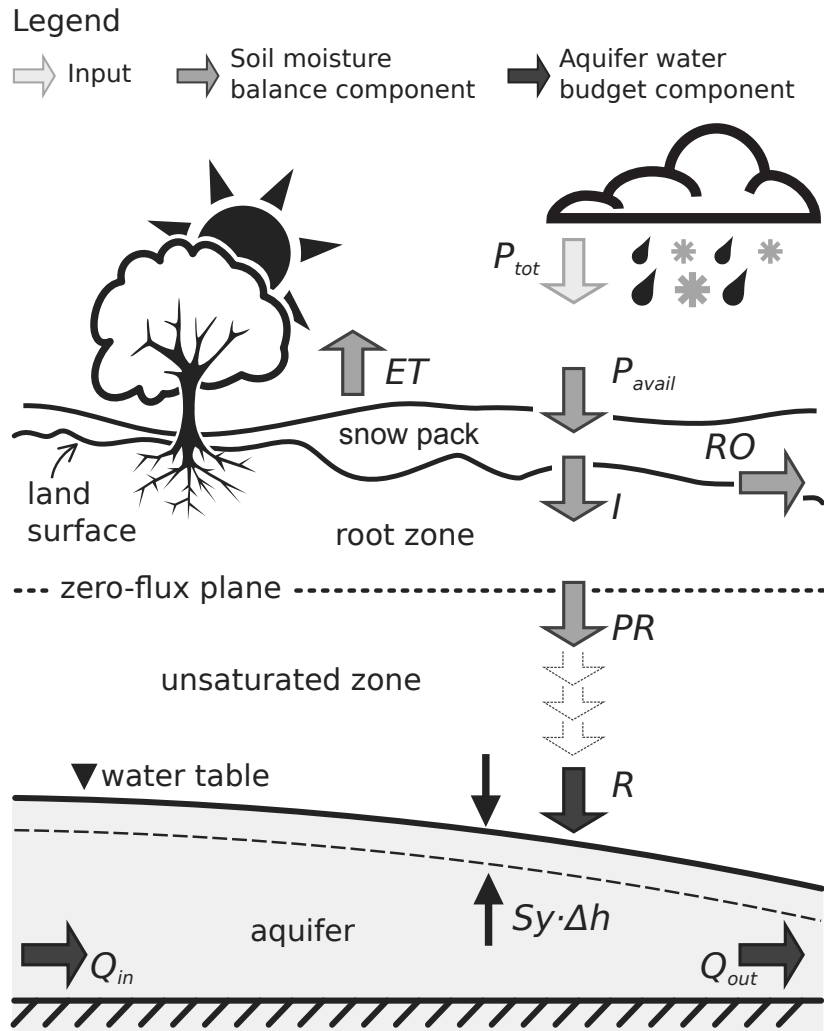


Figure 1 – Diagram showing relations between components of the soil moisture balance and aquifer water budget.

2.1 Surface Water Budget

The excess water that drains below the root zone as potential recharge (PR) is estimated on a daily basis as the residual of a daily soil moisture balance (SMB) (Rushton, 2003; Rushton *et al.*, 2006):

$$PR = I - ET - \Delta RAS = (P_{avail} - RO) - ET - \Delta RAS \quad (1)$$

where I is the infiltration of water in the soil, P_{avail} is available precipitation from snow melt and/or rain, RO is surface runoff, ET is the actual evapotranspiration, and ΔRAS is the daily variation of readily available moisture storage in the root zone.

2.1.1 Available Precipitation

Because during winter precipitation often falls as snow that accumulates (P_{acc}) on the ground surface, total precipitation (P_{tot}) cannot be used directly to compute surface runoff (RO) and water infiltration (I) in the soil. These are computed instead from the available precipitation (P_{avail}), which corresponds to the amount of liquid water available for surface runoff and infiltration after snow accumulation and melting has been resolved. The flowchart of figure 2 presents the methodology that is followed to compute P_{avail} and the amount of accumulated precipitation (P_{acc}) on the ground surface based on the total precipitation (P_{tot}), mean air temperature (T_{air}), and melt potential (MP).

The melt potential (MP) is computed from daily mean air temperature using a simple degree-day method (USDA NRCS, 2004). This is the most common melt index approach used to calculate snow melt and it can be formulated as follows:

$$MP = C_M \cdot (T_{air} - T_{melt}) \quad \text{where} \quad MP \geq 0 \quad (2)$$

where MP is the potential snowmelt in mm/d, C_M is the degree-day melt coefficient in mm/ $^{\circ}\text{C}$, and T_{air} and T_{melt} are the mean daily and base air temperature of melting in $^{\circ}\text{C}$. The coefficient C_M varies geographically and seasonally, with typical values ranging between 1.6 to 6.0 mm/ $^{\circ}\text{C}$. When information is lacking, a constant value of 2.74 mm/ $^{\circ}\text{C}$ can be used as suggested by USDA NRCS (2004).

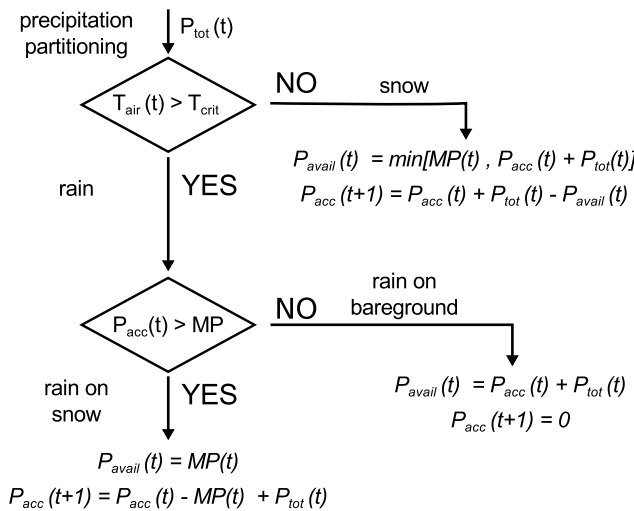


Figure 2
Flowchart showing the functional relationships used to compute daily accumulated P_{acc} and available (P_{avail}) precipitation from mean air temperature (T_{air}) and total precipitation (P_{tot}).

The first step in the calculation of P_{avail} and P_{acc} is to determine the phase of P_{tot} (snow or rain). Multiple methods, encompassing a wide range of complexity and data requirements, exist to partition total precipitation into snow, mixed precipitation or rain (Kienzle, 2008). In this study, a simple static threshold approach is used, where precipitation for a single day is assumed 100 % solid if mean air temperature (T_{air}) is equal or lower than a critical temperature value (T_{crit}) and 100 % liquid otherwise (Kienzle, 2008).

If precipitation is assumed falling as snow, any $P_{avail}(t)$ for the day is from snow melt at ground surface due to the upward heat flux from the soil. Value for $P_{avail}(t)$ is then set as the minimum between MP and the sum of P_{tot} and $P_{acc}(t)$ at the beginning of the day. Daily variation of P_{acc} corresponds to the amount of solid precipitation that has fallen over the day, minus the melt. If the value of T_{melt} is greater or equal to T_{crit} , MP will always equal to zero, and so will $P_{avail}(t)$. All precipitation falling during the day as snow will then be added to P_{acc} .

If precipitation is assumed to be liquid, melt potential (MP) is first calculated and compared to the P_{acc} . If $P_{acc}(t)$ is less than MP at the beginning of the day, all remaining accumulated precipitation on the ground surface is melted during the day ($P_{acc}(t+1) = 0$) and rain is thus assumed to fall on bare ground. All water from snow melt and falling precipitation is then accounted as available precipitation for the day. If $P_{acc}(t)$ is larger than MP , it is then assumed that the snow cover is not fully melted during the day and $P_{avail}(t)$ is set equals MP . Since rain is assumed to fall on snow, precipitation that has fallen during the day is added to the remaining accumulated precipitation.

The above approach assumes that, in all cases, rain falling on snow is instantly refrozen on top of the snow pack. Latent and sensible heat effects involved in these rain-on-snow events are, however, not taken into account in the computation. The model also does not consider that rain can freely percolate through an isothermal porous snowpack and reach the ground surface as available precipitation. Even though this overly simplistic approach does not accurately represent snow melting and timing of snow melt, it is not a critical element of the groundwater recharge assessment method presented in this paper because it does not influence significantly the water budget on a yearly basis.

2.1.2 Surface Runoff

Surface runoff is calculated as a linear fraction of available precipitation (Rushton, 2003; Rushton *et al.*, 2006):

$$RO = C_{RO} \cdot P_{avail} \quad (3)$$

where RO is surface runoff in mm/d, C_{RO} is the runoff coefficient, and P_{avail} are available precipitation in mm/d.

Runoff corresponds in this study to an average value for a single day over an area of one to several km² around an observation well. It also accounts indirectly for precipitation interception from vegetation cover. The runoff coefficient is thus considered to be a best constant value in the model.

The above approach was chosen to facilitate the calibration process and uncertainty assessment. More complex approaches could be considered, such as the one presented by Rushton *et al.* (2006) where runoff is calculated with a set of functional relationships based on the intensity of precipitation and soil moisture deficit.

2.1.3 Infiltration

Infiltration is calculated as the available precipitation computed from rain and snow melt, less surface runoff:

$$I(t) = P_{avail}(t) \cdot (1 - C_{RO}) \quad (4)$$

where I is the infiltration in the soil, P_{avail} are the available precipitation, and C_{RO} is the runoff coefficient.

2.1.4 Readily Available Storage, Actual Evapotranspiration, and Potential Recharge

Readily Available Storage (RAS) corresponds to the amount of water within the root zone that is available for plant evapotranspiration. Its maximum value (RAS_{max}) is related to the field capacity

of the soil, the root depth, and the wilting point (Rushton *et al.*, 2006):

$$RAS_{max} = (\theta_{FC} - \theta_{WP}) \cdot h_{roots} \quad (5)$$

where RAS_{max} is maximum readily available storage, θ_{FC} is field capacity of the soil, θ_{WP} is the wilting point, and h_{roots} is the root depth. The field capacity is the soil moisture content at which the rate of drainage in the soil becomes insignificant (Healy & Cook, 2002), while the wilting point is the soil moisture content below which plant roots cannot extract moisture (Rushton *et al.*, 2006).

Variation of RAS over time is computed with a book keeping procedure. The principle of the approach is described below, as illustrated by figure 3 on which are drawn two soil moisture profiles: one before and another after a rain event that was significant enough to produce recharge.

Before the rain event, soil moisture was below the field capacity due to water uptake from plants. The amount of water required to bring the soil moisture to field capacity is called the soil moisture deficit (SMD) and is illustrated as the light shaded area in figure 3. During the rain event, the infiltration of water was larger than the SMD, bringing the soil moisture over the field capacity. An intermediary value for RAS is then calculated:

$$RAS^*(t + 1) = RAS_t + I \quad (6)$$

where I is water infiltration in the soil, and RAS_t and $RAS^*(t + 1)$ are the readily available storage, respectively at the beginning of the day (before the rain event) and after the rain event.

The amount of water in excess of the field capacity, illustrated in figure 3 as the dark shaded area, is then assumed to drains below the root zone as potential recharge:

$$PR(t) = \min[0, RAS^*(t + 1) - RAS_{max}] \quad (7)$$

where $PR(t)$ is potential recharge calculated for the day. In cases when $RAS^*(t + 1)$ is lower than RAS_{max} due to the soil moisture being below field capacity, potential recharge will equal zero.

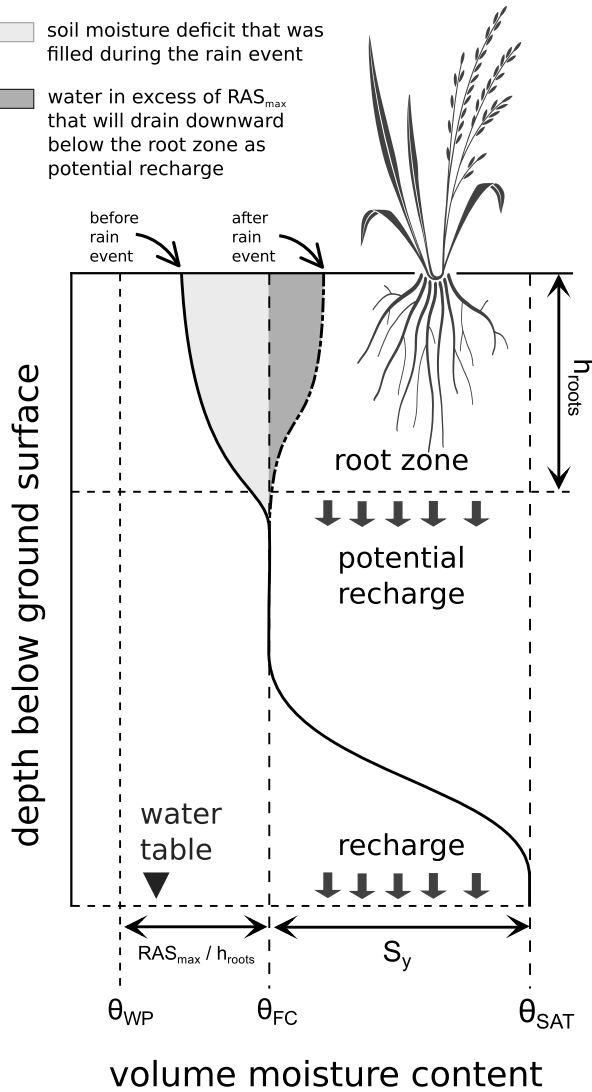


Figure 3

Diagram showing two soil moisture profiles within the unsaturated zone: one before and another after a rain event that was significant enough to produce recharge. The light shaded area corresponds to the Soil Moisture Deficit (SMD), while the dark shaded area corresponds to water in excess of the field capacity (θ_{FC}) of the soil that is assumed to drain below the root zone as potential recharge.

Potential recharge is then subtracted from the soil moisture storage to compute a second intermediary value of *RAS*:

$$RAS^{**}(t+1) = RAS^*(t+1) - PR(t) \quad (8)$$

where $RAS^{**}(t+1)$ is the readily available water after drainage. If no drainage occurred, $RAS^{**}(t+1)$ will then simply equal $RAS^*(t+1)$.

Potential evapotranspiration is then subtracted from the soil, up to RAS^{**} , to compute RAS at the begining of the next day:

$$RAS(t+1) = RAS^{**}(t+1) - ET(t) = RAS^{**}(t+1) - \min[RAS^{**}(t+1), PET(t)] \quad (9)$$

where ET is the actual evapotranspiration and PET is the potential evapotranspiration calculated with [Thorntwaite \(1948\)](#). In cases where PET is larger than RAS^{**} , soil is considered to be under stress and the actual evapotranspiration will be lower than the potential value.

Actual evapotranspiration is resolved in this approach after recharge. Thus, evapotranspiration cannot occur concurrently with precipitation. This approach is supported by the assumption that water drainage occurs in coarse soils on a time scale that is faster than evapotranspiration. This has also some merit for the calibration of the model since it allows evapotranspiration to be increased monotonically, from 0 up to a maximum value, as a function of potential evapotranspiration and total precipitation, by increasing the value of RAS_{max} .

2.2 Aquifer Water Budget

As in the water table fluctuation method, the aquifer water budget (AWB) is based on the assumption that variation of groundwater storage in the aquifer equals recharge, minus the losses at the aquifer boundaries (net lateral outflow) ([Healy & Cook, 2002](#)):

$$S_y \frac{\partial h}{\partial t} = R - Q_{net} \quad (10)$$

where $\partial h / \partial t$ is the variation rate of the water table depth over time, R is the daily amount of groundwater recharge reaching the water table, Q_{net} is the net lateral outflow from the aquifer, and S_y is the specific yield of the aquifer.

Specific yield is a storage term that is defined as the ratio of the volume of water a saturated rock or soil will yield by gravity to its own volume ([Healy & Cook, 2002](#)). In the model, S_y is considered to be a constant value, averaged over time and representative over an area of one to several km² around the observation well, over the entire depth-range in which the water table is fluctuating. This means that specific yield measured on a soil sample will not necessarily be representative of S_y as defined in the model. These laboratory measurements give values of S_y for the soil matrix at a

specific point in space, and do not take into account macro heterogeneity of the soil such as roots, cracks, and rock fragments. Specific yield values estimated from pumping tests (e.g. [Neuman, 1987](#)) will most likely be more representative estimates of S_y for use in this method because they represent an integrated value over a larger area. When information is lacking though, measured or published values from soil samples can be used (e.g., [Rawls *et al.*, 1982](#)).

2.2.1 Aquifer Lateral Outflow

The net outflow of groundwater to aquifer boundaries (mostly rivers) can be estimated directly by interpreting the periods in the well hydrograph where water levels monotonically recede in the absence of recharge. Under temperate continental climates, recharge occurs mostly during spring snow melt and in the fall. Typically, water level will recede during summer and winter, as most precipitation will be used by plants if it infiltrates in the summer and will accumulate on the soil surface as snow in winter.

The average behavior of the declining water-table can be described with a Master Recession Curve (MRC). The strength of this correlation, and thus the validity of the MRC, depends on many factors, including the local topography, seasonality of the climate, hydraulic properties of the subsurface porous medium, and depth to the water-table ([Heppner & Nimmo, 2005](#); [Heppner *et al.*, 2007](#)).

The first-order time derivative of the MRC corresponds to the ratio Q_{out}/S_y , which can take the form of a linear relationship between water-table elevation and water-table declining rate. During periods where recharge is assumed zero ($R = 0$), [equation \(10\)](#) can be rewritten as:

$$\frac{\partial h}{\partial t} = -Q_{out}/S_y = -(a \cdot h(t) + b) \quad (11)$$

where a and b are parameter constants. It is assumed that [equation \(11\)](#), which was established during period when recharge is zero, is also valid during periods when recharge is non-nul.

Estimation of the a and b constants is done in two steps. The first step consists in identifying from the well hydrograph the periods when groundwater recharge is supposed negligible and water levels recede. The second step consists in reproducing the receding water levels with a simple

Crank-Nicolson numerical scheme of [equation \(11\)](#):

$$h(t+1) = \left[\left(1 + \frac{a \cdot \Delta t}{2} \right) h(t) + b \cdot \Delta t \right] \left[1 - \frac{a \cdot \Delta t}{2} \right]^{-1} \quad (12)$$

These simulated water levels are then compared to measurements and the a and b parameters are optimized using a Gauss-Newton optimization algorithm ([Menke, 1989](#)).

2.2.2 Recharge

Daily groundwater recharge is assumed to equate directly the potential recharge that is calculated with the surface water budget with [equation \(7\)](#). A lag sometimes needs to be added to the simulated potential recharge to take into account time taken by the water to drain through the unsaturated zone and reach the water table. This lag can be estimated by running a cross correlation between the synthetic and observed well hydrographs. A more sophisticated approach could be considered, such as modeling the transport of water through the unsaturated zone with a water routing procedure ([Schroeder *et al.*, 1994](#)) or a transfer function ([Besbes & De Marsily, 1984](#)).

2.2.3 Synthetic Well Hydrograph

Using the MRC mathematical description and daily recharge rates as input, the synthetic well hydrograph is computed with a simple explicit time-forward numerical discretization of [equation \(10\)](#):

$$h(t+1) = (R/S_y - (a \cdot h(t) + b)) \cdot \Delta t + h(t) \quad (13)$$

2.3 Model Calibration

One of the problems with traditional approaches to calibrate models is that they are based on finding a unique set of parameters that best fits the observations. Uncertainty is then estimated by looking at the model sensitivity around the optimal point in the parameter space. However, this optimization approach was not adequate for recharge assessment with the model presented in this study because of high level of intercorrelation between the various parameters of the SMB and AWB. Therefore,

multiple combinations of parameter values, which are not necessarily in close proximity within the parameter space, seemed to give equally acceptable results when compared to observations.

Therefore, model calibration and uncertainty estimation is done with the global optimization methodology GLUE ([Beven & Binley, 1992, 2014](#)). The GLUE approach was applied as follows:

1. Define the MRC from the observed well hydrograph.
2. Define an initial distribution range of plausible values for the hydrologic parameters.

Only the runoff coefficient (C_{RO}), maximum readily available water supply (RAS_{max}), and specific yield of the aquifer (S_y) are used for model calibration. All other model parameter values are fixed using available information about the study site or based on expert judgment.

3. Produce multiple synthetic well hydrographs using various sets of model parameter values drawn from the parameter space defined in (2).

More specifically, the range of plausible values for C_{RO} and RAS_{max} is first discretized in a numerical grid of discrete parameter values with uniform intervals. For each unique set of C_{RO} and RAS_{max} values in the grid, the synthetic well hydrograph produced with the model is fitted to the observations by optimizing the value of S_y with a Gauss-Newton gradient approach ([Menke, 1989](#)).

4. Calculate the informal likelihood measure for each synthetic well hydrograph produced in (3).

The informal likelihood measure in this study is based on the sum of squares of the residuals between the simulated and measured hydrographs ([Beven & Binley, 1992](#)):

$$\mathcal{L}[p] = 1/(\sigma_p^2) \quad (14)$$

where $\mathcal{L}[p]$ is the informal likelihood value and σ_p^2 is the variance of the residuals for the synthetic hydrograph produced for a set of model parameters p . However, if the value of S_y in p falls outside the range of plausible values defined as prior information in (2), the model is assumed non-behavioural and its likelihood value $\mathcal{L}[p]$ is set to zero.

5. Compute uncertainty limits for the predicted variable of interest

The informal likelihood values calculated with [equation \(14\)](#) are first scaled so that their sum for the entire population of behavioral models is equal to 1. For each time step of the

simulation, the scaled informal likelihood values are used as probabilistic weighting function to produce a Cumulative Distribution Function (CDF) of the predicted water level and daily recharge rates. Uncertainty limits are then defined on both predicted variables by taking the 5th and 95th percentiles of their respective CDF and the 50th percentile as a measure of the modal behavior.

3 Case Study

3.1 Material and Method

3.1.1 Study Area

The study area is an unconfined deltaic aquifer along the Jacques-Cartier river, in the Portneuf area located on the north shore of the St. Lawrence River (see [figure 4](#)), where many scientific and groundwater characterization studies have been carried out in the past (e.g., [Fagnan et al., 1999](#); [Larose-Charette et al., 2000](#); [Paradis et al., 2007](#); [Lefebvre et al., 2011](#)).

The regional geology consists mainly of surficial quaternary sediments of marine and continental origin, overlying Precambrian Grenville rocks to the north and Ordovician sedimentary rocks (limestones and shales) of the St. Lawrence Platform to the south. [Figure 4](#) shows the five hydrogeological contexts that were defined based on the geology of the study area ([Fagnan et al., 1999](#)): A) deltaic sands and gravel, B) Saint-Narcisse Moraine, C) sedimentary rocks, D) igneous and metamorphic rocks, and E) silts and marine clays. Deltaic aquifers are the most productive and have the best groundwater quality in the study area. These deltaic aquifers are associated to the two main rivers in the area, Sainte-Anne and Jacques-Cartier, and they cover 525 km² with an average thickness of 12 m. The thickness is controlled by irregularities in the underlying till-covered bedrock surface or its local erosion. The hydraulic conductivity of the sands varies between 1×10^{-5} and 7×10^{-3} m/s ([Larose-Charette et al., 2000](#)). Deltaic sand overlays Champlain Sea silts and clays. Most of the Jacques-Cartier River is in hydraulic contact with the adjacent deltaic aquifer ([Larose-Charette et al., 2000](#); [Lefebvre et al., 2011](#)).

HYDROGEOLOGICAL CONTEXTS

A	Deltaic sands and gravels	C	Sedimentary rocks	E	Marine silts and clays
B	Saint-Narcisse Moraine	D	Igneous and metamorphic rocks		

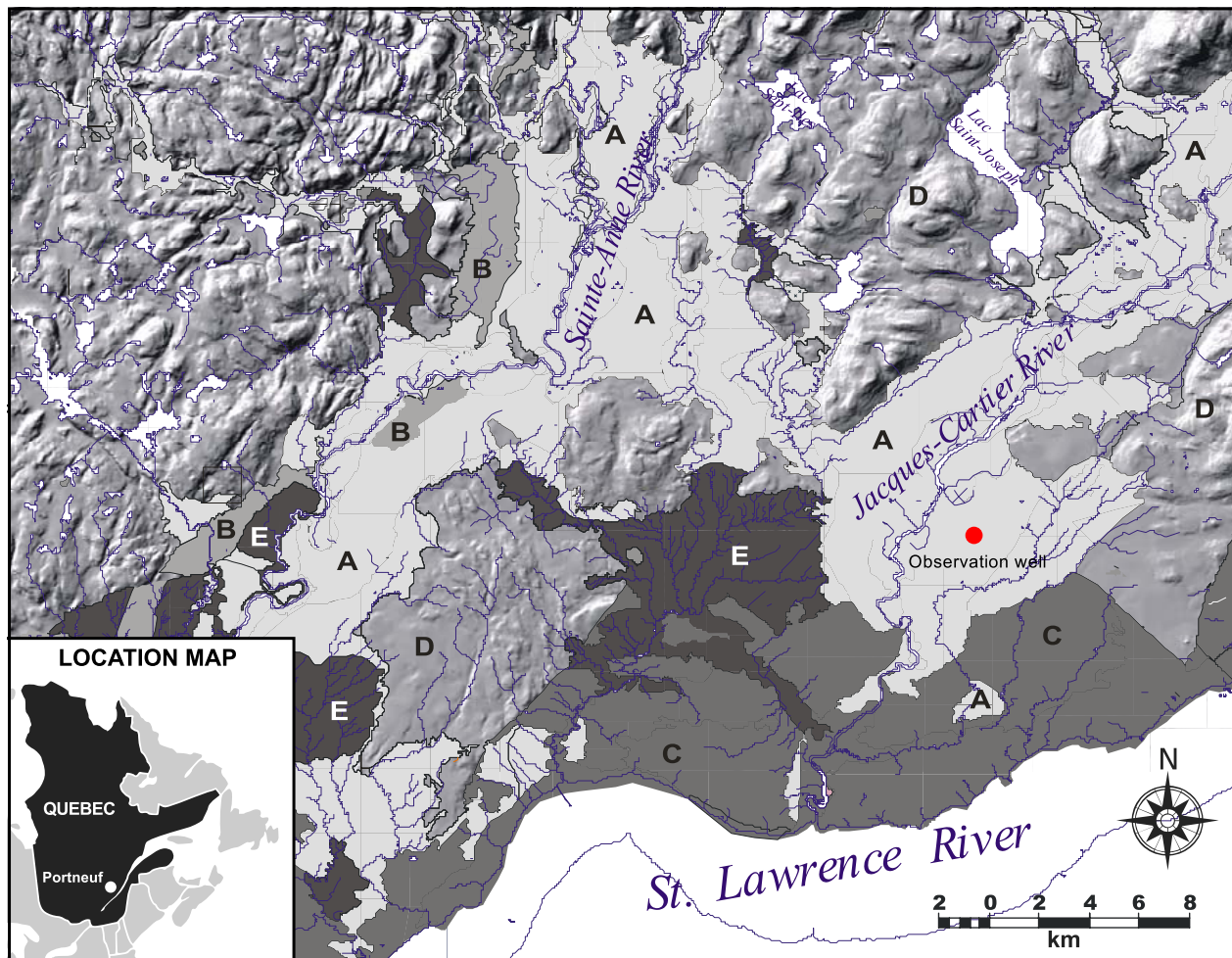


Figure 4 – Location of the Portneuf area in the St. Lawrence Lowlands, Quebec, Canada (modified after Fagnan *et al.*, 1999). The map shows the observation well (red circle) located in an unconfined deltaic aquifer whose hydrograph is interpreted in this paper.

3.1.2 Previous Work

Paradis *et al.* (1997) assessed groundwater recharge in the Portneuf River watershed with hydrological modeling using the CEQUEAU hydrological matrix balance model (Morin & Paquet, 1995). For total mean precipitations of 1174 mm/y, the mean recharge obtained over the entire basin for that period was 299 mm/y. However, the Portneuf watershed has only about half of its surface over deltaic aquifers, the rest being over marine clay. Still, these results provide an indication of probable recharge range in the study area.

Recharge was estimated with a monthly soil moisture balance by [Larose-Charette et al. \(2000\)](#) for 13 weather stations over the Portneuf area. A range of recharge values was calculated based on a range of potential values of hydrologic parameters: runoff coefficient C_{RO} from 0.2 to 0.4 and maximum readily available water supply $RASmax$ from 0 to 150 mm. They obtained minimum and maximum recharge estimates that varied by more than 200 mm/y, with mean recharge values covering a wide range from 250 to 500 mm/y. Their results showed that, without more constraints on the hydrologic input parameters to monthly SMB calculations, recharge rates estimated with this approach are associated with large uncertainties.

[Larose-Charette et al. \(2000\)](#) also calculated initial estimates of recharge with the water table fluctuation method based on the early water level measurements (from the fall of 1996 to the fall of 1998) in four different wells located in the Portneuf area. Analysis of these hydrographs led to recharge estimates between 199 to 284 mm/y. [Larose-Charette et al. \(2000\)](#) also developed numerical models of groundwater flow for three parts of the deltaic aquifers of the Portneuf area (Jacques-Cartier River, Ste-Anne North and Ste-Anne South River). To match these numerical models, a best constant recharge value of 250 mm/y was used. However, a sensitivity study showed that the models were not very sensitive to recharge. Recharge values wider than 200 to 300 mm/y could have also provided a good match between measured and simulated water levels.

[Lefebvre et al. \(2011\)](#) adapted the approach described in [Baalousha \(2005\)](#) to estimate recharge in the Portneuf area using daily weather data and water level measurements from the same four wells as those used by [Larose-Charette et al. \(2000\)](#). Like the method presented in this paper, their approach consisted in converting SMB-derived recharge rates to synthetic groundwater levels and to compare the results with real water level measurements. They estimated average yearly recharge rates of about 300 mm/y, with recharge varying from year to year from about 200 to 450 mm/y. They also estimated that the time taken by the water to reach the water table from the ground surface was about 40 to 50 days for sites with unsaturated zone thickness of 8 to 16 m. Though uncertainty ranges were estimated for the calibrated hydrologic parameters, no uncertainty on groundwater recharge was estimated.

The method used by [Lefebvre et al. \(2011\)](#) to calibrate their model was based on a local optimization approach that is traditionally used in hydrogeology, in which a unique set of optimal model parameters was sought based on a qualitative comparison between simulated and measured

water levels. Uncertainty in the parameters was estimated based on a qualitative sensitivity analysis made around this set of optimal parameters in the parameter space. However, because the inter-correlation between the parameters are important, this approach most likely overestimated the information content of the calibration data, which resulted in the uncertainty ranges being too narrow. In this study, we recognize that multiple sets of parameters can produce synthetic hydrographs that provide a fit to the water levels measured in the well that is equally likely. Therefore, calibration of the model is done with the global optimization method GLUE. This approach defines uncertainty limits on the predicted recharge values, which do not overestimate the information content in the observed well hydrograph.

3.1.3 Water Level and Weather Data

Daily groundwater level measurements from an observation well of the national monitoring network of Quebec ([Gouvernement du Québec, 2015](#)) are available from 1996 to the present. The well is installed in the unconfined deltaic aquifer along the Jacques-Cartier River (see red dot on [figure 4](#)). Sand thickness near the well is about 10 to 15 m ([Lefebvre et al., 2011](#)). [Figure 5](#) shows a drawing of the well. The 12.3 m deep well is installed in medium to fine sand and is screened at the bottom over a 1.5 m interval.

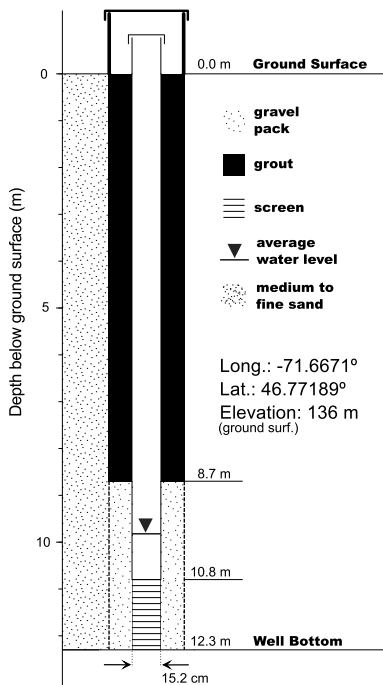


Figure 5
Completion of observation well #5080001 of the Quebec monitoring network ([Gouvernement du Québec, 2015](#)) located at Pont-Rouge, in the Portneuf area (see map on [figure 4](#)).

The closest weather station (STE CHRISTINE) is located 20 km from the well. Weather data were downloaded for that station from the government of Canada website (<http://climate.weather.gc.ca/>). Figure 6 presents annual and monthly averages for precipitation and air temperature for the period 1960-2015. Average annual total precipitation and air temperature are, respectively, 1210 mm/y and 3.5 °C. Monthly total precipitation, as rain or snow, are distributed rather evenly throughout the year, but are slightly more important during summer. Precipitation as rain also occurs frequently in the winter season during mild spells.

Figure 7 shows the well hydrograph recorded in the well for the years 1996-2014. Mean water level is 9.6 m below ground surface during this period. Total monthly precipitation and mean air temperature from the nearest weather station are also plotted in the top portion of the graph. Figure 7 suggests that groundwater recharge is occurring principally following spring snowmelt, around the end of March. The large precipitation events at the end of summer and beginning of fall (sometimes over 200 mm/month in August and September) do not seem to cause important rises of groundwater level, suggesting that recharge is not important during this period.

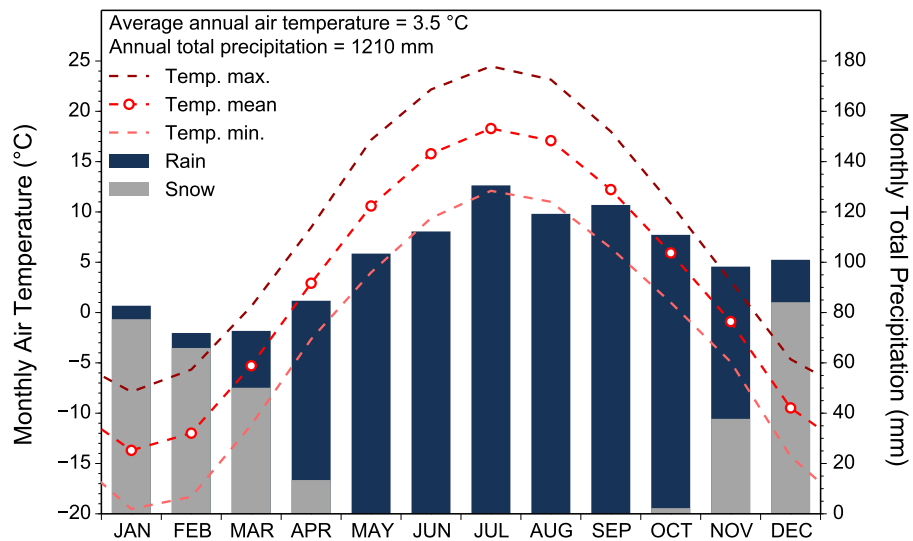


Figure 6 – Yearly and monthly weather normals, calculated for the years 1960-2015, for the weather stations STE CHRISTINE located 20 km from the observation well at Pont-Rouge.

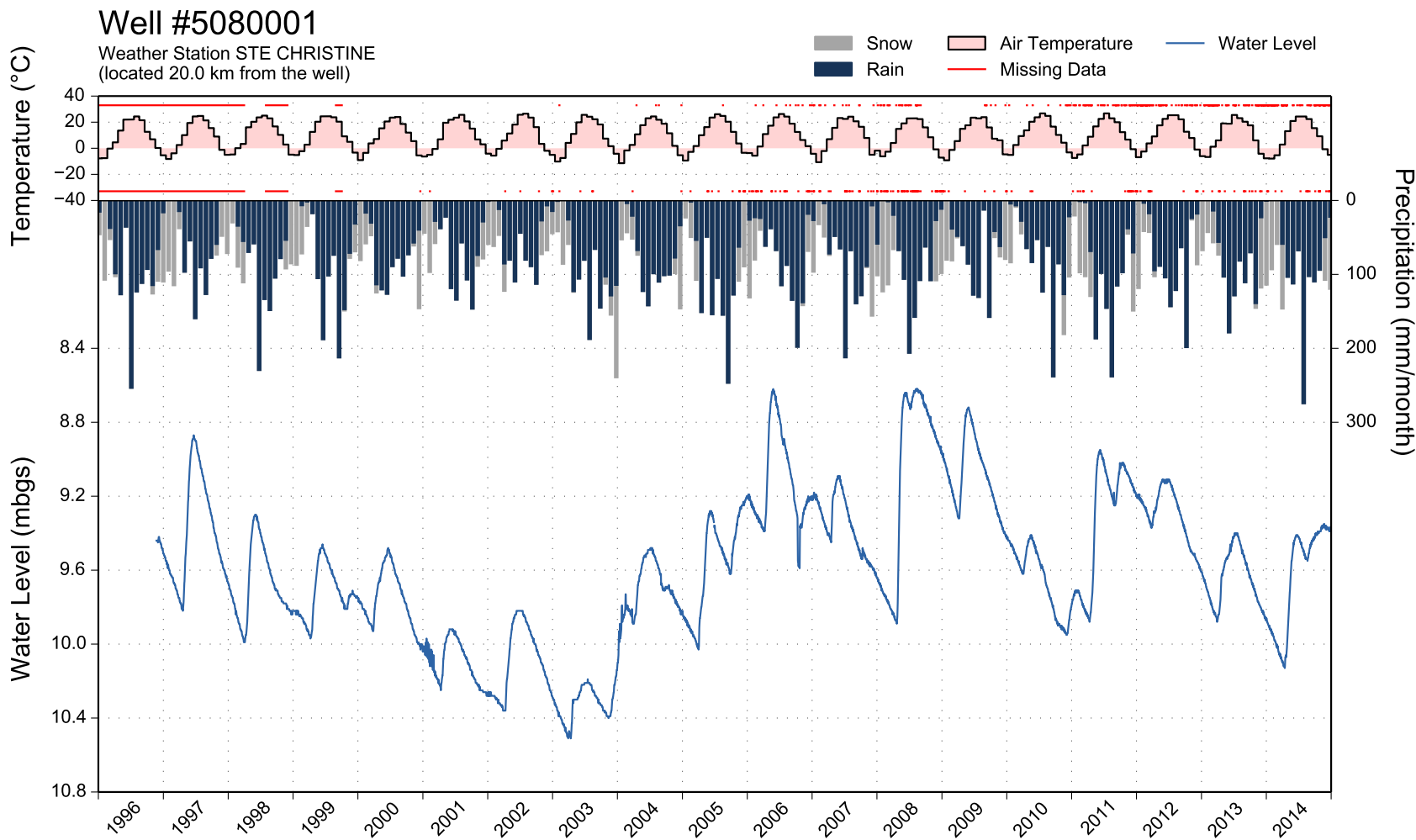


Figure 7 – Monthly weather data and hydrograph for the years 1996-2014. (Lower Part): Daily water levels in meters below ground surface (mbgs) from the well #5080001 of the Quebec monitoring network ([Gouvernement du Québec, 2015](#)) located at Pont-Rouge, in the Portneuf area ([figure 4](#)). (Middle part): Monthly cumulative precipitation. (Top part): Average monthly maximum daily air temperatures. Weather data were compiled from daily values from weather station STE CHRISTINE located 20 km from the well (<http://climate.weather.gc.ca/>).

3.1.4 Master Recession Curve

The master recession curve was defined from 31 different segments in the hydrograph where water level receded due to assumed negligible recharge. The rate of water level decline was defined as a constant, with values for the a and b parameters in [equation \(11\)](#) of 0 d^{-1} and 3.12 mm/d . The root-mean-square error between the observed and simulated water levels during the recession periods was 0.0657 m . [Figure 8](#) presents the fit between the predicted water levels with the MRC and the measurements.

3.1.5 Hydrologic parameters

The second step in the methodology described in [section 2.3](#) consists in defining a range of plausible parameter values in the model. [Table 1](#) presents the range of values that were selected for the calibration of the model.

All paramters were given a fixed value, except S_y , RAS_{max} , and C_{RO} . The range for RAS_{max} and C_{RO} were set to be as in [Larose-Charette et al. \(2000\)](#) in order to obtain results that are comparable with previous studies. The range of values for S_y was established by using a $\pm 20\%$ uncertainty on the nominal value of 0.25 used by [Larose-Charette et al. \(2000\)](#) and [Lefebvre et al. \(2011\)](#). The value for C_M was defined to the typical value suggested in [USDA NRCS \(2004\)](#) when information is lacking. Finally, values for T_{crit} and T_{melt} were set to the temperature of congelation of pure water. A constant delay of 10 days was also added to potential recharge rates based on cross-correlation analysis made between the synthetic and measured hydrographs.

Table 1 – List of model hydrological parameters and calibration ranges.

Parameter	Description	Calibration range
S_y	Aquifer specific yield	0.2 to 0.3
RAS_{max}	Maximum readily available storage	0 to 150 mm
C_{RO}	Runoff coefficient	0.2 to 0.4
T_{crit}	Critical temperature for snow-to-rain partitioning	0°C
C_M	Degree-day melt coefficient	$2.74 \text{ mm} / {}^\circ\text{C}$
T_{melt}	Base air temperature at which snow melt begin	0°C
a	Master recession curve coefficient	0 d^{-1}
b	Master recession curve coefficient	3.12 mm/d

3.2 Results

The parameter space for RAS_{max} and C_{RO} were defined by dividing uniformly the calibration range in intervals of 1 mm and 0.05 respectively. This corresponds to a number of 3171 possible set of $RAS_{max} - C_{RO}$ parameters. Multiple synthetic hydrographs were produced using these sets of parameters following the third step of the approach described in section 2.3. A total of 1195 models were considered to be behavioral based on the optimized value of S_y and the calibration range defined in table 1.

The population of behavioural models was then used to compute uncertainty limits for water level and daily recharge rates as described in steps 4 and 5 of the approach described in section 2.3. Figure 8 shows the 5 % and 95 % GLUE uncertainty limits of the predicted water levels compared to the observation.

Figure 9 shows the annual recharge values computed with the GLUE 5, 50 and 95 % uncertainty limits. Annual recharge values computed for the GLUE 50 % uncertainty limit have a minimal value of 150 mm/y for the hydrological year 2009-2010 and a maximum value of 470 mm/y for the hydrological year 2010-2011. The largest GLUE 5/95 uncertainty range is 253 mm/y for the hydrological year 2004-2005 and the smallest is 77 mm/y for the year 2005-2006.

Mean annual recharge values for the GLUE 50 % uncertainty limit is 286 mm/y, while the 5 % and 95 % uncertainty limits are, respectively, 223 and 384 mm/y. This corresponds to a mean uncertainty range of 161 mm/y. Among the population of behavioral models, S_y varies between 0.2 to 0.3, RAS_{max} between 24 to 150 mm, and C_{RO} between 0.26 to 0.4. The method thus reduced the prior calibration range defined in table 1 for RAS_{max} and C_{RO} .

3.3 Discussion

Results presented in figure 8 show that the predicted water level Containment Ratio (CR), which specifies the percentage of observations captured within the GLUE uncertainty bounds (Xiong & O'Connor, 2008), is only 19.3 %. Many factors can explain this poor CR score. First of all, weather data used in the application of the method were taken from a weather station located 20 km from the well. It is most likely that there were local differences between weather at the weather station and the well that could have caused large epistemic errors in the prediction of the water levels. Where

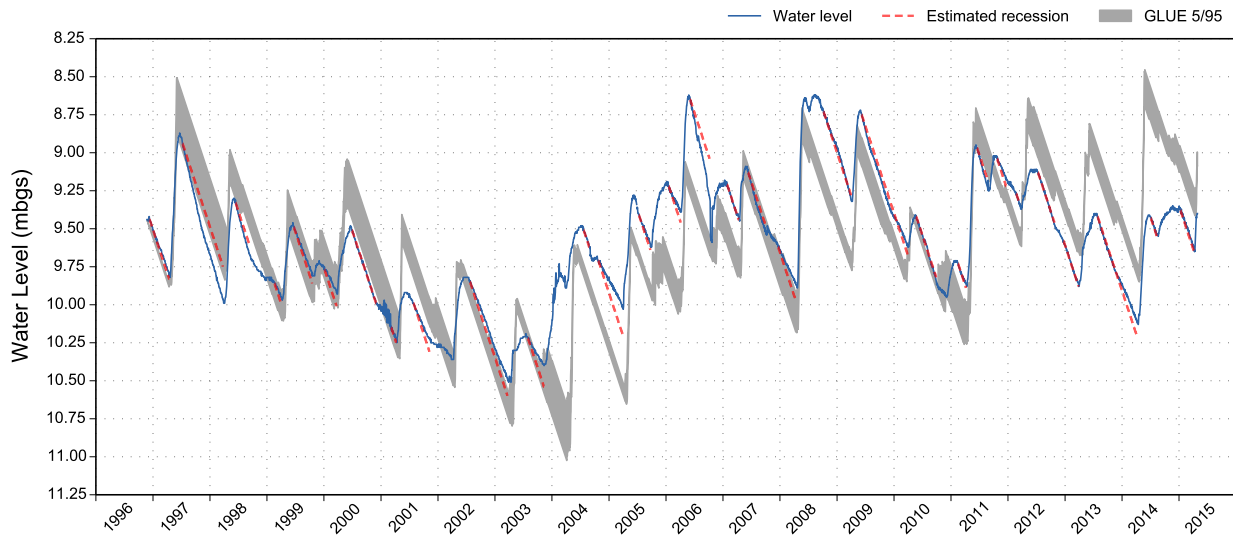


Figure 8 – GLUE 5/95 uncertainty limits (grey) for predicted water levels and observed hydrograph (solid blue line). Simulated water levels with the calibrated master recession curve are shown with dashed red lines.

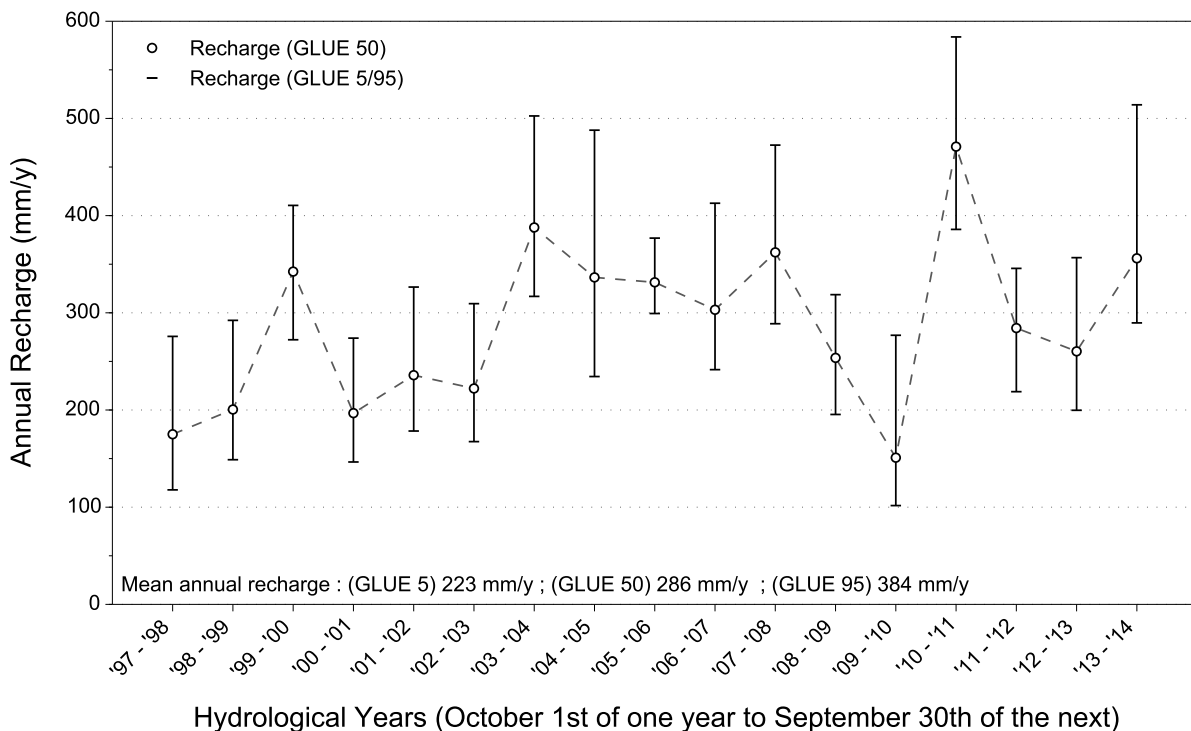


Figure 9 – GLUE modal values for predicted annual groundwater recharge (GLUE 50). The whiskers correspond to the GLUE 5/95 uncertainty limits. Values were calculated for hydrological years by summing daily recharge rates from October 1st of one year to September 30th of the next.

available, application of the method using weather dataset from multiples location around the well could help improve the prediction.

This result also suggests that the combined SMB-AWB model may need to be improved further to better predict short-term fluctuations of the water levels. For example, as seen in [figure 8](#), the MRC is not matched closely with water level observations for all the recession periods. Therefore, the MRC parameters a and b could be made to vary on an annual or even seasonal basis in the model. Also, uncertainty on the MRC parameter values a and b should be taken into account in the calibration process. Additionally, instead of using a fixed delay, transport of water from the base of the root zone to the water table could be simulated with a transfer function as suggested by [Besbes & De Marsily \(1984\)](#). Better definition of T_{crit} and T_{melt} with values that match observations on the site may also help improve the fit between predicted values and observations. Since spring melt recharge is very important in the study area, a better representation of the timing of recharge due to snow melt should help improve the performance of the predicted water levels. Finally, taking into account vertical heterogeneity of the soil by allowing S_y to vary as a function of depth below the ground surface may also improve the model further.

Nonetheless, even though combined SMB-AWB model failed to represent accurately short-term variations of the water levels, the general trend and behavior of the observed hydrograph over the whole 17 year monitoring period is still well represented. Matching the well hydrograph over the long term is the most important aspect for daily SMB recharge estimates. However, since individual recharge events are not closely matched, this means that caution needs to be used in the application of daily SMB over a short monitoring period or to estimate single recharge events.

Moreover, application of the method reduced the uncertainty range on the mean annual estimates of groundwater recharge compared to [Larose-Charette et al. \(2000\)](#) from well above 200 mm/y to about 161 mm/y at the Pont-Rouge site. The uncertainty range could be reduced further by a better prior knowledge of the calibration range of the hydrologic parameters. For example, if an uncertainty of 10 percent is considered on the nominal value of S_y instead of 20 %, the range for S_y is reduced to 0.225 to 0.275 compared to 0.2 to 0.3. Mean annual recharge values for the GLUE 50 % uncertainty limit then becomes 284 mm/y, while the 5 % and 95 % uncertainty limits become, respectively, 231 and 355 mm/y. This corresponds to a mean uncertainty range of 124 mm/y, for a modal value that is still the same as for the case with a wider range on S_y .

Unfortunately, it is not possible to validate the estimated confidence intervals for the groundwater recharge as for water levels because actual measurements of groundwater recharge are not available. Application of the method to a set of synthetic data produced with a complex coupled model, such as CATHY ([Paniconi & Wood, 1993](#)), would allow the full validation of the approach.

4 Conclusion

This paper presents a simple method to assess groundwater recharge in unconfined aquifers based on readily available data, namely daily time series of air temperature, total precipitation, and water level. The principle of the method is to convert daily potential recharge rates, computed with a soil moisture balance model, into a synthetic well hydrograph based on an aquifer water budget. Calibration of the method is done by producing a population of synthetic well hydrographs using multiple sets of model parameters defined from plausible parameter ranges that are defined as prior information. Calibration and quantification of the uncertainty is then achieved with the GLUE methodology.

The method was tested in an unconfined deltaic aquifer in the Portneuf area, Quebec, Canada, where many other studies were carried out in the past. Mean yearly recharge over 17 years was estimated to be 286 mm/y, but year to year recharge varied from about 150 to 470 mm/y. Results showed that application of the combined surface and aquifer water budget method reduced uncertainty on mean annual estimate of groundwater recharge compared to [Larose-Charette et al. \(2000\)](#) from well above 200 mm/y to about 161 mm/y. Unlike [Lefebvre et al. \(2011\)](#) who calibrated their model with a traditional local optimization approach, the use of the global optimization method GLUE provides uncertainty ranges on recharge estimates, while not overestimating the information content in the calibration data.

Adaptation of the method was also done from [Lefebvre et al. \(2011\)](#) to make the calibration process automated and based on a quantitative performance criteria, instead of qualitative. The method was implemented in the Python programming language and a computer software WHAT (Well Hydrograph Analysis Toolbox; [Gosselin et al., 2016a](#)) was developed to allow the application of the method with a graphical user interface. In addition, WHAT covers the entire workflow needed for the application of the method, including the creation of serially complete daily weather data

series, estimation of the master recession curve, and production of publication quality figures of the well hydrograph and weather data.

The combined surface and aquifer water budget method presented in this study shows potential as a recharge assessment method for unconfined aquifers under temperate continental climates. It has advantages compared to well hydrographs and water balance methods used alone. It is simple to use and based on readily available weather data. It allows a better recognition of diffuse recharge events than well hydrographs that tend to underestimate such recharge. The method also provides a means to restrict estimated ranges of hydrologic parameters. It provides recharge estimates over the entire period for which weather data are available. However, more work needs to be done to improve the short-term prediction of groundwater level variations. The method should also be validated against a set of synthetic data produced with a 3D coupled surface-unsaturated-saturated hydrologic model.

5 Acknowledgments

This research was supported by the NSERC Scholarship of Jean-Sébastien Gosselin, the NSERC-discovery grant (326975-2011) of Dr. Richard Martel, by funds from the Groundwater Geoscience Program of the Geological Survey of Canada, and the Projet Montérégie Est of the PACES program of the Ministère du Développement durable, de l'Environnement et de la Lutte contre le changement climatique. The climate data for this study were taken free of charge from the Government of Canada website (www.climate.weather.gc.ca).

Article 4

An Algorithm to Automate the Filling of Gaps in Daily Weather Records

Titre traduit

Un algorithme pour combler automatiquement les données manquantes dans les séries journalières de données météorologiques

Auteurs

Jean-Sébastien Gosselin¹, Richard Martel¹ et Christine Rivard²

¹ Institut national de la recherche scientifique, Centre Eau Terre Environnement, 490 rue de la Couronne, Québec, Qc, Canada

² Commission Géologique du Canada, Division Québec, 490 rue de la Couronne, Québec, Qc, Canada

À soumettre

Computer & Geosciences

Résumé

Cet article présente un algorithme gratuit et libre nommé PyGWD (Python Gap-filling Weather Data algorithm) rédigé dans le langage de programmation Python. Cet algorithme a été développé pour combler les valeurs manquantes dans les séries journalières de données météorologiques avec une méthode automatisée, robuste et efficace. Les valeurs manquantes à une station donnée sont estimées par un modèle de régression linéaire multiple généré avec les données synchronisées aux stations voisines. L'algorithme a été testé pour 19 stations météorologiques situées en Montérégie Est, au Québec, à l'est du Canada. Cette région est caractérisée par une topographie variable induisant des tendances spatiales dans les conditions météorologiques. L'incertitude sur les valeurs estimées a été évaluée avec une routine incluse dans l'algorithme permettant de faire de la validation croisée. La méthode a donné des résultats cohérents pour les températures quotidiennes minimales, moyennes et maximales et pour les précipitations totales pour les 19 stations testées. Les valeurs d'incertitude obtenues sont comparables à celles des autres études publiées qui ont utilisé une approche similaire. De plus, une interface graphique a été développée pour l'utilisation de PyGWD et a été incluse dans le logiciel WHAT (Well Hydrograph Analysis Toolbox).

Abstract

This paper presents a free and open-source algorithm written in the Python programming language called PyGWD (Python Gap-filling Weather Data algorithm). This algorithm was developed to fill the gaps in daily weather datasets with an automated, robust, and efficient method. The missing data for a given weather station are estimated using a multiple linear regression model, generated using synchronous data from neighboring stations. The algorithm was tested for 19 weather stations located in the Montérégie Est region, Quebec, eastern Canada. This region has a variable topography inducing spatial trends in weather conditions. The uncertainty of the estimates were assessed with a built-in cross-validation resampling technique, which is included in PyGWD. The method gave consistent results for the daily mean, maximum, and minimum air temperature and daily total precipitation for the 19 weather stations tested. Uncertainty of the results compared well with other studies that also used a similar approach. Furthermore, PyGWD can be used with a graphical

user interface that is part of the free and open source software WHAT (Well Hydrograph Analysis Toolbox).

1 Introduction

Daily weather data are useful in several fields of science, including hydrology, hydrogeology and agronomy. However, weather datasets are, most of the time, incomplete, with gaps in some of the recorded weather parameters for short or extended periods due to instrument malfunction. This can represent a major hindrance in various applications, such as for the use of hydrological or hydrogeological simulators which need continuous data. Filling the gaps in weather datasets can quickly become a tedious task as the number and length of data records increase over time. Moreover, it can be quite complex when aspects such as time-efficiency of the method and accuracy of the estimated missing values are taken into account. This is especially true for the estimation of missing daily precipitation data because of their high spatial and temporal variability ([Simolo et al., 2010](#)) and due to the complexity of the physical processes involved. Although various methods to estimate missing daily weather data are documented in technical papers (e.g. [DeGaetano et al., 1995](#); [Eischeid et al., 2000](#); [Simolo et al., 2010](#)), few published tools perform this task efficiently and automatically.

This paper addresses this issue by presenting a free and open-source algorithm written in the Python programming language called PyGWD (Python Gap-filling Weather Data algorithm). This algorithm was developed to automate the filling of gaps in daily weather datasets with a robust and efficient approach. The missing data in the records of a given weather station (hereafter called the target station) are estimated with a Multiple Linear Regression (MLR) model using simultaneous measurements at neighboring stations. PyGWD also includes a built-in cross-validation resampling technique to assess the validity of the method and the uncertainty of the estimated missing values. A graphical user interface is also available as part of the software WHAT ([Gosselin et al., 2016a](#)). WHAT was originally developed to estimate groundwater recharge from daily weather data and observation well hydrographs. It uses a method combining a surface and an aquifer water budget ([Gosselin et al., 2016b](#)).

This paper first presents the theoretical basis and methodology underlying the algorithm, followed by technical information on the use of PyGWD to produce serially complete daily weather datasets.

An application to a network of 19 weather stations located in the Montérégie Est study area (Quebec, eastern Canada) is also presented at the end of this paper.

2 Description of the Algorithm

The estimation of missing daily weather data in PyGWD is based on the robust and widely used regression-based MLR (Multiple Linear Regression) technique presented in [Eischeid *et al.* \(2000\)](#). Since the spatial interpolation is based on the strength of the correlation between the simultaneous weather data series, the MLR method can indirectly account for local effects such as topography, land cover, land use and surface water. While creating serially complete daily datasets of air temperature and total precipitation for the western United-States, [Eischeid *et al.* \(2000\)](#) found that the MLR method consistently outperformed the other classical methods tested (normal ratio, inverse distance, optimal interpolation, and single best estimator). The same conclusion was drawn by [Xia *et al.* \(1999\)](#) for a study in Bavaria, Germany. Moreover, in a study carried out in Iran for different climate conditions (dry to extra humid conditions), [Kashani & Dimpashoh \(2011\)](#) found that monthly weather data estimations obtained with the MLR method compared well with those obtained with more recent and complex methods, such as the artificial neural network (e.g., [Coulibaly & Evora, 2007](#); [Dastorani *et al.*, 2009](#)) and the genetic programming (e.g., [Ustoorkar & Deo, 2008](#)) techniques.

[Figure 1](#) presents a flowchart of the methodology followed in PyGWD to produce serially complete daily weather datasets. The algorithm consists of two nested loops: the external *Loop A* iterates over the weather variables of the dataset (minimum, maximum, and mean air temperature and total precipitation), while the inner *Loop B* iterates over the missing values in each weather data series. Each missing value is estimated independently with a two-step procedure in *Loop B*. The first step consists in the selection of the neighboring stations. The second step consists in building a MLR model, estimating the missing value, and filling the corresponding gap in the data series. The PyGWD algorithm is described in more detail in the following sections of this paper.

2.1 Correlation Coefficients Calculations

Correlation coefficients for each weather variable are calculated between all the available measured data at the target station and those at the neighboring stations. However, neighboring stations that

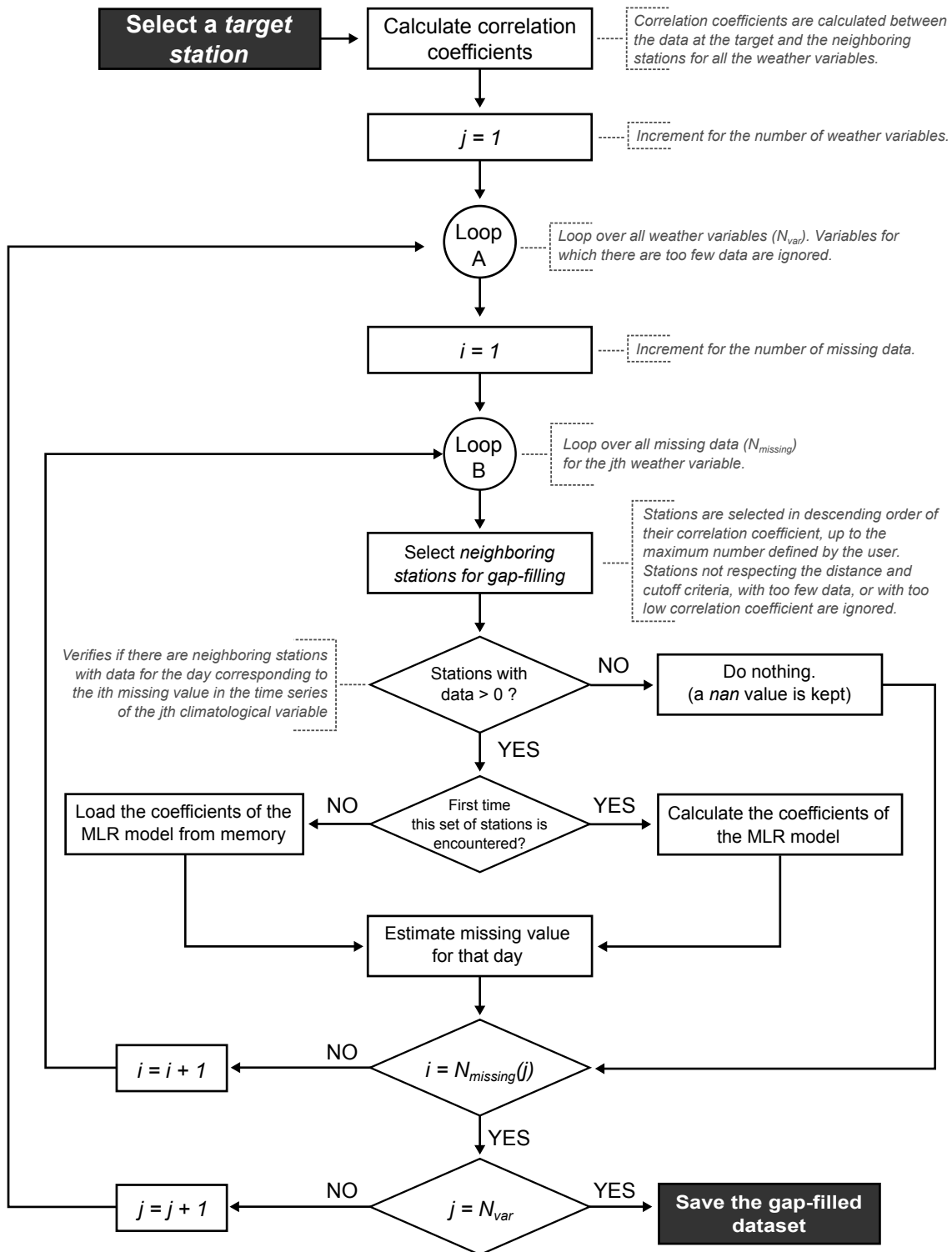


Figure 1 – Flowchart of the methodology followed in PyGWD to produce serially complete daily weather datasets. *Loop A* iterates over the weather variables of the dataset (minimum, maximum, and mean air temperature and total precipitation), while the inner *Loop B* iterates over the missing values in each weather data series. $N_{missing}$ and N_{var} correspond to the total number of missing values and weather variables. *nan* = not a number.

have less than 182 days (half a year) of simultaneous data with the target station or that have a correlation coefficient below 0.35 for a given weather variable are not used to fill the gaps in the data series for that weather variable. The 0.35 threshold is based on the value established by [Eischeid et al. \(2000\)](#) in their application of the method.

Neighboring stations can also be discarded based on specified threshold values for the distance and elevation difference with the target station. The default threshold values are set to 100 km and 350 m for distance and elevation difference respectively, based on values found in the literature ([Tronci et al., 1986](#); [Xia et al., 1999](#); [Simolo et al., 2010](#)).

2.2 Selection of the Neighboring Stations

The selection of neighboring stations is critically important for the accurate estimation of missing weather data ([Eischeid et al., 2000](#)). However, problems arise because the set of neighboring stations with available data may vary from one day to the other. Therefore, the process of selecting neighboring stations used for the generation of a MLR model must be performed separately for each missing value in the dataset of the target station.

For a given day with missing data, the neighboring stations with available data on that day are selected in descending order of correlation coefficient, up to a maximum number of stations that is specified by the user. The default value for the maximum number of neighboring stations used for the generation of the MLR models is 4. Tests run by [Eischeid et al. \(2000\)](#) showed that using more than 4 neighboring stations does not significantly improve, and may even degrade, the accuracy of the estimates. If none of the neighboring stations has a measured value on a day with a missing data, no calculation is performed and a *nan* (not-a-number) value is kept in the dataset.

2.3 Generation of the Multiple Linear Regression Model

Days with no observed precipitation at all the selected neighboring and target stations were not used in the generation of the MLR model for daily precipitation. Otherwise, all available data at the selected neighboring and target station were used in the generation of the MLR model. Therefore, the effect of seasons and long-term climatic changes on the relations between stations are not currently considered in this method.

The MLR models can be generated using either an Ordinary Least Square (OLS) or a Least Absolute Deviations (LAD) criterion. Since daily precipitation series are generally characterized by long-tailed and positively skewed distributions, the LAD method is more appropriate than the OLS method as it is more robust to outliers (Menke, 1989; Eischeid *et al.*, 2000). The downside of using the LAD method is an increase in computation time by about an order of magnitude compared to the OLS method. The resolution of the MLR models with the LAD method is achieved using an iterative reweighted least-squares method (Björck, 1996).

Each time a MLR model is generated for a unique set of neighboring stations, this model is stored into memory. Therefore, whenever a set of neighboring stations is selected for a given day with missing data, PyGWD first verifies if a MLR model already exists in memory for this set of stations. If so, the missing data is estimated from the stored MLR model. Otherwise, a new MLR model is generated to estimate the missing data and is stored into memory. Because a MLR model is generated only once for a unique set of neighboring stations, the algorithm becomes faster with time as the number of MLR models stored into memory increases.

2.4 Estimating Missing Daily Values

Each missing value in the weather dataset of the target station is estimated from simultaneous measurements at the neighboring stations using the MLR model with the following equation:

$$Y_t = a_0 + \sum_{k=1}^N a_k \cdot X_k(t_i) \quad (1)$$

where $Y(t)$ is the value estimated at the target station at time t , $X_k(t)$ is the simultaneous measured data at the k^{th} neighboring station, a_k are the coefficients of the MLR model, and N is the total number of neighboring stations that were used for the regression. The intercept term, a_0 , is estimated for air temperature, but is set to zero for precipitation. Estimated missing data at a given time t are not used to estimate missing values at a later time in the records.

It is possible to have negative coefficients a_k for the less correlated neighboring stations used to generate the MLR model. If so, the MLR model will sometimes yield small negative values for daily precipitation. To correct this, negative values estimated for daily precipitation are set to zero.

2.5 Uncertainty Assessment of the Estimated Values

The uncertainty of the estimated values can be assessed by computing the root-mean-square of residuals of the MLR models that were used for the estimation.

Furthermore, the validity and accuracy of the method can be assessed with PyGWD for the whole dataset of a given weather station using a built-in Leave One Out (LOO) cross-validation resampling technique. This assessment is performed using the procedure described in sections 2.2 to 2.4 to estimate successively a value for each day of the data series for which a measured value is available, rather than for days with missing data. To do so, before estimating a value for a given day, the corresponding measured data is temporarily discarded from the dataset to avoid self-influence of this observation on the estimation procedure. The series of estimated values are then compared with the respective non-missing observations in the original dataset of the target station to compute the Root-Mean-Square Error (RMSE), the Mean-Absolute Error (MAE), the Mean Error (ME) and the correlation coefficient (r).

During the cross-validation procedure described above, a new MLR model is generated for each day independently and the models are not stored in memory. This increases significantly the computation time of the gap-filling procedure, especially if the MLR models are generated with the LAD method. For this reason, the cross-validation procedure is by default not activated in PyGWD.

3 Technical Information on the Use of PyGWD

It is possible to use PyGWD with the graphical user interface that is included in WHAT. Alternately, the algorithm can be run directly from the command line in a Python interpreter version 2.7 or 3.4 (or later). This section will cover this approach. The external libraries *NumPy* (www.numpy.org), *Matplotlib* (www.matplotlib.org), *xlrd* (www.python-excel.org), and *PySide* (www.qt-project.org/wiki/PySide) are required for the program to run. A minimal working example is presented in appendix 7.1. Data samples, required to run the example, are also provided with PyGWD.

The present section of this paper covers the format of the input data that is required for running PyGWD, the parameters of the method, and the various outputs that are generated after a gap-filled

weather dataset has been successfully produced. Additional information about the input and output of PyGWD is also provided in the user guide of the WHAT software ([Gosselin *et al.*, 2016a](#)).

3.1 Input Data

It is possible to use weather data from any sources with PyGWD, as long as the data are saved in a file with tab-separated values with a *.csv* extension. Also, the labels in the file headers must be faithfully observed since the algorithm is reading these to know where to retrieve the station information and the weather data within the file. An example of a data input file is presented in [appendix 7.2](#).

It is recommended to use a copy of one of the sample files that are provided with PyGWD and fill-in directly the station information and the weather data. A *nan* value must be entered where data are missing. The daily data must also be in chronological order, but do not need to be continuous over time. That is, missing blocks of data (i.e., several days, months or years) can be completely omitted from the time-series.

All the input weather data files must be saved in a single input directory that is specified by the user (see Step 2 in [appendix 7.1](#)). It is subsequently possible to tell the algorithm to read the data files contained in the input directory and store the information (weather station's info and data) in memory for the gap-filling procedure (Step 3 in the example of [appendix 7.1](#)).

3.2 Parameters

The command line interface of PyGWD is written as a Python class object in which the parameters of the method are represented as instance attributes whose value can be specified directly (see steps 4 to 6 in [appendix 7.1](#)). [Table 5](#) of [appendix 7.3](#) also presents a list of the parameters that are available in version 1.0 of PyGWD, along with their default values and a description of their role in the algorithm.

3.3 Outputs

The outputs that are produced after a gap-filled weather dataset has been successfully created are saved in a sub-folder that is named after the target station name and its climate identifier, in a directory that is specified by the user (see Step 2 in [appendix 7.1](#)). A detailed list of the output files that are produced by version 1.0 of PyGWD, along with their file type and description, is presented in [table 6](#) in [appendix 7.3](#). A brief overview is also presented below.

The gap-filled weather datasets are saved in a file with tab-separated values with a *.out* extension. Detailed information about the estimated values that were used to fill the gaps in the data series (e.g., parameter values used in the method, uncertainty of the estimated values, simultaneous data at neighboring stations used for the estimations) are also saved in an accompanying file with a *.log* extension. A histogram showing the yearly and monthly weather normals, calculated from the gap-filled data series generated with PyGWD, is also produced and saved in a pdf format.

Results from the cross-validation procedure, if the option is enabled in PyGWD, are saved in a file with tab-separated values with a ‘err’ extension. A figure comparing the probability density function of the original and the estimated daily precipitation series is also produced and saved in a pdf format. Scatter plots comparing the estimated and measured daily weather data are also produced for each variable of the dataset and saved in a pdf format. Examples of the figure produced with PyGWD are shown in [section 4](#), where a case study is presented.

4 Application: The Montérégie Est Case Study

4.1 Materials and Method

4.1.1 Study Area

The Montérégie Est region is located in Quebec, eastern Canada (see [figure 2](#)). This region covers an area of more than 9000 km², from the St. Lawrence River at its northern limit to the United States border (states of New York and Vermont) at its southern boundary. It is characterized by highly variable topography (0 to 800 m) and land cover conditions, and by warm summers and cold winters (climate normals are provided below, [Carrier et al., 2013](#)).



Figure 2
Location of the Montérégie Est region, Quebec, Eastern Canada.

4.1.2 Weather Stations

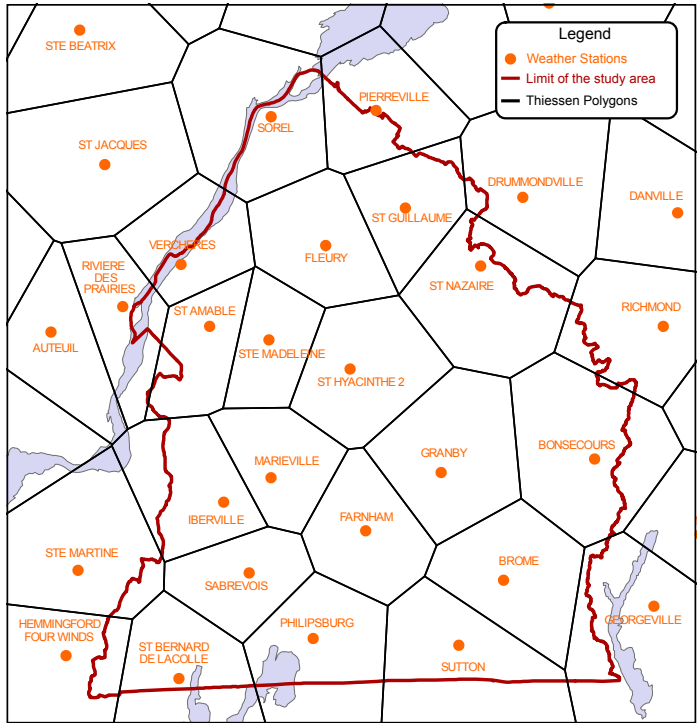
A total of 32 Canadian weather stations located in and around the Montérégie Est region were selected from the Canadian Daily Climate Database (CDCD) based on the availability and continuity of the measured weather data between 1980 and 2009 inclusively. Out of these 32 weather stations, 19 stations within the study area were used to test the algorithm. Data from the 13 stations located just outside the study area were used as neighboring stations to improve the spatial distribution of the weather data.

Using the graphical interface to the online CDCCD that is included in WHAT, the daily data were automatically downloaded from the Government of Canada website (www.climate.weather.gc.ca) and reorganized in a format that is compatible with PyGWD. Table 1 presents the 19 stations used to test the algorithm with their corresponding location coordinates (latitude and longitude), altitude, percentage of days with missing data, and yearly averages for each of the four weather variables. Most of the information presented in table 1 is generated automatically when loading data in PyGWD and is saved in a file named *weather_datasets_summary.log*. The geographical distribution of the weather stations is presented in figure 3.

On average for the 19 stations, the mean annual total precipitation is 1090 mm/y. The highest total annual precipitation is observed at the *Sutton* station (1300 mm/y), while the lowest is found at the *Vercheres* station (974 mm/y). Mean annual air temperature over the study area is 6.1 °C, ranging from 4.0 °C at the *Philipsburg* station to 7.1 °C at the *Bonsecours* station.

Table 1 – List of the 19 weather stations located in the study area along with their location coordinates (Lat. and Long.), elevation (Elev.), percentage of days with missing data, yearly averages for the 1980-2009 period, and mean and standard deviation (SD) for daily precipitation intensity. The mean, maximum, and minimum values for each column are also provided at the bottom. The four weather variables are daily minimum, mean, and maximum daily air temperatures (T_{\min} , T_{mean} , T_{\max}) and daily total precipitation (P_{tot}).

Stations	% of days with missing data				Yearly averages				P _{tot} intensity				
	Lat. °N	Lon. °W	Elev. m	T _{max} °C	T _{min} %	T _{mean} %	P _{tot} %	T _{max} °C	T _{min} °C	T _{mean} °C	P _{tot} mm	Mean mm/day	SD mm/day
Bonsecours	45.40	72.27	297.2	4.7	5.1	6.3	3.2	10.0	-0.8	4.0	1226	7.2	8.5
Brome	45.18	72.57	205.7	2.0	2.3	3.0	2.3	11.0	-0.4	5.3	1297	7.1	8.3
Farnham	45.30	72.90	68.0	5.2	4.7	6.1	3.7	11.5	1.1	6.3	1132	6.6	8.3
Fleury	45.80	73.00	30.5	1.1	1.2	1.6	1.1	10.8	0.8	5.8	1097	7.6	8.9
Granby	45.38	72.72	175.0	1.3	1.3	2.1	0.5	10.7	1.6	6.2	1219	6.8	8.6
Iberville	45.33	73.25	30.5	7.3	7.5	9.7	4.2	11.5	1.6	6.6	1098	7.3	8.4
Marieville	45.40	73.13	38.0	10.2	10.4	11.2	9.8	11.5	1.4	6.4	1102	7.2	8.9
Philipsburg	45.03	73.08	53.3	4.9	5.1	6.9	3.2	11.9	2.2	7.1	1066	6.4	7.8
Pierreville	46.08	72.83	15.2	6.3	5.4	6.9	4.9	10.7	0.8	5.8	979	6.8	8.1
Sabrevois	45.22	73.20	38.1	25.5	26.0	27.1	5.2	11.6	1.4	6.5	1021	6.6	8.5
Sorel	46.03	73.12	14.6	5.7	5.9	6.2	4.5	11.1	1.2	6.2	1000	6.8	8.5
St Amable	45.67	73.30	41.1	8.6	10.4	11.8	7.7	11.4	1.0	6.2	1007	7.6	8.6
St Bernard	45.08	73.38	49.3	9.6	9.7	10.5	9.0	11.7	1.7	6.7	980	6.6	8.6
St Guillaume	45.88	72.77	43.9	4.3	4.6	5.7	3.0	11.0	0.4	5.7	1023	6.6	8.0
St Hyacinthe 2	45.57	72.92	33.0	6.7	6.9	7.5	6.6	11.3	1.3	6.3	1061	6.7	8.2
St Nazaire	45.73	72.62	68.6	3.8	3.8	5.4	2.7	11.0	0.4	5.7	1088	7.0	8.2
Ste Madeleine	45.62	73.13	30.0	5.8	6.4	7.0	5.1	11.4	1.1	6.3	1035	6.7	8.6
Sutton	45.07	72.68	243.8	0.4	0.6	0.7	0.5	11.1	1.0	6.1	1300	6.7	8.6
Vercheres	45.77	73.37	21.0	3.5	3.5	4.7	2.2	11.3	1.8	6.5	974	7.1	7.7
Min	45.03	72.27	14.6	0.4	0.6	0.7	0.5	10.0	-0.8	4.0	974	6.4	7.7
Mean	45.50	72.96	78.8	6.2	6.4	7.4	4.2	11.2	1.0	6.1	1090	6.9	8.4
Max	46.08	73.38	297.2	25.5	26.0	27.1	9.8	11.9	2.2	7.1	1300	7.6	8.9

**Figure 3**

Spatial distribution of the weather stations in (19) and around (13) the Montérégie Est area, southern Quebec, Eastern Canada.

Yearly and monthly averages for total precipitation and maximum, minimum, and mean air temperatures for the *Sutton*, *Vercheres*, *Philipsburg*, and *Bonsecours* weather stations are shown in [figure 4](#). From these graphs, it can be seen that the climate of the region is characterized by significant seasonal differences in temperature, resulting in warm summers and cold winters. The minimum monthly temperatures are observed in January, while the maximum monthly temperatures are observed in July. Total precipitation, including rain and snow, are distributed rather evenly throughout the year. Rain events also occur quite frequently in the winter season due to mild spells.

4.1.3 Validation with the Cross-Validation Procedure

In order to validate PyGWD with real data, the uncertainty of the weather estimates was evaluated using the 19 stations located in the Montérégie Est region with the cross-validation procedure described in [section 2.5](#). The method was tested with the parameter values that are set by default in the algorithm, as shown in [table 5](#) in [appendix 7.3](#). That is, the maximum number of neighboring stations was set to 4, the horizontal distance and elevation thresholds were kept at 100 km and 350 m, respectively. However, the OLS method was chosen for the regression instead of the LAD to save computation time.

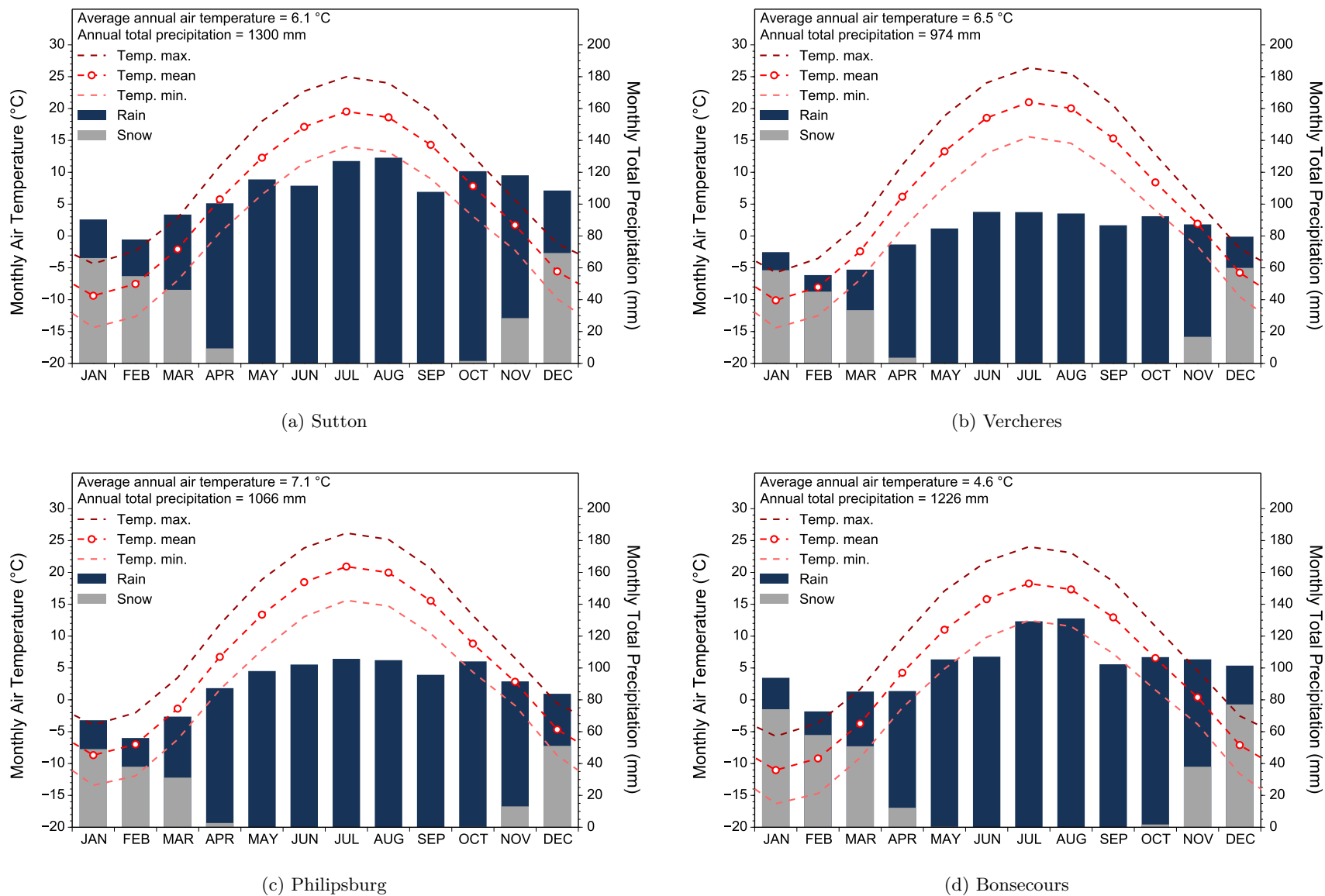


Figure 4 – Monthly weather normals for the weather stations with the highest (*Sutton*) and lowest (*Verchere*) annual total precipitation and the warmer (*Philipsburg*) and colder (*Bonsecours*) air temperature.

4.2 Results and Discussion

[Table 2](#) presents results of the cross-validation procedure. The Root-Mean-Square Error (RMSE), the Mean-Absolute Error (MAE), the Mean Error (ME) and the correlation coefficient (r) are given for each of the 19 weather stations, and each of the 4 weather variables tested: maximum, minimum, and mean air temperature and total precipitation (T_{\max} , T_{\min} , T_{mean} , and P_{tot}). Minimum, mean, and maximum values for each estimator (RMSE, MAE, ME, and r) are also provided at the bottom of the table.

4.2.1 Air Temperature

[Table 2](#) shows that the method gave consistent results for each of the three temperature-related weather variables, for all the 19 weather stations. The RMSE and MAE are both below 2.0 and 1.4 °C for minimum, mean, and maximum daily air temperatures, even for stations that have the highest percentage of missing data (*Sabrevois*, *Marieville* and *St Amable*). There is also no bias in the estimations for any of the temperature-based variable with a ME that is, on average for all the stations, less than 0.01 °C for the minimum, mean, and maximum temperature time series. The correlation coefficient between the estimated and measured time series is also above 0.987 for all the weather stations and temperature-based variables. An example of the goodness of fit between the estimated and observed values for the minimum, mean, and maximum daily temperatures is presented in the graphs of [figures 5a](#) to [5c](#) for the *Granby* station, located in the center of the study area. These graphs are generated automatically by PyGWD at the end of the gap-filling procedure when the cross-validation option is set to *True*.

4.2.2 Total Precipitation

Unlike air temperature, daily precipitation is characterized by large spatial and temporal variability and is thus more difficult to estimate accurately. Nevertheless, [table 2](#) shows that the method provided overall good and consistent results for the Montérégie Est region. Firstly, the correlation coefficient between the estimated and measured daily total precipitation is above 0.847 for all the stations. An example of the goodness of fit between the estimates and measurements is presented in [figure 5d](#) for the Granby station. Secondly, the RMSE and MAE on daily precipitation are less

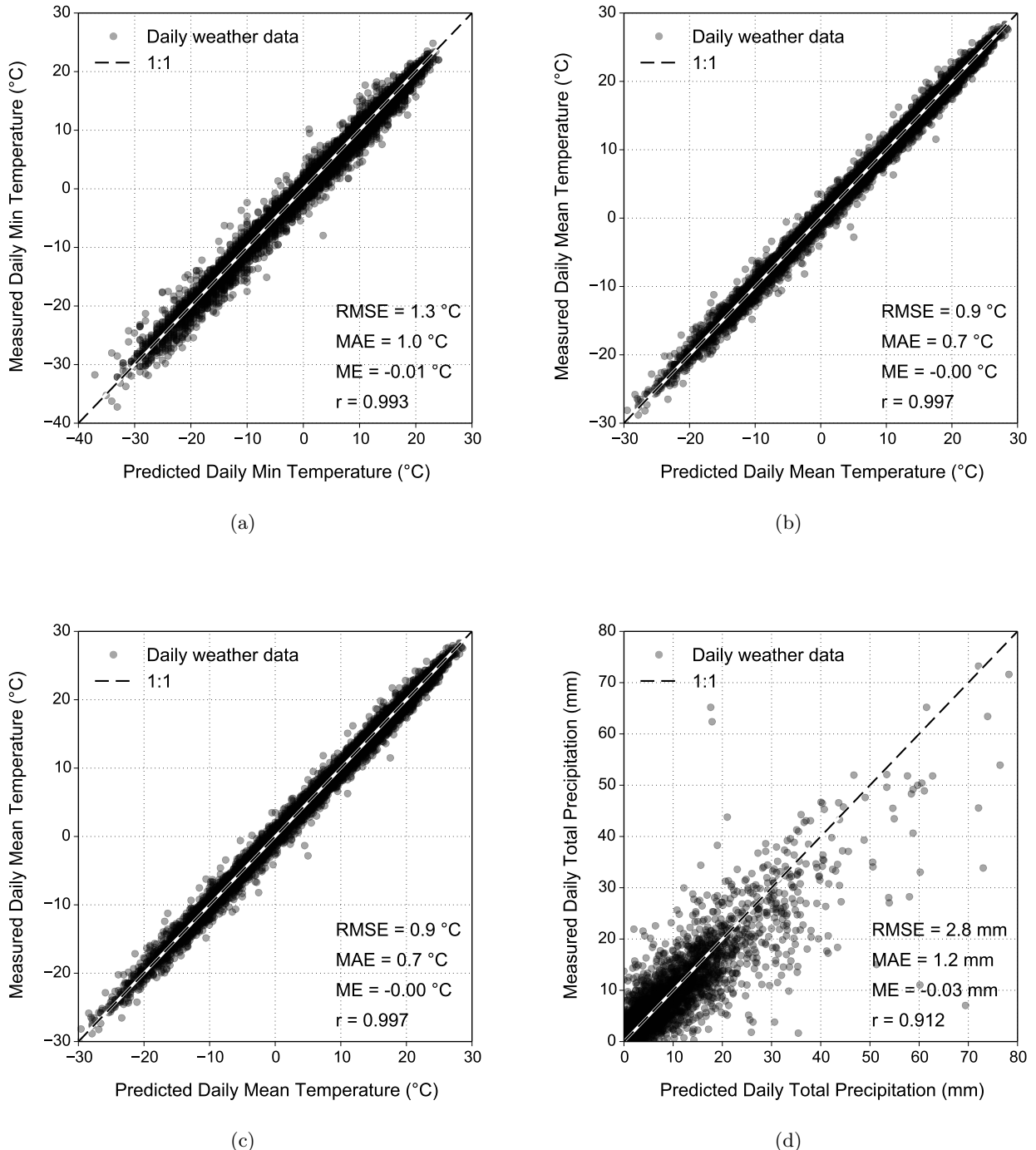


Figure 5 – Scatter plots comparing the predicted versus the measured daily values for (a) minimum air temperature, (b) mean air temperature, (c) maximum air temperature, and (d) precipitation for the *Granby* weather station.

Table 2 – Results of the cross-validation procedure for the 19 weather stations located within the Montérégie Est study area for the 1980-2009 period. The Root-Mean-Square Error (RMSE), the Mean-Absolute Error (MAE), the Mean Error (ME) and the correlation coefficient (r) are given for each weather variable. The measured, predicted, and estimation error on the mean number of wet days per year ($P_{tot} > 0 \text{ mm/d}$) are also presented at the end. The minimum, mean, and maximum values for each column are provided at the bottom. The four weather variables are daily minimum, mean, and maximum daily air temperatures (T_{min} , T_{mean} , T_{max}) and daily total precipitation (P_{tot}).

Stations	T _{max}				T _{min}				T _{mean}				P _{tot}				Wet days per year		
	RMSE °C	MAE °C	ME °C	r -	RMSE °C	MAE °C	ME °C	r -	RMSE °C	MAE °C	ME °C	r -	RMSE* mm	MAE* mm	ME* mm	r -	Meas. days	Pred. days	Error days (%)
Bonsecours	1.2	0.8	0.00	0.995	1.7	1.3	0.15	0.989	1.1	0.8	0.02	0.996	3.1	1.4	-0.10	0.890	179	217	39 (22.5)
Brome	1.1	0.7	-0.07	0.996	1.8	1.3	-0.11	0.989	1.1	0.8	-0.08	0.996	3.0	1.3	-0.17	0.902	181	221	41 (22.5)
Farnham	1.0	0.7	-0.02	0.997	1.3	1.0	-0.03	0.994	0.9	0.6	-0.02	0.997	2.7	1.1	-0.09	0.912	164	197	32 (19.7)
Fleury	0.9	0.6	0.00	0.997	1.2	0.9	0.00	0.995	0.8	0.6	0.00	0.998	2.5	1.0	-0.04	0.928	145	196	51 (35.4)
Granby	0.9	0.6	0.02	0.997	1.3	1.0	-0.01	0.993	0.9	0.7	0.00	0.997	2.8	1.2	-0.03	0.912	179	217	39 (21.8)
Iberville	0.9	0.6	0.00	0.997	1.2	0.9	0.06	0.994	0.8	0.6	0.03	0.998	2.6	1.1	-0.12	0.915	149	200	51 (34.0)
Marieville	0.9	0.6	0.00	0.997	1.2	0.8	0.03	0.995	0.8	0.5	0.01	0.998	2.8	1.1	0.00	0.908	138	182	44 (31.5)
Philipsburg	1.2	0.8	0.02	0.995	1.4	1.0	0.00	0.993	0.9	0.7	0.01	0.997	2.8	1.1	0.00	0.908	163	216	53 (32.6)
Pierreville	1.0	0.7	0.00	0.997	1.3	1.0	-0.02	0.994	0.9	0.7	-0.01	0.997	2.6	1.0	-0.01	0.903	136	179	44 (32.2)
Sabrevois	1.1	0.7	0.00	0.996	1.2	0.8	0.01	0.995	0.8	0.6	0.01	0.998	3.1	1.2	-0.20	0.875	148	194	46 (30.7)
Sorel	1.2	0.8	0.01	0.996	2.0	1.4	0.13	0.987	1.1	0.8	0.07	0.996	2.9	1.1	-0.06	0.886	142	175	33 (23.1)
St Amable	1.5	1.0	-0.01	0.993	1.8	1.3	0.02	0.988	1.2	0.9	0.00	0.995	2.9	1.2	-0.04	0.890	122	169	48 (39.2)
St Bernard	1.4	1.0	-0.03	0.993	1.6	1.1	-0.06	0.990	1.1	0.8	-0.04	0.995	3.4	1.3	0.03	0.847	133	197	64 (48.1)
St Guillaume	1.0	0.7	0.00	0.997	1.2	0.8	-0.01	0.995	0.8	0.6	0.00	0.998	2.3	1.0	-0.01	0.927	151	184	33 (21.9)
St Hyacinthe 2	0.9	0.6	-0.01	0.997	1.2	0.9	-0.01	0.995	0.8	0.6	-0.02	0.998	2.5	1.0	-0.06	0.921	150	186	35 (23.4)
St Nazaire	1.0	0.7	0.01	0.997	1.4	1.0	0.02	0.993	0.9	0.6	0.01	0.997	2.6	1.1	-0.08	0.911	151	193	41 (27.1)
Ste Madeleine	1.0	0.7	0.02	0.996	1.2	0.8	-0.01	0.995	0.8	0.6	0.00	0.998	2.6	1.0	0.01	0.919	146	180	33 (22.9)
Sutton	0.9	0.6	0.00	0.997	1.2	0.9	0.00	0.994	0.8	0.6	0.00	0.998	2.9	1.3	-0.07	0.912	195	221	26 (13.2)
Vercheres	1.1	0.7	0.03	0.996	1.3	1.0	0.05	0.993	0.9	0.6	0.04	0.997	2.6	1.1	-0.10	0.895	136	208	72 (52.8)
Min	0.9	0.6	-0.07	0.993	1.2	0.8	-0.11	0.987	0.8	0.5	-0.08	0.995	2.3	1.0	-0.20	0.847	122	169	26 (13.2)
Mean	1.1	0.7	0.00	0.996	1.4	1.0	0.01	0.993	0.9	0.7	0.00	0.997	2.8	1.1	-0.06	0.901	153	196	43 (29.2)
Max	1.5	1.0	0.03	0.997	2.0	1.4	0.15	0.995	1.2	0.9	0.07	0.998	3.4	1.4	0.03	0.928	195	221	72 (52.8)

*RMSE, MAE, and ME on daily precipitation were calculated for each station with all available data, including wet and dry days.

than 3.4 and 1.4 mm for all the stations, while mean daily precipitation intensity ranges between 6.4 to 7.6 mm/day (see [table 1](#)). Finally, the ME values show only a small bias, with a mean of -0.06 mm and a range of -0.20 to 0.03 mm. The tendency for the method to have a slight negative bias (15 out of 19 stations have a negative ME) is indicative of the positive skewness observed in the distribution of the precipitation events. The residuals of the interpolated values will tend to cluster around the median error rather than the mean error. An example of the daily precipitation distribution for the Granby station that illustrates well this positive skewness is shown in [figure 6](#) (light blue histogram).

Regression-based techniques, like the MLR method used in PyGWD, tend to systematically underestimate heavy precipitation events, while overestimating the occurrence of wet days (days with precipitation). This is illustrated in [figure 6](#) that compares gamma probability density functions that were derived from the estimated (dashed red line) and measured (solid blue line) daily precipitation at the Granby station.

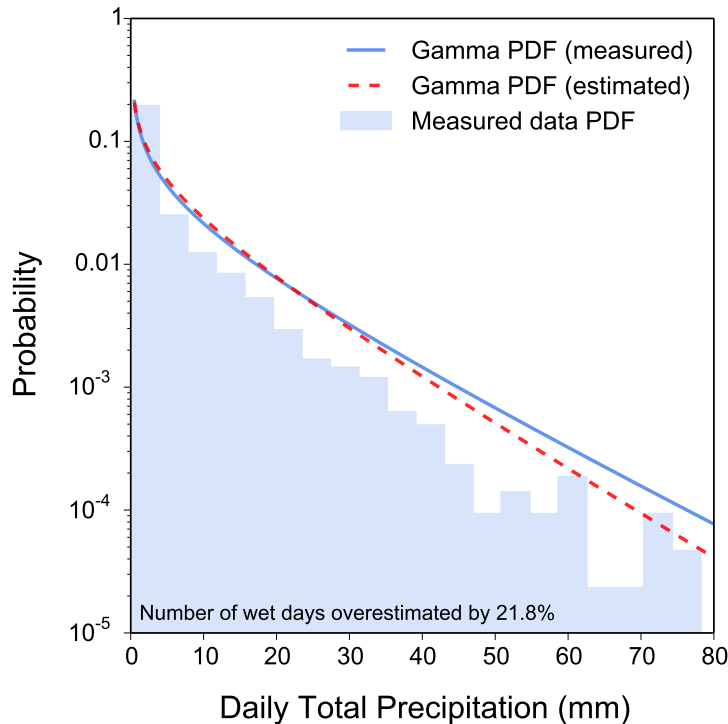


Figure 6 – Gamma probability density functions (PDF) that were estimated from the estimated (dashed red line) and measured (solid blue line) daily precipitation time series for the *Granby* weather station. The histogram of the distribution of the measured daily precipitation events is also shown in light blue.

This topic is investigated further in [table 3](#) where the RSME, MAE, and ME values are presented. These values were computed over limited daily precipitation ranges in increments of 10 mm/day, using all the data pooled together from the 19 stations tested. The ME values show that small precipitation events (10 mm/day and less) tend to be slightly overestimated by the method (positive ME), while heavier events are increasingly underestimated as the intensity of the precipitation increases (negative ME).

Moreover, the positive trend observed in the RMSE and MAE values clearly highlights the heteroscedasticity of the estimation errors that was also slightly apparent in the scatter plot of [figure 5d](#). This implies that important errors ($MAE > 15$ mm/day) can be associated to heavy precipitation events (> 50 mm/day) estimated with the method. This can be explained mainly by the large spatial variability of the precipitation, where a heavy precipitation event that occurred at a single station cannot be reconstructed correctly if the precipitation received at the other surrounding stations were moderate for that same event.

Table 3 – The Root-Mean-Square Error (RMSE), Mean-Absolute Error (MAE), and Mean Error (ME) on daily precipitation are presented for limited ranges in increments of 10 mm/day. These values were computed using all the data pooled together from the 19 stations tested. Mean value and number of occurrences for each range is also presented.

P _{tot} intensity					
Ranges mm/day	Mean mm/day	Occurrences days	RMSE mm/day	MAE mm/day	ME mm/day
= 0	0.0	114 169	0.9	0.2	0.2
] 0 10]	3.4	67 949	2.6	1.6	0.3
] 10 20]	14.2	12 845	5.1	3.8	-1.5
] 20 30]	24.1	4053	7.5	5.7	-3.6
] 30 40]	34.2	1318	10.5	8.0	-6.1
] 40 50]	44.3	421	14.4	11.4	-9.4
] 50 60]	54.3	193	20.3	16.5	-15.2
] 60 70]	64.4	77	23.7	18.7	-15.7
] 70 80]	74.1	37	26.1	19.7	-18.3
] 80 90]	84.1	23	36.9	29.8	-26.4
> 90	105.3	20	45.4	37.1	-36.9

Similarly, a wet day will be estimated at the target station each time there is at least one neighboring station with a non-zero precipitation observation, even if all the other neighboring stations have no observed precipitation on that day. This will generally yield to an overestimation of the occurrence of wet days at the target station. In this regard, the last two columns of [table 2](#) show that the number of wet days for the Montérégie Est region were overestimated by 29 % (+43 days per year) on average for the 19 weather stations tested, with a minimum value of 13 % (+26 days per year) for the *Sutton* station and a maximum value of 53 % (+72 days per year) for the *Vercheres* station. These results were obtained by considering *wet days* as days for which precipitation is greater than 0 mm/day.

Although this overestimation may appear large, it does not have a significant impact on overall results, as small precipitation events (on the order of 0.5 mm/day or less) will not really affect precipitation statistics over long periods of time. This bias could, however, have implications for soil moisture balance models that sometimes do not allow evapotranspiration to occur during wet days. To limit the impact of this overestimation, a threshold value of 0.5 mm/day (instead of 0 mm/day) can be used to partition dry and wet days. The overestimation of wet days then becomes on average 9 % (+12 days per year) and range from 0.7 % (+1 days per year) to 18.2 % (+20 days per year).

4.3 Future Perspectives

The limitations discussed in the above section were addressed by [Simolo et al. \(2010\)](#), who proposed a two-step procedure to limit the overestimation of the number of wet days and the underestimation of the heavy precipitation events in the MLR method. Though they tested their improved method with a set of weather data in the Reno River basin, in northern Italy, they have not compared their results with the basic application of the MLR method. It is therefore not clear exactly what improvements these changes have provided compared to what the conventional application of the method would have produced.

The results shown in this study stress some of the limitations of the basic MLR method and suggest that an improvement of the method, such as the one suggested by [Simolo et al. \(2010\)](#), could be incorporated and tested in a future version of PyGWD. The in built cross-validation resampling technique that is included in PyGWD should facilitate the comparison of the results with and without the proposed modification to the method made by [Simolo et al. \(2010\)](#). Moreover,

according to [Xia et al. \(1999\)](#), the two most important factors in climatology for the estimation of missing daily data are the inter-correlations in the station network and the seasonal variations of these inter-correlations. The later point was not addressed in this work since the MLR models are generated in PyGWD using all the available data. An alternative approach is to partition the data on a seasonal basis to calculate the correlation coefficient and MLR models. This would allow for a better representation of the seasonal variations in the relationships between the stations. The downsides include a more complex algorithm to implement, a reduction of the method robustness, and longer computation times. This is an aspect that should also be considered in a future version of PyGWD.

5 Conclusion

This article presented the main features and capabilities of a free and open-source algorithm called PyGWD (Python Gap-filling Weather Data algorithm) written in the Python programming language. This algorithm was developed for filling the gaps in daily weather data with an automated, robust and efficient method. In addition to the fact that it is free and open source, this algorithm also offers an integrated procedure for the uncertainty assessment of the produced estimates.

PyGWD has been validated against a set of data from 19 weather stations located in the Montérégie Est region, Quebec, eastern Canada. For this purpose, the built-in cross-validation procedure was used to conveniently assess the uncertainty of the estimates for each of the 19 weather stations. The method yielded overall consistent and reliable estimates for all the tested weather stations, based on different basic performance criteria, including the RMSE, MAE, ME, and the correlation coefficient calculated between the estimated and measured values for maximum, minimum, and mean daily air temperatures and total daily precipitation. The results compare well with other published studies that used a similar multiple linear regression method (MLR).

One of the main advantages of PyGWD also resides in the fact it can be used with a graphical user interface that is part of the free and open-source software WHAT (Well Hydrograph Analysis Toolbox). Among other things, WHAT includes a graphical interface to easily search for weather stations in the online Canadian Daily Climate Database (CDCD) and to automatically download and format the available daily data to be used directly in PyGWD. The serially complete daily

weather series can then be used in combination with an observation well hydrograph to estimate groundwater recharge in unconfined aquifer conditions.

PyGWD is a powerful tool that could save consultants, students and researchers a lot of time in any project requiring the use of daily weather datasets. Development of PyGWD is still in progress and new features are regularly being added.

6 Acknowledgments

This research was supported by the NSERC Scholarship of Jean-Sébastien Gosselin, the NSERC-discovery grant (326975-2011) of Dr. Richard Martel, by funds from the Groundwater Geoscience Program of the Geological Survey of Canada, and the Projet Montérégie Est of the PACES program of the Ministère du Développement durable, de l'Environnement et de la Lutte contre le changement climatique. The climate data for this study were taken free of charge from the Government of Canada website (www.climate.weather.gc.ca).

7 Appendix

7.1 Minimal Working Example of the Gapfilling Algorithm

Step 1 - Create an instance of the class *GapFillWeather*

```
gapfill_weather = GapFillWeather()
```

The command line interface of the algorithm is built as a base class of the *Qt GUI Framework* using the *PySide* binding. This has been done to facilitate the addition of a graphical user interface on top of the algorithm with the *Qt GUI Development framework*.

Step 2 - Setup input and output directory

```
gapfill_weather.inputDir = '../Projects/Example/Meteo/Input'  
gapfill_weather.outputDir = '../Projects/Example/Meteo/Output'
```

Weather data files must be put together in a single input directory (*inputDir*). The outputs produced by PyGWD when a gap-less weather dataset is produced are saved in a single output directory (*outputDir*), in a sub-folder named after the name of the target station and its climate ID. Both *inputDir* and *outputDir* must be specified in PyGWD (see also [table 5](#)).

Step 3 - Load weather data files

Data files are loaded directly from the input directory that was setup in Step 2 by doing the following command:

```
stanames = gapfill_weather.load_data()  
print(stanames)
```

Step 4 - Define the time limits

```
gapfill_weather.time_start = 39838
```

```
gapfill_weather.time_end = 42199
```

Gaps in the weather data will be filled only between *time_start* and *time_end* (see also [table 5](#)). Time must be specified in Excel numerical data format. For example, 39838 corresponds to the date 25/01/2009, while 42199 to 14/07/2015 in dd/mm/yyyy format.

Step 5 - Set up method parameters

See [table 5](#) for a description of each parameter.

```
gapfill_weather.Nbr_Sta_max = 4
gapfill_weather.limitDist = 100
gapfill_weather.limitAlt = 350
gapfill_weather.regression_mode = 0 # 0 is LAD, 1 is OLS
```

Step 6 - Define additional options

See [table 5](#) for a description of each option.

```
gapfill_weather.full_error_analysis = False
gapfill_weather.add_ETP = False
```

Step 7 - Set up target station

The target station (for which daily weather data will be gap-filled) must be specified from its index in the *staname* list, which will automatically be displayed in the Python console at the end of Step 3.

```
gapfill_weather.set_target_station(5)
```

Step 8 - Gap-fill the data of the target station

```
gapfill_weather.fill_data()
```

A gap-less weather dataset will be produced for the target weather station defined in Step 7, over the time period defined in Step 4, with the parameters and options defined in Steps 5 and 6.

To run the gap-filling algorithm in batch, simply loop over all the indexes of the *staname* list and redo Step 7 and 8 for each station, such as:

```
for i , staname in enumerate(stanames):
    print(staname)
    gapfill_weather.set_target_station(i)
    gapfill_weather.fill_data()
```

7.2 Example of a weather data input file

Table 4 – Example of a weather data input file for weather station BONSECOURS located in Quebec, Canada. Missing data are represented by not-a-number (nan) values.

Station Name	BONSECOURS					
Province	QUEBEC					
Latitude	45.40					
Longitude	-72.27					
Elevation	297.2					
Climate Identifier	7020828					
Year	Month	Day	Max Temp (deg C)	Min Temp (deg C)	Mean Temp (deg C)	Total Precip (mm)
2010	12	1	nan	nan	nan	nan
2010	12	2	2.0	-1.0	0.5	0.0
2010	12	3	nan	-2.0	nan	4.0
2010	12	4	-2.5	-5.0	-3.8	0.6
2010	12	5	nan	-8.0	nan	1.4
2010	12	6	-5.5	-7.5	-6.5	11.0
2010	12	7	-6.0	-7.5	-6.8	14.0
2010	12	8	nan	nan	nan	7.6
2010	12	9	-11.0	-14.0	-12.5	1.6
2010	12	10	-5.0	-21.0	-13.0	0.0
2010	12	11	-1.0	-9.0	-5.0	0.2
2010	12	12	7.0	nan	nan	14.2
2010	12	13	2.0	-7.0	-2.5	7.0
2010	12	14	nan	-16.0	nan	0.0
2010	12	15	-13.0	-18.0	-15.5	7.0
2010	12	16	-7.5	-16.5	-12.0	nan
2010	12	17	-7.0	nan	nan	0.0
...

7.3 Inputs and Functions

Table 5 – List of parameters for version 1.0 of PyGWD.

Parameter name	Default value	Description
Nbr_Sta_max	4	Sets the maximum number of neighboring stations that is used for the generation of the MLR models to estimate the missing daily weather data.
limitDist	100 km	Maximum distance from the target station. Neighboring stations that are farther away from the target station than the specified value are excluded from the gap-filling procedure.
limitAlt	350 m	Maximum elevation difference. Neighboring stations with an absolute elevation difference with the target station that is higher than the specified value are excluded from the gap-filling procedure.
regression_mode	LAD	Defines the optimization criterion that is used for the regression in the generation of the MLR model as described in section 2.3 . The two options available are <i>OLS</i> (Ordinary Least Squares) or <i>LAD</i> (Least Absolute Deviations).
full_error_analysis	False	When set to <i>True</i> , the accuracy of the method, for the dataset of the target station, will be estimated with the cross-validation procedure described in section 2.5 .
add_ETP	False	When set to <i>True</i> , daily potential evapotranspiration will be estimated from the daily temperature data series with the Thornthwaite (1948) method and will be saved in the ‘out’ file, along with the gapless data series produced with the gap-filling algorithm.
inputDir	-	This is the directory where the algorithm searches for valid weather data file.
outputDir	-	This is the directory where all the outputs data files and figures are saved when the gap-filling procedure for a station is completed successfully. Files associated with a given station are saved in a sub-folder named after the weather station.
time_start	-	Sets the initial time in the weather dataset at which the gap-filling procedure will start.
time_end	-	Sets the final time in the weather dataset at which the gap-filling procedure will be completed.

Table 6 – List of outputs for version 1.0 of PyGWD. The name of the different files are given for the BROME (7020840) weather station.

File name	File type	Description
BROME (7020840)_1980-2009.out	data	Tab-separated values file containing the gapless weather dataset.
BROME (7020840)_1980-2009.log	data	Tab-separated values file containing detailed information about each daily weather value estimated to fill the gaps in the original weather data series.
BROME (7020840)_1980-2009.err	data	Tab-separated values file containing the results of the cross-validation procedure.
weather_datasets_summary.log	data	Tab-separated values file listing all the weather station for which a data file was available in the <i>inputDir</i> . For each station, information about the location coordinates (latitude and longitude), elevation, years for which data are available, and proportion of missing data are also provided.
weather_normals.pdf	figure	Graphs presenting the yearly and monthly weather normals for precipitation and max, min, and mean air temperatures, calculated from the gapless weather dataset. Examples of these graphs are shown in figure 4 .
precip_PDF.pdf	figure	Graph showing the gamma probability density functions that were estimated from the estimated and measured daily precipitation time series. The histogram of the distribution of the observed daily precipitation events is also shown. An example is provided in figure 6 .
min_temp_deg_c.pdf	figure	Scatter plot comparing the goodness of fit between the measured and estimated daily min temperature series. An example is presented in figure 5a .
mean_temp_deg_c.pdf	figure	Scatter plot comparing the goodness of fit between the measured and estimated daily mean temperature series. An example is presented in figure 5b .
max_temp_deg_c.pdf	figure	Scatter plot comparing the goodness of fit between the measured and estimated daily max temperature series. An example is presented in figure 5c .
total_precip_mm.pdf	figure	Scatter plot comparing the goodness of fit between the measured and estimated daily total precipitation series. An example is presented in figure 5d .

Références

- Alley WM & Leake SA (2004). The journey from safe yield to sustainability. *Ground Water*, 42(1):12–16. DOI:10.1111/j.1745-6584.2004.tb02446.x.
- Anderson MP (2005). Heat as a Ground Water Tracer. *Ground Water*, 43(6):951–968. DOI:10.1111/j.1745-6584.2005.00052.x.
- Arnold JG, Muttiah RS, Srinivasan R & Allen PM (2000). Regional estimation of base flow and groundwater recharge in the upper Mississippi river basin. *J. of Hydrology*, 227:21–40.
- Aurand KR & Thamke JN (2014). A comparison of groundwater recharge estimation methods in the Williston and Powder river structural basins. *Rocky Mountain and Cordilleran Joint Meeting*, Geological Society of America, volume 46, 87 pages, Montana State University, Bozeman, MT, USA.
- Baalousha H (2005). Using CRD method for quantification of groundwater recharge in the Gaza Strip, Palestine. *Environmental Geology*, 48:889–900. DOI:10.1007/s00254-005-0027-x.
- Baskaran S, Brodie RS, Ransley T & Baker P (2009). Time-series measurements of stream and sediment temperature for understanding river-groundwater interactions: Border Rivers and Lower Richmond catchments, Australia. *Australian Journal of Earth Sciences*, 56:21–30. DOI:10.1080/08120090802541903.
- Bear J (1972). *Dynamics of Fluids in Porous Media*. Dover Publications, Mineola, New York, USA.
- Bendjoudi H, Cheviron B, Guérin R & Tabbagh A (2005). Determination of upward/downward groundwater fluxes using transient variations of soil profile temperature: test of the method with Voyons (Aube, France) experimental data. *Hydrological Processes*, 19:3735–3745. DOI:10.1002/hyp.5856.
- Besbes M & De Marsily G (1984). From infiltration to recharge: use of a parametric transfer function. *Journal of Hydrology*, 74(3–4):271–293. DOI:10.1016/0022-1694(84)90019-2.
- Beven K & Binley A (1992). The future of distributed models: Model calibration and uncertainty prediction. *Hydrological Processes*, 6(3):279–298. DOI:10.1002/hyp.3360060305.
- Beven K & Binley A (2014). GLUE: 20 years on. *Hydrological Processes*, 28:5897–5918. DOI:10.1002/hyp.10082.
- Björck A (1996). *Numerical Methods for Least Squares Problems*. Other Titles in Applied Mathematics. Society for Industrial and Applied Mathematics.
- Boyle JM & Saleem ZA (1979). Determination of recharge rates using temperature-depth profiles in wells. *Water Resources Research*, 15:1616–1622. DOI:10.1029/WR015i006p01616. D034.

- Bredehoeft JD & Papadopoulos IS (1965). Rates of vertical groundwater movement estimated from the earth's thermal profile. *Water Resources Research*, 1(2):325–328. DOI:10.1029/WR001i002p00325.
- Bredenkamp DB, Botha L, Van Tonder G & Van Rensburg HJ (1995). *Manual on quantitative estimation of groundwater recharge and aquifer storativity*. Water Research Commission.
- Brooks RH & Corey AT (1966). Properties of porous media affecting fluid flow. *Journal of the Irrigation and Drainage Division, Proceedings of the American Society of Civil Engineers*, 92(IR2):61–88.
- Campbell GS (1974). A simple method for determining unsaturated conductivity from moisture retention data. *Soil Science*, 117(6):311–314.
- Carrier MA, Lefebvre R, Rivard C, Parent M, Ballard JM, Benoît N, Vigneault H, Beaudry C, Malet X, Laurencelle M, Gosselin JS, Ladevèze P, Thériault R, Beaudin I, Michaud A, Pugin A, Morin R, Crow H, Gloaguen E, Bleser J, Martin A & Lavoie D (2013). Portrait des ressources en eau souterraine en Montérégie Est, Québec, Canada. Projet réalisé conjointement par l'INRS, la CGC, l'OBV Yamaska et l'IRDA dans le cadre du Programme d'acquisition de connaissances sur les eaux souterraines. Institut national de la recherche scientifique, Centre Eau Terre Environnement. Quebec City, Quebec, Canada, 318 pages.
- Cheviron B, Guérin R, Tabbagh A & Bendjoudi H (2005). Determining long-term effective groundwater recharge by analyzing vertical soil temperature profiles at meteorological stations. *Water Resources Research*, 41(9):W09501. DOI:10.1029/2005WR004174.
- Coes AL, Spruill TB & Thomasson MJ (2007). Multiple-method estimation of recharge rates at diverse locations in the North Carolina Coastal Plain, USA. *Hydrogeology Journal*, 15(4):773–788. DOI:10.1007/s10040-006-0123-3.
- Constantz J (2008). Heat as a tracer to determine streambed water exchanges. *Water Resources Research*, 44(4):W00D10. DOI:10.1029/2008WR006996.
- Coulibaly P & Evora ND (2007). Comparison of neural network methods for infilling missing daily weather records. *Journal of Hydrology*, 341(1–2):27–41. DOI:10.1016/j.jhydrol.2007.04.020.
- Croteau A, Nastev M & Lefebvre R (2010). Groundwater recharge assessment in the Chateauguay river watershed. *Canadian Water Resources Journal*, 35:451–468. DOI:10.4296/cwrj3504451.
- Dastorani MT, Moghadamnia A, Piri J & Rico-Ramirez M (2009). Application of ANN and ANFIS models for reconstructing missing flow data. *Environmental Monitoring and Assessment*, 166(1–4):421–434. DOI:10.1007/s10661-009-1012-8.
- de Vries DA (1966). Thermal Properties of Soils. *Physics of Plant Environment*. Van Wijk WR, éditeur, American Elsevier Publishing Company, Inc., pages 210–235. New York, N.Y., second edition edition.
- de Vries JJ & Simmers I (2002). Groundwater recharge: an overview of processes and challenges. *Hydrogeology Journal*, 10(1):5–17. DOI:10.1007/s10040-001-0171-7.
- Decagon Devices (2010). 5tm water content and temperature sensors operator's manual (version 0). Decagon Devices.

- DeGaetano AT, Eggleston KL & Knapp WW (1995). A Method to Estimate Missing Daily Maximum and Minimum Temperature Observations. *Journal of Applied Meteorology*, 34(2):371–380. DOI:10.1175/1520-0450-34.2.371.
- Delin GN, Healy RW, Lorenz DL & Nimmo JR (2007). Comparison of local- to regional-scale estimates of ground-water recharge in Minnesota, USA. *Journal of Hydrology*, 334(1–2):231–249. DOI:10.1016/j.jhydrol.2006.10.010.
- Dell CI (1959). A study of the mineralogical composition of sand in southern Ontario. *Canadian Journal of Soil Science*, 39(2):185–196. DOI:10.4141/cjss59-024.
- Dell CI (1963). A study of the mineralogical composition of sand in southern Ontario. *Canadian Journal of Soil Science*, 43(2):189–200. DOI:10.4141/cjss63-024.
- Devlin JF & Sophocleous M (2005). The persistence of the water budget myth and its relationship to sustainability. *Hydrogeology Journal*, 13(4):549–554. DOI:10.1007/s10040-004-0354-0.
- Eischeid JK, Bruce Baker C, Karl TR & Diaz HF (1995). The quality control of long-term climatological data using objective data analysis. *Journal of Applied Meteorology*, 34(12):2787–2795.
- Eischeid JK, Pasteris PA, Diaz HF, Plantico MS & Lott NJ (2000). Creating a serially complete, national daily time series of temperature and precipitation for the Western United States. *Journal of Applied Meteorology*, 39:1580–1591. DOI:1520-0450(2000)039<1580:CASCND>2.0.CO;2.
- Environment Canada (2011). *Climate Data - Environment Canada*. <http://climate.weather.gc.ca/>. 2014-06-30.
- Environnement et Changement climatique Canada (2013). *Les eaux souterraines*. <https://www.ec.gc.ca>. 2013-09-09.
- Fagnan N, Bourque E, Michaud Y, Lefebvre R, Boisvert E, Parent M & Martel R (1999). Hydrogéologie des complexes deltaïques sur la marge nord de la mer de Champlain, Québec (in French). *Hydrogéologie*, 4:9–22.
- Farouki OT (1981). Thermal properties of soils. Cold Regions Research and Engineering Laboratory. Hanover, New Hampshire.
- Flerchinger GN (2000). The Simultaneous Heat and Water (SHAW) Model: Technical Documentation. Northwest Watershed Research Center. Boise, Idaho.
- Flerchinger GN, Hanson CL & Wight JR (1996). Modeling evapotranspiration and surface energy budgets across a watershed. *Water Resources Research*, 32(8):2539–2548. DOI:10.1029/96WR01240.
- Flerchinger GN & Saxton KE (1987). Simultaneous heat and water model of a freezing snow-residue-soil system. *American Society of Agricultural Engineers (Microfiche collection) (USA)*.
- Freeman LA, Carpenter MC, Rosenberry DO, Rousseau JP, Unger R & McLean JS (2004). Use of submersible pressure transducers in water-resources investigations. U.S. Geological Survey.
- Freeze RA & Cherry JA (1979). *Groundwater*. Prentice Hall, Upper Saddle River, New Jersey, USA.

Gee GW, Newman BD, Green SR, Meissner R, Rupp H, Zhang ZF, Keller JM, Waugh WJ, van der Velde M & Salazar J (2009). Passive wick fluxmeters: Design considerations and field applications. *Water Resources Research*, 45(4):W04420. DOI:10.1029/2008WR007088.

Goodrich DC, Williams DG, Unkrich CL, Hogan JF, Scott RL, Hultine KR, Pool D, Coes AL & Miller S (2004). Comparison of methods to estimate ephemeral channel recharge, Walnut Gulch, San Pedro river basin, Arizona. *Water Science and Application Series Volume 9*, pages 77–99.

Gosselin JS, Rivard C & Martel R (2016a). User manual for WHAT (Well Hydrograph Analysis Toolbox). Institut National de la Recherche Scientifique, Centre Eau Terre Environnement. Quebec city, Quebec, Canada.

Gosselin JS, Rivard C, Martel R & Lefebvre R (2013). Estimating recharge from observed well hydrographs combined with meteorological data. *GéoMontréal 2013, 66th Canadian Geotechnical Conference and the 11th Joint CGS/IAH-CNC Groundwater Conference proceedings*, Montreal, Quebec, Canada.

Gosselin JS, Rivard C, Martel R & Lefebvre R (2016b). Application limits of the interpretation of near-surface temperature time series to assess groundwater recharge. *Journal of Hydrology*, 538:96–108. DOI:10.1016/j.jhydrol.2016.03.055.

Gosselin JS, Rivard C, Paniconi C & Martel R (2011). Applicability of temperature profile techniques for estimating recharge fluxes through the vadose zone. *GeoHydro2011, Joint IAH-CNC, CANQUA and AHQ conference proceedings*, pages 1–7, Quebec City, Quebec, Canada.

Goto S, Yamano M & Kinoshita M (2005). Thermal response of sediment with vertical fluid flow to periodic temperature variation at the surface. *Journal of Geophysical Research: Solid Earth*, 110(B1):B01106. DOI:10.1029/2004JB003419.

Gouvernement du Québec (2015). Eaux souterraines. Gouvernement du Québec, ministère du Développement durable, Environnement et Lutte contre les changements climatiques. <http://www.mddelcc.gouv.qc.ca/eau/souterraines/> (visité le 12 janvier 2016).

Green WH & Ampt G (1911). Studies on soil physics. *The Journal of Agricultural Science*, 4(01):1–24.

Grismer ME, Bachman S & Powers T (2000). A comparison of groundwater recharge estimation methods in a semi-arid, coastal avocado and citrus orchard (Ventura County, California). *Hydrological Processes*, 14(14):2527–2543. DOI:10.1002/1099-1085(200001015)14:14<2527::AID-HYP112>3.0.CO;2-T.

Healy RW (2010). *Estimating Groundwater Recharge*. Cambridge University Press, Cambridge, United Kingdom.

Healy RW & Cook PG (2002). Using groundwater levels to estimate recharge. *Hydrogeology Journal*, 10(1):91–109. DOI:10.1007/s10040-001-0178-0.

Heppner CS & Nimmo JR (2005). A computer program for predicting recharge with a master recession curve. U.S. Geological Survey. 7 pages.

Heppner CS, Nimmo JR, Folmar GJ, Gburek WJ & Risser DW (2007). Multiple-methods investigation of recharge at a humid-region fractured rock site, Pennsylvania, USA. *Hydrogeology Journal*, 15(5):915–927. DOI:10.1007/s10040-006-0149-6.

- Hill MC & Tiedman CR (2007). *Effective groundwater model calibration with analysis of data, sensitivities, predictions, and uncertainty*. Wiley, Hoboken, New Jersey.
- Hoffman JD (2001). *Numerical methods for engineers and scientists*. CRC Press, New York, 2 edition.
- Huet M, Chesnaux R, Boucher MA & Poirier C (2015). Comparing various approaches for assessing groundwater recharge at a regional scale in the Canadian Shield. *Hydrological Sciences Journal*, 0(ja):null. DOI:10.1080/02626667.2015.1106544.
- Kashani MH & Dinpashoh Y (2011). Evaluation of efficiency of different estimation methods for missing climatological data. *Stochastic Environmental Research and Risk Assessment*, 26(1):59–71. DOI:10.1007/s00477-011-0536-y.
- Keshari AK & Koo MH (2007). Simulating subsurface temperature under variable recharge. *Journal of Porous Media*, 10(8):769–782. DOI:10.1615/JPorMedia.v10.i8.30.
- Kienzle SW (2008). A new temperature based method to separate rain and snow. *Hydrological Processes*, 22(26):5067–5085. DOI:10.1002/hyp.7131.
- Koo MH & Kim Y (2008). Modeling of water flow and heat transport in the vadose zone: numerical demonstration of variability of local groundwater recharge in response to monsoon rainfall in Korea. *Geosciences Journal*, 12(2):123–137. DOI:oui.
- Ladevèze P, Rivard C, Lefebvre R, Lavoie D, Parent M, Malet X, G B & Gosselin JS (2016). Travaux de caractérisation hydrogéologique dans la plateforme sédimentaire du Saint-Laurent, région de Saint-Édouard-de-Lotbinière, Québec. Commission géologique du Canada. Québec, Quebec, Canada.
- Lapham WW (1989). Use of temperature profiles beneath streams to determine rates of vertical ground-water flow and vertical hydraulic conductivity, US Geol. Survey Water-Supply Paper 2337. US Dept. of the Interior, Washington, D.C. 35 p pages.
- Larose-Charette D, Lefebvre R, Fagnan N, Michaud Y & Therrien R (2000). Groundwater flow dynamics in unconfined deltaic aquifers of the Portneuf area, Quebec, Canada. *53rd Can. Geotech. Conf., 1st Joint IAH-CNC and CGS Groundwater Speciality Conf. proceedings*, Montréal, Qc, Canada; Oct. 15-18, 2000.
- Lefebvre R, Maltais I, Paradis D & Michaud Y (2011). Recharge assessment from daily soil moisture balance and well hydrographs for the Portneuf unconfined aquifers. *Geohydro 2011, proceedings of the joint meeting of the Canadian Quaternary Association and the Canadian Chapter of the International Association of Hydrogeologists*, Quebec City, Qc, Canada; August 28-31, 2011.
- Lerner DN, Isaar AS & Simmers I (1990). *Groundwater Recharge: A Guide to Understanding and Estimating Natural Recharge*. Hanover VHH, éditeur. volume 8 de *International Contributions to hydrogeology*. Verlag Heinz Heise GmbH & Co. KG., Hannover, West Germany.
- Mackay JD, Jackson CR, Brookshaw A, Scaife AA, Cook J & Ward RS (2015). Seasonal forecasting of groundwater levels in principal aquifers of the United Kingdom. *Journal of Hydrology*, 530:815–828. DOI:10.1016/j.jhydrol.2015.10.018.
- Mackay JD, Jackson CR & Wang L (2014a). AquiMod User Manual (v1.0) - Environmental Modelling Programme. British Geological Survey. Keyworth, Nottingham, UK.

Mackay JD, Jackson CR & Wang L (2014b). A lumped conceptual model to simulate groundwater level time-series. *Environmental Modelling & Software*, 61:229–245. DOI:10.1016/j.envsoft.2014.06.003.

Menke W (1989). *Geophysical Data Analysis: Discrete Inverse Theory*. Academic Press, San Diego, 1 edition edition.

Morin G & Paquet P (1995). Le modèle de simulation de quantité et de qualité CEQUEAU - Manuel de référence. INRS-Eau. 318 pages.

Neuman SP (1987). On Methods of Determining Specific Yield. *Ground Water*, 25(6):679–684. DOI:10.1111/j.1745-6584.1987.tb02208.x.

Obiefuna GI & Orazulike DM (2011). Application and comparison of groundwater recharge estimation methods for the semiarid Yola area, northeast, Nigeria. *Global Journal of Geological Sciences*, 9(2):177–204. DOI:10.4314/gjgs.v9i2.

Paniconi C & Wood EF (1993). A detailed model for simulation of catchment scale subsurface hydrologic processes. *Water Resources Research*, 29:1601–1620. DOI:10.1029/92WR02333.

Paradis D, Lefebvre R & Michaud Y (1997). Analyse hydrologique pour l'évaluation de la recharge en eau souterraine dans le bassin versant de la rivière Portneuf sur le piémont laurentien, Québec. Commission Géologique du Canada. pages 83–88.

Paradis D, Martel R, Karanta G, Lefebvre R, Michaud Y, Therrien R & Nastev M (2007). Comparative study of methods for WHPA delineation. *Ground Water*, 45(2):158–167. DOI:10.1111/j.1745-6584.2006.00271.x.

Parsons ML (1970). Groundwater thermal regime in a glacial complex. *Water Resources Research*, 6(6):1701–1720. DOI:10.1029/WR006i006p01701.

Pettijohn FJ (1975). *Sedimentary Rocks*. Harper & Row, New York, N.Y., 3 edition.

Posavec K, Bačani A & Nakić Z (2006). A visual basic spreadsheet macro for recession curve analysis. *Ground Water*, 44(5):764–767. DOI:10.1111/j.1745-6584.2006.00226.x.

Posavec K, Parlov J & Nakić Z (2010). Fully automated objective-based method for master recession curve separation. *Ground Water*, 48(4):598–603. DOI:10.1111/j.1745-6584.2009.00669.x.

Rasmussen WC & Andreassen GE (1959). Hydrologic budget of the Beaverdam Creek Basin, Maryland. *US Geological Survey Water-Supply*, Paper 1972.

Rau GC, Andersen MS, McCallum AM, Roshan H & Acworth RI (2014). Heat as a tracer to quantify water flow in near-surface sediments. *Earth-Science Reviews*, 129:40–58. DOI:10.1016/j.earscirev.2013.10.015.

Rawls WJ, Brakensiek DL & Saxton KE (1982). Estimation of soil water properties. *Transactions of the ASAE [American Society of Agricultural Engineers] (USA)*.

Ringleb J, Sallwey J & Stefan C (2015). Comparison of different estimation techniques to quantify groundwater recharge in Pirna, Germany. *Geophysical Research Abstracts for EGU General Assembly*, volume 17, 3594 pages.

- Risser DW, Gburek WJ & Folmar GJ (2009). Comparison of recharge estimates at a small watershed in east-central Pennsylvania, USA. *Hydrogeology Journal*, 17(2):287–298. DOI:10.1007/s10040-008-0406-y.
- Rivard C, Lefebvre R & Paradis D (2014). Regional recharge estimation using multiple methods: an application in the Annapolis Valley, Nova Scotia (Canada). *Environmental Earth Sciences*, 71(3):1389–1408. DOI:10.1007/s12665-013-2545-2.
- Rushton KR (2003). *Groundwater Hydrology: Conceptual and Computational Models*. John Wiley & Sons Ltd, Chichester, West Sussex, England.
- Rushton KR, Eilers VHM & Carter RC (2006). Improved soil moisture balance methodology for recharge estimation. *Journal of Hydrology*, 318:379–399. DOI:10.1016/j.jhydrol.2005.06.022. D134.
- Sanford W (2002). Recharge and groundwater models: an overview. *Hydrogeology Journal*, 10(1):110–120.
- Scanlon BR, Healy RW & Cook PG (2002). Choosing appropriate techniques for quantifying groundwater recharge. *Hydrogeology Journal*, 10:18–39. DOI:10.1007/s10040-001-0176-2.
- Schroeder PR, Lloyd CM, Zappi PA & Aziz NM (1994). The Hydrologic Evaluation of Landfill Performance (HELP) Model: User's Guide for Version 3. U.S. Environmental Protection Agency, Office of Research and Development, Risk Reduction Engineering Laboratory. Washington, DC, USA.
- Shanafield M, Hatch C & Pohll G (2011). Uncertainty in thermal time series analysis estimates of streambed water flux. *Water Resources Research*, 47(3). DOI:10.1029/2010WR009574.
- Shiklomanov IA & Rodda JC (2003). *World Water Resources at the Beginning of the Twenty-First Century*. International Hydrology Series. Cambridge University Press, Cambridge, United kingdom.
- Sibanda T, Nonner JC & Uhlenbrook S (2009). Comparison of groundwater recharge estimation methods for the semi-arid Nyamandhlovu area, Zimbabwe. *Hydrogeology Journal*, 17(6):1427–1441. DOI:10.1007/s10040-009-0445-z.
- Silliman SE, Ramirez J & McCabe RL (1995). Quantifying downflow through creek sediments using temperature time series: one-dimensional solution incorporating measured surface temperature. *Journal of Hydrology*, 167(1):99–119. DOI:10.1016/0022-1694(94)02613-G.
- Simolo C, Brunetti M, Maugeri M & Nanni T (2010). Improving estimation of missing values in daily precipitation series by a probability density function-preserving approach. *International Journal of Climatology*, 30:1564–1576. DOI:10.1002/joc.1992.
- Sophocleous M & Devlin JF (2004). Comment on "The water budget myth revisited: why hydrogeologists model." by J.D. Bredehoeft. *Ground Water*, 42(4):618.
- Sorey ML (1971). Measurement of vertical groundwater velocity from temperature profiles in wells. *Water Resources Research*, 7(4):963–970. DOI:10.1029/WR007i004p00963.
- Soto-López CD, Meixner T & Ferré T (2011). Effects of measurement resolution on the analysis of temperature time series for stream-aquifer flux estimation. *Water Resources Research*, 47(12). DOI:10.1029/2011WR010834.

Stallman RW (1963). Computation of Groundwater Velocity from Temperature Data. *Methods of collecting and interpreting ground-water data*, USGS, numéro 1544-H de Water Supply Paper, pages 36–46. Washington, DC.

Stallman RW (1965). Steady one-dimensional fluid flow in a semi-infinite porous medium with sinusoidal surface temperature. *Journal of Geophysical Research*, 70(12):2821–2827. DOI:10.1029/JZ070i012p02821.

Stonestrom DA & Blasch KW (2003). Determining temperature and thermal properties for heat-based studies of surface-water ground-water interactions. *Heat as a tool for studying the movement of ground water near streams*. Stonestrom DA & Constantz J (éditeurs), U.S. Geological Survey, USGS Circular 1260 Appendix A, pages 73–80. Reston, Virginia.

Stonestrom DA & Constantz J (2003). Heat as a tool for studying the movement of ground water near streams. U.S. Geological Survey. Reston, Virginia.

Suzuki S (1960). Percolation measurements based on heat flow through soil with special reference to paddy fields. *Journal of Geophysical Research*, 65:2883–2885. DOI:10.1029/JZ065i009p02883.

Tabbagh A, Bendjoudi H & Benderitter Y (1999). Determination of recharge in unsaturated soils using temperature monitoring. *Water Resources Research*, 35(8):2439–2446. DOI:10.1029/1999WR900134.

Tabbagh A, Guérin R, Bendjoudi H, Cheviron B & Bechkit MA (2009). Pluri-annual recharge assessment using vertical soil temperature profiles: exemple of the Seine River Basin (1984–2001). *Comptes Rendus Geoscience*, 341:949–956. DOI:10.1016/j.crte.2009.08.007.

Taniguchi M (1993). Evaluation of vertical groundwater fluxes and thermal properties of aquifers based on transient temperature-depth profiles. *Water Resources Research*, 29:2021–2026. DOI:10.1029/93WR00541.

Taniguchi M (1994). Estimated recharge rates from groundwater temperatures in the Nara Basin, Japan. *Applied Hydrogeology*, 2(4):7–14. DOI:10.1007/s100400050031.

Thornthwaite CW (1948). An approach toward a rational classification of climate. *Geographical review*, 38:55–94.

Timlin D, Starr J, Cady R & Nicholson T (2003). Comparing ground-water recharge estimates using advanced monitoring techniques and models. United States Department of Agriculture, Agricultural Research Service. Beltsville, MD, USA.

Todd DK & Mays LW (2005). *Groundwater Hydrology*. Wiley, Hoboken, New Jersey, 3 edition.

Tronci N, Molteni F & Bozzini M (1986). A comparison of local approximation methods for the analysis of meteorological data. *Archives for Meteorology, Geophysics, and Bioclimatology, Series B*, 36(2):189–211. DOI:10.1007/BF02278328.

UNESCO-WWAP (2006). Water a Shared Responsibility. The United Nations World Water Development report 2. UNESCO. Paris, France.

USDA NRCS (2004). Snowmelt. *National Engineering Handbook: Part 630 - Hydrology, Chapter 11*, United States Department of Agriculture (USDA), Natural Resources Conservation Service (NRCS). Washington, DC, USA.

- Ustoorkar K & Deo MC (2008). Filling up gaps in wave data with genetic programming. *Marine Structures*, 21(2–3):177–195. DOI:10.1016/j.marstruc.2007.12.001.
- Vandenbohede A & Lebbe L (2010a). Parameter estimation based on vertical heat transport in the surficial zone. *Hydrogeology Journal*, 18:931–943. DOI:10.1007/s10040-009-0557-5.
- Vandenbohede A & Lebbe L (2010b). Recharge assessment by means of vertical temperature profiles: analysis of possible influences. *Hydrological Sciences Journal*, 55(5):792–804. DOI:10.1080/02626667.2010.490531.
- Williams PJ & Smith MW (1991). *The Frozen Earth: Fundamentals of Geocryology (Studies in Polar Research)*. Cambridge University Press, The Edinburgh Building, Cambridge, UK.
- WWAP (2015). Water for a Sustainable World. The United Nations World Water Development report 2015. UNESCO, Paris, France.
- Xia Y, Fabian P, Stohl A & Winterhalter M (1999). Forest climatology: estimation of missing values for Bavaria, Germany. *Agricultural and Forest Meteorology*, 96:131–144. DOI:10.1016/S0168-1923(99)00056-8.
- Xiong L & O'Connor KM (2008). An empirical method to improve the prediction limits of the GLUE methodology in rainfall-runoff modeling. *Journal of Hydrology*, 349(1–2):115–124. DOI:10.1016/j.jhydrol.2007.10.029.
- Yin L, Hu G, Huang J, Wen D, Dong J, Wang X & Li H (2011). Groundwater-recharge estimation in the Ordos Plateau, China: comparison of methods. *Hydrogeology Journal*, 19(8):1563–1575. DOI:10.1007/s10040-011-0777-3.
- Zhang T & Osterkamp TE (1995). Considerations in determining thermal diffusivity from temperature time series using finite difference methods. *Cold Regions Science and Technology*, 23:333–341. DOI:oui. D103.
- Šimůnek J, Šejna M, Saito H, Sakai M & van Genuchten MT (2013). The Hydrus-1d Software Package for Simulating the Movement of Water, Heat, and Multiple Solutes in Variably Saturated Media, Version 4.17, HYDRUS Software Series 3. Department of Environmental Sciences, University of California Riverside. Riverside, California, USA.

Appendix A

User Manual for WHAT

1 Introduction

1.1 What is WHAT

WHAT (Well Hydrograph Analysis Toolbox) is a free, open source, and cross-platform interactive computer program whose main focus is the interpretation of observation well hydrographs. It is written in the Python 2.7 programming language and is currently maintained and developed by Jean-Sébastien Gosselin at INRS-ETE (www.ete.inrs.ca). The source code and a stand-alone executable for Windows 7 are available free of charge for download on GitHub (www.github.com/jnsebgosselin/WHAT).

If you encounter any problems or errors during program execution, have any questions, or have suggestions on how to improve WHAT, please contact Jean-Sébastien Gosselin at this email address: jean-sebastien.gosselin@ete.inrs.ca.

1.2 Features

Below are listed the features that are available in the current version of WHAT, as well as the ones that are going to be incorporated in future versions of the software.

Features available in current version of WHAT :

- Gapless Daily Weather Time Series Preparation :
 - Graphical interface to the online Canadian Daily Climate Database (CDCD) to search for weather station by location coordinate.
 - Automatic downloading and formatting of available data from the CDCD.
 - Estimation of missing data and automatic gapfilling of the datasets.
- Data Visualization:
 - Data exploration in a user-friendly and dynamic graphical environment.
 - Production of publication-quality graphs in vectorial formats (pdf or svg).
- Weather Data Analysis :
 - Estimation of yearly and monthly normals.
 - Estimation of the daily potential evapotranspiration.
- Water Level Analysis :
 - Calculation of the master recession curve (MRC).
 - Estimation of groundwater recharge from the MRC using a continuous water-table fluctuation (WTF) method.

Features planned for future versions of WHAT :

- Synthetic hydrograph production for the estimation of groundwater recharge and prediction of water levels.
- Assessment of the level of confinement of the aquifer at the well location based on an analysis of the barometric response function of the water level record.

1.3 Installation and Update

WHAT can run on Windows, Linux, or OS X computer operating systems. However, a stand-alone executable of the program is currently released and tested only for the Windows 7 platform. This executable should also be compatible with Windows XP. For the Linux and OS X platforms, the software can be run directly from the source code, provided that Python 2.7 and all the required third party packages are installed on the computer (PySide, NumPy, matplotlib, xlrd, xlwt).

The stand-alone executable for Windows 7 is distributed in a Zip archive that can be downloaded freely on GitHub (<https://github.com/jnsebgosselin/WHAT/releases>). This archive contains:

- the GNU General Public License;
- a folder named “WHAT” that contains all the necessary system files for the program to run, including the file “WHAT.exe” from which the software can be started;
- a folder named “Projects” where all input and output files used or created by WHAT are stored by default. This folder includes samples of input and output files that provide a quick and convenient way to test and learn the various features of the program.

Once the content of the Zip archive has been extracted, the program can be started directly from the “WHAT.exe” executable file that is contained within the folder named “WHAT”. The software can conveniently run from any location on the computer or from any storage device without the need to install the program beforehand.

It is possible to update WHAT by downloading the Zip archive of a later version of the software, extracting the content, and by manually overwriting the “WHAT” folder of the older version with the newer one that was just downloaded.

1.4 Overview of the Graphical User Interface

The Graphical User Interface (GUI) of WHAT mainly consists of a menu bar, a console area, and a central view panel ([figure 1](#)). The *menu bar* is located in the top right corner of the GUI. This is where the name of the current project is displayed and where it is possible to open an existing project or create a new one. The *console* is located at the bottom of the GUI and is used to report technical information about the various tasks accomplished by the program as well as warning and error messages. The console can be collapsed vertically to save space, or can be extended to the entire window area. The *central view panel* is the main component of the GUI. It is where the various features of the software are displayed. The content of this panel is divided into four tabs: *Download Data*, *Fill Data*, *Hydrograph*, and *About*. These tabs are described in more details below and are shown in [figure 2](#).

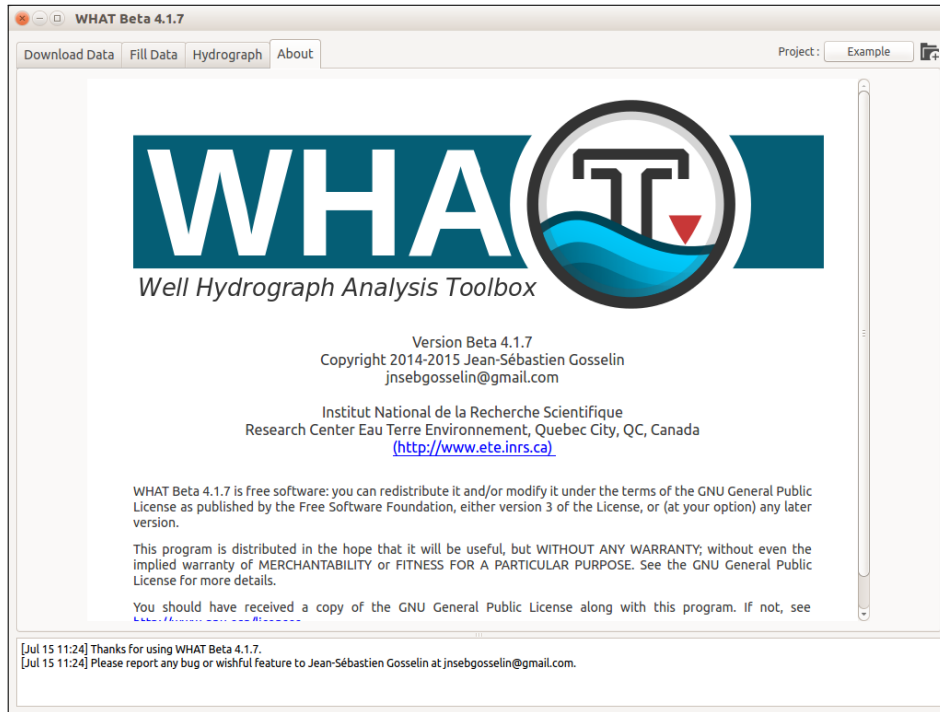


Figure 1 – Screenshot of WHAT v4.1.7-beta in Ubuntu-Linux 15.04 showing the *About* tab.

Download Data : This tab ([figure 2a](#)) provides a graphical interface to the online Canadian Daily Climate Database (CDCD), owned and operated by Environment Canada, from which it is

possible to interactively search for stations by location coordinates, download the available data, and automatically organize the data in a format compatible with WHAT.

Fill Data : This tab ([figure 2b](#)) provides an automated procedure to estimate and fill the missing values in the daily weather datasets. Missing data in a dataset from a given station are estimated with data from selected neighboring weather stations using a multiple linear regression model.

Hydrograph : This tab is used for viewing and plotting both groundwater level and weather time series. For this purpose, two modes are available: the *layout* and the *computation* mode. Both modes share the same weather and water level datasets and it is possible to switch from one mode to the other at anytime. The **layout** mode ([figure 2c](#)) provides a graphical interface to interactively produce publication-quality graphs. The **computation** mode ([figure 2d](#)) consists in a dynamic graphical environment where data can be visualized, manipulated and analyzed. Various computational tools are available in this mode, including the estimation of the Master Recession Curve (MRC) and the estimation of groundwater recharge.

About : This tab ([figure 1](#)) displays copyright, licensing and general information about WHAT.

2 Data Management by Projects

2.1 Introduction

The data are managed in WHAT by project, that is to say, all input and output files relative to a particular project are stored in a common folder named “project folder”. This file management system allows to easily backup or copy the data related to a particular project since all the files are saved at the same location.

The first time WHAT is started, the software will automatically open the project “Example”, which includes all the files necessary to easily and quickly test the different features of the software. The title of the current project is shown in the menu bar located in the upper right corner of the WHAT window. Only one project at a time can be open per instance of WHAT.

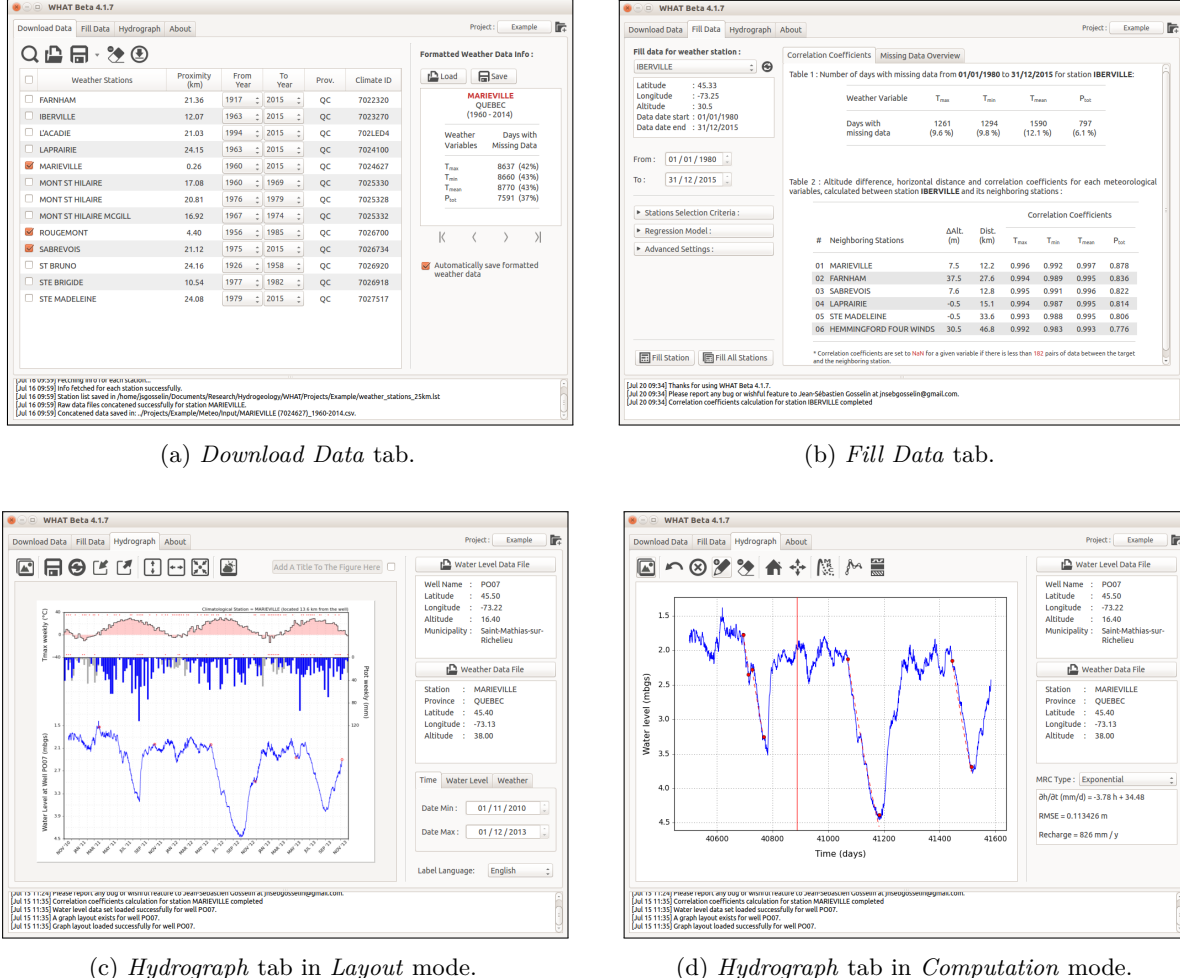


Figure 2 – Screenshots of WHAT v4.1.7-beta captured in Ubuntu Linux 15.04. showing : (a) the Download Data tab, (b) the Fill Data tab (c) the Hydrograph tab in Layout mode, and (d) the Hydrograph tab in Computation mode.

2.2 Create a New Project

The creation of a new project can be started by clicking on the *New Project* button located in the menu bar ([figure 1](#)). This will open a new dialog window ([figure 3](#)) where information about the project can be entered such as its title, author, and location coordinates. Clicking on the button *Save* will create a new project folder named after the project's title. Moreover, information related to

the project are saved in a file with an extension “.what”. It is possible to change the directory where the project is saved by clicking the folder  icon located next to the *Save in Folder* directory path.

For example, information related to the project *My New Project* by John Doe, in [figure 3](#), would be saved in the file named “My_New_Project.what”, in the folder named “My New Project”, located in the directory “...\\WHAT\\Projects”.

2.3 Open a Project

It is possible to open an existing project by clicking on the button *Project*, which displays the name of the current project, in the upper right corner of the WHAT window. This will open a new dialog window, from which an existing project file (*.what) can be selected and opened. The current project name will then change for the name of the project that was just selected.

The path to the project folder is stored in a relative format. This means that if the location of the project folder is changed relative the executable of the software (“WHAT.exe”), WHAT will need to be redirected to the new location of the project by repeating the procedure described in the paragraph above.

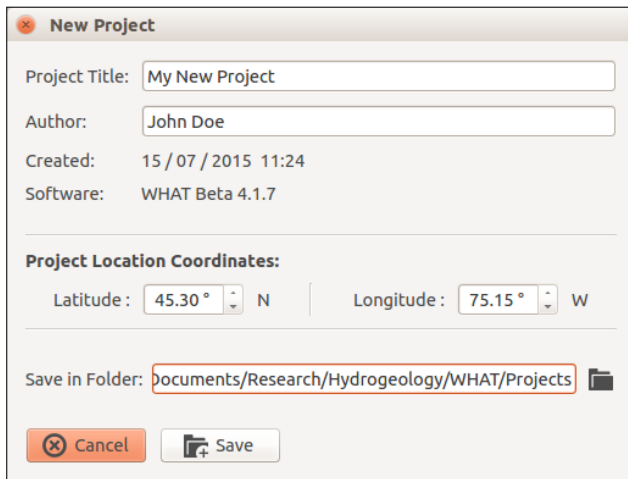


Figure 3
Screenshot of WHAT v4.1.7-beta in Ubuntu-Linux 15.04 showing the *New Project* dialog window.

2.4 Project Folder Structure Overview

In addition to the project folder and the “.what” file that are created when saving a new project, WHAT automatically generates various files and sub-folders that are required for its execution. This file organization is briefly described below and an example is presented in [figure 4](#). The project folder contains two sub-folders named “Meteo” and “Waterlvl” and a few other files.

Meteo : The sub-folder *Meteo* contains three sub-folders named respectively Raw, Input and Output. The **Raw** folder is where the weather data downloaded from the CDCCD are saved, for each year separately, as csv (comma-separated values) files. All the files related to a same station are saved within a common folder, named after the name of the station and its climate ID. For example, in [figure 4](#), the raw data file “eng-daily-01011980-12311980.csv”, which contains weather data from the station “Marieville” for the year 1980, is saved within a folder named “MARIEVILLE (7024627)”, where the number in parentheses is the climate ID of the station.

The folder **Input** contains the formatted weather data files produced from the raw data files. These are tsv (tab-separated values) files that are named after the name of the station, its climate ID, and the first and last year of the data record.

The folder **Output** is where the gapless weather time-series are saved in tsv files with the extension “.out”. The files with the extension “.log” are tsv files that contain detailed information about the missing daily weather values that were estimated to fill the gaps in the weather datasets. The files with the extension “.err” contains a time-series of estimated weather values that were produced with a cross-validation re-sampling technique. These estimated values can be used to evaluate the accuracy of the method.

Waterlvl : The sub-folder “Waterlvl” is the preferred location where the water level datasets related to a same project should be stored. These files can be either in a Microsoft Excel spreadsheet file format (xls) or in a tab-separated values text format (tsv).

Other Files : The files with an “.lst” extension correspond to the lists of weather stations from the Canadian Daily Climate Database (CDCCD) that were saved by the user from the *Download Data* tab.

The file “graph.layout.lst” is a resource file, in which are stored the layout of the well hydrographs that were produced from the *Hydrograph* tab. The file “weather_datasets_summary.log” is a tsv file that contains a summary of all the weather data files included in the “Input” folder. The file “waterlvl_manual_measurements.xls” contains all the manual water-level measurements from field visits.

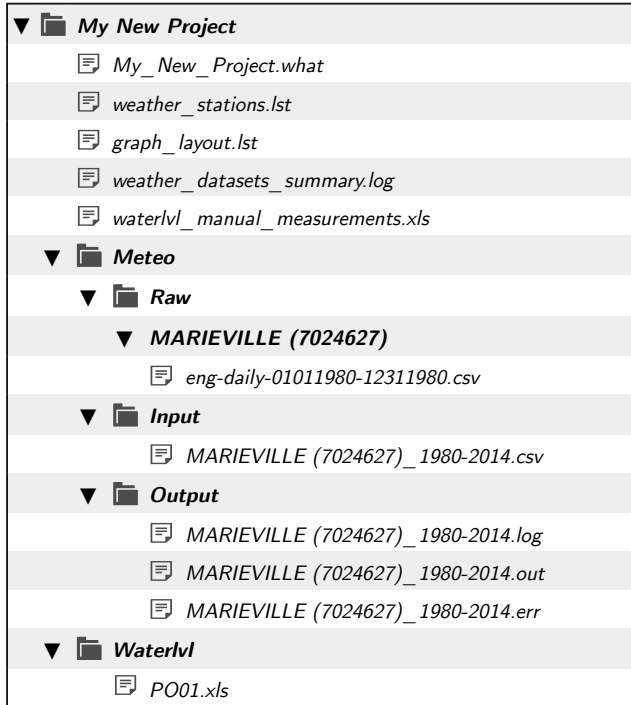


Figure 4
File organization of the project folders.

3 Creating Gapless Daily Weather Datasets

3.1 Downloading and formatting data from the CDCCD

3.1.1 Introduction

WHAT provides a graphical interface to the online Canadian Daily Climate Database (CDCCD), which contains daily data for air temperature and precipitation dating back to 1840 to the present for about 8450 stations distributed across Canada (www.climate.weather.gc.ca). The interface allows to search for stations interactively using location coordinates, download the available data

for the selected weather stations, and automatically organize the data in a format compatible with WHAT. These features are available in the *Download Data* tab shown in [figure 5](#). This tab consists of a toolbar located at the top of the interface, an area where are displayed the current list of weather stations for which data can be downloaded, and a side-panel to the right where can be manage the formatting of the weather data files that were downloaded for each year individually.

3.1.2 Searching for weather stations

Before any weather data can be downloaded from the online CDCCD, a list of stations must first be provided to WHAT. This can be done by selecting an already existing list of stations (files with a “lst” extension) by clicking on the opened document  icon located in the toolbar.

Alternatively, it is possible to search for weather stations in the online CDCCD by clicking on the magnifying glass  icon in the toolbar. This will open a new dialog window (see [figure 6](#)) where it is possible to search for weather stations located within a given radius around a set of location coordinates (latitude and longitude) in decimal degrees. It is possible to further narrow down the search by including only stations with data available within a given period and/or with data available for a minimum number of years.

When all the parameters have been specified, the search for weather stations in the online CDCCD can be initiated by clicking on the *Search Stations*  button. The resulting stations are automatically displayed in a table, along with information regarding their proximity to the location coordinates used for the search, the years for which data are available, their province, and their climate ID. Selecting stations and clicking on the *Add Stations*  button will add them to the current list of weather stations displayed in the *Download Data* tab.

It is possible to remove any weather station from the current list by selecting them and clicking on the toolbar eraser  icon. The station list can be saved by clicking on the toolbar floppy disk  icon. Alternatively, it is also possible to generate a list of weather stations by creating manually a lst file without using the graphical interface. This is done by retrieving station information from their unique url directly on the government of Canada website (www.climate.weather.gc.ca) and saving the information in a tsv (tabular-separated values) text file with a “lst” extension.

3.1.3 Downloading the weather data

Daily weather data can be downloaded from the online CDCD by selecting the desired stations from the list displayed in the *Download Data* tab and clicking on the toolbar icon with the encircled downward arrow . Data will be downloaded for the years specified for each selected station and

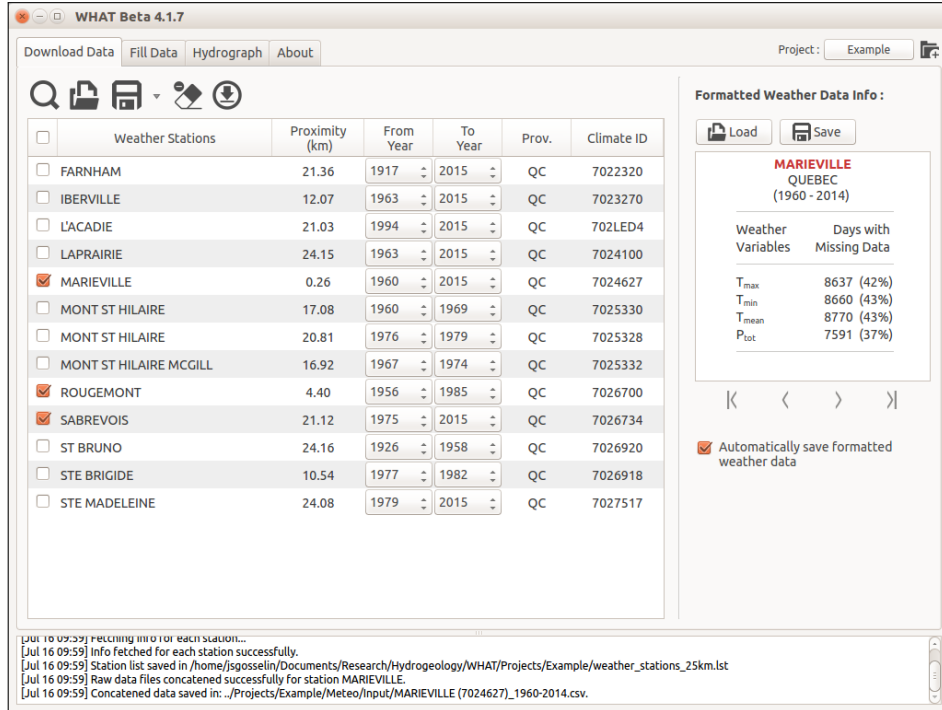


Figure 5 – Screenshot of WHAT v4.1.7-beta in Ubuntu-Linux 15.04 showing the *Download Data* tab.

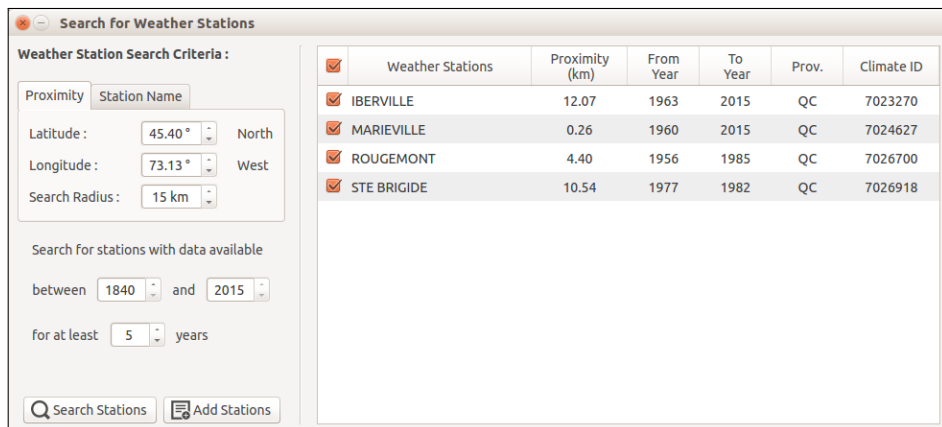


Figure 6 – Screenshot of WHAT v4.1.7-beta in Ubuntu-Linux 15.04 showing the graphical interface to the online CDCD database.

the results will be saved automatically as a csv (comma-separated values) file in the *Raw* folder (see [appendix 2.4](#)). Weather data for a given station won't be downloaded for the years for which a data file already exist in the *Raw* folder. Detailed information about the downloading process are printed in the console area located at the bottom of the interface (see [appendix 1.4](#)). The downloading process can be stopped at any time by clicking on the stop  icon that appears in the toolbar as soon a downloading task is started.

3.1.4 Formatting the weather data

WHAT automatically formats the data as soon as they have been successfully downloaded for a given weather station. To do this, data from each annual file are put together end to end in chronological order. Only the data related to air temperature (mean, max and min) and total precipitation are kept. In addition, days with missing data in the dataset are filled with a NaN (not a number) value. Finally, information on the number of days with missing data for each meteorological variable are displayed in the right side-panel. Alternatively, it is possible to open and format previously downloaded weather data files by clicking on the *Load*  button in the right side-panel and selecting the desired files from the dialog window that will open.

By default, WHAT will automatically save the formatted data in a single tsv (tabular-separated values) file in the *Input* folder (see [appendix 2.4](#)). The automatic saving of the formatted data series can be disabled by unchecking the *Automatically save concatenated data* option. From the right side-panel, it is then possible to navigate through the datasets that were formatted over the course of a given session using the left-right arrows and save any dataset manually by clicking on the save  button.

3.2 Filling the gaps in daily weather records

3.2.1 Introduction

WHAT provides an automated, robust, and efficient method to quickly and easily fill the gaps in the daily weather datasets from the files that were produced as described in [appendix 3.1.4](#). It is also possible to fill the gaps in weather datasets from files that were not produced with WHAT, provided

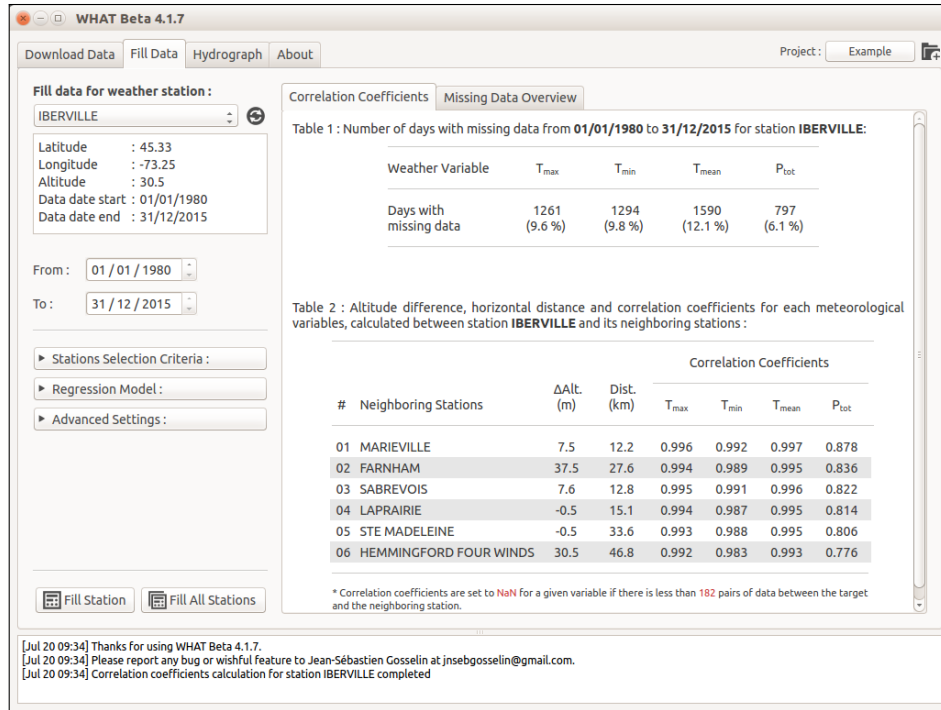


Figure 7 – Screenshot of WHAT v4.1.7-beta in Ubuntu-Linux 15.04 showing the *Fill Data* tab.

that the data are formatted in the right format. In addition, WHAT includes the framework to easily validate and assess the uncertainty of the estimated missing values with a cross-validation resampling technique. These features are available in the *Fill Data* tab shown in figure 7. This tab consists in a side-panel to the left where the gapfilling procedure can be managed and configured and an area to the right where various outputs are displayed.

3.2.2 Loading the weather data files

When starting WHAT or when a project is opened, the content of the *Input* folder is automatically scanned for weather data files. The results are displayed in a list of weather stations, located under the label *Fill data for weather station* shown in figure 8. A summary of the number of days with missing data for each dataset is also produced and displayed in the tab *Missing Data Overview* of the display area, to the right. The icon with the circular arrows located next to the list of stations, can be clicked to re-scan the *Input* folder for new weather data files to update the list of stations and the summary.

3.2.3 Setting the model parameters

The first step is to select the station for which missing values in the dataset need to be filled. This is done from the drop-down list located under the *Fill data for station* section shown in [figure 8](#). Under this list are automatically posted information about the currently selected weather station. It is also possible to define the period for which the data of the selected station will be filled by editing the date fields located next to the *From* and *To* labels. By default, dates are set as the first and the last date for which data are available for any of the stations of the list.

The method used to estimate the missing data for the selected weather station consists in the generation of a multiple linear regression (MLR) model, using synchronous data from selected neighboring stations from the list. The neighboring stations are selected mainly on the basis of the correlation coefficients computed between their data and those of the selected weather station. The values of these coefficients are automatically displayed in the table located in the right side of the interface when a new weather station is selected from the list. Moreover, among the selected neighboring stations, the ones with the highest correlation coefficients have more weight in the model than those with weak correlation coefficients. For this reason, correlation coefficients that fall below a value of 0.7 are shown in red in the table, as a guidance for the user. There are several settings that can be used to control the selection of the neighboring stations, the generation of the MLR model, and the outputs of the gapfilling procedure. An overview of these settings is presented below.

The screenshot shows a user interface for filling data for a weather station. At the top, it says "Fill data for weather station :". Below that is a dropdown menu showing "MARIEVILLE". To the right of the dropdown is a small circular icon with a refresh symbol. The main area contains the following information:

Latitude	:	45.4
Longitude	:	-73.13
Altitude	:	38.0
Data date start : 01/01/1980		
Data date end : 31/12/2015		

At the bottom, there are two date input fields:

- "From :" followed by a dropdown menu containing "01 / 01 / 1980".
- "To :" followed by a dropdown menu containing "31 / 12 / 2015".

Figure 8
Screenshot of WHAT v4.1.7-beta in Ubuntu-Linux 15.04 showing the *Fill data for station* section. For this setup, missing values in the datasets of the selected weather station (MARIEVILLE) would be filled for the 01/01/1980 to 31/12/2015 period.

Station Selection Criteria : A MLR model is generated for each day for which a data is missing in the dataset of the selected station. This is done because the number of neighboring stations with available data can vary in time. Therefore, for a given date with missing data in the dataset of the selected station, the neighboring stations are selected in decreasing order of their correlation coefficients. Neighboring stations that also have a missing data at this particular date are excluded from the selection process. The maximum number of station that are selected for the generation of the MLR model can be specified in the *Nbr. of stations* field, located in the *Stations Selection Criteria* menu shown in [figure 9](#). The number of neighboring station that is selected by default is 4. If for a given date, all the neighboring stations have missing data synchronously with the selected station, a NaN value is kept in the dataset at this particular date.

Moreover, the correlation between the data of two stations will, in general, decreases as the distance and the altitude difference between them increase. Therefore, the fields *Max. Distance* and *Max. Elevation Diff.* allow to specify thresholds for the distance and altitude difference. Neighboring stations exceeding either one of these thresholds will not be used to fill the gaps in the dataset of the selected station. The default values for the distance and altitude difference are set to 100 km and 350 m, respectively, based on a literature review ([Tronci et al., 1986](#); [Xia et al., 1999](#); [Simolo et al., 2010](#)). The horizontal distances and elevation differences calculated between the selected station and its neighbors are shown in the table to the right, alongside the correlation coefficients. The values that exceed their corresponding threshold are shown in red.

Regression Model : It is possible to select whether the MLR model is generated using a Ordinary Least Squares (OLS) or a Least Absolute Deviations (LAD) criteria from the *Regression Model*

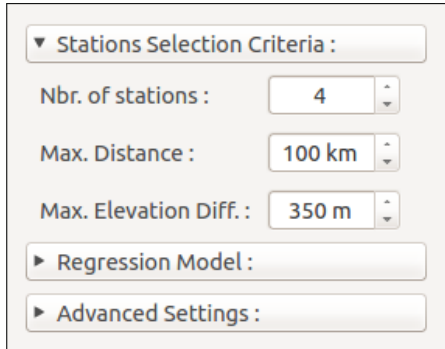


Figure 9
Screenshot of WHAT v4.1.7-beta in Ubuntu-Linux 15.04 showing the *Advanced Settings* menu.

menu shown in [figure 10](#). A regression based on a LAD is more robust to outliers than a regression based on a OLS, but is more expensive in computation time.

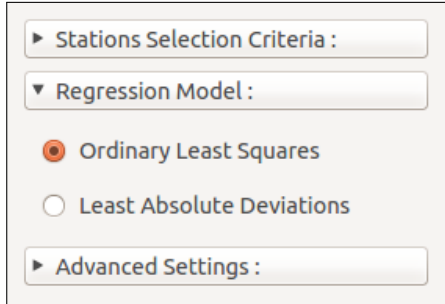


Figure 10
Screenshot of WHAT v4.1.7-beta in Ubuntu-Linux 15.04 showing the *Regression Model* menu.

Advanced Settings : It is possible to automatically estimate and add the daily Potential Evapotranspiration (ETP) to the output data file produced at the end of the gapfilling procedure of the selected station. This option is enabled by checking the *Add ETP to data file* option in the menu *Advanced Settings* shown in [figure 11](#). The daily ETP is estimated with a method adapted from [Thornthwaite \(1948\)](#), using the daily mean air temperature time series of the selected station. Alternatively, it is possible to add manually the ETP to an existing weather data file by clicking on the open file icon located next to the *Add ETP to data file* option.

The *Full Error Analysis* option can be checked to perform a cross-validation resampling analysis during the gapfilling procedure. The results from this analysis can be used afterward to estimate the accuracy of the method. This option is discussed in more details in [appendix 3.2.5](#).

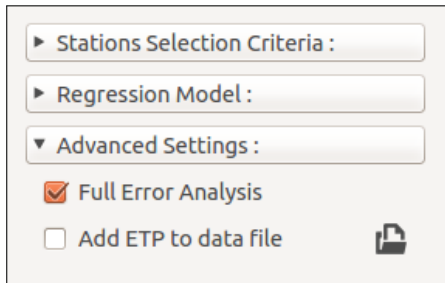


Figure 11
Screenshot of WHAT v4.1.7-beta in Ubuntu-Linux 15.04 showing the *Advanced Settings* menu.

3.2.4 Filling the gaps in the data

The automated procedure to fill the gaps in the dataset of the selected weather station can be started by clicking the button *Fill*  located at the bottom of the left side-panel. It is also possible to run this procedure in batch mode to fill the gaps in the datasets of the entire list of weather station by clicking on the button *Fill All Stations* 

Once the process is completed for a station, the resulting gapless daily weather dataset is automatically saved in a tsv (tabular-separated values) file with the extension “.out” in the *Output* folder (see [appendix 2.4](#)). The file is named after the weather station name, climate ID, and first and last year of the dataset. For example, the resulting output file for the station MARIEVILLE in [figure 7](#) would be “MARIEVILLE (7024627) 1980-2015.out”. In addition, detailed information on the values estimated for filling the gaps in the data are saved in a file with the same name as the “.out” file, but with a “.log” extension. Information includes, the names of the neighboring stations, the values of the data used for the estimations, as well as the expected uncertainty of the estimates.

3.2.5 Uncertainty of the estimated values

By default, each time a new MLR model is generated to estimate a missing value in the dataset of the selected station, the model is also used to predict the values in the dataset that are not missing. The accuracy of the MLR model is then approximated by computing a Root-Mean-Square Error (RMSE) between the values estimated with the model and the respective non-missing observations in the dataset of the selected station. The RMSE thus calculated is saved, along with the estimated value, in the “.log” file.

When the *Full Error Analysis* option in the *Advanced Settings* menu is enabled, WHAT will also perform a cross-validation resampling procedure to estimate the accuracy of the model, in addition to fill the gaps in the dataset. More specifically, the procedure consists in estimating alternately a weather data value for each day of the selected station’s dataset, even for days for which data are not missing. Before estimating a value for a given day, the corresponding measured data in the dataset of the selected station is temporarily discarded to avoid self-influence of this observation on the generation of the MLR model. The model is then generated and used to estimate a value

on this given day and the corresponding observed data is put back in the dataset of the selected station. When a value for every day of the dataset has thus been estimated, the estimated values are saved in a tsv (tabular-separated values) file in the *Output* folder with the extension “.err”, along with the “.log” and “.out” files described in [appendix 3.2.4](#). The accuracy of the method can then be estimated by computing the RMSE between the estimated weather data and the respective non-missing observations in the original dataset of the selected station. Activating this feature will significantly increase the computation time of the gap filling procedure, especially if the least absolute deviation regression model is selected, but can provide interesting insights on the performance of the procedure for the specific datasets used for a project.